Nonlinear Resonance of Trapped Waves on a Plane Beach

by

Guangda Li

B.S., Tsinghua University (1997)
S.M., Tsinghua University (2000)

Submitted to the Department of Civil & Environmental Engineering in partial fulfillment of the requirements for the degree of

Doctor of Philosophy in Environmental Fluid Mechanics

at the

MASSACHUSETTS INSTITUTE OF TECHNOLOGY

February 2007

Author 9/15/06
Department of Civil & Environmental Engineering
September 15, 2006

Certified by 9/15/06
Chiang C. Mei
Ford Professor of Engineering
Department of Civil & Environmental Engineering
Thesis Supervisor

Accepted by ....
Andrew J. Whittle
Professor of Civil & Environmental Engineering
Chairman, Department Committee on Graduate Students

Nonlinear Resonance of Trapped Waves on a Plane Beach

by

Guangda Li

Submitted to the Department of Civil & Environmental Engineering
on September 15, 2006, in partial fulfillment of the
requirements for the degree of
Doctor of Philosophy in Environmental Fluid Mechanics

Abstract

Linear edge waves were first found mathematically by Stokes (1846). It has long been a topic of interest, since edge waves are believed to be responsible for the formation of beach cusps. Galvin (1965) was the first to observe in the laboratory that edge wave mode of frequency ω can be excited by incident waves of frequency 2ω. Guza and Bowen (1976) gave a theoretical explanation of the nonlinear mechanism of subharmonic resonance. This type of theory has been extended by Minzoni & Whitham (1977), Rockliff (1978), and Rockliff & Smith (1985), among others. Rockliff also initiated a theory whereby subharmonic resonance can be achieved by an incident wave of frequency ω, which leads to second harmonic at the second order to excite the edge wave. Their theory was however incomplete.

The goal of this thesis is to extend the existing theories in order to show other paths to resonance. The nearshore region is a plane beach of small slope. For all cases we shall derive the evolution equations governing the edge wave amplitudes and analyze the stability of the equilibrium (static or dynamic) state. We first study in Chapter 2 synchronous resonance as a special case. We shall show that interaction between the edge wave and the incident/reflected wave also generates circulation cells on the beach. Comparison is made between our theoretical results and the experiments by Bowen & Inman. We then give a corrected version of the work of Rockliff and Rockliff & Smith. Next, in Chapter 3 we generalize the idea of Chapter 2 and examine the excitation of an edge wave by a pair of incident waves of magnitudes comparable to the saturated edge wave but the sum of their frequencies can cause subharmonic resonance nonlinearly. In the development of theory, singularities were discovered at certain incident wave frequencies, each of which coincides with the difference of natural frequencies of two edge wave modes. Hence lower-order resonance happens. To remove this singularity we consider in Chapter 4 the simultaneous excitation of two modes of edge waves by one incident wave. The two edge waves are shown to be coupled by both linear and nonlinear terms. Instead of a fixed point, the dynamical system has two limit cycles as dynamic equilibria. Nonlinear numerical simulation and linear instability are analyzed.

Thesis Supervisor: Chiang C. Mei
Title: Ford Professor of Engineering
Department of Civil & Environmental Engineering

Acknowledgments

I owe my gratitude to all the people who have made this thesis possible and because of whom my graduate experience has been one that I will cherish forever.

First and foremost I'd like to thank my advisor, Professor Chiang C. Mei for giving me an invaluable opportunity to work on challenging and extremely interesting projects over the past six years. He has always made himself available for help and advice. It has been a pleasure to work with and learn from such an extraordinary individual.

I would also like to thank Prof. Ole S. Madsen and Prof. Triantaphyllos Akylas for agreeing to serve on my thesis committee and for sparing their invaluable time reviewing the thesis draft. Without their help, this thesis would have been a distant dream.

My friends and my colleagues at Parson's Lab have enriched my graduate life in many ways and deserve a special mention. I thank Lei Chen, Zhiyu Zhang, Lixian Liu, Yuan Xiao, Matthew Lim, Zhenhua Huang, Yile Li, Matthew Hancock, Mengyi Chen, Andrea Adamo and Sheila Fay for all your help.

I owe my deepest thanks to my family — my mother and father who have always stood by me. Words cannot express the gratitude I owe them. I also thank my mother-in-law for her long-lasting support and sharing housework. Most importantly, I would like to thank my wife Liying and my son Alexander for all the joys they bring to me.

I acknowledge with gratitude the financial support from Magistato alle Acqua & Consorzio Venezia Nuova, U.S. Office of Naval Research (Grant N00014-04-1-0077), US National Science Foundation (Grant CTS oo75713) and US-Israel BiNational Science Foundation (Grant 2004205).

It is impossible to remember all, and I apologize to those I've inadvertently left out.

Contents

1 Introduction **19**

1.1 Basic linearized theory 22

2 Synchronous excitation of edge wave by incident wave of comparable magnitude **25**

2.1 Normalization 26

2.2 Harmonics and nonlinear forcing terms 27

2.3 Multiple-scale expansions 31

2.4 The leading-order solution 32

2.5 The second-order solution 33

2.5.1 ϕ_1 — Radiated second-harmonic 33

2.5.2 ψ_{12} — Forced second-harmonic trapped wave 38

2.5.3 Series solution 39

2.5.4 ψ_{10} — zeroth harmonic and steady circulation 46

2.5.5 Wave set-up/set-down at equilibrium 49

2.6 The third-order problem 52

2.6.1 Governing equation and forcing 52

2.6.2 Solvability and evolution equation 54

2.6.3 The coupling coefficients 55

2.7 Initial growth 60

2.8 Effects of detuning 61

2.9 Analysis of nonlinear dynamical system 62

2.9.1 Equilibrium state — mature edge wave and the second-order steady flow . . . 64
2.9.2 Local dynamics around the fixed point . . . 74
2.10 Summary . . . 78

3 Edge wave generation by a pair of incident waves of comparable magnitude 83

3.1 Harmonics and nonlinear forcing terms . . . 84
3.2 Multiple-scale expansions . . . 90
3.3 The leading order . . . 91
3.4 The second order solutions . . . 92
3.4.1 ϕ_1 — Radiated wave of frequency 2 . . . 92
3.4.2 ψ_{11} — Trapped wave of frequency $(1-\omega_1)$ . . . 95
3.4.3 ψ_{12} — Trapped wave of frequency $(1-\omega_2)$ . . . 97
3.4.4 ψ_{13} — Trapped wave of frequency $(1+\omega_1)$ . . . 97
3.4.5 ψ_{14} — Trapped wave of frequency $(1+\omega_2)$ . . . 99
3.4.6 1-D Finite element formulation . . . 99
3.5 The third order . . . 100
3.5.1 Solvability and evolution equation . . . 106
3.5.2 The coupling coefficients . . . 107
3.6 Effects of detuning . . . 116
3.7 Initial growth . . . 121
3.8 Analysis of nonlinear dynamical system . . . 121
3.9 Conclusion . . . 137

4 Resonance of two edge waves by one incident/reflected wave system 139

4.1 Harmonics and the nonlinear forcing terms . . . 142
4.2 Multiple-scale expansion . . . 145
4.3 The leading-order solution . . . 146
4.4 The second-order solution . . . 147
4.4.1 ϕ_{11} to ϕ_{14} — Radiated harmonics . . . 147

4.4.2 ψ_{11} to ψ_{14} — Trapped harmonics 151
4.5 The third-order problem 154
4.5.1 Governing equations and forcing 154
4.6 Initial evolution 167
4.7 Nonlinear evolution equations 173
4.7.1 Nonlinear term coefficients for case (1): $p = 0,\ q = 1$ 173
4.8 Nonlinear dynamics of Stuart-Landau equations 183
4.8.1 Effects of detuning 184
4.8.2 Initial growth rate from infinitesimal disturbance with effect of detuning 185
4.8.3 Energy equation 187
4.9 Analysis of nonlinear dynamical system for $\bar{B}_p$ and $\bar{B}_q$ 188
4.9.1 Fixed point of $\bar{B}_p$ and $\bar{B}_q$ 190
4.9.2 Numerical verification for the existence of limit cycles 196
4.9.3 Physical implication of the equilibrium 199
4.9.4 Local stability of limit cycles 203
4.10 Conclusion 218

5 Other considerations and future works **223**
5.1 Competition between two subharmonic edge waves driven by two smaller incident and reflected waves 223
5.1.1 Governing equations 224
5.1.2 Fixed points 226
5.2 Simultaneous resonance of two subharmonic edge waves of the same eigen frequency by one incident/reflected wave 230

A Analytical solution by Guza and Davis, Rockliff **235**

B Confirmation of $C_2 = 0$ by the no-flux boundary condition at shoreline **241**

C Analytical solution similar to Guza and Davis **243**

D Convergence of integrals **249**

E Numerical solution by finite element method for synchronous resonance **251**

F Evaluation of the integral in (2.66) **259**

G Low-frequency incident wave — case of $\omega = \omega_q - \omega_p$ **261**

G.1 Governing equations 261

G.2 Initial growth 264

G.3 Effects of Detuning 269

G.4 Analysis of nonlinear dynamical system 271

G.5 Fixed point — the equilibrium state 272

H Numerical solution by finite element method for cross resonance **275**

I The coefficients c's and d's for other two cases **279**

I.1 Case (2). $p = 0,\ q = 2$ 279

I.2 Case (3). $p = 1,\ q = 2$ 288

J Subharmonic resonance as a special case **299**

J.1 Initial growth rate 304

J.2 Equilibrium state — mature edge wave amplitude 305

List of Figures

1-1 Reflective beach and beach cusps at Duck, North Carolina (photo by Steve Elgar). 20

1-2 Wedge-like water body on a confined plane sloping beach 22

2-1 Curves for $u_1^i(x)$ and $u_2^i(x)$. 37

2-2 Curves for $u_1^e(x)$ and $u_2^e(x)$. To be filled in. 37

2-3 $f_{11}(x)$ reconstructed using first 5($N = 4$, solid line) and 10($N = 9$, crosses) Laguerre polynomials. 45

2-4 $f_{12}(x)$ reconstructed using first 5($N = 4$, solid line) and 10($N = 9$, crosses) Laguerre polynomials. 51

2-5 Bifurcation diagram of equilibrium branches. 65

2-6 The normalized surface elevation $\zeta'(0, y, t)$ along shore line at different time $t = \frac{n\pi}{12}$, n=1, 2, 3,..., 12, which are labeled on corresponding curves. 66

2-7 Photo cited from Bowen & Inman's 6.4 sec test. 69

2-8 The normalized steady flow velocity $(u, v) = (\frac{\partial f}{\partial x}, \frac{\partial f}{\partial y})$. The two lines in the bottom figure represent the instantaneous edge wave surface elevation and the solid line is half period away from the dashed line. AN— Antinode, N— Node. 70

2-9 Normalized wave set-up on the beach. The two curves at $x = 0$ represent the instantaneous edge wave surface elevation at shoreline and the solid line is half period away from the dashed line. 72

2-10 Normalized wave set-up at the shoreline $x = 0$. The dashed curves represent the instantaneous edge wave surface elevation at shoreline and the two curves are half period away from each other. 73

2-11 Phase portrait near the perfect resonance stable equilibrium $(I_0, \theta_0) = (0.1673, -1.3052)$. 75

2-12 Bifurcation diagram. 77

2-13 Attraction domain demarcation by the saddle separatix for $\hat{a} = 1.15$. . 79

2-14 A trajectory starting from $(I(0), \theta(0)) = (0.25, 0.2)$ in between the PQ curve is suppressed by the MN branch. 80

2-15 Attraction domain demarcation by the saddle separatix for $\hat{a} = 1.15$. . 81

2-16 A trajectory with a starting point in between the PQ curve is suppressed by the MN branch. 81

3-1 Coefficients a_1 (solid lines), a_2 (dash lines) and absolute value of a_3 (dash-dot line) v.s. ω_1. The three vertical dot lines indicate positions of discontinuities at $\omega_1 = 0.354, 0.732$ and 0.764, where resonance occurs. 117

3-2 Coefficients a_0 v.s. ω_1 for zero detuning $\Omega = 0$ and $(|A_1|, |A_2|) = (\frac{1}{2}, \frac{3}{2})$— dash lines, $(|A_1|, |A_2|) = (1, 1)$— solid lines, $(|A_1|, |A_2|) = (\frac{3}{2}, \frac{1}{2})$— dash-dot lines. Note the singularities at $\omega_1 = 0.354, 0.732$ and 0.764. 119

3-3 Coefficients b v.s. ω_1 for zero detuning $\Omega = 0$ and $(|A_1|, |A_2|) = (\frac{1}{4}, \frac{7}{4})$— dash-dot line, $(|A_1|, |A_2|) = (\frac{1}{2}, \frac{3}{2})$— dash line, $(|A_1|, |A_2|) = (1, 1)$— solid line. 120

3-4 Growth rate r^2 v.s. ω_1 for zero detuning $\Omega = 0$ and $(|A_1|, |A_2|) = (\frac{1}{2}, \frac{3}{2})$— dash lines, $(|A_1|, |A_2|) = (1, 1)$— solid lines, $(|A_1|, |A_2|) = (\frac{3}{2}, \frac{1}{2})$—dash-dot lines. Singularities occur at $\omega_1 = 0.354, 0.732$ and 0.764. 122

3-5 A closer look of growth rate r^2 v.s. ω_1 for zero detuning $\Omega = 0$ and $(|A_1|, |A_2|) = (\frac{1}{2}, \frac{3}{2})$— dash lines, $(|A_1|, |A_2|) = (1, 1)$— solid lines, $(|A_1|, |A_2|) = (\frac{3}{2}, \frac{1}{2})$—dash-dot lines. Singularities occur at $\omega_1 = 0.354, 0.732$ and 0.764. 123

3-6 Growth rate r^2 v.s. $|A_1|$ for zero detuning $\Omega = 0$ and $\omega_1 = 0.1$— dash-dot line, $\omega_1 = 0.14$— solid line, $\omega_1 = 0.18$— dash line. 124
3-7 Equilibrium branches I_0/b with respect to $\hat{a}$. 126
3-8 Parametrized surface $\hat{a} = -1$. 126
3-9 Parametrized surface $\hat{a} = 0.82$. 127
3-10 Parametrized surface $\hat{a} = 1$. 128
3-11 Parameterized surface $\hat{a} = 1.29$. 129
3-12 $\hat{a}$ v.s. Ω curves for critical value of ω_1 with $A_1 = 0.25, A_2 = 1.75$— First branch of a_0. 130
3-13 $\hat{a}$ v.s. Ω curves for critical value of ω_1 with $A_1 = 0.25, A_2 = 1.75$— Second branch of a_0. 131
3-14 $\hat{a}$ v.s. Ω curves for critical value of ω_1 with $A_1 = 0.25, A_2 = 1.75$— Third branch of a_0. The dashed line in the middle is for $\omega_1 = 0.749$. . . 132
3-15 $\hat{a}$ v.s. Ω curves for critical value of ω_1 with $A_1 = 0.25, A_2 = 1.75$— Forth branch of a_0 133
3-16 $\hat{a}$ v.s. ω_1 curves for $A_1 = 1$ and several Ω's: $\Omega = 0$— solid lines, $\Omega = -2$— dash lines, $\Omega = 2$— dash-dot lines. Note the singularities at $\omega_1 = 0.354, 0.732$ and 0.764. 134
3-17 $\hat{a}$ v.s. ω_1 curves for $A_1 = 0.5$ and several Ω's: $\Omega = 0$— solid lines, $\Omega = -2$— dash lines, $\Omega = 2$— dash-dot lines. Note the singularities at $\omega_1 = 0.354, 0.732$ and 0.764. 135
3-18 $\hat{a}$ v.s. ω_1 curves for $A_1 = 1.5$ and several Ω's: $\Omega = 0$— solid lines, $\Omega = -2$— dash lines, $\Omega = 2$— dash-dot lines. Note the singularities at $\omega_1 = 0.354, 0.732$ and 0.764. 136

4-1 Numerical solutions to f_{11}— solid line, f_{12}— dash line, and f_{14}— dash-dot line for Case (1): $p = 0,\ q = 1$. 175
4-2 Equilibrium branches of I_q^0 v.s. Ω–$p = 0,\ q = 1$. 192
4-3 Equilibrium branches of I_q^0 v.s. Ω–$p = 0,\ q = 2$. 193
4-4 Equilibrium branches of I_q^0 v.s. Ω–$p = 1,\ q = 2$. 193

4-5 Equilibrium branches of Θ^0 v.s. Ω. The solid line represents the stable equilibrium branch and the dot line represents the unstable branch. . . 194
4-6 Detuning of the two edge wave modes Ω_p^0 and Ω_q^0 v.s. Ω, i.e. the detuning of the incident wave. The solid lines represent the stable equilibrium branch and the dot lines represent the unstable branch. . . 195
4-7 Phase angles evolution curves for $\Omega = 0$. $\Omega_p = -0.1166$ and $\Omega_q = 0.1166$. 197
4-8 Flow map (I_p,I_q) for fixed point (I_p^0,I_q^0)=(0.1497, 0.4560) — ($p = 0, q = 1$). 198
4-9 Two limit cycles corresponding to two edge wave amplitudes with $\Omega = 0$ ($p = 0, q = 1$). The inner circle is B_p, the outer is B_q. 199
4-10 Phase angles evolution curves for $\Omega = 0$. $\Omega_p = \Omega_q = 0$. 200
4-11 Two limit cycles corresponding to two edge wave amplitudes with $\Omega = 0$ ($p = 0, q = 2$). The inner circle is B_p, the outer is B_q. 200
4-12 Two limit cycles corresponding to two edge wave amplitudes with $\Omega = 0$ ($p = 1, q = 2$). The inner circle is B_p, the outer is B_q. 201
4-13 The instantaneous surface elevation by addition of two edge wave modes as steady state is reached ($p = 0, q = 1$). 202
4-14 Projection of eigen directions of the unstable fixed point U on (I_p, I_q) plane for $\Omega = 0.54$. 206
4-15 The 3D view of the eigen directions of the unstable point U for $\Omega = 0.54$. 207
4-16 The 3D view of the separatix by the unstable fixed point U for $\Omega = 0.54$. 208
4-17 Flow map of the nonlinear dynamical system for $\Omega = -0.2$. 209
4-18 Flow map of the nonlinear dynamical system for $\Omega = 0$. 209
4-19 Flow map of the nonlinear dynamical system for $\Omega = 0.2$. 210
4-20 Flow map of the nonlinear dynamical system for $\Omega = 0.54$. 210
4-21 Flow map of the nonlinear dynamical system for $\Omega = 0.54$. 213
4-22 Flow map of the nonlinear dynamical system for $\Omega = 0.376$ with a starting point (I_p, I_q, Θ)=(0.001, 0.001, 0.01). 216
4-23 Temporal evolution of I_p and I_q v.s. τ for $\Omega = 0.376$ with a starting point (I_p, I_q, Θ)=(0.001, 0.001, 0.01). 216

4-24 Temporal evolution of I_p v.s. τ for $\Omega = 0.376$ with a starting point (I_p, I_q, Θ)=(0.00001, 0.00001, 0.1). 217

4-25 Temporal evolution of I_q v.s. τ for $\Omega = -0.380$ with a starting point (I_p, I_q, Θ)=(0.00001, 0.00001, 0.1). 217

4-26 Flow map of the nonlinear dynamical system for $\Omega = -0.380$ with a starting point (I_p, I_q, Θ)=(0.001, 0.001, 0.01). 218

4-27 Temporal evolution of I_p v.s. τ for $\Omega = -0.380$ with a starting point (I_p, I_q, Θ)=(0.001, 0.001, 0.01). 219

4-28 Temporal evolution of I_q v.s. τ for $\Omega = -0.380$ with a starting point (I_p, I_q, Θ)=(0.001, 0.001, 0.01). 219

4-29 Flow map of the nonlinear dynamical system for $\Omega = -0.380$ with a starting point (I_p, I_q, Θ)=(0.003, 0.007, 0.1). 220

4-30 Temporal evolution of I_p (dash line) and I_q (solid line) v.s. τ for $\Omega = -0.380$ with a starting point (I_p, I_q, Θ)=(0.003, 0.007, 0.1). 220

4-31 Flow map of the nonlinear dynamical system for $\Omega = -0.370$. 221

5-1 Equilibrium branch for $J_2^0 = 0$— Equilibrium of the first kind. 227

5-2 Equilibrium branch for $J_1^0 = 0$— Equilibrium of the second kind. 228

5-3 The bifurcation diagram. 229

5-4 Flow map (x_j,y_j), $j = 1, 2$ for $\Omega = 0.5$ — ($p = 1, q = 3$). 232

5-5 Temporal evolution of x_2 and y_2 for $\Omega = 0.5$ — ($p = 1, q = 3$). 233

A-1 Comparison of two solutions: Analytical formula — solid line; Solution by variation of parameters — crosses. 238

C-1 $\hat{u}_1(\infty)$ and $\hat{u}_2(\infty)$ v.s. ω_1. 244

C-2 Comparison of the two solutions for $\omega_1 = 0.5$: Solid line — Eq. (C.3); Crosses — Eq. (C.7). 245

C-3 Comparison of the two solutions for $\omega_1 = 0.25$: Solid line — Eq. (C.3); Crosses — Eq. (C.7). 246

C-4 Comparison of the two solutions for $\omega_1 = 0.75$: Solid line — Eq. (C.3); Crosses — Eq. (C.7). 247

D-1 Behavior of the integrand ζ 250

E-1 Local coordinate system for 1-D linear element 253

E-2 Numerical solution of $f(x)$ (solid line) and exact solution (dots) for special force $g(x) = e^{-x}$. 255

E-3 The numerical solution for f_{11}(solid line) and f_{12}(dashed line). The circles and crosses are their series expansion solutions respectively. . . . 257

I-1 Numerical solutions to f_{11}— solid line, f_{12}— dash line, and f_{14}— dash-dot line for Case (2). $p = 0,\ q = 2$. 280

I-2 Numerical solutions to f_{11}— solid line, f_{12}— dash line, f_{13}— dot line, and f_{14}— dash-dot line for Case (3): $p = 1,\ q = 2$. 290

List of Tables

2.1 Coefficients C_n from (2.61) by Rockliff and Smith. 40

2.2 Coefficients C_n for the Fourier-Laguerre series expansion of $f_{11}(x)$ by analytical formula (2.68). 43

2.3 Coefficients a_n for the final solution of f_{11}. 43

2.4 Computed $f_{11}(x)$ using different truncation number N. Error is defined by $100 \times \frac{f_{11}(N=9)-f_{11}(N=4)}{f_{11}(N=9)}$. 44

2.5 Coefficients C_n for the Fourier-Laguerre series expansion of $f_{12}(x)$. . . . 48

2.6 Coefficients a_n for the final solution of f_{12}. 49

2.7 Computed $f_{12}(x)$ using different truncation number N. Error is defined by $100 \times \frac{f_{12}(N=9)-f_{12}(N=4)}{f_{12}(N=9)}$. 50

2.8 All the numerically evaluated coefficients for the governing equation. . . 59

2.9 Quoted records of the longshore variation of breaker height from Bowen and Inman [3]. 68

3.1 Effective second-order harmonics and their further interactions. 87

4.1 Check for the eigen value condition for several combinations of (p, q). . 153

4.2 Coefficients pairs (c_1, d_1) for different edge wave modes combinations. . 173

4.3 The growth rate factor $\sqrt{c_1 d_1}$ for different edge wave modes combinations. 173

4.4 Coefficients of α's by numerical integration. 176

4.5 Coefficients of β's by numerical integration. 177

4.6 Coefficients of γ's by numerical integration. 178

4.7 Coefficients of κ's by numerical integration. 182

4.8 Coefficients of c's and d's for $\omega = \omega_q + \omega_p$. 184

4.9 The steady state phase angles θ_p^0 and θ_q^0— $(p = 0, q = 1)$. 196
4.10 Parameter θ_j for the starting point and the corresponding backward evolution time t. 205
4.11 Eigen values for upper nontrivial equilibrium branch BD. 211
4.12 Eigen values for lower nontrivial equilibrium branch CD. 212

5.1 Coefficients c_j's for case $p = 1$, $q = 3$. 231
5.2 Coefficients d_j's for case $p = 1$, $q = 3$. 231

A.1 Confirmation for the numerical integral of $u_1^i(\infty) = -1$, $u_2^i(\infty) = 0$. . 237

E.1 Comparison of FEM solution with the exact solution for $g(x) = e^{-x}$. Error is defined by $100 \times \frac{f(EXACT)-f(FEM)}{f(EXACT)}$. 256
E.2 Comparison of FEM solution with the series solution of $f_{11}(x)$ and $f_{12}(x)$. 258

G.1 Coefficients pairs (a_1, b_1) for different edge wave modes combinations. Low frequency incident wave. 269
G.2 Coefficients of a's and b's for $\omega = \omega_q - \omega_p$. 270

Chapter 1

Introduction

Rhythmic or periodic features such as rip currents, beach cusps and crescentic bars, are often found among many plane sandy beaches. The photograph (Figure 1-1) by Steve Elgar [33] clearly shows beach cusps running down the shoreline.

Since the nineteen sixties (Eckart [7] and Ursell [31]), the formation of beach cusps has been attributed to edge-waves (e.g. Galvin [10], Bowen and Inman [3], Komar [21], Guza and Bowen [13]). There is increasing evidence from field observations (Coco et al. [5]) that these edge waves are often excited subharmonically by waves incident upon the beach, i.e., edge waves of frequency ω is excited by incoming wind waves of frequency 2ω. For these edge waves, sandy horns coincide with the edge-wave nodes, where swash excursion is the minimum, and bays coincide with the antinodes, where swash excursion is the maximum. Different edge wave modes have different node and antinode structures, in both longshore and cross-shore directions. These edge-wave modes are believed to be responsible for the formation of beach cusps and longshore bars. Multiple edge wave modes can also be excited simultaneously, implying that several length scales may coexist on one beach. A striking feature of beach cusps is their regular or quasi-regular spacing along-shore, even in the random sea condition. To explain this, theories that beach cusps are evolving features resulting from self-organizing feedback processes have been proposed by Werner and Fink [32], Coco et al. [6]. Recent field work in this direction has been focused mainly in two areas. Firstly high resolution beach experiments have been conducted in order to discern the

Figure 1-1: Reflective beach and beach cusps at Duck, North Carolina (photo by Steve Elgar).

nearshore dynamics and to identify harmonic forcing signals. Secondly mathematical models are used to test features of self-organizing processes. Such computational models have shown that with a simple grid on a beach and using irregular chaotic waves as forcing, cuspate patterns can begin to evolve, if an initial edge wave signal is introduced into the model.

Edge waves are first found mathematically by Stokes [29] (1846), and extended by Ursell [30] (1951). They can be excited linearly by a moving storm (Greenspan [11], 1956) but not by incident waves of the same frequency. Galvin [10] (1965) was the first to observe in the laboratory that edge wave mode of frequency ω can be excited by incident waves of frequency 2ω. Guza & Bowen [12] gave a theoretical explanation of the nonlinear mechanism of subharmonic resonance. This type of theory has been extended by Minzoni & Whitham [23] (1977), Rockliff [26] (1978), and Rockliff & Smith [27] (1985), among others. Rockliff also initiated a theory whereby subharmonic resonance can be achieved by an incident wave of frequency ω, whose second harmonic at the second order excites the edge wave. Their theory was however incomplete.

The goal of this thesis is to extend the existing theories where subharmonic resonance of one edge wave mode is achieved by a single incident/reflected wave system of much smaller amplitude and twice the frequency. Throughout the thesis, we treat the incident wave as the energy source of the dynamical system and its amplitude is always considered as a constant. The nearshore region is assumed to consist of many natural modes of longshore oscillation, i.e. the edge waves. We first study synchronous resonance as a special case. In this part, we shall show that interaction between the edge wave and the incident/reflected wave also generates circulation cells on the beach. To check the correctness of the theory, we make a comparison between our theoretical results and the experiments by Bowen and Inman [3]. While somewhat similar to the work of Rockliff [26] and Rockliff & Smith [27], our theory clears the errors in Rockliff & Smith. The technique solving second-order problem are typical and will be used in the rest of chapters. Next, we generalize the idea of synchronous resonance to the excitation of an edge wave by a pair of incident waves of magnitudes comparable to the final edge wave. Then we consider the simultaneous excitation of two modes of edge waves by one incident wave. The two edge waves are selected so that cross resonance can happen. Next, we study the generation of two edge wave modes by two incident/reflected wave systems subharmonically. The initial growth of the two waves are independent, whereas the nonlinear interaction adds new features to the nonlinear dynamical system as soon as one of the edge wave reaches a finite amplitude. In the last case, we choose two edge wave modes sharing same eigen frequency and let them compete under the excitation of one incident wave of frequency twice of theirs. In particular we shall find if it is possible that only one of the eigen mode finally survives the competition. The nodal structure of the dominant mode should be relevant to beach cusps and bars observed in field and laboratory experiments. Otherwise the interaction of the two edge waves would generate a steady circulation on the beach.

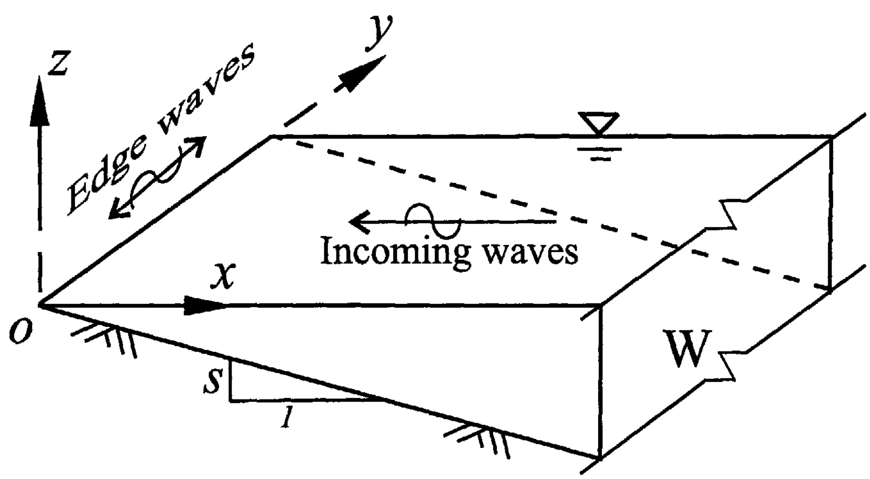

Figure 1-2: Wedge-like water body on a confined plane sloping beach

1.1 Basic linearized theory

As an introduction, we first recall the solutions of the edge waves and the incident/reflected waves on a sloping beach, according to the linearized theory.

An idealized plane beach of constant slope s is chosen, as shown in Figure 1-2. The sloping beach is infinitely long in the x (cross-shore) direction, while bounded by vertical walls laterally in the y (longshore) direction. The width of the bay is W, which can be taken as an integral multiple of the wave length on an infinitely long beach. The origin of the coordinate system is located at the intersection of the still water beach line and one of the walls.

The linearized Airy's shallow-water equation for the velocity potential is [22]

$$\mathcal{L}\Phi = -\Phi_{tt} + sg\left[(x\Phi_x)_x + x\Phi_{yy}\right] = 0 \tag{1.1}$$

where $\mathcal{L}$ is a linear operator. And the corresponding boundary conditions are

i) No flux on the channel walls, i.e. $\Phi_y = 0$ on $y = 0$ and $y = W$.

ii) No flux at shore, i.e. $x\Phi_x = 0$ at $x = 0$.

iii) The edge wave must diminish to zero as $x \to \infty$.

Along the free surface, vanishing of surface pressure requires,

$$g\zeta + \frac{\partial \Phi}{\partial t} = 0. \tag{1.2}$$

Two kinds of eigen solutions to the linearized equation (1.1) are of our interest.

1) Edge wave of frequency ω:

$$\Phi_e = \psi_0(x) \cos ky e^{-i\omega t} + *$$

The longshore wave number k is related to the bay width by the eigenvalue condition in y:

$$k = \frac{m\pi}{W}, \quad m = 1, 2, 3... \tag{1.3}$$

The cross-shore factor $\psi_0(x)$ satisfies

$$(x\psi_{0x})_x + \left(\frac{\omega^2}{gs} - k^2 x\right)\psi_0 = 0$$

which is a confluent hypergeometric equation and has two homogeneous solutions

$$e^{-kx}M(a, 1, 2kx), \quad \text{or} \quad e^{-kx}U(a, 1, 2kx)$$

with

$$a = \frac{1}{2}\left(1 - \frac{\omega^2}{gks}\right).$$

Of the two the first is bounded at the beach and is of physical interest. To satisfy the condition at infinity M must satisfy the eigenvalue condition

$$\omega_n^2 = (2n+1)gks, \quad n = 0, 1, 2... \tag{1.4}$$

Note that the lowest mode has the eigen frequency $\omega_0^2 = kgs$.

With this eigen value condition, the confluent hypergeometric function M becomes the Laguerre polynomials L_n, i.e.

$$M(-n, 1, \xi) = L_n(\xi) = \frac{(-1)^n}{n!}\left[\xi^n - \frac{n^2}{1!}\xi^{(n-1)} + \frac{n^2(n-1)^2}{2!}\xi^{(n-2)} - \cdots + (-1)^n n!\right] \tag{1.5}$$

with $\xi = 2kx$. The final solution for the edge wave is

$$\Phi_e = -\frac{igB}{\omega_n} e^{-kx} L_n(2kx) \cos ky e^{-i\omega_n t} + * \tag{1.6}$$

where B is half of the edge wave amplitude at the shoreline.

2) Normally incident/reflected wave:

Considering the long-crested wave without y-dependence:

$$\Phi_0 = \phi_0(x)e^{-i\omega t} + *$$

Then $\phi_0(x)$ satisfies

$$(x\phi_{0x})_x + \frac{\omega^2}{gs}\phi_0 = 0$$

which is a Bessel equation and has solutions of the form

$$J_0\left(2\omega\sqrt{\frac{x}{gs}}\right), \quad \text{or} \quad Y_0\left(2\omega\sqrt{\frac{x}{gs}}\right)$$

The Bessel function Y_0 has a logarithmic singularity at $x = 0$, which must be discarded for boundedness. The solution for the standing wave is

$$\Phi_0 = -\frac{igA}{\omega}J_0\left(2\omega\sqrt{\frac{x}{gs}}\right)e^{-i\omega t} + * \tag{1.7}$$

where A is half of the incident/reflected wave amplitude at the shoreline.

Chapter 2

Synchronous excitation of edge wave by incident wave of comparable magnitude

It is known that an edge wave of frequency ω and amplitude of order $O(\epsilon)$ can be excited by incident wave of frequency 2ω and amplitude (ϵ^2)[14]. Their quadratic interaction at the third order, combining with the cubic interaction of the first-order edge wave, generates a forcing of frequency ω, which resonates the edge wave at the order $O(\epsilon^3)$. If there are both an incident wave of frequency ω and an edge wave of the same frequency at the same order $O(\epsilon)$, then the quadratic self-interaction of the incident/reflected wave system will generate harmonic of 2ω frequency at order $O(\epsilon^2)$, which can trigger subharmonic resonance of the edge wave at the third order. This idea has been recognized by Rockliff [26]. Her theory is however incomplete and contain algebraic errors, as will be pointed out later. For simplicity, we consider an edge wave of the lowest cross-shore mode. Therefore the eigen frequency is

$$\omega = \omega_0 = \sqrt{kgs} \tag{2.1}$$

Airy's theory is the leading order approximation for very long waves of finite amplitude in shallow water. Its validity requires that $kh \ll 1$ and $A/h \sim O(1)$. Edge waves are appreciable only near the shore because of their exponentially decaying eigenfunctions as in (1.6). Hence any interactions with incident/reflected waves can be regarded as taking place within a distance comparable with the longshore wavelength. As a plane wave approaches a sloping plane beach, its incidence becomes increasingly normal to the shoreline due to refraction. We treat it absolutely normal when it enters the interaction domain. The mathematical infinity for x refers only to the nearshore shallow-water region, where it is appropriate to apply Airy's theory as in [12] by Guza and Bowen. Using primes to denote physical variables, we cite below the nonlinear shallow-water equation of Airy [22]:

$$\mathcal{L}\Phi' = -\Phi'_{t't'} + sg\left[(x'\Phi'_{x'})_{x'} + x'\Phi'_{y'y'}\right] = Q(\Phi') + C(\Phi') \tag{2.2}$$

where $\mathcal{L}$ is the same linear operator in Eq. (1.1). $Q(\Phi')$ and $C(\Phi')$ are the quadratic and cubic nonlinear forcing terms defined below

$$Q(\Phi') = 2\left(\Phi'_{x'}\Phi_{x't'} + \Phi'_{y'}\Phi_{y't'}\right) + \Phi'_{t'}\left(\Phi'_{x'x'} + \Phi_{y'y'}\right) \tag{2.3}$$

$$C(\Phi') = \frac{1}{2}\left({\Phi'_{x'}}^2 + {\Phi'_{y'}}^2\right)\left(\Phi'_{x'x'} + \Phi'_{y'y'}\right) + {\Phi'_{x'}}^2\Phi'_{x'x'} + {\Phi'_{y'}}^2\Phi'_{y'y'} + 2\Phi'_{x'}\Phi'_{y'}\Phi'_{x'y'} \tag{2.4}$$

The corresponding nonlinear free surface condition is

$$\zeta' + \frac{\partial\Phi'}{\partial t'} + \frac{1}{2}|\nabla\Phi'|^2 = 0. \tag{2.5}$$

2.1 Normalization

We use the following nondimensionalized variables:

$$x = kx', \quad y = ky', \quad t = \omega t', \quad \zeta = \frac{\zeta'}{|A'|}, \quad \Phi = \frac{\omega}{|A'|g}\Phi'$$

where $|A'|$ is one-half the absolute amplitude of the incident wave at shoreline. The complex amplitude $A' = |A'|e^{i\varphi}$ contains the phase angle φ. Upon substitution into Eq. (2.2) we get

$$-\Phi_{tt} + (x\Phi_x)_x + x\Phi_{yy} = \epsilon Q(\Phi) + \epsilon^2 C(\Phi) \tag{2.6}$$

where we have introduced the small parameter

$$\epsilon = \frac{k|A'|}{s} \ll 1. \tag{2.7}$$

The quadratic and cubic nonlinear terms remain the same

$$Q(\Phi) = 2\left(\Phi_x\Phi_{xt} + \Phi_y\Phi_{yt}\right) + \Phi_t\left(\Phi_{xx} + \Phi_{yy}\right) \tag{2.8}$$

$$C(\Phi) = \frac{1}{2}\left(\Phi_x^2 + \Phi_y^2\right)\left(\Phi_{xx} + \Phi_{yy}\right) + \Phi_x^2\Phi_{xx} + \Phi_y^2\Phi_{yy} + 2\Phi_x\Phi_y\Phi_{xy} \tag{2.9}$$

Use has been made of the eigenvalue condition for the edge wave (2.1). We also normalize the free surface boundary condition (2.5) to get

$$\zeta + \frac{\partial\Phi}{\partial t} + \frac{\epsilon}{2}|\nabla\Phi|^2 = 0. \tag{2.10}$$

The parameter defined in (2.7) implies that the wave slope must be much less than the bed slope. It is known empirically that standing wave breaks when the following surf parameter exceeds a critical value [22]

$$\xi = s\left(\frac{\pi}{k_\infty A_b}\right)^{1/2}.$$

This critical value roughly implies the following incident wave slope

$$k_\infty A_b = \left(\frac{\pi}{4}\right)^2 s^2$$

Since breaking waves are beyond the scope of present theory, we require that

$$\epsilon = \frac{k|A'|}{s} < \frac{k}{k_\infty}\left(\frac{\pi}{4}\right)^2 s. \tag{2.11}$$

Notice that k is the edge wave number, k_∞ is the incident wave number in deep water, A' is one-half the incident/reflected wave amplitude at the shoreline and A_b is the breaking wave amplitude. We have replaced A_b with $2|A'|$ in (2.11).

2.2 Harmonics and nonlinear forcing terms

We represent the solution as a perturbation expansion:

$$\Phi = \Phi_0 + \epsilon\Phi_1 + \epsilon^2\Phi_2 + \cdots \tag{2.12}$$

At the leading order we assume the co-existence of one edge wave and one normally incident and reflected wave of the same frequency (unity because of normalization):

$$\Phi_0 = \Phi_e + \Phi_i \tag{2.13}$$

where

$$\Phi_e = \psi_0 \; e^{-it} + *; \quad \text{with} \;\; \psi_0 = -iB(\tau)e^{-x}\cos y; \tag{2.14}$$

is the edge wave, and

$$\Phi_i = \phi_0 \; e^{-it} + *; \quad \text{with} \;\; \phi_0 = -ie^{i\varphi}J_0(2\sqrt{x}) \tag{2.15}$$

is the normally incident and reflected waves.

Quadratic interaction at the second order $O(\epsilon)$ leads to forcing terms with the following time-harmonics :

$$(\Phi_e, \Phi_e), (\Phi_e, \Phi_i), (\Phi_i, \Phi_i) \longrightarrow 0, \pm 2. \tag{2.16}$$

We shall use the spatial parts of the first order solutions to symbolize the nonlinear forcing (2.8) and (2.9), where their complex conjugate counterparts are implied. For example, (ψ_0, ϕ_0) represents the quadratic terms due to the interaction of edge wave and the incident wave, and gives rise to a second harmonic. From the same interaction, (ψ_0, ϕ_0^*) produces zero harmonic. We now give the details:

Second harmonic

[Q-1]. (ψ_0, ψ_0) and its complex conjugate:

$$\begin{aligned}(\psi_0, \psi_0) &= 2\left[\psi_{0x}\psi_{0x}(-i) + \psi_{0y}\psi_{0y}(-i)\right] = -2i\left(\psi_{0x}^2 + \psi_{0y}^2\right) \\ &= -2i\left(-iBe^{-x}\right)^2\left(\cos^2 y + \sin^2 y\right) = 2iB^2e^{-2x}\end{aligned} \tag{2.17}$$

after using

$$\psi_{0xx} + \psi_{0yy} = 0.$$

[Q-2]. (ϕ_0, ϕ_0) and its complex conjugate:

$$\begin{aligned}(\phi_0, \phi_0) &= 2\left[\phi_{0x}\phi_{0x}(-i)\right] + \phi_0(-i)\phi_{0xx} \\ &= -ie^{i\varphi}\left(-ie^{i\varphi}\right)\left\{-2i\left(\frac{dJ_0(2\sqrt{x})}{dx}\right)^2 - iJ_0(2\sqrt{x})\frac{d^2J_0(2\sqrt{x})}{dx^2}\right\} \\ &= ie^{i2\varphi}\left\{2\left(\frac{dJ_0(2\sqrt{x})}{dx}\right)^2 + J_0(2\sqrt{x})\frac{d^2J_0(2\sqrt{x})}{dx^2}\right\}\end{aligned} \tag{2.18}$$

[Q-3]. (ψ_0, ϕ_0) and its complex conjugate:

$$\begin{aligned}
(\psi_0, \phi_0) &= 2\left[\psi_{0x}\phi_{0x}(-i) + \phi_{0x}\psi_{0x}(-i)\right] + (-i)\psi_0\phi_{0xx} \\
&= -ie^{i\varphi}(-iB)\,e^{-x}\cos y\left\{2(-2i)(-1)\frac{dJ_0(2\sqrt{x})}{dx} - i\frac{d^2J_0(2\sqrt{x})}{dx^2}\right\} \\
&= -ie^{i\varphi}Be^{-x}\left\{4\frac{dJ_0(2\sqrt{x})}{dx} - \frac{d^2J_0(2\sqrt{x})}{dx^2}\right\}\cos y \\
&\equiv -ie^{i\varphi}Bg_{11}(x)\cos y \qquad (2.19)
\end{aligned}$$

where we introduced

$$g_{11}(x) = e^{-x}\left\{4\frac{dJ_0(2\sqrt{x})}{dx} - \frac{d^2J_0(2\sqrt{x})}{dx^2}\right\} \qquad (2.20)$$

for brevity.

Zeroth harmonic

[Q-4]. (ψ_0, ϕ_0^*) and its complex conjugate:

$$\begin{aligned}
(\psi_0, \phi_0^*) &= 2\left[\psi_{0x}\phi_{0x}^*(i) + \phi_{0x}^*\psi_{0x}(-i)\right] + (-i)\psi_0\phi_{0xx}^* \\
&= ie^{-i\varphi}(-iB)\,e^{-x}\cos y\left[-i\frac{d^2J_0(2\sqrt{x})}{dx^2}\right] \\
&= -ie^{-i\varphi}Be^{-x}\frac{d^2J_0(2\sqrt{x})}{dx^2}\cos y \\
&\equiv -ie^{-i\varphi}Bg_{12}(x)\cos y \qquad (2.21)
\end{aligned}$$

where we introduced

$$g_{12}(x) = e^{-x}\frac{d^2J_0(2\sqrt{x})}{dx^2} \qquad (2.22)$$

for brevity.

There are two terms that do not give any forcing:

[Q-5].

$$\begin{aligned}
(\psi_0, \psi_0^*) &= 2\left[\psi_{0x}\psi_{0x}^*(i) + \psi_{0x}^*\psi_{0x}(-i) + \psi_{0y}\psi_{0y}^*(i) + \psi_{0y}^*\psi_{0y}(-i)\right] \\
&\quad -i\psi_0\left(\psi_{0xx}^* + \psi_{0yy}^*\right) + i\psi_0^*\left(\psi_{0xx} + \psi_{0yy}\right) = 0. \qquad (2.23)
\end{aligned}$$

and

[Q-6].

$$(\phi_0, \phi_0^*) \;=\; 2\left[\phi_{0x}\phi_{0x}^*(i) + \phi_{0x}^*\phi_{0x}(-i) + \phi_{0y}\phi_{0y}^*(i) + \phi_{0y}^*\phi_{0y}(-i)\right]$$
$$-i\phi_0\left(\phi_{0xx}^* + \phi_{0yy}^*\right) + i\phi_0^*\left(\phi_{0xx} + \phi_{0yy}\right) = 0. \qquad (2.24)$$

Therefore, we have four pairs of effective forcing terms producing zeroth and second harmonics. In response to these forcing terms, the following types of second-order solutions will be excited:

i) $(\psi_0, \psi_0) + (\phi_0, \phi_0) \rightarrow \phi_1(x)e^{-i2t}$;

ii) $(\psi_0, \phi_0) \rightarrow \psi_{12}(x, y, \tau)e^{-i2t}$;

iii) $(\psi_0, \phi_0^*) \rightarrow \psi_{10}(x, y, \tau)$.

With these first- and second-order solutions, we can work out all the effective resonance-forcing terms at the third order, guided by two rules : 1) Only the first harmonic (frequency 1) will force resonance and is of interest; and 2) The forcing first harmonic must be proportional to $\cos y$. It follows immediately that the edge wave Φ_e can appear once or three times, but not twice, in each combination (since all combinations of the incident/reflected waves do not depend on y.). The cubic nonlinear terms which can produce first harmonics are [C-1]:$(\psi_0^*, \psi_0, \psi_0)$, [C-2]:$(\psi_0^*, \phi_0, \phi_0)$, [C-3]:$(\psi_0, \phi_0, \phi_0^*)$, [C-4]:$(\psi_0^*, \psi_0, \phi_0)$ and [C-5]:$(\psi_0, \psi_0, \phi_0^*)$.

Among these first harmonics, both [C-4] and [C-5], where the edge wave appears twice, produces quadratic terms of the form $\sin y \sin y$, $\cos y \cos y$ or $\sin y \cos y$. By recalling the trigonometric identities that all these products do not give rise to $\cos y$. The number of effective cubic-nonlinear resonance terms reduces to three. From (2.9), (2.14) and (2.15), we now calculate the three effective forcing terms in detail:

[C-1].

$$\begin{aligned}
&(\psi_0^*, \psi_0, \psi_0) \\
&= \psi_{0xx}2\psi_{0x}\psi_{0x}^* + \psi_{0xx}^*\psi_{0x}\psi_{0x} + \psi_{0yy}2\psi_{0y}\psi_{0y}^* + \psi_{0yy}^*\psi_{0y}\psi_{0y} \\
&+ 2\left(\psi_{0x}\psi_{0y}\psi_{1xy}^* + \psi_{0x}\psi_{0y}^*\psi_{1xy} + \psi_{0x}^*\psi_{0y}\psi_{1xy}\right) \\
&= (-iB)^2 iB^* e^{-3x}\left\{3\cos^3 y - 2\cos y\sin^2 y - \cos y \sin^2 y\right. \\
&+ \left. 2\left[-\cos y\left(-\sin^2 y - \sin^2 y\right) + \cos y \sin^2 y\right]\right\}
\end{aligned}$$

$$
\begin{aligned}
&= -iB^2B^*e^{-3x}\left\{3\cos^3 y + 3\cos y\sin^2 y\right\} \\
&= -3iB^2B^*e^{-3x}\cos y \equiv \hat{h}_{C1}(x)B^2B^*\cos y
\end{aligned} \tag{2.25}
$$

[C-2].

$$
\begin{aligned}
&(\psi_0^*, \phi_0, \phi_0) \\
&= \psi_{0xx}^*\phi_{0x}^2 + 3\left(\phi_{0xx}\phi_{0x}\right)\psi_{0x}^* \\
&= B^*i\left(-ie^{i\varphi}\right)\left(-ie^{i\varphi}\right)e^{-x}\cos y\left[\left(\frac{dJ_0(2\sqrt{x})}{dx}\right)^2 - 3\frac{d^2J_0(2\sqrt{x})}{dx^2}\frac{dJ_0(2\sqrt{x})}{dx}\right] \\
&= -ie^{i2\varphi}e^{-x}\cos y\left[\left(\frac{dJ_0(2\sqrt{x})}{dx}\right)^2 - \frac{3}{2}\frac{d}{dx}\left(\frac{dJ_0(2\sqrt{x})}{dx}\right)^2\right]B^* \\
&\equiv ie^{i2\varphi}\hat{g}_{C2}(x)B^*\cos y
\end{aligned} \tag{2.26}
$$

[C-3].

$$
\begin{aligned}
&(\psi_0, \phi_0, \phi_0^*) \\
&= \phi_{0xx}\phi_{0x}^*\psi_{0x} + \phi_{0xx}^*\phi_{0x}\psi_{0x} + 2\phi_{0x}\phi_{0x}^*\psi_{0xx} + 2\psi_{0x}\phi_{0x}^*\phi_{0xx} + 2\psi_{0x}\phi_{0x}\phi_{0xx}^* \\
&= 2\psi_{0xx}\phi_{0x}^*\phi_{0x} + 3\left(\phi_{0xx}\phi_{0x}^* + \phi_{0xx}^*\phi_{0x}\right)\psi_{0x} \\
&= -i\left(-ie^{i\varphi}\right)\left(ie^{-i\varphi}\right)e^{-x}\cos y\left[2\left(\frac{dJ_0(2\sqrt{x})}{dx}\right)^2 - 6\frac{d^2J_0(2\sqrt{x})}{dx^2}\frac{dJ_0(2\sqrt{x})}{dx}\right]B \\
&= -ie^{-x}\cos y\left[2\left(\frac{dJ_0(2\sqrt{x})}{dx}\right)^2 - 3\frac{d}{dx}\left(\frac{dJ_0(2\sqrt{x})}{dx}\right)^2\right]B \\
&= i\hat{f}_{C3}B\cos y
\end{aligned} \tag{2.27}
$$

Additional contributions will come from quadratic interactions of the pairs (ϕ_1, ψ_0^*), (ψ_{12}, ϕ_0^*), (ψ_{10}, ϕ_0), and (ψ_{10}^*, ϕ_0). Details of these forcing terms will be given after the second-order solutions $\phi_1, \psi_{12}, \psi_{10}$ are derived.

2.3 Multiple-scale expansions

With these preparations, we now proceed with the solution via multiple-scale expansions

$$
\Phi = \left[\psi_0(x, y, \tau)e^{-it} + *\right] + \left[\phi_0(x)e^{-it} + *\right]
$$

$$
\begin{aligned}
&+ \quad \epsilon\left\{\left[\phi_1(x,\tau)e^{-i2t}+*\right]+\left[\psi_{12}(x,y,\tau)e^{-i2t}+*\right]+\left[\psi_{10}(x,y,\tau)+*\right]\right\}\\
&+ \quad \epsilon^2\left[\psi_2(x,y,\tau)e^{-it}+*\right]+\dots
\end{aligned}
\tag{2.28}
$$

where two time variables are introduced: fast time t and slow time $\tau=\epsilon^2 t$. Accordingly time derivatives will be changed as follows

$$
\frac{\partial}{\partial t}\longrightarrow\frac{\partial}{\partial t}+\epsilon^2\frac{\partial}{\partial\tau},\quad \frac{\partial^2}{\partial t^2}\longrightarrow\frac{\partial^2}{\partial t^2}+2\epsilon^2\frac{\partial}{\partial t}\frac{\partial}{\partial\tau}+\epsilon^4\frac{\partial^2}{\partial\tau^2}
$$

Substituting (2.28) into Eq. (2.2) and separating different orders, we get

$$
\begin{aligned}
&\left\{\left[\psi_0+(x\psi_{0x})_x+x\psi_{0yy}\right]e^{-it}+*\right\}+\left\{\left[\phi_0+(x\phi_{0x})_x\right]e^{-it}+*\right\}\\
&\quad+\epsilon\left\{\left[4\phi_1+(x\phi_{1x})_x\right]e^{-i2t}+*\right\}\\
&\quad+\epsilon\left\{\left[4\psi_{12}+(x\psi_{12x})_x+x\psi_{12yy}\right]e^{-i2t}+*\right\}\\
&\quad+\epsilon\left\{\left[(x\psi_{10x})_x+x\psi_{10yy}\right]+*\right\}\\
&\quad+\epsilon^2\left\{\left[\psi_2+(x\psi_{2x})_x+x\psi_{2yy}\right]e^{-it}+*\right\}\\
= &\quad \epsilon\left\{\left[(\psi_0,\psi_0)+(\phi_0,\phi_0)\right]e^{-i2t}+*\right\}\\
&\quad+\epsilon\left\{(\psi_0,\phi_0)e^{-i2t}+*\right\}+\epsilon\left\{(\psi_0,\phi_0^*)+*\right\}\\
&\quad+\epsilon^2\left\{\left[(\phi_1,\psi_0^*)+(\psi_{12},\phi_0^*)+(\psi_{10},\phi_0)+(\psi_{10}^*,\phi_0)\right]e^{-it}+*\right\}\\
&\quad+\epsilon^2\left\{\left[(\psi_0^*,\psi_0,\psi_0)+(\psi_0,\phi_0,\phi_0^*)+(\psi_0^*,\phi_0,\phi_0)\right]e^{-it}+*\right\}\\
&\quad+\epsilon^2\left\{-2i\frac{\partial\psi_0}{\partial\tau}e^{-it}+*\right\}+\dots
\end{aligned}
\tag{2.29}
$$

2.4 The leading-order solution

For convenience we repeat the leading order solution here. The governing equations are

$$
\psi_0+(x\psi_{0x})_x+x\psi_{0yy}=0
$$

$$
\phi_0+(x\phi_{0x})_x=0
$$

The homogeneous solutions to the first is an edge wave,

$$
\psi_0=-iB(\tau)e^{-x}\cos y \tag{2.30}
$$

and to the second is the incident /reflected wave

$$\phi_0 = -ie^{i\varphi} J_0(2\sqrt{x}) \tag{2.31}$$

Note that $B(\tau)$ is the slowly varying, dimensionless, complex amplitude of the edge wave at the shore. The physical amplitude of edge wave is

$$B' = 2|A'|B. \tag{2.32}$$

For later use note that the function $F = e^{-x}$ which describes the x dependence of the edge wave satisfies

$$F + \left[(xF_x)_x - xF\right] = 0, \tag{2.33}$$

and the boundary conditions

$$xF_x = 0, \quad x = 0; \quad \text{and} \quad F \to 0, \quad x \sim \infty. \tag{2.34}$$

2.5 The second-order solution

At O(ϵ), there are two harmonics, but three components : $\phi_1(x)e^{-i2t}$, $\psi_{12}(x, y, \tau)e^{-i2t}$ and $\psi_{10}(x, y, \tau)$. They are solved separately.

2.5.1 ϕ_1 — Radiated second-harmonic

From previous discussion we know that both (ψ_0, ψ_0) and (ϕ_0, ϕ_0) contribute to the excitation force for this harmonic. From (2.29), we have

$$4\phi_1 + (x\phi_{1x})_x = (\psi_0, \psi_0) + (\phi_0, \phi_0) \tag{2.35}$$

The details of the two quadratic forcing terms are given in (2.17) and (2.18). Let us introduce the abbreviation

$$\begin{aligned} g(x) &= 2iB^2 g_e + ie^{i2\varphi} g_i \equiv 2iB^2 e^{-2x} \\ &+ ie^{i2\varphi} \left\{ 2\left(\frac{dJ_0(2\sqrt{x})}{dx}\right)^2 + J_0(2\sqrt{x})\frac{d^2 J_0(2\sqrt{x})}{dx^2} \right\} \end{aligned} \tag{2.36}$$

where

$$g_e \equiv e^{-2x} \tag{2.37}$$

represents the self-interaction of edge wave and

$$g_i \equiv \left\{ 2\left(\frac{dJ_0(2\sqrt{x})}{dx}\right)^2 + J_0(2\sqrt{x})\frac{d^2J_0(2\sqrt{x})}{dx^2} \right\} \tag{2.38}$$

the self-interaction of incident/reflected wave. With these we can rewrite the inhomogeneous Eq. (2.35) as

$$\phi_{1xx} + \frac{1}{x}\phi_{1x} + \frac{4}{x}\phi_1 = \frac{g(x)}{x} \tag{2.39}$$

We shall solve the inhomogeneous equation by method of variation of parameters. To ensure correctness, we compare our solution with others in Appendix A.

By the method of variation of parameters, the general solution of this inhomogeneous equation takes the form

$$\phi_1 = C_1 J_0(4\sqrt{x}) + C_2 Y_0(4\sqrt{x}) + u_1(x) J_0(4\sqrt{x}) + u_2(x) Y_0(4\sqrt{x}) \tag{2.40}$$

where

$$u_1(x) = -\int_0^x \frac{Y_0(4\sqrt{\xi})g(\xi)}{\xi W(J_0, Y_0)(\xi)} d\xi = -\pi \int_0^x Y_0(4\sqrt{\xi})g(\xi)d\xi \tag{2.41}$$

$$u_2(x) = \int_0^x \frac{J_0(4\sqrt{\xi})g(\xi)}{\xi W(J_0, Y_0)(\xi)} d\xi = \pi \int_0^x J_0(4\sqrt{\xi})g(\xi)d\xi \tag{2.42}$$

where the Wronskian W is

$$W(J_0, Y_0)(x) = J_0\frac{dY_0}{dx} - Y_0\frac{dJ_0}{dx} = (J_0Y_0' - Y_0J_0')\frac{d(4\sqrt{x})}{dx} = \frac{2}{\pi 4\sqrt{x}}\frac{2}{\sqrt{x}} = \frac{1}{\pi x}$$

The constant coefficients C_1, C_2 are to be determined by boundary conditions. Use has been made of the properties

$$J_0' = -J_1,\ Y_0' = -Y_1, \quad J_1(z)Y_0(z) - J_0(z)Y_1(z) = \frac{2}{\pi z}$$

Here primes " $'$ " denote derivatives with respect to the argument z, which is equal to $4\sqrt{x}$.

At the shoreline $x = 0$, boundedness of the solution (2.40) requires that $C_2 = 0$. For detailed confirmation please refer to Appendix B.

At large x, we shall require that ϕ_1 behaves as an outgoing wave. To impose this condition, we need the asymptotic behavior of both the forcing $g(x)$ and the solution. Using the facts that

$$J_0(z) \sim \sqrt{\frac{2}{\pi z}} \cos\left(z - \frac{\pi}{4}\right); \quad Y_0(z) \sim \sqrt{\frac{2}{\pi z}} \sin\left(z - \frac{\pi}{4}\right)$$

and

$$\frac{dJ_0(2\sqrt{x})}{dx} \sim x^{-3/4} \sin\left(2\sqrt{x} - \frac{\pi}{4}\right); \quad \frac{d^2 J_0(2\sqrt{x})}{dx^2} \sim x^{-5/4} \cos\left(2\sqrt{x} - \frac{\pi}{4}\right)$$

we find

$$g(x) \sim 2iB^2 e^{-2x} + x^{-3/2} \{\sin(\cdot)\sin(\cdot), \cos(\cdot)\cos(\cdot)\} \tag{2.43}$$

The sinusoidal factors inside the curly brackets {} oscillate fast at large x and do not affect the magnitude. When integrated, these fast oscillatory terms make the integral converge fast due to cancelations. Even without accounting for the oscillatory factor,

$$Y_0(4\sqrt{\xi})g(\xi) \sim J_0(4\sqrt{\xi})g(\xi) \sim x^{-7/4}$$

The integral $u_1(x)$ and $u_2(x)$ diminish like $x^{-3/4}$ at infinity. Therefore, $u_1(x)$ and $u_2(x)$ converge to constants as $x \to \infty$. Finally, the solution $\phi_1 \sim x^{-1/4}$ like $J_0(4\sqrt{x})$ and $Y_0(4\sqrt{x})$ at $x = \infty$.

By comparison we can see that at large x, the forcing function $g(x)$ diminishes faster than the solution $\phi_1(x)$ ($x^{-3/2}$ versus $x^{-1/4}$), i.e. relative to the solution $\phi_1(x)$, the forcing $g(x)$ is a local disturbance. Therefore, we impose the radiation condition that $\phi_1(x)$ should appear as outgoing wave at infinity. It is easy to see that

$$\phi_1 \sim -iu_2(\infty)H_0^{(1)}(4\sqrt{x}) \sim -iu_2(\infty)\sqrt{\frac{2}{4\pi\sqrt{x}}}e^{i\left(4\sqrt{x}-\frac{\pi}{4}\right)} \quad as \quad x \to \infty$$

representing the propagating wave if we let

$$C_1 = -u_1(\infty) - iu_2(\infty).$$

We recall from (2.36) that $g(x) = 2iB^2 g_e + ie^{i2\varphi} g_i$, where g_e and g_i are defined in (2.37) and (2.38). Let us denote

$$u_1(x) = 2iB^2 u_1^e(x) + ie^{i2\varphi}u_1^i(x), \quad u_2(x) = 2iB^2 u_2^e(x) + ie^{i2\varphi}u_2^i(x) \tag{2.44}$$

The coefficients have contributions from the edge wave through

$$\begin{aligned} u_1^e(x) &= -\int_0^x \frac{Y_0(4\sqrt{\xi})g_e(\xi)}{\xi W(J_0,Y_0)(\xi)}d\xi = -\pi\int_0^x Y_0(4\sqrt{\xi})g_e(\xi)d\xi \\ &= -\pi\int_0^x Y_0(4\sqrt{\xi})e^{-2\xi}d\xi \end{aligned} \tag{2.45}$$

$$\begin{aligned} u_2^e(x) &= \int_0^x \frac{J_0(4\sqrt{\xi})g_e(\xi)}{\xi W(J_0,Y_0)(\xi)}d\xi = \pi\int_0^x J_0(4\sqrt{\xi})g_e(\xi)d\xi \\ &= \pi\int_0^x J_0(4\sqrt{\xi})e^{-2\xi}d\xi \end{aligned} \tag{2.46}$$

and from the incident and reflected waves through

$$\begin{aligned} u_1^i(x) &= -\int_0^x \frac{Y_0(4\sqrt{\xi})g_i(\xi)}{\xi W(J_0,Y_0)(\xi)}d\xi = -\pi\int_0^x Y_0(4\sqrt{\xi})g_i(\xi)d\xi \\ &= -\pi\int_0^x Y_0(4\sqrt{\xi})\left\{2\left(\frac{dJ_0(2\sqrt{\xi})}{d\xi}\right)^2 + J_0(2\sqrt{\xi})\frac{d^2J_0(2\sqrt{\xi})}{d\xi^2}\right\}d\xi \end{aligned} \tag{2.47}$$

$$\begin{aligned} u_2^i(x) &= \int_0^x \frac{J_0(4\sqrt{\xi})g_i(\xi)}{\xi W(J_0,Y_0)(\xi)}d\xi = \pi\int_0^x J_0(4\sqrt{\xi})g_i(\xi)d\xi \\ &= \pi\int_0^x J_0(4\sqrt{\xi})\left\{2\left(\frac{dJ_0(2\sqrt{\xi})}{d\xi}\right)^2 + J_0(2\sqrt{\xi})\frac{d^2J_0(2\sqrt{\xi})}{d\xi^2}\right\}d\xi \end{aligned} \tag{2.48}$$

By numerical integration, the variations of $u_1^i(x)$ and $u_2^i(x)$ are shown in Figure 2-1. Note that $u_2^i(\infty) = 0$.

In Figure 2-2 we show the calculated variations of $u_1^e(x)$ and $u_2^e(x)$. Note that $u_2^e(\infty)$ is finite, implying finite radiation to infinity.

In summary, the final solution for the second-harmonic forced by self-interactions is

$$\phi_1 = 2iB^2\phi_1^e + ie^{i2\varphi}\phi_1^i \tag{2.49}$$

with

$$\phi_1^e = \left[-u_1^e(\infty) - iu_2^e(\infty)\right]J_0(4\sqrt{x}) + u_1^e(x)J_0(4\sqrt{x}) + u_2^e(x)Y_0(4\sqrt{x}) \tag{2.50}$$

and

$$\begin{aligned} \phi_1^i &= \left[-u_1^i(\infty) - iu_2^i(\infty)\right]J_0(4\sqrt{x}) + u_1^i(x)J_0(4\sqrt{x}) + u_2^i(x)Y_0(4\sqrt{x}) \\ &= J_0(4\sqrt{x}) + u_1^i(x)J_0(4\sqrt{x}) + u_2^i(x)Y_0(4\sqrt{x}) \end{aligned} \tag{2.51}$$

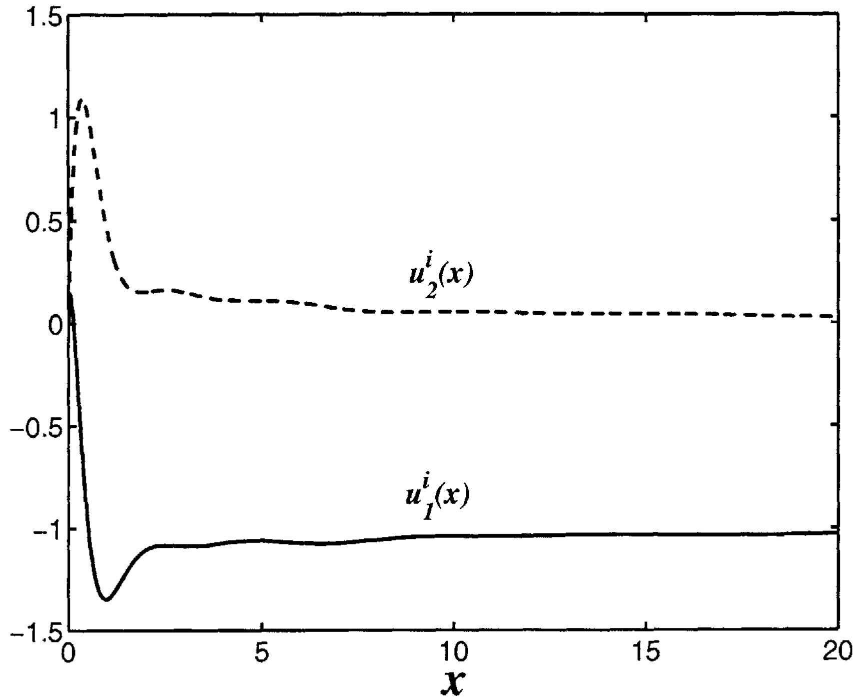

Figure 2-1: Curves for $u_1^i(x)$ and $u_2^i(x)$.

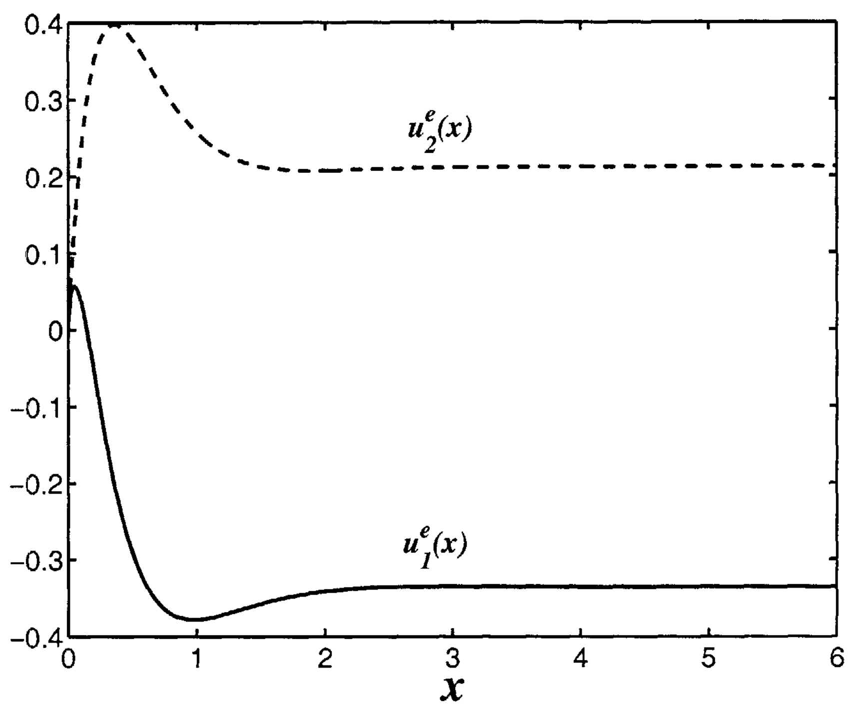

Figure 2-2: Curves for $u_1^e(x)$ and $u_2^e(x)$. To be filled in.

Use has been made of $u_1^i(\infty) = -1, \quad u_2^i(\infty) = 0$ as discussed in Appendix A. Note that ϕ_1^e is complex, whereas ϕ_1^i is real.

– – – – – – – –

For later use in (2.93), we record that

$$\left.\frac{d\phi_1(x)}{dx}\right|_{x=0} = C_1(-4) + g(0) = 4\left(u_1(\infty) + iu_2(\infty)\right) + g(0) \tag{2.52}$$

and

$$\phi_1(0) = C_1 = -u_1(\infty) - iu_2(\infty) \tag{2.53}$$

2.5.2 ψ_{12} — Forced second-harmonic trapped wave

From (2.29), this harmonic is governed by

$$4\psi_{12} + (x\psi_{12x})_x + x\psi_{12yy} = (\psi_0, \phi_0) \tag{2.54}$$

The details of the quadratic forcing term (ψ_0, ϕ_0) are given in (2.19), which suggests a solution of the form

$$\psi_{12} = -ie^{i\varphi} B f_{11}(x) \cos y \tag{2.55}$$

where $f_{11}(x)$ satisfies

$$x f_{11xx} + f_{11x} - [x - 4] f_{11} = g_{11}(x) \tag{2.56}$$

with the abbreviation

$$g_{11}(x) = e^{-x}\left\{4\frac{dJ_0(2\sqrt{x})}{dx} - \frac{d^2 J_0(2\sqrt{x})}{dx^2}\right\} \tag{2.57}$$

Let us first study the differential operator. By the change of variables

$$\xi = 2x, \quad f_{11} = e^{-\frac{\xi}{2}} f(\xi)$$

(2.56) reduces to the confluent hypergeometric equation,

$$\xi f'' + (1-\xi) f' - \frac{1-4}{2} f = \frac{1}{2} g_{11}\left(\frac{\xi}{2}\right) e^{\frac{\xi}{2}}$$

The left-hand-side possesses non-trivial eigen-solutions only if the third coefficient is an integer n. Since

$$\frac{3}{2} \neq n, \ n = 0, 1, 2... ,$$

the inhomogeneous equation can always be solved uniquely provided that the boundary conditions are well posed. For this, let us first examine the property of this equation.

A solution of an inhomogeneous ODE consists of two parts: the homogeneous solution and the particular one. In our problem, the forcing $g_{11}(x)$ decays exponentially as x increases. As $x \to \infty$, Eq. (2.56) becomes a homogeneous modified Bessel equation

$$x f_{11xx} + f_{11x} - x f_{11} = 0$$

which has the general solution in terms of zeroth-order modified Bessel function of the first and second kind

$$f_{11} = C_1 I_0(x) + C_2 K_0(x)$$

For boundedness at $x = 0$, I_0 is excluded. Therefore, the solution of our problem behaves like K_0, which vanishes as e^{-x} at ∞. Because of this property of ψ_{11} is localized and trapped.

Now we can impose the boundary condition at a large distance

$$f_{11} \to 0 \quad \text{at} \quad x \to \infty \tag{2.58}$$

and the no flux condition on the shore:

$$x f_{11x} = 0 \quad \text{as} \quad x \to 0 \tag{2.59}$$

This problem can be solve analytically as well as numerically by the standard Finite Element Method (See Appendix E.).

2.5.3 Series solution

In their study of topographic effects on nonlinear edge waves, Rockliff and Smith [27] solved the inhomogeneous equation

$$x f_{11xx} + f_{11x} - (x - 4) f_{11} = e^{-x} \left\{ 4 \frac{dJ_0(2\sqrt{x})}{dx} - \frac{d^2 J_0(2\sqrt{x})}{dx^2} \right\} \tag{2.60}$$

by Fourier-Laguerre series expansion:

$$f_{11} = e^{x} \sum_{n=0}^{\infty} C_n L_n(2x)$$

with

$$C_n = \left\{ 1 - e^{-1/2} \sum_{p=0}^{n} \left[\frac{1}{2^p p!} + \frac{1}{n!} \left(\frac{1}{2} \right)^e e^{-1/2} \frac{1}{3-2n} \right] \right\} \tag{2.61}$$

Refer to Case 5 in [26] for their inhomogeneous forcing and (5.4a, b) in [27] for the solution. For convenience of comparison, we isolated this problem from others and changed it to the normalized form. By repeating their analysis we found a different solution. For later comparison the first 10 coefficients obtained from the formula above are listed in Table 2.1.

Table 2.1: Coefficients C_n from (2.61) by Rockliff and Smith.

C_0	C_1	C_2	C_3	C_4
0.37483560608	-0.02159839480	0.09823948189	0.01417411203	0.00250133241
C_5	C_6	C_7	C_8	C_9
0.00041345924	0.00006138948	0.00000812875	0.00000096328	0.00000010287

A correct calculation is given below which will be checked by an independent method of finite elements.

Let us first carry out the differentiations on the right of (2.56):

$$\frac{dJ_0(2\sqrt{x})}{dx} = -\frac{J_1(2\sqrt{x})}{\sqrt{x}} = -x^{-1/2} J_1(2\sqrt{x})$$

$$\frac{d^2 J_0(2\sqrt{x})}{dx^2} = \frac{1}{2} x^{-3/2} J_1(2\sqrt{x}) - x^{-1} \left[J_0(2\sqrt{x}) - \frac{1}{2} x^{-1/2} J_1(2\sqrt{x}) \right]$$

Therefore, R.H.S. of Eq. (2.60) becomes

$$\begin{aligned} g_{11}(x) &= e^{-x} \left[-4x^{-1/2} J_1 - \frac{1}{2} x^{-3/2} J_1 + x^{-1} J_0 - \frac{1}{2} x^{-3/2} J_1 \right] \\ &= e^{-x} \left[-4x^{-1/2} J_1 - x^{-3/2} J_1 + x^{-1} J_0 \right] \end{aligned} \tag{2.62}$$

By the change of variables

$$\xi = 2x, \quad f_{11} = e^{-\frac{\xi}{2}} f(\xi)$$

we get

$$\xi f'' + (1-\xi)f' - \frac{1-4}{2}f = \frac{1}{2}g\left(\frac{\xi}{2}\right)e^{\frac{\xi}{2}} \tag{2.63}$$

We now construct the inhomogeneous solution by series of Laguerre polynomials, i.e.

$$f(\xi) = \sum_{n=0}^{\infty} C_n L_n(\xi)$$

where $L_n(\xi)$ is the Laguerre polynomial. Substituting the series into the equation, we get the L.H.S.

$$\begin{aligned}
& \sum_{n=0}^{\infty} C_n \left[\xi L_n'' + (1-\xi)L_n' + \frac{3}{2}L_n\right] \\
= & \sum_{n=0}^{\infty} C_n \left[\xi L_n'' + (1-\xi)L_n' + nL_n\right] + \sum_{n=0}^{\infty} C_n \left(\frac{3}{2} - n\right) L_n
\end{aligned} \tag{2.64}$$

The first summation on the right of above equation is equal to zero and only the second series of Laguerre polynomial remains on the left of (2.63). The R.H.S. is

$$\begin{aligned}
& \frac{1}{2}g\left(\frac{\xi}{2}\right)e^{\frac{\xi}{2}} \\
= & \frac{1}{2}\left[-4x^{-1/2}J_1 - x^{-3/2}J_1 + x^{-1}J_0\right] \\
= & \frac{x^{-1}}{2}\left(\frac{1}{\Gamma(1)} - \frac{1}{\Gamma(2)}\right) + \sum_{k=0}^{\infty}\left[\frac{2(-1)^{k+1}}{k!\Gamma(k+2)} + \frac{(-1)^{k+1}}{2(k+1)!}\left(\frac{1}{\Gamma(k+2)} - \frac{1}{\Gamma(k+3)}\right)\right]x^k \\
= & \sum_{k=0}^{\infty}\left[2 + \frac{1}{2(k+1)}\left(1 - \frac{1}{k+2}\right)\right]\frac{(-1)^{k+1}}{k!\Gamma(k+2)}x^k \\
= & \sum_{k=0}^{\infty}\frac{(-1)^{k+1}(2k+9/2)}{k!(k+2)!}x^k \\
= & \sum_{k=0}^{\infty}\frac{(-1)^{k+1}(2k+9/2)}{2^k k!(k+2)!}\xi^k
\end{aligned}$$

Use has been made of

$$J_n(x) = \sum_{k=0}^{\infty}\frac{(-1)^k (x/2)^{n+2k}}{k!\Gamma(n+k+1)}$$

and

$$J_0(2\sqrt{x}) = \sum_{k=0}^{\infty}\frac{(-1)^k x^k}{k!\Gamma(k+1)}$$

$$J_1(2\sqrt{x}) = \sum_{k=0}^{\infty}\frac{(-1)^k x^{k+1/2}}{k!\Gamma(k+2)}$$

$$\Gamma(n+1) = n!$$

Equating the left and right-hand sides, we get

$$\sum_{n=0}^{\infty} C_n \left(\frac{3}{2} - n\right) L_n = \sum_{k=0}^{\infty} \frac{(-1)^{k+1}(2k+9/2)}{2^k k!(k+2)!} \xi^k$$

Invoking orthogonality :

$$\int_0^{\infty} d\xi \, e^{-\xi} L_n(\xi) L_m(\xi) = \delta_{nm}, \tag{2.65}$$

we find the coefficient

$$C_n \left(\frac{3}{2} - n\right) = \int_0^{\infty} e^{-\xi} L_n(\xi) \left\{ \sum_{k=0}^{\infty} \frac{(-1)^{k+1}(2k+9/2)}{2^k k!(k+2)!} \xi^k \right\} d\xi$$

Replacing L_n by Rodrigue's formula

$$L_n(\xi) = \frac{e^{\xi}}{n!} \frac{d^n}{d\xi^n} \left(\xi^n e^{-\xi}\right)$$

we get

$$C_n \left(\frac{3}{2} - n\right) = \sum_{k=0}^{\infty} \frac{(-1)^{k+1}(2k+9/2)}{2^k k!(k+2)! n!} \int_0^{\infty} \xi^k \frac{d^n}{d\xi^n} \left(\xi^n e^{-\xi}\right) d\xi \tag{2.66}$$

For $k < n$, the right-hand-side integral becomes zero (Refer to Appendix F for detail.). Otherwise, we can evaluate it by partial integration and get

$$C_n \left(\frac{3}{2} - n\right) = \sum_{k=n}^{\infty} \frac{(-1)^{k+1}(2k+9/2)k!(-1)^n k!}{2^k k!(k+2)! n!(k-n)!} \tag{2.67}$$

Evaluation of the integral can be found in Appendix F. Therefore,

$$C_n = \sum_{k=n}^{\infty} \frac{(-1)^{k+n+1}(2k+9/2)k!}{(3-2n)2^{k-1}(k+2)! n!(k-n)!} \tag{2.68}$$

By truncating the series at $k = 15,\ 20,\ 30$, the first 10 coefficients are computed as listed in Table 2.2. It is obvious that after truncation at $k = 15$ the computed C_n do not change anymore. The results listed here are different from those in Table 2.1 by Rockliff & Smith.

For numerical computation we only need to compute the first $N + 1$ Laguerre polynomials and rewrite the the solution as

$$f_{11}(x) = e^{-x} \sum_{n=0}^{N} a_n x^n \tag{2.69}$$

Table 2.2: Coefficients C_n for the Fourier-Laguerre series expansion of $f_{11}(x)$ by analytical formula (2.68).

k	C_0	C_1	C_2	C_3	C_4
15	-1.1912924537	-0.7869386806	0.1228573090	0.0049207918	0.0002875715
20	-1.1912924537	-0.7869386806	0.1228573090	0.0049207918	0.0002875715
30	-1.1912924537	-0.7869386806	0.1228573090	0.0049207918	0.0002875715
k	C_5	C_6	C_7	C_8	C_9
15	1.67989×10^{-5}	9.20254×10^{-7}	4.6548×10^{-8}	2.169×10^{-9}	9.3×10^{-11}
20	1.67989×10^{-5}	9.20254×10^{-7}	4.6548×10^{-8}	2.169×10^{-9}	9.3×10^{-11}
30	1.67989×10^{-5}	9.20254×10^{-7}	4.6548×10^{-8}	2.169×10^{-9}	9.3×10^{-11}

Table 2.3: Coefficients a_n for the final solution of f_{11}.

N	a_0	a_1	a_2	a_3	a_4
4	-1.8501654620	1.0506228021	0.2786902271	-0.0080947705	0.0001917143
9	-1.8501476940	1.0504430821	0.2790558959	-0.0083456405	0.0002581084
N	a_5	a_6	a_7	a_8	a_9
9	-6.2483×10^{-6}	1.16860×10^{-7}	-1.708×10^{-9}	1.9×10^{-11}	-1.3×10^{-13}

The coefficients a_n for $N = 4$ and $N = 9$ are listed in Table 2.3, suggesting that five terms are sufficient.

The computed solution $f_{11}(x)$ by different N is plotted in Figure 2-3 and the numerical values are listed in Table 2.4 as well. The analytical solution will be confirmed by a numerical solution later. For later comparison we use only the first 5 Laguerre polynomials.

Table 2.4: Computed $f_{11}(x)$ using different truncation number N. Error is defined by $100 \times \frac{f_{11}(N=9)-f_{11}(N=4)}{f_{11}(N=9)}$.

x	$f_{11}(x), N=4$	$f_{11}(x), N=9$	Error (%)
0	-1.850165462	-1.850147694	-0.000960354
0.5	-0.761912514	-0.761917413	0.000643013
1	-0.194518274	-0.194513452	-0.002478997
1.5	0.072845851	0.072849027	0.004358618
2	0.176497552	0.176495342	-0.001252441
2.5	0.196939438	0.196934915	-0.002296632
3	0.179576232	0.17957311	-0.001738616
3.5	0.148651919	0.148651856	-0.000042421
4	0.116164796	0.11616744	0.002276656
4.5	0.087339966	0.087343951	0.00456297
5	0.06386347	0.063867325	0.006035813
5.5	0.045719948	0.045722606	0.00581237
6	0.032190094	0.032191037	0.002927422
6.5	0.022360261	0.022359445	-0.003650993
7	0.015359571	0.015357266	-0.015009274
7.5	0.010451882	0.010448509	-0.032278513
8	0.00705536	0.007051367	-0.056626681
8.5	0.004729634	0.004725416	-0.089252263
9	0.003151405	0.00314727	-0.131379004
9.5	0.002088652	0.00208481	-0.184251502
10	0.001377772	0.001374349	-0.249131465
10.5	0.000905028	0.000902076	-0.327294501
11	0.000592258	0.000589781	-0.420027319
11.5	0.000386268	0.000384237	-0.52862529
12	0.000251153	0.00024952	-0.654390276

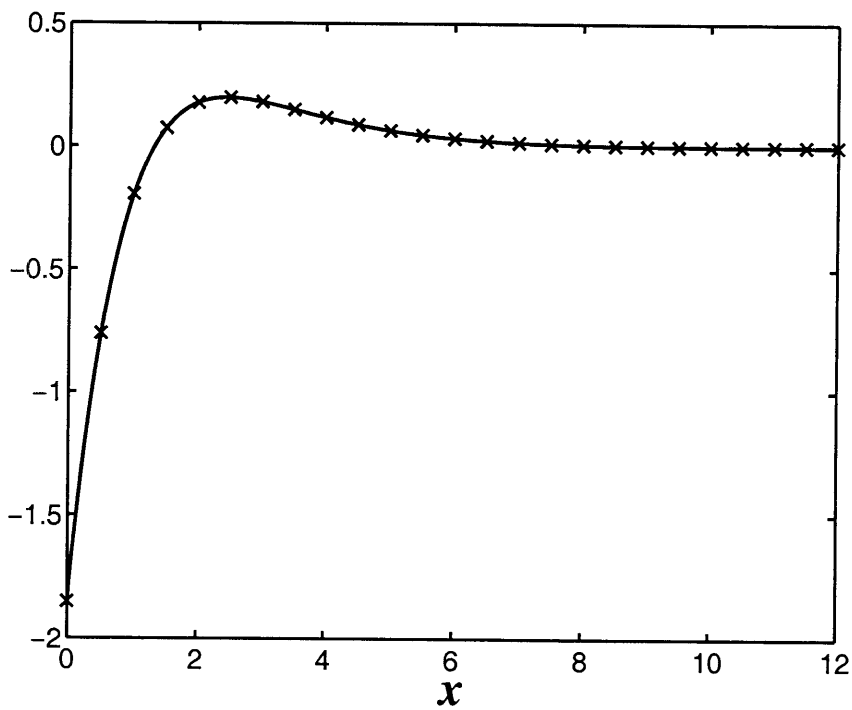

Figure 2-3: $f_{11}(x)$ reconstructed using first $5(N = 4$, solid line) and $10(N = 9$, crosses) Laguerre polynomials.

2.5.4 ψ_{10} — zeroth harmonic and steady circulation

Collecting the coefficient of zeroth harmonic in (2.29) we get

$$(x\psi_{10x})_x + x\psi_{10yy} = (\psi_0, \phi_0^*) \tag{2.70}$$

In (2.21) the details of the quadratic nonlinear forcing (ψ_0, ϕ_0^*) are given. We propose a solution of the following form

$$\psi_{10} = -ie^{-i\varphi} B f_{12}(x) \cos y \tag{2.71}$$

where $f_{12}(x)$ satisfies

$$x f_{12xx} + f_{12x} - x f_{12} = g_{12}(x), \tag{2.72}$$

with the abbreviation

$$g_{12}(x) \equiv e^{-x} \left[\frac{d^2 J_0(2\sqrt{x})}{dx^2} \right].$$

subject to the boundary conditions

$$x f_{12x} = 0 \quad \text{as} \quad x \to 0$$

$$f_{12x} = 0 \quad \text{as} \quad x \to \infty$$

To solve this boundary value problem, the standard Finite Element Method can be applied as described in Appendix E. Again, an analytical solution can be constructed by a Fourier-Laguerre series.

Recalling the recurrence relation of Bessel function, we have

$$\frac{dJ_0(2\sqrt{x})}{dx} = -\frac{J_1(2\sqrt{x})}{\sqrt{x}} = -x^{-1/2} J_1(2\sqrt{x})$$

$$\frac{d^2 J_0(2\sqrt{x})}{dx^2} = \frac{1}{2} x^{-3/2} J_1(2\sqrt{x}) - x^{-1} \left[J_0(2\sqrt{x}) - \frac{1}{2} x^{-1/2} J_1(2\sqrt{x}) \right].$$

the R.H.S. of Eq. (2.72) can be written as

$$g(x) = e^{-x} \left[\frac{1}{2} x^{-3/2} J_1 - x^{-1} J_0 + \frac{1}{2} x^{-3/2} J_1 \right] = e^{-x} \left[x^{-3/2} J_1 - x^{-1} J_0 \right]$$

By the change of variables

$$\xi = 2x, \quad f_{12} = e^{-\frac{\xi}{2}} f(\xi)$$

we get the Laguerre differential equation

$$\xi f'' + (1-\xi)f' - \frac{1}{2}f = \frac{1}{2}g\left(\frac{\xi}{2}\right)e^{\frac{\xi}{2}}$$

Note again the left-hand side does not possess eigen solutions since

$$-\frac{1}{2} \neq n \quad n = 0, 1, 2...$$

By assuming a series of Laguerre polynomials as the inhomogeneous solution, i.e.

$$f(\xi) = \sum_{n=0}^{\infty} C_n L_n(\xi)$$

we get

$$\begin{aligned} & \sum_{n=0}^{\infty} C_n \left[\xi L_n'' + (1-\xi)L_n' - \frac{1}{2}L_n\right] \\ = & \sum_{n=0}^{\infty} C_n \left[\xi L_n'' + (1-\xi)L_n' + nL_n\right] + \sum_{n=0}^{\infty} C_n \left(-\frac{1}{2} - n\right) L_n \end{aligned} \tag{2.73}$$

Again the first summation is equal to zero, leaving only the second series of Laguerre polynomial on the right. The R.H.S. is

$$\begin{aligned} \frac{1}{2}g\left(\frac{\xi}{2}\right)e^{\frac{\xi}{2}} &= \frac{1}{2}\left[x^{-3/2}J_1 - x^{-1}J_0\right] \\ &= \sum_{k=0}^{\infty} \frac{1}{2}\left[\frac{(-1)^k}{k!\Gamma(k+2)} - \frac{(-1)^k}{k!\Gamma(k+1)}\right] x^{k-1} \\ &= \sum_{k=1}^{\infty} \left[\frac{1}{\Gamma(k+2)} - \frac{1}{\Gamma(k+1)}\right] \frac{(-1)^k}{2k!} x^{k-1} \\ &= \sum_{k=1}^{\infty} \frac{(-1)^{k-1}k}{2(k+1)!k!} x^{k-1} \\ &= \sum_{k=1}^{\infty} \frac{(-1)^{k-1}k}{2^k(k+1)!k!} \xi^{k-1} \end{aligned}$$

Use has been made of

$$J_n(x) = \sum_{k=0}^{\infty} \frac{(-1)^k (x/2)^{n+2k}}{k!\Gamma(n+k+1)}$$

and

$$J_0(2\sqrt{x}) = \sum_{k=0}^{\infty} \frac{(-1)^k x^k}{k!\Gamma(k+1)}$$

$$J_1(2\sqrt{x}) = \sum_{k=0}^{\infty} \frac{(-1)^k x^{k+1/2}}{k!\Gamma(k+2)}$$

$$\Gamma(n+1) = n!$$

In order for the coefficients C_n to satisfy

$$\sum_{n=0}^{\infty} C_n \left(-\frac{1}{2} - n\right) L_n = \sum_{k=1}^{\infty} \frac{(-1)^{k-1}k}{2^k(k+1)!k!} \xi^{k-1}$$

we require

$$C_n \left(-\frac{1}{2} - n\right) = \int_0^{\infty} e^{-\xi} L_n(\xi) \left\{ \sum_{k=1}^{\infty} \frac{(-1)^{k-1}k}{2^k(k+1)!k!} \xi^{k-1} \right\} d\xi$$

by orthogonality of Laguerre polynomials. Therefore,

$$\begin{aligned} C_n &= -\frac{2}{1+2n} \sum_{k=0}^{\infty} \frac{(-1)^k(k+1)}{2^{k+1}(k+1)!(k+2)!} \int_0^{\infty} e^{-\xi}\xi^k L_n(\xi) d\xi \\ &= -\frac{2}{1+2n} \sum_{k=0}^{\infty} \frac{(-1)^k(k+1)}{2^{k+1}(k+1)!(k+2)!n!} \int_0^{\infty} \xi^k \frac{d^n}{d\xi^n} \left(\xi^n e^{-\xi}\right) d\xi \\ &= \frac{1}{1+2n} \sum_{k=n}^{\infty} \frac{(-1)^{k+n+1}}{2^k(k+1)(k+2)n!(k-n)!} \end{aligned} \tag{2.74}$$

Listed in Table 2.5 are the first 10 coefficients of the series computed by above formula with truncation of $k = 20$. After that, the computed C_n shows no difference anymore.

Table 2.5: Coefficients C_n for the Fourier-Laguerre series expansion of $f_{12}(x)$.

C_0	C_1	C_2	C_3	C_4
-0.4261226389	-0.0217688657	-0.0015511771	-0.0001070564	-0.0000067703
C_5	C_6	C_7	C_8	C_9
-3.884×10^{-7}	-2.025×10^{-8}	-9.6388×10^{-10}	-4.213×10^{-11}	-1.70×10^{-12}

Similar to f_{11}, we can use the first $N+1$ Laguerre polynomials and rewrite the the solution as

$$f_{12}(x) = e^{-x} \sum_{n=0}^{N} a_n x^n \tag{2.75}$$

The coefficients a_n for $N = 4$ and $N = 9$ are listed in Table 2.6.

Table 2.6: Coefficients a_n for the final solution of f_{12}.

N	a_0	a_1	a_2	a_3	a_4
4	-0.4495565083	0.0504389405	-0.0038259361	0.0001788501	-4.5135×10^{-6}
9	-0.4495569180	0.0504430820	-0.0038343552	0.0001846175	-6.0354×10^{-6}
N	a_5	a_6	a_7	a_8	a_9
9	1.4207×10^{-7}	-2.51726×10^{-9}	3.459×10^{-11}	-3.6×10^{-13}	0×10^{-14}

The computed solution $f_{12}(x)$ by different N is plotted in Figure 2-4 and the numerical values are listed in Table 2.7 as well. The analytical solution will be confirmed by a numerical solution later. For later comparison we use only the first 5 Laguerre polynomials.

2.5.5 Wave set-up/set-down at equilibrium

In terms of the first-order waves the steady component of the second-order free surface displacement, i.e., the wave set-up and set-down, can be determined by taking the time-average of Bernoulli equation over a period $T = 2\pi$

$$\begin{aligned}
\overline{\zeta} &= -\overline{\left(\frac{\partial \Phi}{\partial t} + \frac{\epsilon}{2}|\nabla\Phi|^2\right)} \\
&= -\frac{\epsilon}{2}\overline{\left\{\left[(\psi_{0x}e^{-it} + *) + (\phi_{0x}e^{-it} + *)\right]^2 + (\psi_{0y}e^{-it} + *)^2\right\}} \\
&= -\frac{\epsilon}{2}2\left(\psi_{0x}\psi_{0x}^* + \psi_{0y}\psi_{0y}^* + \phi_{0x}\phi_{0x}^* + \psi_{0x}\phi_{0x}^* + \phi_{0x}\psi_{0x}^*\right) \\
&= -\epsilon\left[BB^*e^{-2x}\left(\cos^2 y + \sin^2 y\right) + \left(\frac{dJ_0(2\sqrt{x})}{dx}\right)^2 - (B + B^*)\,e^{-x}\frac{dJ_0(2\sqrt{x})}{dx}\cos y\right] \\
&= -\epsilon\left[BB^*e^{-2x} + \left(\frac{dJ_0(2\sqrt{x})}{dx}\right)^2 - (B + B^*)\,e^{-x}\frac{dJ_0(2\sqrt{x})}{dx}\cos y\right] \qquad (2.76)
\end{aligned}$$

Please refer to (2.10) for the normalized free surface boundary condition, (2.28) for the total solution Φ, (2.30) and (2.31) for ψ_0 and ϕ_0. We have replaced B in (2.30) with $Be^{i\varphi}$ due to change of variable in (2.91).

Table 2.7: Computed $f_{12}(x)$ using different truncation number N. Error is defined by $100 \times \frac{f_{12}(N=9)-f_{12}(N=4)}{f_{12}(N=9)}$.

x	$f_{12}(x), N=4$	$f_{12}(x), N=9$	Error (%)
0	-0.449556508	-0.449556918	0.000091132
0.5	-0.257940172	-0.257940059	-0.000043855
1	-0.148170496	-0.148170607	0.000075019
1.5	-0.085219139	-0.085219213	0.000086181
2	-0.049075793	-0.049075742	-0.000103575
2.5	-0.028299052	-0.028298948	-0.000368948
3	-0.016340601	-0.016340529	-0.000442258
3.5	-0.009448672	-0.009448670	-0.000017909
4	-0.005471335	-0.005471396	0.001113502
4.5	-0.003172836	-0.003172928	0.002901020
5	-0.001842659	-0.001842749	0.004839700
5.5	-0.001071759	-0.001071821	0.005749068
6	-0.000624334	-0.000624356	0.003526254
6.5	-0.000364267	-0.000364249	-0.005122848
7	-0.000212875	-0.000212822	-0.024970259
7.5	-0.000124611	-0.000124533	-0.062565908
8	-0.000073071	-0.000072978	-0.126546139
8.5	-0.000042927	-0.000042829	-0.227946019
9	-0.000025267	-0.000025171	-0.380510884
9.5	-0.000014903	-0.000014814	-0.601003198
10	-0.000008810	-0.000008730	-0.909501667
10.5	-0.000005220	-0.000005152	-1.329689118
11	-0.000003101	-0.000003044	-1.889129913
11.5	-0.000001848	-0.000001801	-2.619532843
12	-0.000001105	-0.000001067	-3.557000336

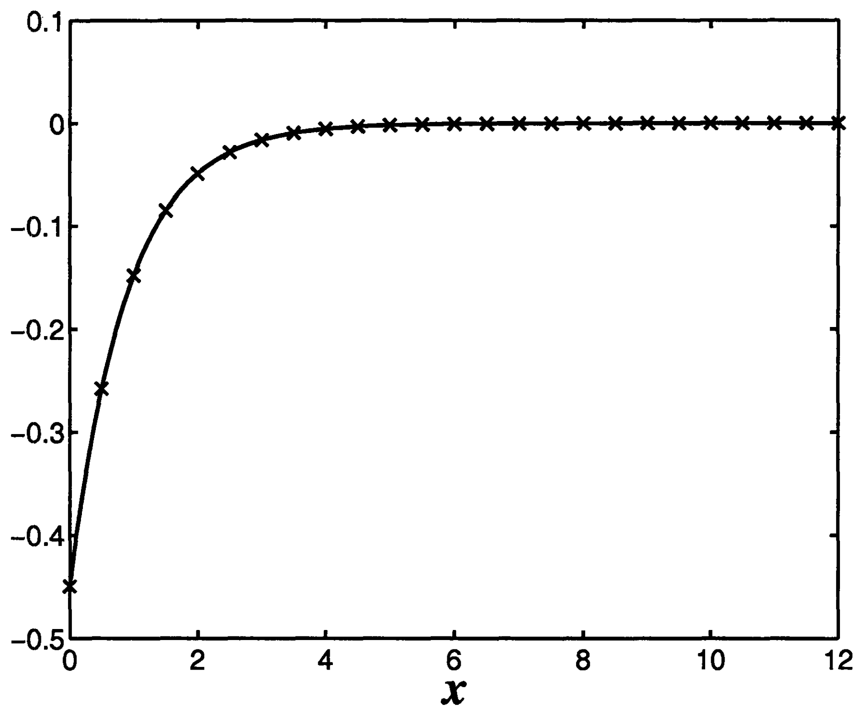

Figure 2-4: $f_{12}(x)$ reconstructed using first $5(N = 4$, solid line) and $10(N = 9$, crosses) Laguerre polynomials.

Physical implications will be discussed later after the edge-wave amplitude B is found.

2.6 The third-order problem

2.6.1 Governing equation and forcing

From (2.29) the governing equation for the first harmonic at $O(\epsilon^2)$ is

$$\psi_2 + (x\psi_{2x})_x + x\psi_{2yy} = -2\frac{\partial B}{\partial \tau}e^{-x}\cos y + \mathcal{E}(x)\cos y \tag{2.77}$$

where $\mathcal{E}(x)$ denotes all the resonance-forcing terms from quadratic interactions of first and second-order solutions, and from cubic interactions of first-order solution, of frequency 1. Noticing that all of these forcing terms are proportional to $\cos y$, we get

$$\begin{aligned}\mathcal{E}(x)\cos y &= (\psi_0^*, \psi_0, \psi_0) + (\psi_0^*, \phi_0, \phi_0) + (\psi_0, \phi_0, \phi_0^*) \\ &+ (\phi_1, \psi_0^*) + (\psi_{12}, \phi_0^*) + (\psi_{10}, \phi_0) + (\psi_{10}^*, \phi_0)\end{aligned} \tag{2.78}$$

The first three terms on the right have been labeled as [C-1], [C-2] and [C-3] respectively. The last four will be labeled as [C-4], [C-5], [C-6] and [C-7] respectively. It is obvious that [C-2] to [C-7] are proportional to $\cos y$ since only one edge wave component is present in each of the forces. For [C-1], refer to (2.25) for the detail.

We now propose the solution to be

$$\psi_2 = H(x)\cos y \tag{2.79}$$

so that

$$H + [(xH_x)_x - xH] = -2\frac{\partial B}{\partial \tau}e^{-x} + \mathcal{E}(x) \tag{2.80}$$

Details of the nonlinear forcing terms involving cubic interaction of the leading-order contributions ([C-1], [C-2] and [C-3]) are given in (2.25), (2.26) and (2.27). We shall now work out the third-order forcing terms due to quadratic interactions of first- and second-order solutions:

[C-4].

$$
\begin{aligned}
(\phi_1, \psi_0^*) &= 2\left[\phi_{1x}\psi_{0x}^*(i) + \psi_{0x}^*\phi_{1x}(-2i)\right] + \psi_0^*(i)\phi_{1xx} \\
&= -2i\phi_{1x}\psi_{0x}^* + i\phi_{1xx}\psi_0^* \\
&= e^{-x}\cos y\left\{-2i\frac{d\phi_1}{dx}iB^*(-1) + i\frac{d^2\phi_1}{dx^2}iB^*\right\} \\
&= -B^*e^{-x}\cos y\left(2\frac{d\phi_1}{dx} + \frac{d^2\phi_1}{dx^2}\right) \\
&= i\hat{h}_{C4}B^2B^*\cos y + ie^{i2\varphi}\hat{g}_{C4}B^*\cos y
\end{aligned} \tag{2.81}
$$

where use has been made of

$$\psi_{0xx}^* + \psi_{0yy}^* = 0.$$

and we have recalled that $\phi_1 = 2iB^2\phi_1^e + ie^{i2\varphi}\phi_1^i$ with ϕ_1^e and ϕ_1^i defined in (2.50) and (2.51). Therefore, $\hat{g}_{C4}$ is real due to real ϕ_1^i, whereas $\hat{h}_{C4}$ is complex due to complex ϕ_1^e.

[C-5].

$$
\begin{aligned}
&(\psi_{12}, \phi_0^*) \\
&= 2\left[\psi_{12x}\phi_{0x}^*(i) - i2\phi_{0x}^*\psi_{12x}\right] - i2\psi_{12}\phi_{0xx}^* + i\phi_0^*\left(\psi_{12xx} + \psi_{12yy}\right) \\
&= -ie^{i\varphi}B(ie^{-i\varphi})\cos y\left[-i2f_{11x}\frac{dJ_0(2\sqrt{x})}{dx} - i2f_{11}\frac{d^2J_0(2\sqrt{x})}{dx^2} + iJ_0(2\sqrt{x})\left(f_{11xx} - f_{11}\right)\right] \\
&= -iB\cos y\left[2f_{11x}\frac{dJ_0(2\sqrt{x})}{dx} + 2f_{11}\frac{d^2J_0(2\sqrt{x})}{dx^2} - J_0(2\sqrt{x})\left(f_{11xx} - f_{11}\right)\right] \\
&= i\hat{f}_{C5}B\cos y
\end{aligned} \tag{2.82}
$$

where f_{11} is given by (2.56) and plotted in Figure E-3

[C-6].

$$
\begin{aligned}
&(\psi_{10}, \phi_0) \\
&= 2\left[\psi_{10x}\phi_{0x}(-i)\right] - i\phi_0\left(\psi_{10xx} + \psi_{10yy}\right) \\
&= -ie^{-i\varphi}B(-ie^{i\varphi})\cos y\left[-i2f_{12x}\frac{dJ_0(2\sqrt{x})}{dx} - iJ_0(2\sqrt{x})\left(f_{12xx} - f_{12}\right)\right] \\
&= iB\cos y\left[2f_{12x}\frac{dJ_0(2\sqrt{x})}{dx} + J_0(2\sqrt{x})\left(f_{12xx} - f_{12}\right)\right] \\
&= i\hat{f}_{C5}B\cos y
\end{aligned} \tag{2.83}
$$

[C-7].

$$
\begin{aligned}
& (\psi_{10}^*, \phi_0) \\
= \;& 2\left[\psi_{10x}^*\phi_{0x}(-i)\right] - i\phi_0\left(\psi_{10xx}^* + \psi_{10yy}^*\right) \\
= \;& ie^{i\varphi}B^*(-ie^{i\varphi})\cos y\left[-i2f_{12x}\frac{dJ_0(2\sqrt{x})}{dx} - iJ_0(2\sqrt{x})\left(f_{12xx} - f_{12}\right)\right] \\
= \;& -ie^{i2\varphi}B^*\cos y\left[2f_{12x}\frac{dJ_0(2\sqrt{x})}{dx} + J_0(2\sqrt{x})\left(f_{12xx} - f_{12}\right)\right] \\
= \;& ie^{i2\varphi}\hat{g}_{C7}B^*\cos y \qquad (2.84)
\end{aligned}
$$

where f_{12} is given by (2.72) and plotted in Figure E-3.

In summary, we group the terms according to B, B^* and B^2B^*, and get

$$
\mathcal{E}(x) = i\hat{f}(x)B + ie^{i2\varphi}\hat{g}(x)B^* + \hat{h}(x)B^2B^* \qquad (2.85)
$$

where $i\hat{f}, ie^{i2\varphi}\hat{g}, \hat{h}$ are the sum of coefficients of B, B^* and $|B|^2B$ respectively. Specifically

- $i\hat{f}(x)$ is collected from [C-3] in (2.27),[C-5] in (2.82) and [C-6] in (2.83), i.e.,

$$
i\hat{f} = i(\hat{f}_{C3} + \hat{f}_{C5} + \hat{f}_{C6}). \qquad (2.86)
$$

- $\hat{g}(x)$ is collected from [C-2] in (2.26), [C-4] in (2.81) and [C-7] in (2.84), i.e.,

$$
ie^{i2\varphi}\hat{g} = ie^{i2\varphi}(\hat{g}_{C2} + \hat{g}_{C4} + \hat{g}_{C7}) \qquad (2.87)
$$

- $\hat{h}(x)$ is collected from [C-1] in (2.25) and [C-4] in (2.81), i.e.

$$
\hat{h}(x) = \hat{h}_{C1}(x) + \hat{h}_{C4}(x). \qquad (2.88)
$$

Obviously, $\hat{f}$ and $\hat{g}$ are real while $\hat{h}$ is complex.

2.6.2 Solvability and evolution equation

Since the homogeneous version of (2.80) has nontrivial solution $F = e^{-x}$, as described in (2.33) and (2.34), H must satisfy a solvability condition which is found by Green's formula

$$\int_0^\infty (H\mathcal{L}F - F\mathcal{L}H)dx = \int_0^\infty \left[H(xF_x)_x - F(xH_x)_x\right] dx$$
$$= \int_0^\infty \left[(xHF_x)_x - (xFH_x)_x\right] dx = 0$$

The last equality follows after integration and applying the boundary conditions. Since $\mathcal{L}F = 0$, we must have

$$\int_0^\infty F\mathcal{L}H dx = 0$$

which gives the solvability condition

$$\int_0^\infty dx e^{-x} \left(-2\frac{\partial B}{\partial \tau} e^{-x} + \mathcal{E}(x)\right) = 0$$

or, the evolution of the edge wave amplitude

$$\boxed{\frac{\partial B}{\partial \tau} = \int_0^\infty dx e^{-x} \mathcal{E}(x) = i\alpha B + i\beta e^{i2\varphi} B^* + \kappa B^2 B^*} \tag{2.89}$$

where

$$[\alpha, \beta, \kappa] = \int_0^\infty e^{-x} [\hat{f}(x), \hat{g}(x), \hat{h}(x)] dx, \tag{2.90}$$

By the change of variable

$$B = \bar{B} e^{i\varphi} \Rightarrow \bar{B} = \frac{B}{e^{i\varphi}} \tag{2.91}$$

the phase of the incident wave φ can be eliminated from the governing equation (2.89):

$$\boxed{\frac{\partial \bar{B}}{\partial \tau} = i\alpha \bar{B} + i\beta \bar{B}^* + \kappa \bar{B}^2 \bar{B}^*} \tag{2.92}$$

This shows that the phase φ is of no consequence dynamically and will be taken to be zero from here on.

2.6.3 The coupling coefficients

We now derive the coefficients α, β and κ explicitly.

[C-1]. From $(\psi_0^*, \psi_0, \psi_0)$ in (2.25):

$$\int_0^\infty dx e^{-x} (-3i) \, e^{-3x} B^2 B^* = -\frac{3i}{4} B^2 B^*$$

[C-2]. From $(\psi_0, \phi_0, \phi_0^*)$ in (2.27), we perform partial integration to get

$$\begin{aligned}
&\int_0^\infty dx e^{-x} (-i) \, e^{-x} \left[2 \left(\frac{dJ_0(2\sqrt{x})}{dx} \right)^2 - 3 \frac{d}{dx} \left(\frac{dJ_0(2\sqrt{x})}{dx} \right)^2 \right] B \\
= \; & -i \int_0^\infty dx e^{-2x} \left[2 \left(\frac{dJ_0(2\sqrt{x})}{dx} \right)^2 - 3 \frac{d}{dx} \left(\frac{dJ_0(2\sqrt{x})}{dx} \right)^2 \right] B \\
= \; & -i \left[3 \left(\frac{dJ_0(2\sqrt{x})}{dx} \right)^2 \Bigg|_{x=0} - 4 \int_0^\infty dx e^{-2x} \left(\frac{dJ_0(2\sqrt{x})}{dx} \right)^2 \right] B \\
= \; & -i \, (3 - 4\alpha_1) \, B
\end{aligned}$$

with

$$\alpha_1 = \int_0^\infty dx e^{-2x} \left(\frac{dJ_0 \, (2\sqrt{x})}{dx} \right)^2$$

[C-3]. From $(\psi_0^*, \phi_0, \phi_0)$ in (2.26):

$$\begin{aligned}
&\int_0^\infty dx e^{-x} \left(-i e^{i2\varphi} \right) e^{-x} \left[\left(\frac{dJ_0(2\sqrt{x})}{dx} \right)^2 - \frac{3}{2} \frac{d}{dx} \left(\frac{dJ_0(2\sqrt{x})}{dx} \right)^2 \right] B^* \\
= \; & -i e^{i2\varphi} \left[\frac{3}{2} - 2\beta_9 \right] B^*
\end{aligned}$$

with

$$\beta_9 = \alpha_1 = \int_0^\infty dx e^{-2x} \left(\frac{dJ_0 \, (2\sqrt{x})}{dx} \right)^2$$

[C-4]. From (ϕ_1, ψ_0^*) in (2.81), we perform partial integration to get :

$$\begin{aligned}
&\int_0^\infty dx e^{-x} (-B^*) \, e^{-x} \left(2 \frac{d\phi_1}{dx} + \frac{d^2\phi_1}{dx^2} \right) \\
= \; & -B^* \int_0^\infty dx e^{-2x} \left(2 \frac{d\phi_1}{dx} + \frac{d^2\phi_1}{dx^2} \right) \\
= \; & -B^* \left(-4\phi_1(0) - \frac{d\phi_1(x)}{dx} \Bigg|_{x=0} + 8 \int_0^\infty dx e^{-2x} \phi_1(x) \right) \\
= \; & -B^* \left(-g(0) + 8 \int_0^\infty dx e^{-2x} \phi_1(x) \right) \\
= \; & g(0) B^* - 8 B^* \int_0^\infty dx e^{-2x} \phi_1(x)
\end{aligned} \tag{2.93}$$

Use has been made of (2.52) and (2.53). We recall that $g(0) = 2iB^2 + \frac{5}{2}ie^{i2\varphi}$ from (B.2) and $\phi_1 = 2iB^2\phi_1^e + ie^{i2\varphi}\phi_1^i$ with ϕ_1^e and ϕ_1^i defined in (2.50) and (2.51). Therefore,

$$g(0)B^* = 2iB^2B^* + \frac{5}{2}ie^{i2\varphi}B^*$$

and

$$\begin{aligned}
&-8B^*\int_0^\infty dxe^{-2x}\phi_1(x) \\
&= -16iB^2B^*\int_0^\infty dxe^{-2x}\phi_1^e - 8ie^{i2\varphi}B^*\int_0^\infty dxe^{-2x}\phi_1^i \\
&= -16iB^2B^*\int_0^\infty dxe^{-2x}\left\{\left[-u_1^e(\infty) - iu_2^e(\infty)\right]J_0(4\sqrt{x})\right. \\
&\quad \left.+u_1^e(x)J_0(4\sqrt{x}) + u_2^e(x)Y_0(4\sqrt{x})\right\} \\
&\quad -8ie^{i2\varphi}B^*\int_0^\infty dxe^{-2x}\left\{\left[-u_1^i(\infty) - iu_2^i(\infty)\right]J_0(4\sqrt{x})\right. \\
&\quad \left.+u_1^i(x)J_0(4\sqrt{x}) + u_2^i(x)Y_0(4\sqrt{x})\right\} \\
&= 16i\int_0^\infty dxe^{-2x}J_0(4\sqrt{x})u_1^e(\infty)B^2B^* + 8ie^{i2\varphi}\int_0^\infty dxe^{-2x}J_0(4\sqrt{x})u_1^i(\infty)B^* \\
&\quad -16i\int_0^\infty dxe^{-2x}J_0(4\sqrt{x})u_1^e(x)B^2B^* - 8ie^{i2\varphi}\int_0^\infty dxe^{-2x}J_0(4\sqrt{x})u_1^i(x)B^* \\
&\quad -16\int_0^\infty dxe^{-2x}J_0(4\sqrt{x})u_2^e(\infty)B^2B^* - 8e^{i2\varphi}\int_0^\infty dxe^{-2x}J_0(4\sqrt{x})u_2^i(\infty)B^* \\
&\quad -16i\int_0^\infty dxe^{-2x}Y_0(4\sqrt{x})u_2^e(x)B^2B^* - 8ie^{i2\varphi}\int_0^\infty dxe^{-2x}Y_0(4\sqrt{x})u_2^i(x)B^*
\end{aligned} \tag{2.94}$$

Therefore, the R.H.S. of (2.93)

$$\begin{aligned}
&g(0)B^* - 8B^*\int_0^\infty dxe^{-2x}\phi_1(x) \\
&= 2iB^2B^* + \frac{5}{2}ie^{i2\varphi}B^* \\
&\quad -16i\pi\kappa_1B^2B^* - 8ie^{i2\varphi}\pi\left(2\beta_1 + \beta_2\right)B^* \\
&\quad +16i\pi\kappa_2B^2B^* + 8ie^{i2\varphi}\pi\left(2\beta_3 + \beta_4\right)B^* \\
&\quad -16\pi\kappa_3B^2B^* - 8e^{i2\varphi}\pi\left(2\beta_5 + \beta_6\right)B^* \\
&\quad -16i\pi\kappa_4B^2B^* - 8ie^{i2\varphi}\pi\left(2\beta_7 + \beta_8\right)B^*
\end{aligned} \tag{2.95}$$

with

$$\kappa_1 = \int_0^\infty dxe^{-2x}J_0(4\sqrt{x})\int_0^\infty d\xi e^{-2\xi}Y_0(4\sqrt{\xi})$$

$$\beta_1 = \int_0^\infty dx e^{-2x} J_0(4\sqrt{x}) \int_0^\infty d\xi Y_0(4\sqrt{\xi}) \left(\frac{dJ_0(2\sqrt{\xi})}{d\xi}\right)^2$$
$$\beta_2 = \int_0^\infty dx e^{-2x} J_0(4\sqrt{x}) \int_0^\infty d\xi Y_0(4\sqrt{\xi}) J_0(2\sqrt{\xi}) \frac{d^2 J_0(2\sqrt{\xi})}{d\xi^2}$$

$$\kappa_2 = \int_0^\infty dx e^{-2x} J_0(4\sqrt{x}) \int_0^x d\xi e^{-2\xi} Y_0(4\sqrt{\xi})$$

$$\beta_3 = \int_0^\infty dx e^{-2x} J_0(4\sqrt{x}) \int_0^x d\xi Y_0(4\sqrt{\xi}) \left(\frac{dJ_0(2\sqrt{\xi})}{d\xi}\right)^2$$
$$\beta_4 = \int_0^\infty dx e^{-2x} J_0(4\sqrt{x}) \int_0^x d\xi Y_0(4\sqrt{\xi}) J_0(2\sqrt{\xi}) \frac{d^2 J_0(2\sqrt{\xi})}{d\xi^2}$$

$$\kappa_3 = \int_0^\infty dx e^{-2x} J_0(4\sqrt{x}) \int_0^\infty d\xi e^{-2\xi} J_0(4\sqrt{\xi})$$

$$\beta_5 = \int_0^\infty dx e^{-2x} J_0(4\sqrt{x}) \int_0^\infty d\xi J_0(4\sqrt{\xi}) \left(\frac{dJ_0(2\sqrt{\xi})}{d\xi}\right)^2$$
$$\beta_6 = \int_0^\infty dx e^{-2x} J_0(4\sqrt{x}) \int_0^\infty d\xi J_0(4\sqrt{\xi}) J_0(2\sqrt{\xi}) \frac{d^2 J_0(2\sqrt{\xi})}{d\xi^2}$$

$$\kappa_4 = \int_0^\infty dx e^{-2x} Y_0(4\sqrt{x}) \int_0^x d\xi e^{-2\xi} J_0(4\sqrt{\xi})$$

$$\beta_7 = \int_0^\infty dx e^{-2x} Y_0(4\sqrt{x}) \int_0^x d\xi J_0(4\sqrt{\xi}) \left(\frac{dJ_0(2\sqrt{\xi})}{d\xi}\right)^2$$
$$\beta_8 = \int_0^\infty dx e^{-2x} Y_0(4\sqrt{x}) \int_0^x d\xi J_0(4\sqrt{\xi}) J_0(2\sqrt{\xi}) \frac{d^2 J_0(2\sqrt{\xi})}{d\xi^2}$$

Use has been made of (2.45) through (2.48). The numerical values of all the integrals are evaluated later.

[C-5]. From (ψ_{12}, ϕ_0^*) in (2.82):

$$\begin{aligned} & -i \int_0^\infty dx e^{-x} \left[2 f_{11x} \frac{dJ_0(2\sqrt{x})}{dx} + 2 f_{11} \frac{d^2 J_0(2\sqrt{x})}{dx^2} - J_0(2\sqrt{x}) \left(f_{11xx} - f_{11}\right) \right] B \\ = & -i\alpha_2 B \end{aligned}$$

with

$$\alpha_2 = f_{11x}(0) + 4 f_{11}(0) + \int_0^\infty dx e^{-x} f_{11} \left[4 \frac{dJ_0(2\sqrt{x})}{dx} - \frac{d^2 J_0(2\sqrt{x})}{dx^2} \right]$$

[C-6]. From (ψ_{10}, ϕ_0) in (2.83):

$$\begin{aligned} & i\int_0^\infty dx e^{-x}\left[2f_{12x}\frac{dJ_0(2\sqrt{x})}{dx} + J_0(2\sqrt{x})\left(f_{12xx} - f_{12}\right)\right]B \\ = \; & i\alpha_3 B \end{aligned}$$

with

$$\alpha_3 = -f_{12x}(0) - \int_0^\infty dx e^{-x} f_{12}\frac{d^2 J_0(2\sqrt{x})}{dx^2}$$

[C-7]. From (ψ_{10}^*, ϕ_0) in (2.84):

$$\begin{aligned} & -ie^{i2\varphi}\int_0^\infty dx e^{-x}\left[2f_{12x}\frac{dJ_0(2\sqrt{x})}{dx} + J_0(2\sqrt{x})\left(f_{12xx} - f_{12}\right)\right]B^* \\ = \; & -ie^{i2\varphi}\beta_{10}B^* \end{aligned}$$

with

$$\beta_{10} = \alpha_3 = -f_{12x}(0) - \int_0^\infty dx e^{-x} f_{12}\frac{d^2 J_0(2\sqrt{x})}{dx^2}$$

All the integrals are evaluated numerically by adaptive Lobatto quadrature within an error of 10^{-6}. To ensure the accuracy of the numerical integration, we did some asymptotic analysis near the two ends 0 and ∞ in Appendix D. The numerical values are list in Table 2.8.

Table 2.8: All the numerically evaluated coefficients for the governing equation.

$\alpha_1 = \beta_9$	α_2	$\alpha_3 = \beta_{10}$	β_1	β_2
0.326330	-2.069132	-0.408492	0.008322	0.004901
β_3	β_4	β_5	β_6	β_7
-0.009742	-0.004169	0.000003	-0.000008	0.016142
β_8	κ_1	κ_2	κ_3	κ_4
0.007550	0.007221	-0.007085	0.004579	0.014306

In summary, we get

$$i\alpha = i(4\alpha_1 - 3 - \alpha_2 + \alpha_3) = -0.0340i; \tag{2.96}$$

$$
\begin{aligned}
i\beta &= \frac{5}{2}i - 8i\pi\left(2\beta_1+\beta_2\right) + 8i\pi\left(2\beta_3+\beta_4\right) - 8\pi\left(2\beta_5+\beta_6\right) - 8i\pi\left(2\beta_7+\beta_8\right) \\
&- i\left[\frac{3}{2} - 2\beta_9\right] - i\beta_{10} = 0.000065 - 0.0760i \qquad (2.97)
\end{aligned}
$$

Referring to (2.94) and (2.95) and comparing with (2.48), we observe that the $Re\{i\beta\} = -8\pi(2\beta_5+\beta_6) = -8\int_0^\infty dx e^{-2x} J_0(4\sqrt{x}) u_2^i(\infty)$, where $u_2^i(\infty)$ is equal to zero as discussed in Appendix A. Here the sum is practically zero (=0.000065) so that $i\beta = -0.0760i$.

$$
\kappa = 2i - 16i\pi\kappa_1 + 16i\pi\kappa_2 - 16\pi\kappa_3 - 16i\pi\kappa_4 - \frac{3i}{4} = -0.2302 - 0.1882i
$$

We point out that the constant $\kappa = -0.2302 - 0.1882i$ is identical to that in the subharmonic resonance [22].

Let us return to physical variables by making following replacements

$$
\bar{B} \to \frac{B'}{A'}, \quad \tau = \epsilon^2 t = \left(\frac{k|A'|}{s}\right)^2 \omega t'
$$

in (2.92). Hence we get the physical evolution equation

$$
\frac{\partial B'}{\partial t'} = i\alpha\left(\frac{k}{s}\right)^2 \omega|A'|^2 B' + i\beta\left(\frac{k}{s}\right)^2 \omega A'^2 B'^* + \kappa\left(\frac{k}{s}\right)^2 \omega|B'|^2 B' \qquad (2.98)
$$

In the following analysis we shall use the simpler equation (2.92) and drop the overbar for brevity. Note that $\bar{B}$ is the ratio of complex amplitude (including the phase) of edge wave to that of incident wave, i.e. phase of $\bar{B}$ is the phase difference of the two waves.

2.7 Initial growth

In the initial stage the edge-wave amplitude is infinitesimally small so that only the linear terms come into play. Eq. (2.92) becomes

$$
\frac{\partial B}{\partial \tau} = i\alpha B + i\beta B^* \qquad (2.99)
$$

It follows that

$$\frac{\partial^2 B}{\partial \tau^2} = i\alpha\frac{\partial B}{\partial \tau} + i\beta\frac{\partial B^*}{\partial \tau} = \left(\beta^2 - \alpha^2\right) B$$

Since from (2.96) and (2.97), $\beta = -0.0760$ and $\alpha = -0.0340$, $|\beta| > |\alpha|$. Therefore, solution to the above equation is

$$B(\tau) = B(0)e^{\pm\sqrt{\beta^2-\alpha^2}\ \tau} = B(0)e^{\pm 0.0679\tau} \tag{2.100}$$

The dimensionless growth rate of unstable disturbances is 0.0679[1]. Note that

$$\tau = \epsilon^2 t = \epsilon\frac{k|A'|}{s}\omega_0 t' = \epsilon\frac{\omega_0^2|A'|}{gs^2}\omega_0 t' = \epsilon\frac{\omega^3|A'|}{gs^2}t'$$

where ω_0 is the edge-wave frequency. This time scale is much longer than that $\frac{\omega^3|A'|}{gs^2}t'$ for subharmonic resonance (See Appendix J.) if $\epsilon \ll 1$. This means that subharmonic resonance has a faster initial growth than the synchronous resonance since $0.2707/8 = 0.0338 \sim O(0.0679)$.

2.8 Effects of detuning

Instead of perfectly synchronous resonance, we now consider the effects of detuning, i.e. the incident wave has a frequency

$$\bar{\omega} = 1 + \epsilon^2\Omega$$

The incident wave becomes

$$\Phi_0 = \phi_0 e^{-i(1+\epsilon^2\Omega)t} + *. \tag{2.101}$$

This amounts to a replacement

$$\phi_0 = -ie^{i\varphi}J_0(2\sqrt{x}) \rightarrow \phi_0 = -ie^{i\varphi}e^{-i\epsilon^2\Omega t}J_0(2\sqrt{x}).$$

i.e., the incident wave amplitude changes from A' to $A'e^{-i\epsilon^2\Omega t}$. This replacement does not affect the coefficient α since it is related to $|A'|^2$ (Refer to Eq. (2.98).). But it does alter the coefficient β to $\beta e^{-2i\Omega\tau}$.

[1]In the classical case of subharmonic resonance the growth rate is 0.2707. See Appendix J.

The evolution equation (2.92) becomes

$$\frac{\partial B}{\partial \tau} = i\alpha B + i\beta e^{-2i\Omega\tau} B^* + \kappa B^2 B^* \tag{2.102}$$

After the change of variable $B = \bar{B}e^{-i\Omega\tau}$, we get

$$\frac{\partial B}{\partial \tau} = \left(\frac{\partial \bar{B}}{\partial \tau} - i\Omega\bar{B}\right) e^{-i\Omega\tau},$$

Hence Eq. (2.102) becomes

$$\frac{\partial \bar{B}}{\partial \tau} = i(\alpha + \Omega)\bar{B} + i\beta\bar{B}^* + \kappa|\bar{B}|^2\bar{B} \tag{2.103}$$

Comparing the above equation with Eq. (2.92) we found that detuning only changes the first coefficient from the constant α to $\alpha + \Omega$, which is a linear function of the bifurcation parameter Ω.

An energy relation can be derived by multiplying (2.103) by $\bar{B}^*$,

$$\bar{B}^*\frac{\partial \bar{B}}{\partial \tau} = i(\alpha + \Omega)\bar{B}\bar{B}^* + i\beta\bar{B}^*\bar{B}^* + \kappa|\bar{B}|^2\bar{B}\bar{B}^* \tag{2.104}$$

The complex conjugate of the preceding equation is

$$\bar{B}\frac{\partial \bar{B}^*}{\partial \tau} = -i(\alpha + \Omega)\bar{B}\bar{B}^* - i\beta\bar{B}\bar{B} + \kappa^*|\bar{B}|^2\bar{B}\bar{B}^* \tag{2.105}$$

The sum of (2.104) and (2.105) is a statement of energy evolution

$$\frac{\partial|\bar{B}|^2}{\partial \tau} = 2\beta Im\{\bar{B}\bar{B}\} + 2Re\{\kappa\}|\bar{B}|^4 \tag{2.106}$$

Since $Re\{\kappa\} = -0.230160$ is negative, the cubic nonlinear term in (2.103) gives rise to damping by radiation of waves.

For simplicity, we drop the overbar from now on.

2.9 Analysis of nonlinear dynamical system

Consider the dynamical system

$$\frac{\partial B}{\partial \tau} = iaB - ibB^* - (\sigma + i\gamma)|B|^2 B \tag{2.107}$$

where

$$a = \Omega + \alpha = \Omega - 0.0340 \tag{2.108}$$

and $b = 0.0760$, $\sigma = 0.2302$, $\gamma = 0.1882$. We make a replacement of $b = -\beta$ so that b is real and positive. Refer to (2.96) and (2.97) for the value of α and β.

Replacing B by its polar form

$$B = \sqrt{I}e^{i\theta}$$

we get from (2.103)

$$\begin{aligned}\frac{\partial B}{\partial \tau} &= \left(\frac{1}{2\sqrt{I}}\dot{I} + i\sqrt{I}\dot{\theta}\right)e^{i\theta} \\ &= ia\sqrt{I}e^{i\theta} - ib\sqrt{I}e^{-i\theta} - (\sigma + i\gamma)I\sqrt{I}e^{i\theta}\end{aligned}$$

where $I = |B|^2$ is the action variable and θ the phase variable. Separating the real and imaginary parts, we obtain

$$\dot{I} = -2\sigma I^2 - 2bI\sin 2\theta \tag{2.109}$$

$$\dot{\theta} = a - \gamma I - b\cos 2\theta \tag{2.110}$$

Now we seek the equilibrium points (I_0, θ_0) by requiring $\dot{I}(I_0, \theta_0) = 0$ and $\dot{\theta}(I_0, \theta_0) =$ 0.

$$2I_0\left(\sigma I_0 + b\sin 2\theta_0\right) = 0 \tag{2.111}$$

$$a - \gamma I_0 - b\cos 2\theta_0 = 0 \tag{2.112}$$

It is obvious that

$$(I_0, \theta_0) = \left(0, \frac{\cos^{-1}\hat{a}}{2}\right) \tag{2.113}$$

is a fixed point, where

$$\hat{a} = \frac{\Omega - \alpha}{b} \tag{2.114}$$

is the bifurcation parameter through Ω. Another fixed point is

$$I_0 = -\frac{b}{\sigma}\sin 2\theta_0, \quad \cos 2\theta_0 = \frac{a - \gamma I_0}{b} \tag{2.115}$$

By eliminating θ_0 we obtain a relation between I_0 and the detuning parameter a,

$$\left(\frac{\sigma}{b}I_0\right)^2 + \left(\frac{a-\gamma I_0}{b}\right)^2 = 1 \tag{2.116}$$

or,

$$\hat{\sigma}^2 I_0^2 + (\hat{a} - \hat{\gamma} I_0)^2 = 1 \tag{2.117}$$

where

$$\hat{\sigma} = \frac{\sigma}{b} = 3.0284, \quad \hat{\gamma} = \frac{\gamma}{b} = 2.4765.$$

are numerical constants and $\hat{a}$ is defined in (2.114). The solutions to this quadratic equation are

$$I_0^{\pm} = \frac{\hat{\gamma}}{\hat{\gamma}^2 + \hat{\sigma}^2}\left[\hat{a} \pm \sqrt{1 + \frac{\hat{\sigma}^2}{\hat{\gamma}^2}\left(1 - \hat{a}^2\right)}\right] \tag{2.118}$$

Since I_0 must be real, we require that

$$|\hat{a}| < \sqrt{\frac{\hat{\gamma}^2 + \hat{\sigma}^2}{\hat{\sigma}^2}} \Rightarrow |\hat{a}| < 1.292$$

Since I_0 must also be positive, there is one finite fixed point I_0^+ when $|\hat{a}| < 1$, and two finite fixed points $I_0^{\pm}$ when $1 < \hat{a} < 1.292$. For $\hat{a} > 1.292$ only the trivial fixed point $I_0 = 0$ exists.

The equilibrium branches are plotted in Figure 2-5. After I_0 is known, we can get θ_0 from (2.115)

$$\theta_0 = \frac{\cos^{-1}\left(\hat{a} - \hat{\gamma} I_0\right)}{2} \tag{2.119}$$

2.9.1 Equilibrium state — mature edge wave and the second-order steady flow

In this section, we discuss some implications of equilibrium state of the dynamical system.

- **First-order**

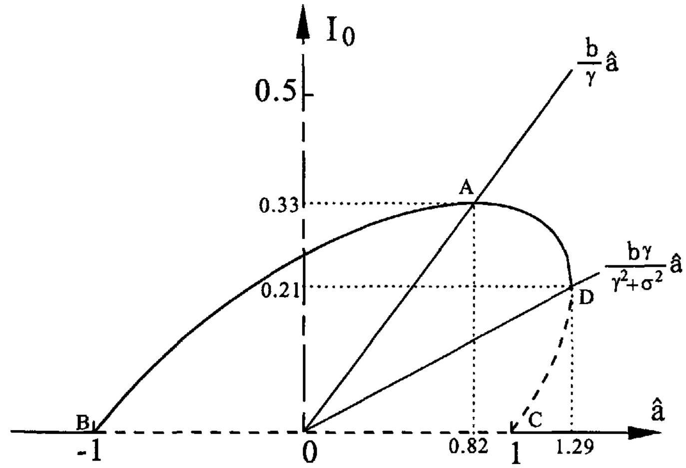

Figure 2-5: Bifurcation diagram of equilibrium branches.

At perfectly synchronous resonance, $\Omega = 0$ and $a = \alpha = -0.0340$ by definition (2.108). Therefore, $\hat{a} = \frac{a}{b} = -0.4479$ from (2.114). Therefore, we can compute the corresponding fixed point from (2.118) and (2.119) to obtain

$$I_0 = 0.1673, \quad \theta_0 = -1.3052 \tag{2.120}$$

which implies that the mature edge wave amplitude $B_0 = |B_0|e^{-i\theta_0}$ with

$$|B_0| = \sqrt{I_0} = 0.409. \tag{2.121}$$

Returning to physical variables, $B_0' = 0.409e^{-1.3052i}A'$, or, $|B_0'| = 0.409|A'|$ [2] and the phase difference between the edge wave and the incident wave is 1.3052, which is closed to $\pi/2$.

To visualize what happens at the shoreline at this steady state, we rewrite the two first-order solutions (2.30) and (2.31) in physical variables

$$\psi_0' = -i\frac{|A'|g}{\omega}B_0 e^{i\varphi}e^{-kx}\cos ky' = -|B_0|e^{i\theta_0}i\frac{A'g}{\omega}e^{-kx'}\cos ky' \tag{2.122}$$

$$\phi_0' = -i\frac{|A'|g}{\omega}e^{i\varphi}J_0(2\sqrt{kx'}) = -i\frac{A'g}{\omega}J_0(2\sqrt{kx'}) \tag{2.123}$$

where we have replaced B in (2.30) by $Be^{i\varphi}$ due to (2.91). Refer to (2.121) and (2.120) for the value of $|B_0|$ and θ_0.

[2]In subharmonic resonance, $|B'| = 0.954\frac{2s}{\omega}(g|A'|)^{1/2}$. See Appendix J.

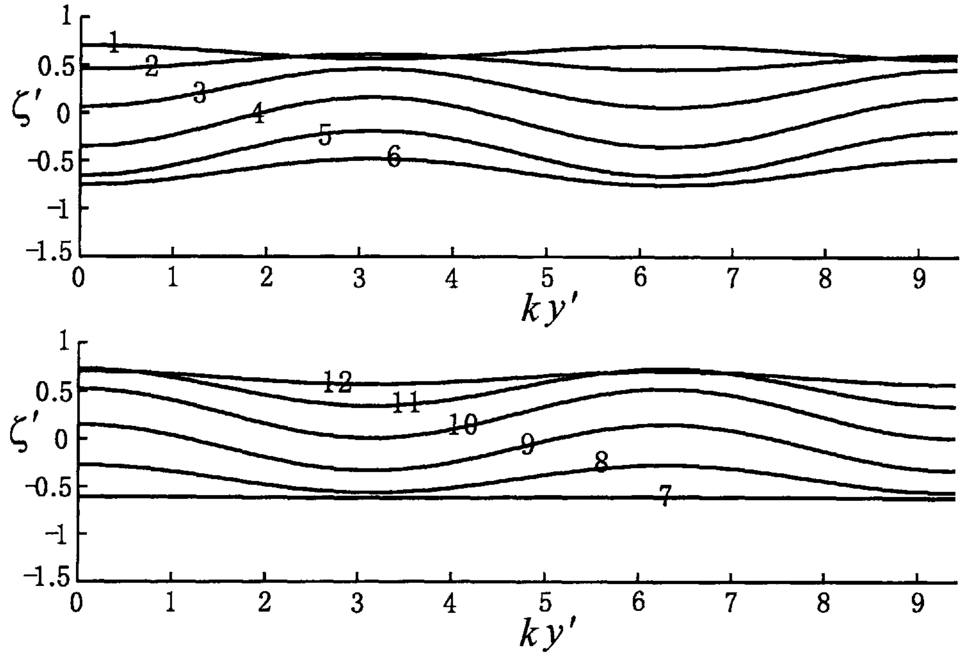

Figure 2-6: The normalized surface elevation $\zeta'(0, y, t)$ along shore line at different time $t = \frac{n\pi}{12}$, n=1, 2, 3,..., 12, which are labeled on corresponding curves.

Applying the surface boundary condition (1.2), we get from (2.122) and (2.123)

$$\zeta'_e = |B_0|A'e^{-kx'}\cos ky' e^{-i(\omega t' - \theta_0)} + * = 2|B_0||A'|e^{-kx'}\cos ky' \cos(\omega t' - \theta_0) \quad (2.124)$$

and

$$\zeta'_i = A' J_0(2\sqrt{kx'})e^{-i\omega t'} + * = 2|A'|J_0(2\sqrt{kx'})\cos(\omega t'). \quad (2.125)$$

where we have set $\varphi = 0$ without loss of generality. The sum of the two elevations along the shoreline $\zeta' = \zeta'_i + \zeta'_e$ is plotted for different times during one period $T = 2\pi/\omega$ in dimensionless form in Figure 2-6.

- **Second order**

In their lab experiment [3], Bowen and Inman generated edge waves with exactly the same period as the input wave and rip currents were observed. The test were performed in a wave basin with $W = 24\ feet = 731.5\ cm$ wide working area and a bottom slope $s = 0.075$. Two kinds of waves were used: In the nonbreaking surge case, they used incident wave of period equal to 6.4 seconds. For a 5.0 second period, the incident wave broke. There was no record in their paper about the incident wave amplitudes. But for 5.0-second incident wave, they recorded the longshore variation of breaker height in Table 2 of their paper. For convenience, we quoted part of the records in Table 2.9. In the nonbreaking case, they observed longshore period which they interpreted as edge waves and rip currents appeared to grow simultaneously and quite rapidly. The pattern was established a few wave periods after the first wave reached the beach. In their test with incident waves of period 6.4 seconds ($\omega \sim 1$ rad /s) rip currents were clearly present at such spacing as seen in Fig. 3 from their paper [3]. We cite the photo in Figure 2-7 for convenience. In the breaking case, they claimed that no edge waves were visible inside the breaker, although the rip currents occurred at the theoretical positions of the alternate antinodes of edge waves having the input frequency. Measurements outside the breakers showed that edge waves were present there.

In their test with incident wave of 5.00 seconds period, Bowen and Inman [3] reported in their Table 2, a breaker height $H_b = 2.41\ cm$ at the distance $x_b = 34\ cm$ from SWL. This measurement was taken at the node of the edge wave, where edge wave makes no contribution to the total wave height. From their Table 1, it can be identified that the edge wave mode $m = 5$ was generated with 4.96 sec eigen period. The longshore wave number should be $k = \frac{5\pi}{W} = 0.0215/cm$. From these data, we can infer the incident wave amplitude at the shoreline $a_0 = 2|A'|$ through (2.125) that

$$a_b = a_0 J_0(2\sqrt{kx_b}) \Rightarrow |A'| = \frac{a_b}{2J_0(2\sqrt{kx_b})} = \frac{H_b}{4J_0(2\sqrt{kx_b})} = 1.536\ cm.$$

Although the incident wave amplitude of the nonbreaking wave of period 6.4 sec was not reported, we assume it to be the same as in the 5.00 sec test. With the amplitude $|A'|$ known, the perturbation parameter in this experiment can be estimated as

$$\epsilon = \frac{k|A'|}{s} = 0.44.$$

which is not small. Therefore, the experimental condition is outside the scope of our theory. Nevertheless we use this value for further comparisons.

With the inferred $|A'|$, the mature edge wave amplitude at shoreline should be $|B_0'| = 2|B_0||A'| = 2 \times 0.409 \times 1.536cm = 1.256cm$ according to (2.32) in our theory (wave height $H = 2.51cm$). Projected onto the sloping beach, this wave height creates an runup of 2.51 $cm/0.075 = 33.5cm$. From their Figure 3 (see Figure 2-7) of the 6.4 sec test, the waterline variation on the beach is roughly $731.5cm \times 0.6cm/11.8cm =$ 37.2 cm, which is close to our theoretical prediction despite the large difference in ϵ.

Table 2.9: Quoted records of the longshore variation of breaker height from Bowen and Inman [3].

	Antinode(Rip)	Node	Antinode(No Rip)
Longshore distance(cm)	0	144	288
Breaker height(cm)	2.05	2.41	3.18
Distance of breaker from SWL(cm)	34	34	40

From (2.71) the steady flow generated by interaction of the incident wave and the edge wave is

$$\psi_{10} = -ie^{-i\varphi}Be^{i\varphi}f_{12}(x)\cos y = -iBf(x,y) \tag{2.126}$$

where we have introduced an abbreviation

$$f(x,y) = f_{12}(x)\cos y$$

The normalized velocity $(u,v) = (\frac{\partial f}{\partial x}, \frac{\partial f}{\partial y})$ is shown in Figure 2-8. Note that the length of the arrow is proportional to the strength of the velocity. The local mass flux is equal to the product of local velocity and water depth. Therefore, the flux at shoreline is zero due to the zero water depth at $x = 0$. Returning to physical variables we have at equilibrium

$$\begin{aligned}\psi_{10}' &= -|B_0|e^{i\theta_0}i\frac{|A'|g}{\omega}f_{12}(kx')\cos ky' \\ &= -|B_0|e^{i(\frac{\pi}{2}+\theta_0)}\frac{|A'|g}{\omega}f_{12}(kx')\cos ky'\end{aligned}$$

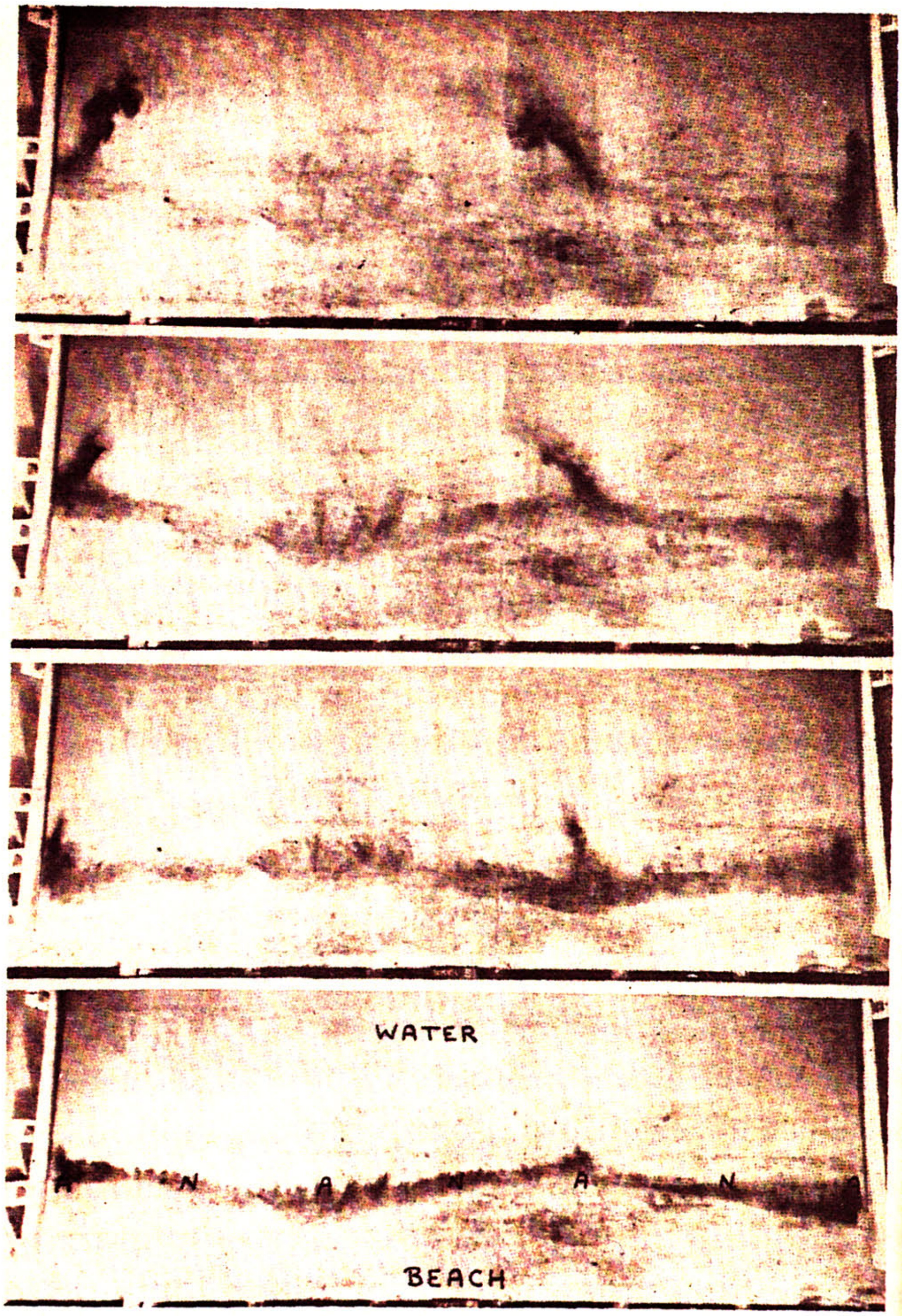

Fig. 3. Edge waves and rip currents in the wave tank for an input wave of period 6.40 seconds. The antinodes A and nodes N of the edge wave are visible at the water line on the beach.

Figure 2-7: Photo cited from Bowen & Inman's 6.4 sec test.

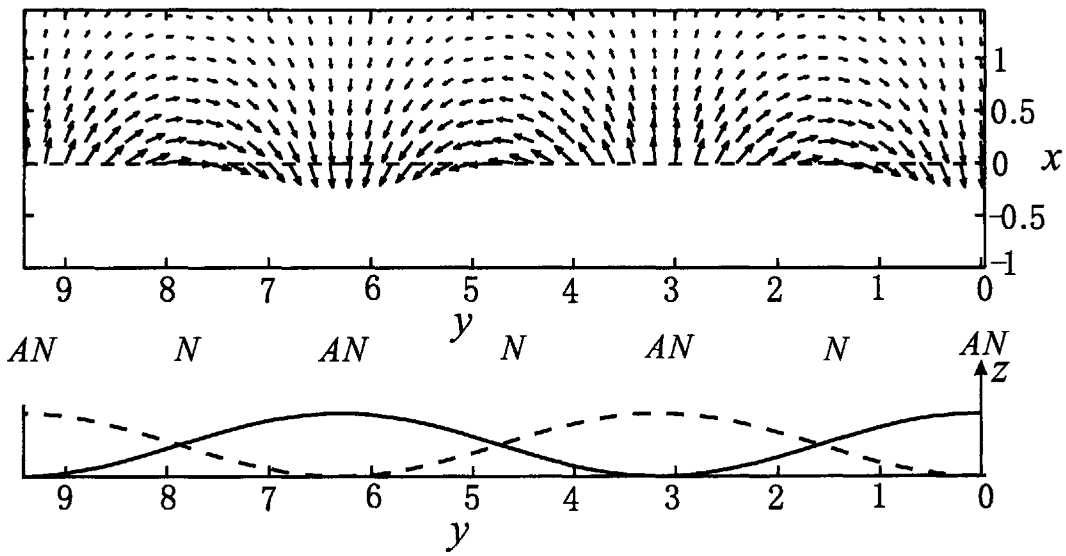

Figure 2-8: The normalized steady flow velocity $(u, v) = (\frac{\partial f}{\partial x}, \frac{\partial f}{\partial y})$. The two lines in the bottom figure represent the instantaneous edge wave surface elevation and the solid line is half period away from the dashed line. AN— Antinode, N— Node.

Adding to its complex conjugate, the total potential for the steady flow

$$\begin{aligned}\Psi'_{10} &= -2|B_0|\cos\left(\frac{\pi}{2}+\theta_0\right)\frac{|A'|g}{\omega}f_{12}(kx')\cos ky' \\ &= 0.789\frac{|A'|g}{\omega}f(kx', ky') \qquad (2.127)\end{aligned}$$

Again, we recall the value of $|B_0|$ and θ_0 from (2.121) and (2.120). Note that the coefficient in front of $f(kx', ky')$ in (2.127) is positive. Starting from the second antinode from the wall at $y = 0$, seaward rip currents are predicted at alternate antinodes (see Figure 2-8) according to (2.127). Comparing Figure 2-8 with Figure 2-7 we can see that our theory predicts an identical circulation pattern as in Bowen & Inman's experiment.

From (2.75) and Table 2.6 we can get

$$f_{12x}(0) = k(a_1 - a_0) = 0.5k.$$

The maximum cross-shore velocity occured at the antinodes, where $\cos y = \pm 1$ and

$$|\Psi'_{10x}| = \left|0.789 \times 0.5k\frac{|A'|g}{\omega}\right| = 0.394\frac{\omega}{s}|A'|.$$

Therefore, the velocity must be

$$u_{max} = 0.394\epsilon\frac{\omega}{s}|A'|. \tag{2.128}$$

As a speculative check, we compute the rip current velocity upon substitution of the incident wave amplitude $|A'| = 1.536\ cm$ into (2.128)

$$u_{max} = 0.394 \times 0.44 \times \frac{2\pi}{5sec \times 0.075} \times 1.536\ cm = 4.46 cm/sec.$$

Thus a 4.46 cm/s maximum rip current should occur at the shoreline in the experiment. In the breaking wave (5sec) experiment, they reported a 5cm/sec maximum rip current velocity. We should remark that breaking was observed in this particular experiments of Bowen and Inman, which may enhance the surf zone circulation. That may explain why our theory, based on non-breaking wave assumption, predicts a smaller velocity. Although the two results are close, the crude agreement is not a confirmation of our theory.

With the small parameter ϵ known, we can compare the initial growth rate of synchronous resonance with that of subharmonic resonance. From Section 2.7 the growth rate of synchronous resonance is

$$0.0679\epsilon\frac{\omega^3|A'|}{gs^2} = 0.030\frac{\omega^3|A'|}{gs^2}, \quad \text{for} \quad \epsilon = 0.44.$$

where the coefficient 0.0679 is from (2.100). On the other hand, according to the classical theory of subharmonic resonance, the initial growth rate is

$$\frac{0.2707}{8}\frac{\omega^3|A'|}{gs^2} = 0.034\frac{\omega^3|A'|}{gs^2}.$$

Thus numerically, the synchronous resonance and subharmonic resonance have almost the same rate of initial growth.

At equilibrium, we recall the edge-wave amplitude $B_0 = 0.409e^{-1.3052i}$. Substituting this result along with $\epsilon = 0.44$ in (2.76), we get the second-order wave setup/setdown

$$\bar{\zeta} = -\epsilon\left[|B_0|^2e^{-2x} + \left(\frac{dJ_0(2\sqrt{x})}{dx}\right)^2 - 2|B_0|\cos\theta_0 e^{-x}\frac{dJ_0(2\sqrt{x})}{dx}\cos y\right] \tag{2.129}$$

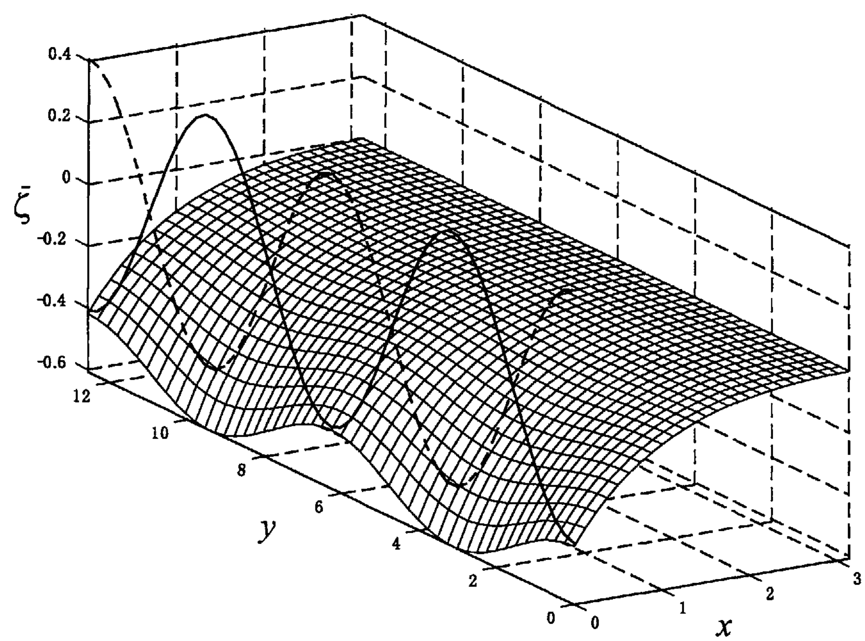

Figure 2-9: Normalized wave set-up on the beach. The two curves at $x = 0$ represent the instantaneous edge wave surface elevation at shoreline and the solid line is half period away from the dashed line.

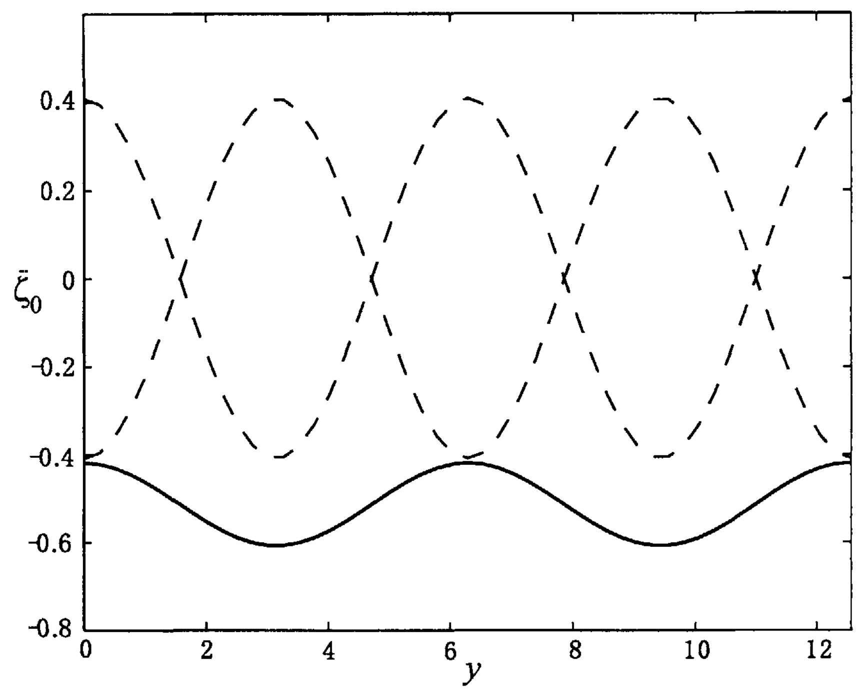

Figure 2-10: Normalized wave set-up at the shoreline $x = 0$. The dashed curves represent the instantaneous edge wave surface elevation at shoreline and the two curves are half period away from each other.

with $|B_0| = 0.409, \theta_0 = -1.3052$. Figure 2-9 shows the normalized wave set-up on the beach according to (2.129).

At the shoreline $x = 0$, this set-up is equal to

$$\bar{\zeta}_0 = -0.44\,(1.1673 + 0.2147\cos y) \tag{2.130}$$

which is plotted in Figure 2-10. Use has been made of $\frac{dJ_0(2\sqrt{x})}{dx} = -1$ at $x = 0$. The dashed curves in the figure shows the node and antinode position of the edge wave. It is actually a set-down due to the negative value. As in Bowen and Inman's experiment, the incident wave has an amplitude $|A'| = 1.536cm$. Therefore, the physical set-up is

$$\bar{\zeta}_0{}' = |A'|\bar{\zeta}_0 = -0.676\,(1.1673 + 0.2147\cos y)$$

From the first anti-node of the edge wave at $y = 0$, the wave set-down increases from its lowest level to reach the maximum at the second anti-node.

2.9.2 Local dynamics around the fixed point

In order to analyze the stability of the equilibrium state, we add some infinitesimal disturbances to both I_0 and θ_0 so that

$$I = I_0 + I', \quad \theta = \theta_0 + \theta'$$

Substituting these into (2.109) and (2.110)and linearizing both equations, we get

$$\begin{pmatrix} \dot{I}' \\ \dot{\theta}' \end{pmatrix} = \begin{bmatrix} -4\sigma I_0 - 2b\sin(2\theta_0) & -4bI_0\cos(2\theta_0) \\ -\gamma & 2b\sin(2\theta_0) \end{bmatrix} \begin{pmatrix} I' \\ \theta' \end{pmatrix} \tag{2.131}$$

Making use of (2.115) we can further simplify the coefficient matrix to

$$\mathbf{A} = \begin{bmatrix} -2\sigma I_0 & 4I_0(-a+\gamma I_0) \\ -\gamma & -2\sigma I_0 \end{bmatrix}$$

Substituting

$$\begin{pmatrix} I' \\ \theta' \end{pmatrix} = \begin{pmatrix} \bar{I}' \\ \bar{\theta}' \end{pmatrix} e^{\lambda t}$$

into (2.131) we get the characteristic equation

$$det(\mathbf{A} - \lambda\mathbf{I}) = \begin{vmatrix} -2\sigma I_0 - \lambda & 4I_0(-a+\gamma I_0) \\ -\gamma & -2\sigma I_0 - \lambda \end{vmatrix} = 0$$

This quadratic equation gives two eigenvalues

$$\lambda_{\pm} = \begin{cases} -2\sigma I_0 \pm i2\sqrt{-\gamma I_0(a-\gamma I_0)}, & \text{if} \quad (a-\gamma I_0) \leq 0 \\ -2\sigma I_0 \pm 2\sqrt{\gamma I_0(a-\gamma I_0)}, & \text{if} \quad (a-\gamma I_0) > 0. \end{cases} \tag{2.132}$$

There are two possibilities:

- Two complex-conjugate eigen values,

  This happens when $(a-\gamma I_0) \leq 0$. For this to happen we require $a \leq \gamma I_0 \Rightarrow I_0 \geq \frac{b}{\gamma}\hat{a}$. In this case, we have $\mathrm{Re}(\lambda) \equiv -2\sigma I_0 < 0$, meaning that the fixed points are asymptotically stable foci. These equilibria correspond to the branch AB of the bifurcation diagram in Figure 2-5 and 2-12. The equilibrium of perfect synchronous resonance is on this branch. All orbits spiral to this fixed point. A sample phase portrait near this equilibrium is shown in Figure 2-11.

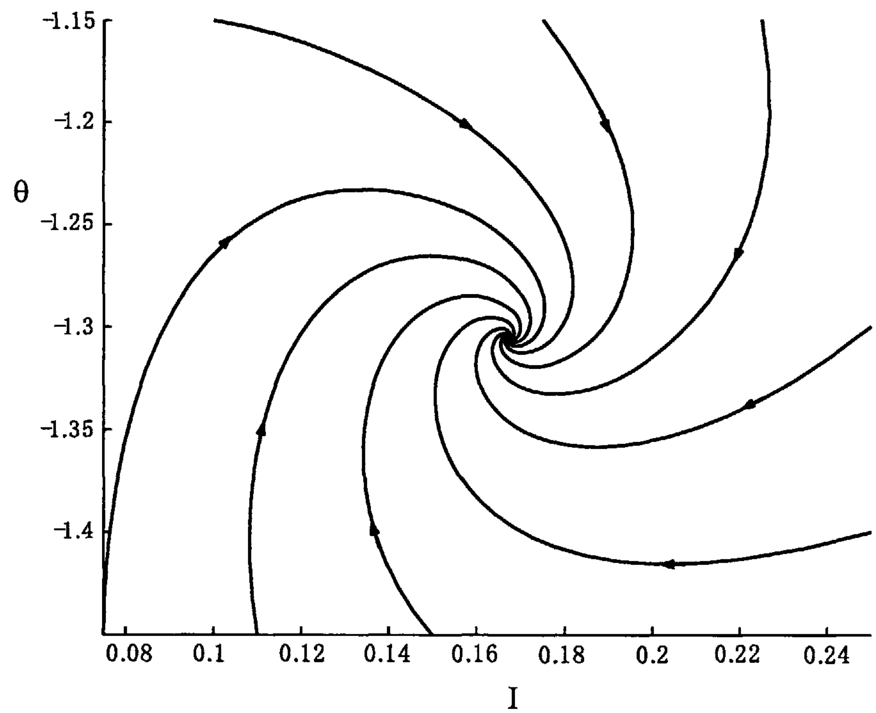

Figure 2-11: Phase portrait near the perfect resonance stable equilibrium $(I_0, \theta_0) = (0.1673, -1.3052)$.

- Two real eigen values,

  This happens when $(a - \gamma I_0) > 0$, or $a > \gamma I_0 \Rightarrow I_0 < \frac{b}{\gamma}\hat{a}$, which corresponds to branch AC of the bifurcation diagram. Within this branch, we have two possibilities:

  a) One positive and one negative eigen value, i.e. one of the eigen value $\lambda_+ > 0$. This happens when $-2\sigma I_0 + 2\sqrt{\gamma I_0(a - \gamma I_0)} > 0$, which requires

$$I_0 < \frac{\gamma a}{\gamma^2 + \sigma^2} = \frac{b\gamma}{\gamma^2 + \sigma^2}\hat{a}.$$

  Therefore, the fix points $I_0 < \frac{b\gamma}{\gamma^2+\sigma^2}\hat{a}$ are unstable saddle, which correspond to branch CD of the bifurcation diagram in Figure 2-5 and 2-12.

  b) Both the eigen values are negative.

  These fix points are asymptotically stable nodes, corresponding to branch AD of the bifurcation diagram in Figure 2-5.

All points with $I_0 = 0$ are trivial equilibrium points, around each we have double zero eigen value $\lambda = 0$ and

$$\cos 2\theta = -\frac{a}{b}$$

Linearization leads to

$$\dot{I} = 2bI \sin 2\theta = \pm 2bI\sqrt{1 - \left(\frac{a}{b}\right)^2}$$

which gives the solution

$$I = I(0)e^{\pm 2b\tau\sqrt{1-\left(\frac{a}{b}\right)^2}} \tag{2.133}$$

Hence the fixed point $I_0 = 0$ is unstable when $b > |a|$ (i.e. $|\hat{a}| < 1$). In order to see what happens beyond $\hat{a} = \pm 1$, we turn to the Cartesian coordinate system and let $B = x + iy$. Then (2.107) can be transfered to two real ODEs

$$\dot{x} = -(a + b)y - (x^2 + y^2)(\sigma x - \gamma y) \tag{2.134}$$

$$\dot{y} = (a - b)x - (x^2 + y^2)(\sigma y + \gamma x) \tag{2.135}$$

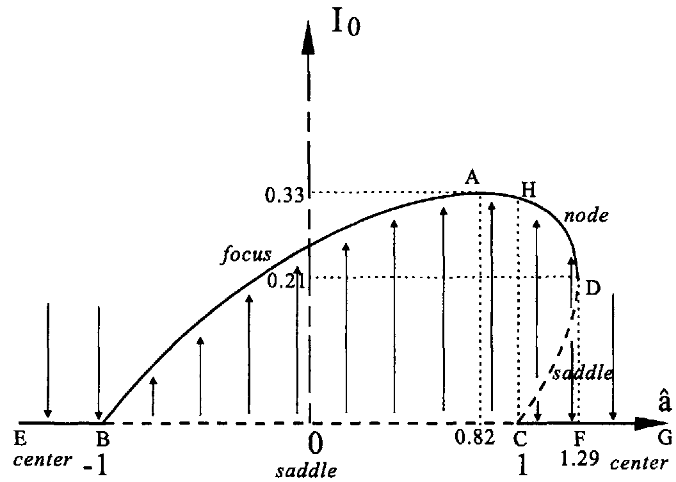

Figure 2-12: Bifurcation diagram.

The linearized dynamical system around fixed point $(x_0, y_0) = (0,0)$ is

$$\begin{pmatrix} \dot{x} \\ \dot{y} \end{pmatrix} = \begin{bmatrix} 0 & -(a+b) \\ a-b & 0 \end{bmatrix} \begin{pmatrix} x \\ y \end{pmatrix} \tag{2.136}$$

With $(x,y) \propto e^{\lambda t}$, the eigen value condition is

$$\begin{bmatrix} -\lambda & -(a+b) \\ a-b & -\lambda \end{bmatrix} \begin{pmatrix} x \\ y \end{pmatrix} = 0$$

There is a pair of eigen values $\lambda = \pm\sqrt{b^2 - a^2}$, which are purely imaginary if $b < |a|$ (i.e. $|\hat{a}| > 1$), corresponding to neutrally stable centers along $I_0 = 0$. Obviously, $|a| = b$ (i.e. $\hat{a} = \pm 1$) are two critical points of bifurcation.

Let us examine the whole bifurcation diagram in Figure 2-12.

Starting from point E, the lower end of $\hat{a}$, we have only one trivial stable center until B, i.e. $\hat{a} = -1$, where the dynamical system start to develop a stable focus besides the trivial unstable saddle. Therefore, the system will jump to this static equilibrium with arbitrarily small perturbation. This jump becomes greater along the branch BA as $\hat{a}$ increases until it reaches its maximum at A, where $I_0 = 0.33$ and $\hat{a} = 0.82$. After that the system jumps to the stable node along section AH. The jump height decreases with the increase of $\hat{a}$. After passing through point H, the system enters a complicated domain of motion. It has two choices, node branch

HD or center branch CF, depending on the initial perturbation. Suggested by the bifurcation diagram, this dependence on initial condition should be closely related to the saddle branch CD. Referring to Figure 2-13 for the separation of the two different motions by a saddle separatix. As an example, we take $\hat{a} = 1.15$. Therefore, the unstable saddle is located at $(I_0, \theta_0) = (0.0697, -0.106)$ and the stable node is at $(I_0, \theta_0) = (0.303, -0.579)$. PQ denotes the stable eigen direction of the saddle, while MN is the unstable direction. All the orbits starting from points on the right-hand side of PQ will be attracted to the stable node, whereas those starting from points in between the periodic PQ curves will be suppressed by MN and finally go to $I_0 = 0$. Here we denote the periodic repetition of PQ curve by $(P)(Q)$, as well as for MN curve in Figure 2-14. Figure 2-14 shows this process. The equivalent phase portrait under Cartesian coordinate system is shown in Figure 2-15 and Figure 2-16, where $x = \sqrt{I}\cos\theta,\ y = \sqrt{I}\sin\theta$. After F, the system dies on the trivial equilibrium again.

In a laboratory experiment, the edge wave has a frequency ω. Let the incoming waves have a frequency $\sigma \neq \omega$ by controlling the wave maker. The detuning frequency is

$$\Omega = \frac{\sigma - \omega}{\omega\epsilon^2} = \frac{s^2}{k^2}\frac{\sigma - \omega}{\omega|A|^2}.$$

As Ω is varied, the dynamical system approaches its critical bifurcation points either along EB or GF, depending on whether $\sigma < \omega$ or $\sigma > \omega$. As soon as the incoming wave amplitude $|A|$ reaches a critical value so that $\hat{a} = \frac{\Omega - 0.03404}{0.0760} > -1$ or $\hat{a} = \frac{\Omega - 0.03404}{0.0760} < 1.29$, the system response grows continuously to a finite value (for EB branch) or discontinuously with a sudden jump (for GF branch). Under either situation, an edge wave is observed.

2.10 Summary

In this chapter we have found the following:

1. For a given incident wave with frequency equal to the eigenfrequency of an edge wave, the edge wave can be excited by the second harmonic resulting from the

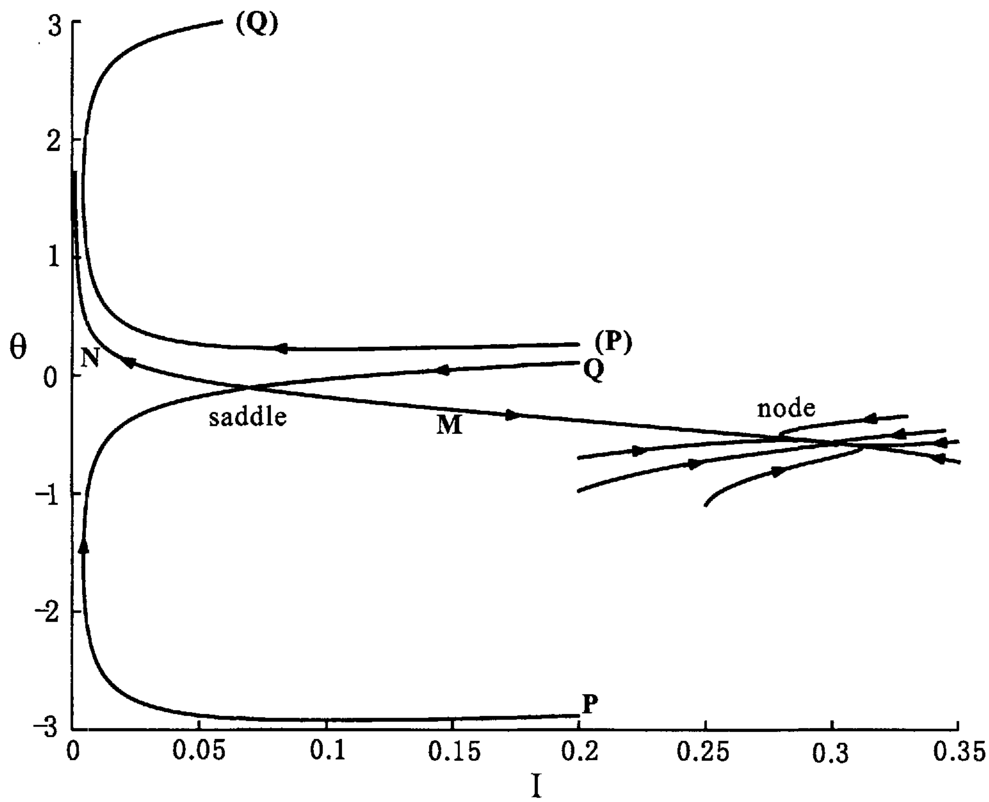

Figure 2-13: Attraction domain demarcation by the saddle separatix for $\hat{a} = 1.15$.

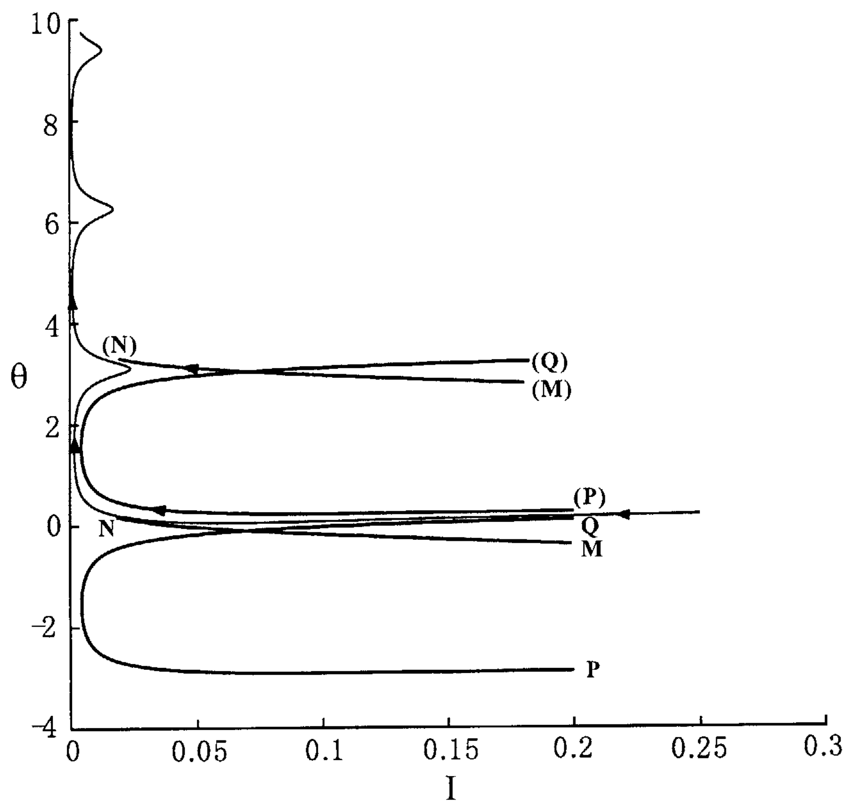

Figure 2-14: A trajectory starting from $(I(0), \theta(0)) = (0.25, 0.2)$ in between the PQ curve is suppressed by the MN branch.

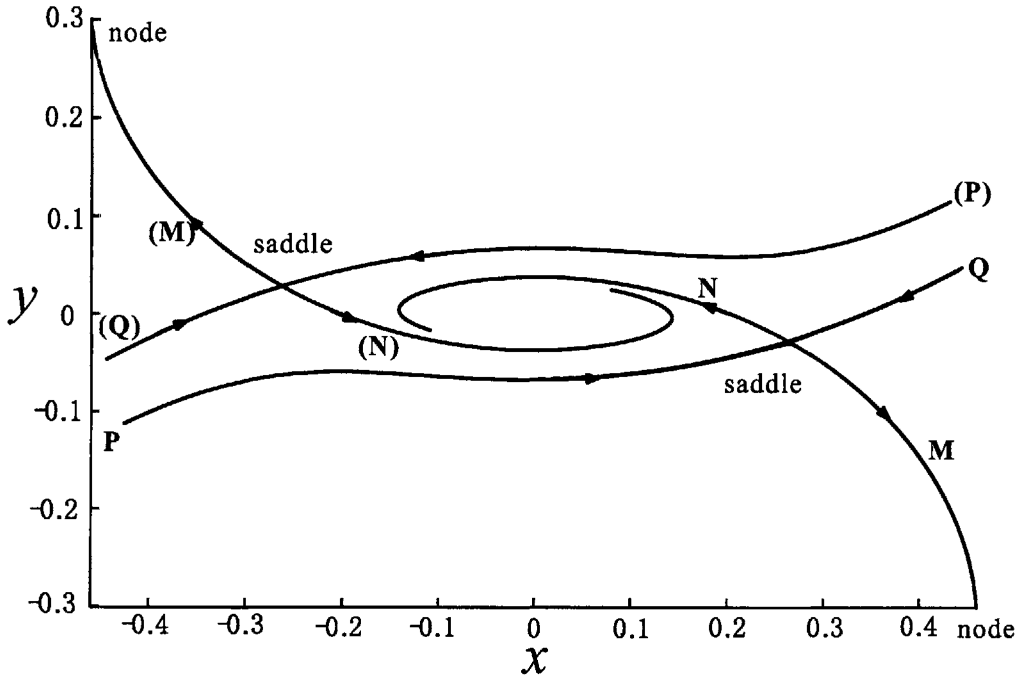

Figure 2-15: Attraction domain demarcation by the saddle separatix for $\hat{a} = 1.15$.

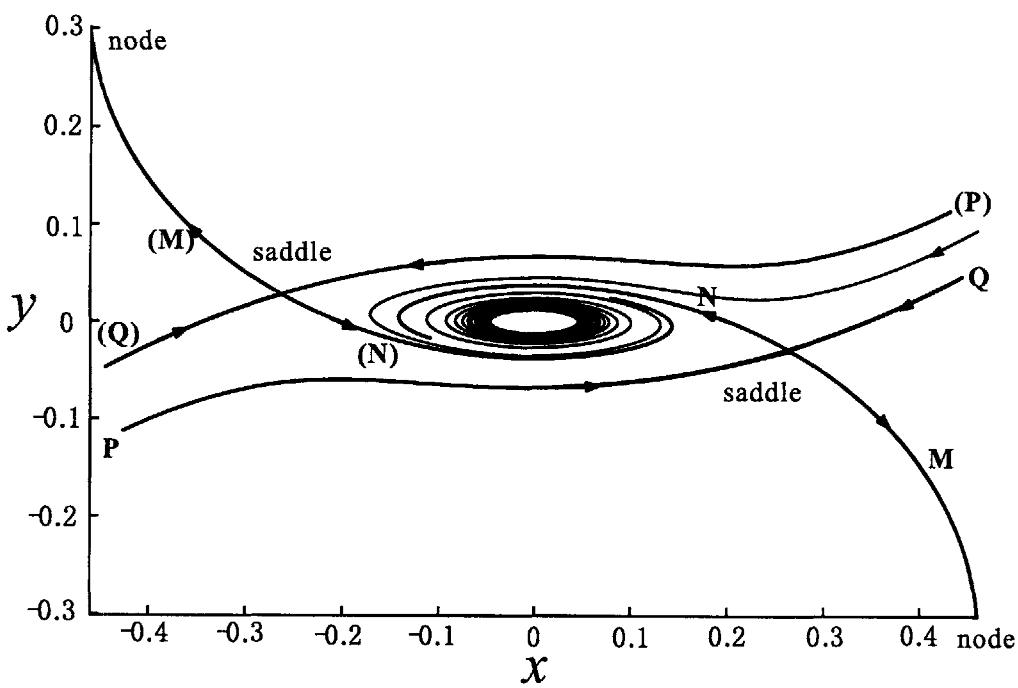

Figure 2-16: A trajectory with a starting point in between the PQ curve is suppressed by the MN branch.

self-interaction of the incident wave. At the first order linear sum of the edge wave and incident/reflected wave creates a periodic pattern of waterline excursion;

2. The nonlinear interaction of the two waves produces second-order circulation cells on the beach. The relative phase between the two waves determines the sign of the flow velocity field, and further determines the location of the rip currents;

3. The rip current velocity can be calculated after both incident and edge wave amplitudes are known;

4. We have studied the synchronous resonance in this chapter as a special case. The ideas here can be generalized to the excitation of one edge wave by an incident wave pair, which can be a part of a broadbanded sea.

Chapter 3

Edge wave generation by a pair of incident waves of comparable magnitude

Instead of the synchronous or subharmonic resonance, we examine how a pair of incident waves can excite one edge wave mode. All the three components are assumed to be present at the first order. Nonlinear interaction of the two incident waves generates harmonics twice of the frequency of the edge wave (ω). This requires that the frequency pair (ω_1', ω_2') from the two incident waves satisfy

$$\omega_1' \pm \omega_2' = 2\omega. \tag{3.1}$$

so that an excitation similar to subharmonic resonance follows at the third order. Generally speaking, here $\omega_1' \neq \omega_2' \neq \omega \neq 0$. For simplicity of analysis, we consider an edge wave with eigen function $\cos ky$ (i.e. longshore wave number k) and the lowest cross-shore mode. Therefore the eigen value condition (1.4) gives

$$\omega = \omega_0 = \sqrt{kgs} \tag{3.2}$$

For other x modes of the edge wave, similar procedure should be followed.

The full version of the nonlinear shallow-water equation is as (2.2) and we use the following nondimensionalized variables:

$$x = kx', \quad y = ky', \quad t = \omega t', \quad \zeta = \frac{\zeta'}{|A'|}, \quad \Phi = \frac{\omega}{|A'|g}\Phi'$$

where $|A'|$ is one-half of the average of the two incident waves amplitudes at shoreline and taken to be a constant, i.e.

$$|A'| = \frac{|A_1'| + |A_2'|}{2} \tag{3.3}$$

with A_1' and A_2' are half of the amplitude of the two incident waves respectively. Then the same set of dimensionless governing equation as (2.6) is obtained, as well as the small parameter ϵ. Note that here the definition of A' is different from the one in the synchronous resonance case.

$$-\Phi_{tt} + (x\Phi_x)_x + x\Phi_{yy} = \epsilon Q(\Phi) + \epsilon^2 C(\Phi) \tag{3.4}$$

with

$$\epsilon = \frac{k|A'|}{s}$$

and quadratic and cubic nonlinear terms

$$Q(\Phi) = 2\left(\Phi_x\Phi_{xt} + \Phi_y\Phi_{yt}\right) + \Phi_t\left(\Phi_{xx} + \Phi_{yy}\right) \tag{3.5}$$

$$C(\Phi) = \frac{1}{2}\left(\Phi_x^2 + \Phi_y^2\right)\left(\Phi_{xx} + \Phi_{yy}\right) + \Phi_x^2\Phi_{xx} + \Phi_y^2\Phi_{yy} + 2\Phi_x\Phi_y\Phi_{xy} \tag{3.6}$$

The normalized free surface boundary condition becomes

$$\zeta + \frac{\partial\Phi}{\partial t} + \frac{\epsilon}{2}|\nabla\Phi|^2 = 0. \tag{3.7}$$

3.1 Harmonics and nonlinear forcing terms

Let the perturbation expansion solution be

$$\Phi = \Phi_0 + \epsilon\Phi_1 + \epsilon^2\Phi_2 + \cdots \tag{3.8}$$

At the leading order we assume the co-existence of one edge wave and two normally incident and reflected waves of frequency ω_1 and ω_2:

$$\Phi_0 = \Phi_e + \Phi_{01} + \Phi_{02} \tag{3.9}$$

where

$$\Phi_e = \psi_0 \, e^{-it} + *; \quad \text{with} \;\; \psi_0 = -iB(\tau)e^{-x}\cos y; \tag{3.10}$$

is the edge wave, and

$$\Phi_{01} = \phi_{01} \, e^{-i\omega_1 t} + *; \quad \text{with} \;\; \phi_{01} = -i\frac{A_1}{\omega_1}J_0(2\omega_1\sqrt{x}); \tag{3.11}$$

$$\Phi_{02} = \phi_{02} \, e^{-i\omega_2 t} + *; \quad \text{with} \;\; \phi_{02} = -i\frac{A_2}{\omega_2}J_0(2\omega_2\sqrt{x}); \tag{3.12}$$

are the two incident and totally reflected waves. Please refer to (1.6) and (1.7) for dimensional form of the two kinds of wave solutions. B, A_1 and A_2 are one half of the normalized amplitudes of those waves at the shoreline $x = 0$. Therefore, their physical amplitudes are

$$B' = |A'|B, \quad A_1' = |A'|A_1, \quad A_2' = |A'|A_2. \tag{3.13}$$

Therefore, $|A_1| + |A_2| = 2$ according to the definition of the nondimensionalization scale $|A|$ in (3.3). ω_1 and ω_2 are the normalized frequencies of the two incident and reflected waves, i.e. $\omega_j = \omega_j'/\omega$, $(j = 1,\ 2)$. Note also that the edge wave solution depends on x and y and is 2-dimensional, whereas the two incident and reflected waves are longcrested 1-dimensional and have no y dependence.

In order to find out what are the harmonics excited by nonlinear interaction at second order $O(\epsilon)$ and consequently contributing to resonance forcing at the third order $O(\epsilon^2)$, we need to look at the quadratic nonlinear forcing terms first. Out of the three first order wave solutions, there are totally six possible combinations, which give different harmonics as follows:

Q-I. $(\Phi_e,\ \Phi_e) \longrightarrow 0,\ \pm 2$

Q-II. $(\Phi_e,\ \Phi_{01}) \longrightarrow \pm(1+\omega_1),\ \pm(1-\omega_1)$

Q-III. $(\Phi_e,\ \Phi_{02}) \longrightarrow \pm(1+\omega_2),\ \pm(1-\omega_2)$

Q-IV. $(\Phi_{01},\ \Phi_{01}) \longrightarrow 0,\ \pm 2\omega_1$

Q-V. $(\Phi_{02},\ \Phi_{02}) \longrightarrow 0,\ \pm 2\omega_2$

Q-VI. $(\Phi_{01},\ \Phi_{02}) \longrightarrow \pm(\omega_1+\omega_2),\ \pm(\omega_1-\omega_2)$

Similar to the classical edge wave theory [22], we try to find all the possible resonance forces for the edge wave, i.e. only those with unit frequency and y-dependence of $\cos y$ are of our ultimate concern. Obviously, the first three combinations will not give harmonic of frequency 1 (For the time being, only one mode of the edge wave is considered and those with frequencies other than 1 are not of interest.). The remaining three combinations can give the right frequency 1. But they only involve incident and reflected waves and there is no y dependence in the forcing term, which is necessary in order to resonate the edge wave. Therefore, resonance of the edge wave of frequency 1 is not expected to happen until the third order.

Now let us look at the third order cubic nonlinear terms. We require that at least one edge wave Φ_e is involved in each combination. Then the remaining two components can come from any of the three first order components and the possible combinations are reduces to 6 (Q-I to Q-VI) as in the quadratic combinations. Furthermore, from the quadratic combination Q-II and Q-III we can see that combination (Φ_e, Φ_e, Φ_{01}) and (Φ_e, Φ_e, Φ_{02}) do not give rise to harmonic of frequency 1. Only combinations with one Φ_e or three Φ_e is possible to resonate the edge wave. From now on, we use the spatial part of the first order solutions to symbolize the combinations, where their complex conjugate counterparts are implied.

C-I. $(\psi_0^*, \psi_0, \psi_0) \longrightarrow \pm 1$

C-II. $(\psi_0, \phi_{01}, \phi_{01}^*) \longrightarrow \pm 1$

C-III. $(\psi_0, \phi_{02}, \phi_{02}^*) \longrightarrow \pm 1$

C-IV. $(\psi_0^*, \phi_{01}, \phi_{02}) \longrightarrow \pm(\omega_1 + \omega_2 - 1)$

C-V. $(\psi_0^*, \phi_{01}, \phi_{02}^*) \longrightarrow \pm(\omega_1 - \omega_2 - 1)$

Among these combinations, ω_1 in C-II and ω_2 in C-III can be arbitrary in order for them to give harmonic of 1. The interaction of the two incident and reflected waves lead to combination C-IV and C-V, which are the excitation force we want to see. Notice that if and only if $\omega_1 + \omega_2 = 2$ in C-IV or $\omega_1 - \omega_2 = 2$ in C-V, then C-IV or C-V can give rise to harmonic of 1. Depending on where the natural frequency of the edge wave ω is located in the spectrum of the incident waves, we can pick either C-IV or C-V in our analysis. Finally, the total number of effective cubic nonlinear combinations are reduced to 4.

Among the quadratic terms at second order, any pair out of the three components

Table 3.1: Effective second-order harmonics and their further interactions.

	2nd-order harmonics	Further interaction with	3rd-order harmonic
[Q-1]	$(\psi_0^*, \psi_0) \longrightarrow 0$	$\psi_0(+1)$	$\longrightarrow 1$
[Q-2]	$(\psi_0, \psi_0) \longrightarrow 2$	$\psi_0^*(-1)$	$\longrightarrow 1$
[Q-3]	$(\phi_{01}, \phi_{01}^*) \longrightarrow 0$	$\psi_0(+1)$	$\longrightarrow 1$
[Q-4]	$(\psi_0, \phi_{01}) \longrightarrow 1 + \omega_1$	$\phi_{01}^*(-\omega_1)$	$\longrightarrow 1$
[Q-5]	$(\psi_0, \phi_{01}^*) \longrightarrow 1 - \omega_1$	$\phi_{01}(+\omega_1)$	$\longrightarrow 1$
[Q-6]	$(\phi_{02}, \phi_{02}^*) \longrightarrow 0$	$\psi_0(+1)$	$\longrightarrow 1$
[Q-7]	$(\psi_0, \phi_{02}) \longrightarrow 1 + \omega_2$	$\phi_{02}^*(-\omega_2)$	$\longrightarrow 1$
[Q-8]	$(\psi_0, \phi_{02}^*) \longrightarrow 1 - \omega_2$	$\phi_{02}(+\omega_2)$	$\longrightarrow 1$
[Q-9]	$(\phi_{01}, \phi_{02}) \longrightarrow \omega_1 + \omega_2 = 2$	$\psi_0^*(-1)$	$\longrightarrow 1$
[Q-10]	$(\psi_0^*, \phi_{01}) \longrightarrow \omega_1 - 1$	$\phi_{02}(+\omega_2)$	$\longrightarrow 1$
[Q-11]	$(\psi_0^*, \phi_{02}) \longrightarrow \omega_2 - 1$	$\phi_{01}(+\omega_1)$	$\longrightarrow 1$
[Q-12]	$(\phi_{01}, \phi_{02}^*) \longrightarrow \omega_1 - \omega_2 = 2$	$\psi_0^*(-1)$	$\longrightarrow 1$
[Q-13]	$(\psi_0^*, \phi_{01}) \longrightarrow \omega_1 - 1$	$\phi_{02}^*(-\omega_2)$	$\longrightarrow 1$
[Q-14]	$(\psi_0^*, \phi_{02}^*) \longrightarrow -\omega_2 - 1$	$\phi_{01}(+\omega_1)$	$\longrightarrow 1$

in each of the 4 effective cubic combinations might generate a certain harmonic and further interact with the third one at the third order to resonate the edge wave. For example, both combinations (ψ_0, ψ_0) and (ϕ_{01}, ϕ_{02}) give rise to a harmonic of 2. Later on we will see that the y dependence will disappear in combination (ψ_0, ψ_0). Q-I and Q-VI will excite the incident and reflected kind of wave ϕ_1 of frequency 2 at second order. Subsequently ϕ_1 will interact with ψ_0 at the third order to resonate the edge wave. All the effective nonlinear forcing and the corresponding harmonics excited at second order are listed in Table 3.1.

First let us deal with the case

$$\omega_1 + \omega_2 = 2.$$

Then combination [Q-1] to [Q-11] are of our concern at the second order. Only when

$\omega_1 - \omega_2 = 2$, [Q-12] to [Q-14] are of interest instead of [Q-9] to [Q-11], hence they will be excluded here. Let's derive from (3.5) the details of these forces one by one in order to determine the effective harmonics at second order for case $\omega_1 + \omega_2 = 2$:

[Q-1].

$$\begin{aligned}(\psi_0^*, \psi_0) &= 2\left[\psi_{0x}^*\psi_{0x}(-i) + \psi_{0x}\psi_{0x}^*(i) + \psi_{0y}^*\psi_{0y}(-i) + \psi_{0y}\psi_{0y}^*(i)\right] \\ &+ i\psi_0^*\left(\psi_{0xx} + \psi_{0yy}\right) - i\psi_0\left(\psi_{0xx}^* + \psi_{0yy}^*\right) = 0.\end{aligned}$$

[Q-2].

$$\begin{aligned}(\psi_0, \psi_0) &= 2\left[\psi_{0x}\psi_{0x}(-i) + \psi_{0y}\psi_{0y}(-i)\right] = -2i\left(\psi_{0x}^2 + \psi_{0y}^2\right) \\ &= -2i\left(-iBe^{-x}\right)^2\left(\cos^2 y + \sin^2 y\right) = 2iB^2e^{-2x} \qquad (3.14)\end{aligned}$$

after noting that

$$\psi_{0xx} + \psi_{0yy} = 0.$$

[Q-3].

$$\begin{aligned}(\phi_{01}, \phi_{01}^*) &= 2\left[\phi_{01x}^*\phi_{01x}(-i\omega_1) + \phi_{01x}\phi_{01x}^*(i\omega_1)\right] + i\omega_1\phi_{01}^*\phi_{01xx} - i\omega_1\phi_{01}\phi_{01xx}^* \\ &= 0\end{aligned}$$

[Q-4].

$$\begin{aligned}(\psi_0, \phi_{01}) &= 2\left[\psi_{0x}\phi_{01x}(-i\omega_1) + \phi_{01x}\psi_{0x}(-i)\right] + (-i)\psi_0\phi_{01xx} \\ &= -i\frac{A_1}{\omega_1}\left(-iB\right)e^{-x}\cos y\left\{-2i(1+\omega_1)(-1)\frac{dJ_0(2\omega_1\sqrt{x})}{dx} - i\frac{d^2J_0(2\omega_1\sqrt{x})}{dx^2}\right\} \\ &= -i\frac{A_1}{\omega_1}Be^{-x}\left\{2(1+\omega_1)\frac{dJ_0(2\omega_1\sqrt{x})}{dx} - \frac{d^2J_0(2\omega_1\sqrt{x})}{dx^2}\right\}\cos y \\ &\equiv -i\frac{A_1}{\omega_1}Bg_{13}(x)\cos y \qquad (3.15)\end{aligned}$$

[Q-5].

$$\begin{aligned}(\psi_0, \phi_{01}^*) &= 2\left[\psi_{0x}\phi_{01x}^*(i\omega_1) + \phi_{01x}^*\psi_{0x}(-i)\right] + (-i)\psi_0\phi_{01xx}^* \\ &= i\frac{A_1^*}{\omega_1}\left(-iB\right)e^{-x}\cos y\left\{2i(\omega_1-1)(-1)\frac{dJ_0(2\omega_1\sqrt{x})}{dx} - i\frac{d^2J_0(2\omega_1\sqrt{x})}{dx^2}\right\} \\ &= -i\frac{A_1^*}{\omega_1}Be^{-x}\left\{2(\omega_1-1)\frac{dJ_0(2\omega_1\sqrt{x})}{dx} + \frac{d^2J_0(2\omega_1\sqrt{x})}{dx^2}\right\}\cos y \\ &\equiv -i\frac{A_1^*}{\omega_1}Bg_{11}(x)\cos y \qquad (3.16)\end{aligned}$$

[Q-6].

$$
\begin{aligned}
(\phi_{02}, \phi_{02}^*) &= 2\left[\phi_{02x}^*\phi_{02x}(-i\omega_2) + \phi_{02x}\phi_{02x}^*(i\omega_2)\right] + i\omega_2\phi_{02}^*\phi_{02xx} - i\omega_2\phi_{02}\phi_{02xx}^* \\
&= 0
\end{aligned}
$$

[Q-7].

$$
\begin{aligned}
(\psi_0, \phi_{02}) &= 2\left[\psi_{0x}\phi_{02x}(-i\omega_2) + \phi_{02x}\psi_{0x}(-i)\right] + (-i)\psi_0\phi_{02xx} \\
&= -i\frac{A_2}{\omega_2}(-iB)\,e^{-x}\cos y\left\{-2i(1+\omega_2)(-1)\frac{dJ_0(2\omega_2\sqrt{x})}{dx} - i\frac{d^2J_0(2\omega_2\sqrt{x})}{dx^2}\right\} \\
&= -i\frac{A_2}{\omega_2}Be^{-x}\left\{2(1+\omega_2)\frac{dJ_0(2\omega_2\sqrt{x})}{dx} - \frac{d^2J_0(2\omega_2\sqrt{x})}{dx^2}\right\}\cos y \\
&\equiv -i\frac{A_2}{\omega_2}Bg_{14}(x)\cos y
\end{aligned}
\tag{3.17}
$$

[Q-8].

$$
\begin{aligned}
(\psi_0, \phi_{02}^*) &= 2\left[\psi_{0x}\phi_{02x}^*(i\omega_2) + \phi_{02x}^*\psi_{0x}(-i)\right] + (-i)\psi_0\phi_{02xx}^* \\
&= i\frac{A_2^*}{\omega_2}(-iB)\,e^{-x}\cos y\left\{2i(\omega_2-1)(-1)\frac{dJ_0(2\omega_2\sqrt{x})}{dx} - i\frac{d^2J_0(2\omega_2\sqrt{x})}{dx^2}\right\} \\
&= -i\frac{A_2^*}{\omega_2}Be^{-x}\left\{2(\omega_2-1)\frac{dJ_0(2\omega_2\sqrt{x})}{dx} + \frac{d^2J_0(2\omega_2\sqrt{x})}{dx^2}\right\}\cos y \\
&\equiv -i\frac{A_2^*}{\omega_2}Bg_{12}(x)\cos y
\end{aligned}
\tag{3.18}
$$

[Q-9].

$$
\begin{aligned}
(\phi_{01}, \phi_{02}) &= 2\left[\phi_{01x}\phi_{02x}(-i\omega_2) + \phi_{02x}\phi_{01x}(-i\omega_1)\right] + \phi_{01}(-i\omega_1)\phi_{02xx} + \phi_{02}(-i\omega_2)\phi_{01xx} \\
&= -i\frac{A_1}{\omega_1}\left(-i\frac{A_2}{\omega_2}\right)\left\{-2i(\omega_1+\omega_2)\frac{dJ_0(2\omega_1\sqrt{x})}{dx}\frac{dJ_0(2\omega_2\sqrt{x})}{dx}\right. \\
&- \left. i\omega_1J_0(2\omega_1\sqrt{x})\frac{d^2J_0(2\omega_2\sqrt{x})}{dx^2} - i\omega_2J_0(2\omega_2\sqrt{x})\frac{d^2J_0(2\omega_1\sqrt{x})}{dx^2}\right\} \\
&= i\frac{A_1}{\omega_1}\frac{A_2}{\omega_2}\left\{4\frac{dJ_0(2\omega_1\sqrt{x})}{dx}\frac{dJ_0(2\omega_2\sqrt{x})}{dx}\right. \\
&+ \left. \omega_1J_0(2\omega_1\sqrt{x})\frac{d^2J_0(2\omega_2\sqrt{x})}{dx^2} + \omega_2J_0(2\omega_2\sqrt{x})\frac{d^2J_0(2\omega_1\sqrt{x})}{dx^2}\right\}
\end{aligned}
\tag{3.19}
$$

[Q-10].

$$(\psi_0^*, \phi_{01}) \equiv (\psi_0, \phi_{01}^*)^*$$

is the complex conjugate of [Q-5].

[Q-11].

$$(\psi_0^*, \phi_{02}) \equiv (\psi_0, \phi_{02}^*)^*$$

is the complex conjugate of [Q-8].

Therefore, we have total 6 effective forcing terms, i.e. [Q-2], [Q-4], [Q-5], [Q-7], [Q-8] and [Q-9]. [Q-1], [Q-3] and [Q-6] are identically zero. In response to these forcing terms, the following types of second-order waves will be excited:

$(\psi_0, \psi_0) + (\phi_{01}, \phi_{02}) \rightarrow \phi_1(x)e^{-i2t}$

$(\psi_0, \phi_{01}^*) \longrightarrow \psi_{11}(x, y, \tau)e^{-i(1-\omega_1)t}$

$(\psi_0, \phi_{01}) \longrightarrow \psi_{13}(x, y, \tau)e^{-i(1+\omega_1)t}$

$(\psi_0, \phi_{02}^*) \longrightarrow \psi_{12}(x, y, \tau)e^{-i(1-\omega_2)t}$

$(\psi_0, \phi_{02}) \longrightarrow \psi_{14}(x, y, \tau)e^{-i(1+\omega_2)t}$

3.2 Multiple-scale expansions

We demonstrate the mathematical derivation of the evolution equation governing the edge wave amplitude using case (The case $\omega_1 - \omega_2 = 2$ can be treated similarly but omitted.)

$$\frac{\omega_1'}{\omega} + \frac{\omega_2'}{\omega} \equiv \omega_1 + \omega_2 = 2$$

Let us assume the multiple-scale expansion

$$\begin{aligned}
\Phi &= \left[\psi_0(x, y, \tau)e^{-it} + *\right] + \left[\phi_{01}(x)e^{-i\omega_1 t} + *\right] + \left[\phi_{02}(x)e^{-i\omega_2 t} + *\right] \\
&\quad + \epsilon\left[\psi_{11}(x, y, \tau)e^{-i(1-\omega_1)t} + *\right] + \epsilon\left[\psi_{13}(x, y, \tau)e^{-i(1+\omega_1)t} + *\right] \\
&\quad + \epsilon\left[\psi_{12}(x, y, \tau)e^{-i(1-\omega_2)t} + *\right] + \epsilon\left[\psi_{14}(x, y, \tau)e^{-i(1+\omega_2)t} + *\right] \\
&\quad + \epsilon\left[\phi_1(x, \tau)e^{-i2t} + *\right] + \epsilon^2\left[\psi_2(x, y, \tau)e^{-it} + *\right] + \ldots \qquad (3.20)
\end{aligned}$$

where two temporal variables are used: fast time t and slow time $\tau = \epsilon^2 t$, implying

$$\frac{\partial}{\partial t} \longrightarrow \frac{\partial}{\partial t} + \epsilon^2\frac{\partial}{\partial \tau}, \quad \frac{\partial^2}{\partial t^2} \longrightarrow \frac{\partial^2}{\partial t^2} + 2\epsilon^2\frac{\partial}{\partial t}\frac{\partial}{\partial \tau} + \epsilon^4\frac{\partial^2}{\partial \tau^2}$$

Plugging 3.20 into Eq. 3.4 and separate different orders, we get

$$\left\{\left[\psi_0 + (x\psi_{0x})_x + x\psi_{0yy}\right]e^{-it} + *\right\} + \left\{\left[\omega_1^2\phi_{01} + (x\phi_{01x})_x\right]e^{-i\omega_1 t} + *\right\}$$

$$
\begin{aligned}
&+\left\{\left[\omega_2^2\phi_{02}+(x\phi_{02x})_x\right]e^{-i\omega_2 t}+*\right\}+\epsilon\left\{\left[4\phi_1+(x\phi_{1x})_x\right]e^{-i2t}+*\right\}\\
&+\epsilon\left\{\left[(1-\omega_1)^2\psi_{11}+(x\psi_{11x})_x+x\psi_{11yy}\right]e^{-i(1-\omega_1)t}+*\right\}\\
&+\epsilon\left\{\left[(1+\omega_1)^2\psi_{13}+(x\psi_{13x})_x+x\psi_{13yy}\right]e^{-i(1+\omega_1)t}+*\right\}\\
&+\epsilon\left\{\left[(1-\omega_2)^2\psi_{12}+(x\psi_{12x})_x+x\psi_{12yy}\right]e^{-i(1-\omega_2)t}+*\right\}\\
&+\epsilon\left\{\left[(1+\omega_2)^2\psi_{14}+(x\psi_{14x})_x+x\psi_{14yy}\right]e^{-i(1+\omega_2)t}+*\right\}\\
&+\epsilon^2\left\{\left[\psi_2+(x\psi_{2x})_x+x\psi_{2yy}\right]e^{-it}+*\right\}\\
= \;&\epsilon\left\{\left[(\psi_0,\psi_0)+(\phi_{01},\phi_{02})\right]e^{-i2t}+*\right\}\\
&+\epsilon\left\{(\psi_0,\phi_{01}^*)e^{-i(1-\omega_1)t}+*\right\}+\epsilon\left\{(\psi_0,\phi_{01})e^{-i(1+\omega_1)t}+*\right\}\\
&+\epsilon\left\{(\psi_0,\phi_{02}^*)e^{-i(1-\omega_2)t}+*\right\}+\epsilon\left\{(\psi_0,\phi_{02})e^{-i(1+\omega_2)t}+*\right\}\\
&+\epsilon^2\left\{\left[(\phi_1,\psi_0^*)+(\psi_0^*,\psi_0,\psi_0)+(\psi_0,\phi_{01},\phi_{01}^*)+(\psi_0,\phi_{02},\phi_{02}^*)\right]e^{-it}+*\right\}\\
&+\epsilon^2\left\{\left[(\psi_0^*,\phi_{01},\phi_{02})+(\psi_{11},\phi_{01})+(\psi_{13},\phi_{01}^*)+(\psi_{12},\phi_{02})\right]e^{-it}+*\right\}\\
&+\epsilon^2\left\{\left[(\psi_{14},\phi_{02}^*)+(\psi_{11}^*,\phi_{02})+(\psi_{12}^*,\phi_{01})\right]e^{-it}+*\right\}\\
&+\epsilon^2\left\{-2i\frac{\partial\psi_0}{\partial\tau}e^{-it}+*\right\}+\ldots \qquad (3.21)
\end{aligned}
$$

3.3 The leading order

At O(1) we separate different harmonics (1, ω_1 and ω_2) to get

$$\psi_0+(x\psi_{0x})_x+x\psi_{0yy}=0$$

$$\omega_1^2\phi_{01}+(x\phi_{01x})_x=0$$

$$\omega_2^2\phi_{02}+(x\phi_{02x})_x=0$$

which give the homogeneous solutions of one edge wave (So far the lowest mode is our concern.)

$$\psi_0=-iB(\tau)e^{-x}\cos y \qquad (3.22)$$

and two normally incident and reflected waves

$$\phi_{01}=-i\frac{A_1}{\omega_1}J_0(2\omega_1\sqrt{x}) \qquad (3.23)$$

$$\phi_{02} = -i\frac{A_2}{\omega_2}J_0(2\omega_2\sqrt{x}) \tag{3.24}$$

$B(\tau)$ is the slowly varying dimensionless amplitude of the edge wave at shore, whose evolution equation is to be obtained at the third order.

For later uses note that the factor $F = e^{-x}$ which describes the x dependence of the edge wave satisfies

$$F + [(xF_x)_x - xF] = 0,$$

$$xF_x = 0 \quad at \quad x = 0; \quad F \to 0, \quad x \sim \infty.$$

3.4 The second order solutions

At O(ϵ), there are totally five harmonics— $\psi_{11}(x, y, \tau)e^{-i(1-\omega_1)t}$, $\psi_{13}(x, y, \tau)e^{-i(1+\omega_1)t}$, $\psi_{12}(x, y, \tau)e^{-i(1-\omega_2)t}$, $\psi_{14}(x, y, \tau)e^{-i(1+\omega_2)t}$ and $\phi_1(x)e^{-i2t}$. We solve them individually.

3.4.1 ϕ_1 — Radiated wave of frequency 2

From previous discussion we know that both (ψ_0, ψ_0) and (ϕ_{01}, ϕ_{02}) contribute to the excitation force for this harmonic. Referring to (3.21), we have

$$4\phi_1 + (x\phi_{1x})_x = (\psi_0, \psi_0) + (\phi_{01}, \phi_{02}) \tag{3.25}$$

The details of the two quadratic terms are given in (3.14) and (3.19). Introducing an abbreviation for the total force

$$\begin{aligned} g(x) &= 2iB^2 g_e + i\frac{A_1}{\omega_1}\frac{A_2}{\omega_2}g_i \equiv 2iB^2 e^{-2x} + i\frac{A_1}{\omega_1}\frac{A_2}{\omega_2}\left\{4\frac{dJ_0(2\omega_1\sqrt{x})}{dx}\frac{dJ_0(2\omega_2\sqrt{x})}{dx}\right. \\ &+ \left.\omega_1 J_0(2\omega_1\sqrt{x})\frac{d^2J_0(2\omega_2\sqrt{x})}{dx^2} + \omega_2 J_0(2\omega_2\sqrt{x})\frac{d^2J_0(2\omega_1\sqrt{x})}{dx^2}\right\} \end{aligned} \tag{3.26}$$

where

$$g_e \equiv e^{-2x} \tag{3.27}$$

represents the self-interaction of edge wave and

$$\begin{aligned} g_i &\equiv \left\{4\frac{dJ_0(2\omega_1\sqrt{x})}{dx}\frac{dJ_0(2\omega_2\sqrt{x})}{dx}\right. \\ &+ \left.\omega_1 J_0(2\omega_1\sqrt{x})\frac{d^2J_0(2\omega_2\sqrt{x})}{dx^2} + \omega_2 J_0(2\omega_2\sqrt{x})\frac{d^2J_0(2\omega_1\sqrt{x})}{dx^2}\right\} \end{aligned} \tag{3.28}$$

the self-interaction of incident/reflected wave. With these we can rewrite the inhomogeneous Eq. (3.25) as the standard form

$$\phi_{1xx} + \frac{1}{x}\phi_{1x} + \frac{4}{x}\phi_1 = \frac{g(x)}{x} \tag{3.29}$$

By the method of variation of parameters, the general solution to this inhomogeneous equation takes the form

$$\phi_1 = C_1 J_0(4\sqrt{x}) + C_2 Y_0(4\sqrt{x}) + u_1(x) J_0(4\sqrt{x}) + u_2(x) Y_0(4\sqrt{x}) \tag{3.30}$$

where

$$u_1(x) = -\int_0^x \frac{Y_0(4\sqrt{\xi})g(\xi)}{\xi W(J_0, Y_0)(\xi)} d\xi = -\pi \int_0^x Y_0(4\sqrt{\xi}) g(\xi) d\xi$$

$$u_2(x) = \int_0^x \frac{J_0(4\sqrt{\xi})g(\xi)}{\xi W(J_0, Y_0)(\xi)} d\xi = \pi \int_0^x J_0(4\sqrt{\xi}) g(\xi) d\xi$$

with the Wronskian

$$W(J_0, Y_0)(x) = J_0 \frac{dY_0}{dx} - Y_0 \frac{dJ_0}{dx} = (J_0 Y_0' - Y_0 J_0') \frac{d(4\sqrt{x})}{dx} = \frac{2}{\pi 4\sqrt{x}} \frac{2}{\sqrt{x}} = \frac{1}{\pi x}$$

and C_1, C_2 are the constants to be determined by boundary conditions. Use has been made of

$$J_0' = -J_1, \; Y_0' = -Y_1, \quad J_1(z)Y_0(z) - J_0(z)Y_1(z) = \frac{2}{\pi z}$$

Also notice that prime " $'$ " is the derivative with respect to argument z, which is equal to $4\sqrt{x}$.

Following the same argument as in last chapter, we can obtain the solution

$$\phi_1 = \left[-u_1(\infty) - i u_2(\infty)\right] J_0(4\sqrt{x}) + u_1(x) J_0(4\sqrt{x}) + u_2(x) Y_0(4\sqrt{x}). \tag{3.31}$$

which is the same in form as the synchronous resonance case except the definition of the forcing function $g(x)$ is different, hence the $u_1(x)$ and $u_2(x)$. We recall from (3.26) that $g(x) = 2iB^2 g_e + i\frac{A_1}{\omega_1}\frac{A_2}{\omega_2} g_i$, where g_e and g_i are defined in (3.27) and (3.28). Let us denote

$$u_1(x) = 2iB^2 u_1^e(x) + i\frac{A_1}{\omega_1}\frac{A_2}{\omega_2} u_1^i(x), \quad u_2(x) = 2iB^2 u_2^e(x) + i\frac{A_1}{\omega_1}\frac{A_2}{\omega_2} u_2^i(x) \tag{3.32}$$

The coefficients have contributions from the edge wave through

$$\begin{aligned} u_1^e(x) &= -\int_0^x \frac{Y_0(4\sqrt{\xi})g_e(\xi)}{\xi W(J_0,Y_0)(\xi)}d\xi = -\pi\int_0^x Y_0(4\sqrt{\xi})g_e(\xi)d\xi \\ &= -\pi\int_0^x Y_0(4\sqrt{\xi})e^{-2\xi}d\xi \end{aligned} \tag{3.33}$$

$$\begin{aligned} u_2^e(x) &= \int_0^x \frac{J_0(4\sqrt{\xi})g_e(\xi)}{\xi W(J_0,Y_0)(\xi)}d\xi = \pi\int_0^x J_0(4\sqrt{\xi})g_e(\xi)d\xi \\ &= \pi\int_0^x J_0(4\sqrt{\xi})e^{-2\xi}d\xi \end{aligned} \tag{3.34}$$

and from the incident and reflected waves through

$$\begin{aligned} u_1^i(x) &= -\int_0^x \frac{Y_0(4\sqrt{\xi})g_i(\xi)}{\xi W(J_0,Y_0)(\xi)}d\xi = -\pi\int_0^x Y_0(4\sqrt{\xi})g_i(\xi)d\xi \\ &= -\pi\int_0^x Y_0(4\sqrt{\xi})\left\{4\frac{dJ_0(2\omega_1\sqrt{\xi})}{d\xi}\frac{dJ_0(2\omega_2\sqrt{\xi})}{d\xi}\right. \\ &\quad \left. +\,\omega_1 J_0(2\omega_1\sqrt{\xi})\frac{d^2J_0(2\omega_2\sqrt{\xi})}{d\xi^2} + \omega_2 J_0(2\omega_2\sqrt{\xi})\frac{d^2J_0(2\omega_1\sqrt{\xi})}{d\xi^2}\right\}d\xi \end{aligned} \tag{3.35}$$

$$\begin{aligned} u_2^i(x) &= \int_0^x \frac{J_0(4\sqrt{\xi})g_i(\xi)}{\xi W(J_0,Y_0)(\xi)}d\xi = \pi\int_0^x J_0(4\sqrt{\xi})g_i(\xi)d\xi \\ &= \pi\int_0^x J_0(4\sqrt{\xi})\left\{4\frac{dJ_0(2\omega_1\sqrt{\xi})}{d\xi}\frac{dJ_0(2\omega_2\sqrt{\xi})}{d\xi}\right. \\ &\quad \left. +\,\omega_1 J_0(2\omega_1\sqrt{\xi})\frac{d^2J_0(2\omega_2\sqrt{\xi})}{d\xi^2} + \omega_2 J_0(2\omega_2\sqrt{\xi})\frac{d^2J_0(2\omega_1\sqrt{\xi})}{d\xi^2}\right\}d\xi \end{aligned} \tag{3.36}$$

In summary, the final solution for the second-harmonic forced by self-interactions is

$$\phi_1 = 2iB^2\phi_1^e + i\frac{A_1}{\omega_1}\frac{A_2}{\omega_2}\phi_1^i \tag{3.37}$$

with

$$\phi_1^e = \left[-u_1^e(\infty) - iu_2^e(\infty)\right]J_0(4\sqrt{x}) + u_1^e(x)J_0(4\sqrt{x}) + u_2^e(x)Y_0(4\sqrt{x}) \tag{3.38}$$

and

$$\begin{aligned} \phi_1^i &= \left[-u_1^e(\infty) - iu_2^e(\infty)\right]J_0(4\sqrt{x}) + u_1^i(x)J_0(4\sqrt{x}) + u_2^i(x)Y_0(4\sqrt{x}) \\ &= -u_1^e(\infty)J_0(4\sqrt{x}) + u_1^i(x)J_0(4\sqrt{x}) + u_2^i(x)Y_0(4\sqrt{x}) \end{aligned} \tag{3.39}$$

Use has been made of $u_2^i(\infty) = 0$ as discussed in Appendix C for the last chapter. Note that ϕ_1^e is complex, whereas ϕ_1^i is real.

— — — — — — — —

For later uses in (3.68), we now work out the constant $g(0)$ as follows. From (D.2) we see that

$$\frac{dJ_0(2c_n\sqrt{x})}{dx} = -c_n^2 + \frac{1}{2}c_n^4 x - O(x^2), \quad \frac{d^2J_0(2c_n\sqrt{x})}{dx^2} = \frac{1}{2}c_n^4 - O(x)$$

as $x \to 0$. Upon substitution into (2.36), we get

$$\begin{aligned} g(0) &= 2iB^2 + i\frac{A_1}{\omega_1}\frac{A_2}{\omega_2}\left\{4(-\omega_1^2)(-\omega_2^2) + \omega_1\frac{\omega_2^4}{2} + \omega_2\frac{\omega_1^4}{2}\right\} \\ &= 2iB^2 + i\frac{A_1}{\omega_1}\frac{A_2}{\omega_2}\omega_1^2\omega_2^2\left\{4 + \frac{\omega_2^2}{2\omega_1} + \frac{\omega_1^2}{2\omega_2}\right\} \end{aligned} \tag{3.40}$$

And also

$$\begin{aligned} \left.\frac{d\phi_1(x)}{dx}\right|_{x=0} &= \omega_1(-4) + g(0) \\ &= 4\left(u_1(\infty) + iu_2(\infty)\right) + g(0) \end{aligned} \tag{3.41}$$

$$\phi_1(0) = C_1 = -u_1(\infty) - iu_2(\infty) \tag{3.42}$$

A guessed partial solution similar to Guza and Davis [14] can be found in Appendix C for the last chapter.

3.4.2 ψ_{11} — Trapped wave of frequency $(1 - \omega_1)$

Referring to (3.21), we have for this particular harmonic

$$(1-\omega_1)^2\psi_{11} + (x\psi_{11x})_x + x\psi_{11yy} = (\psi_0, \phi_{01}^*)$$

The quadratic nonlinear forcing (ψ_0, ϕ_{01}^*) is given in (3.16), which suggests a solution

$$\psi_{11} = -i\frac{A_1^*}{\omega_1}Bf_{11}(x)\cos y$$

with $f_{11}(x)$ satisfying

$$xf_{11xx} + f_{11x} - \left[x - (1-\omega_1)^2\right]f_{11} = g_{11}(x) \tag{3.43}$$

Change of variables

$$\xi = 2x, \quad f_{11} = e^{-\frac{\xi}{2}} f(\xi)$$

leads to the Laguerre differential equation, which belongs to the class of confluent hypergeometric equation.

$$\xi f'' + (1-\xi) f' - \frac{1-(1-\omega_1)^2}{2} f = \frac{1}{2} g_{11}\left(\frac{\xi}{2}\right) e^{\frac{\xi}{2}}$$

Generally speaking, ω_1 is within the range of $(0, 2)$, which does not satisfy the eigen value condition, i.e.

$$-\frac{1-(1-\omega_1)^2}{2} \neq n$$

since

$$\omega_1 = 1 \pm \sqrt{1+2n}, \quad n = 0, 1, 2...$$

is not possible. As in the last chapter, we can apply the standard Finite Element Method. For this, equation (3.43) can be rewritten as

$$-\frac{d}{dx}\left(x f_{11x}\right) + \left[x - (1-\omega_1)^2\right] f_{11} = -g_{11}(x)$$

with the boundary conditions

$$x f_{11x} = 0 \quad \text{as} \quad x \to 0$$

$$x f_{11x} = 0 \quad \text{as} \quad x \to L.$$

It is easy to show that the boundary-value problem above is equivalent to the stationarity of the following functional

$$\mathcal{F}(f_{11}) = \frac{1}{2}\int_0^L \left[p(x)\left(\frac{df_{11}}{dx}\right)^2 + q(x) f_{11}^2\right] dx + \int_0^L g_{11} f_{11} dx \qquad (3.44)$$

where

$$p(x) = x, \quad q(x) = x - (1-\omega_1)^2$$

3.4.3 ψ_{12} — Trapped wave of frequency $(1-\omega_2)$

Referring to (3.21), we have for this particular harmonic

$$(1-\omega_2)^2\psi_{12} + (x\psi_{12x})_x + x\psi_{12yy} = (\psi_0, \phi_{02}^*)$$

The quadratic nonlinear forcing (ψ_0, ϕ_{02}^*) is given in (3.18), which suggests a solution

$$\psi_{12} = -i\frac{A_2^*}{\omega_2}Bf_{12}(x)\cos y$$

where $f_{12}(x)$ satisfies

$$xf_{12xx} + f_{12x} - \left[x-(1-\omega_2)^2\right]f_{12} = g_{12}(x) \tag{3.45}$$

We rewrite (3.45) as

$$-\frac{d}{dx}(xf_{12x}) + \left[x-(1-\omega_2)^2\right]f_{12} = -g_{12}(x)$$

And the corresponding boundary conditions are

$$xf_{12x} = 0 \quad \text{as} \quad x \to 0$$

$$xf_{12x} = 0 \quad \text{as} \quad x \to L$$

Similar to ψ_{11}, ω_2 in the range of $(0,2)$ is not an eigen value.

3.4.4 ψ_{13} — Trapped wave of frequency $(1+\omega_1)$

Referring to (3.21), we have for this harmonic

$$(1+\omega_1)^2\psi_{13} + (x\psi_{13x})_x + x\psi_{13yy} = (\psi_0, \phi_{01})$$

The quadratic nonlinear forcing (ψ_0, ϕ_{01}) is given in (3.15), which suggests a solution

$$\psi_{13} = -i\frac{A_1}{\omega_1}Bf_{13}(x)\cos y$$

with $f_{13}(x)$ satisfies

$$xf_{13xx} + f_{13x} - \left[x-(1+\omega_1)^2\right]f_{13} = g_{13}(x) \tag{3.46}$$

which can be rewritten as

$$-\frac{d}{dx}(xf_{13x}) + \left[x - (1+\omega_1)^2\right] f_{13} = -g_{13}(x) \tag{3.47}$$

And the corresponding boundary conditions are

$$xf_{13x} = 0 \quad \text{as} \quad x \to 0$$

$$xf_{13x} = 0 \quad \text{as} \quad x \to L$$

The eigen value condition can be satisfied, i.e.

$$-\frac{1-(1+\omega_1)^2}{2} = n$$

when

$$\omega_1 = -1 \pm \sqrt{1+2n}, \quad n = 0, 1, 2...$$

For example, within the range of $\omega_1 \in (0, 2)$, the possible values are

$$\omega_1 = \sqrt{3} - 1, \quad \sqrt{5} - 1, \quad \sqrt{7} - 1.$$

corresponding to $n = 1, 2$ and 3 respectively. Therefore, the eigen function are Laguerre polynomials L_n, more specifically

$$L_1 = 1 - \xi, \quad L_2 = 1 - 2\xi + \frac{1}{2}\xi^2, \quad L_3 = 1 - 3\xi + \frac{3}{2}\xi^2 - \frac{1}{6}\xi^3, \quad \xi = 2x.$$

which are mode 1, 2 and 3 of the edge waves. By direct substitution, it is easy to check that they are the eigen solutions to the homogeneous version of (3.47), i.e.

$$xf_{13xx} + f_{13x} - [x - (2n+1)] f_{13} = 0$$

When the eigen value condition is satisfied, a new eigen mode is resonated. A quadratic interaction between one mode of edge wave and one incident/reflected wave can resonate another mode of edge wave, and vice versa. This kind of cross resonance will be discussed in the next chapter. In this chapter, we exclude this situation and simply require that ω_1 is not equal to any of these three values: $\sqrt{3} - 1, \quad \sqrt{5} - 1, \quad \sqrt{7} - 1$.

3.4.5 ψ_{14} — Trapped wave of frequency $(1+\omega_2)$

Referring to (3.21), we have for this harmonic

$$(1+\omega_2)^2\psi_{14} + (x\psi_{14x})_x + x\psi_{14yy} = (\psi_0, \phi_{02})$$

The quadratic nonlinear forcing (ψ_0, ϕ_{02}) is given in (3.17), which suggests a solution

$$\psi_{14} = -i\frac{A_2}{\omega_2} B f_{14}(x)\cos y$$

with $f_{14}(x)$ satisfies

$$x f_{14xx} + f_{14x} - \left[x - (1+\omega_2)^2\right] f_{14} = g_{14}(x) \tag{3.48}$$

, which can be rewritten as

$$-\frac{d}{dx}(x f_{14x}) + \left[x - (1+\omega_2)^2\right] f_{14} = -g_{14}(x)$$

And the corresponding boundary conditions are

$$x f_{14x} = 0 \quad \text{as} \quad x \to 0$$

$$x f_{14x} = 0 \quad \text{as} \quad x \to L$$

Similar to ψ_{13}, the eigen value condition can be satisfied when

$$\omega_2 = \sqrt{3} - 1, \quad \sqrt{5} - 1, \quad \sqrt{7} - 1.$$

within the range of $\omega_2 \in (0, 2)$.

3.4.6 1-D Finite element formulation

From the analysis of the previous four sections we can see that, except for a few special frequencies, the four harmonics of trapped waves share the same generic form of BVP as follows:

$$\frac{d}{dx}(x f_x) - \left[x - w^2\right] f = g(x)$$

with the boundary conditions

$$xf_x = 0 \quad \text{as} \quad x \to 0$$

$$xf_x = 0 \quad \text{as} \quad x \to L$$

Therefore, the Finite Element formula is exactly the same as in the previous chapter (see Appendix E of last chapter.), although we have different definition for ω and $g(x)$ in this chapter. For convenience, we summarize the solution to the four trapped harmonics as follows:

$$\psi_{11} = -i\frac{A_1^*}{\omega_1}Bf_{11}(x)\cos y,$$

with

$$\omega = 1 - \omega_1, \quad g(x) = e^{-x}\left\{2(\omega_1 - 1)\frac{dJ_0(2\omega_1\sqrt{x})}{dx} + \frac{d^2J_0(2\omega_1\sqrt{x})}{dx^2}\right\};$$

$$\psi_{12} = -i\frac{A_2^*}{\omega_2}Bf_{12}(x)\cos y,$$

with

$$\omega = 1 - \omega_2, \quad g(x) = e^{-x}\left\{2(\omega_2 - 1)\frac{dJ_0(2\omega_2\sqrt{x})}{dx} + \frac{d^2J_0(2\omega_2\sqrt{x})}{dx^2}\right\};$$

$$\psi_{13} = -i\frac{A_1}{\omega_1}Bf_{13}(x)\cos y,$$

with

$$\omega = 1 + \omega_1, \quad g(x) = e^{-x}\left\{2(1 + \omega_1)\frac{dJ_0(2\omega_1\sqrt{x})}{dx} - \frac{d^2J_0(2\omega_1\sqrt{x})}{dx^2}\right\};$$

$$\psi_{14} = -i\frac{A_2}{\omega_2}Bf_{14}(x)\cos y,$$

with

$$\omega = 1 + \omega_2, \quad g(x) = e^{-x}\left\{2(1 + \omega_2)\frac{dJ_0(2\omega_2\sqrt{x})}{dx} - \frac{d^2J_0(2\omega_2\sqrt{x})}{dx^2}\right\}.$$

3.5 The third order

At $O(\epsilon^2)$ the governing equation for ψ_2 can be reduced to

$$H + [(xH_x)_x - xH] = -2\frac{\partial B}{\partial \tau}e^{-x} + \mathcal{E}(x) \tag{3.49}$$

after the introduction of

$$\psi_2 = H(x)\cos y$$

by separation of variables. $\mathcal{E}(x)$ denotes all the quadratic and cubic nonlinear terms of frequency 1 and with y-dependence of $\cos y$. Except one of the forcing $(\psi_0^*, \psi_0, \psi_0)$, each of these forcing terms has only one edge wave as its component, which makes them all proportional to $\cos y$. Later on we will show in (3.52) that even $(\psi_0^*, \psi_0, \psi_0)$ is only proportional to $\cos y$. Therefore we get

$$\begin{aligned} \mathcal{E}(x)\cos y &= (\phi_1, \psi_0^*) + (\psi_0^*, \psi_0, \psi_0) + (\psi_0, \phi_{01}, \phi_{01}^*) + (\psi_0, \phi_{02}, \phi_{02}^*) + (\psi_0^*, \phi_{01}, \phi_{02}) \\ &+ (\psi_{11}, \phi_{01}) + (\psi_{13}, \phi_{01}^*) + (\psi_{12}, \phi_{02}) + (\psi_{14}, \phi_{02}^*) + (\psi_{11}^*, \phi_{02}) + (\psi_{12}^*, \phi_{01}) \end{aligned} \tag{3.50}$$

We shall recall from (3.5) and (3.6) and work out all above nonlinear forcing terms as follows:

[C-1].

$$\begin{aligned} (\phi_1, \psi_0^*) &= 2\left[\phi_{1x}\psi_{0x}^*(i) + \psi_{0x}^*\phi_{1x}(-2i)\right] + \psi_1^*(i)\phi_{1xx} \\ &= -2i\phi_{1x}\psi_{0x}^* + i\phi_{1xx}\psi_1^* \\ &= e^{-x}\cos y\left\{-2i\frac{d\phi_1}{dx}iB^*(-1) + i\frac{d^2\phi_1}{dx^2}iB^*\right\} \\ &= -B^*e^{-x}\cos y\left(2k\frac{d\phi_1}{dx} + \frac{d^2\phi_1}{dx^2}\right) \\ &= \hat{h}_{C1}B^2B^*\cos y + \hat{g}_{C1}A_1A_2B^*\cos y \end{aligned} \tag{3.51}$$

where use has been made of

$$\psi_{0xx}^* + \psi_{0yy}^* = 0.$$

We have recalled that $\phi_1 = 2iB^2\phi_1^e + i\frac{A_1}{\omega_1}\frac{A_2}{\omega_2}\phi_1^i$ with ϕ_1^e and ϕ_1^i defined in (3.38) and (3.39). Therefore, $\hat{g}_{C1}$ is real because ϕ_1^i is real, whereas $\hat{h}_{C1}$ is complex because ϕ_1^e is complex.

[C-2].

$$\begin{aligned} &(\psi_0^*, \psi_0, \psi_0) \\ = \; &\psi_{0xx}2\psi_{0x}\psi_{0x}^* + \psi_{0xx}^*\psi_{0x}\psi_{0x} + \psi_{0yy}2\psi_{0y}\psi_{0y}^* + \psi_{0yy}^*\psi_{0y}\psi_{0y} \end{aligned}$$

$$
\begin{aligned}
&+ \quad 2\left(\psi_{0x}\psi_{0y}\psi^*_{1xy} + \psi_{0x}\psi^*_{0y}\psi_{1xy} + \psi^*_{0x}\psi_{0y}\psi_{1xy}\right) \\
&= \quad (-iB)^2\, iB^* e^{-3x}\Big\{3\cos^3 y - 2\cos y\sin^2 y - \cos y \sin^2 y \\
&+ \quad 2\Big[-\cos y\left(-\sin^2 y - \sin^2 y\right) + \cos y \sin^2 y\Big]\Big\} \\
&= \quad -iB^2B^* e^{-3x}\left\{3\cos^3 y + 3\cos y\sin^2 y\right\} \\
&= \quad -3iB^2B^* e^{-3x}\cos y \\
&\equiv \quad \hat{h}_{C2}B^2B^*\cos y
\end{aligned} \tag{3.52}
$$

[C-3] & [C-4].

$$
\begin{aligned}
& (\psi_0, \phi_{0n}, \phi^*_{0n}) \\
= \quad & \phi_{0nxx}\phi^*_{0nx}\psi_{0x} + \phi^*_{0nxx}\phi_{0nx}\psi_{0x} + 2\phi_{0nx}\phi^*_{0nx}\psi_{0xx} \\
& +2\psi_{0x}\phi^*_{0nx}\phi_{0nxx} + 2\psi_{0x}\phi_{0nx}\phi^*_{0nxx} \\
= \quad & 2\psi_{0xx}\phi^*_{0nx}\phi_{0nx} + 3\left(\phi_{0nxx}\phi^*_{0nx} + \phi^*_{0nxx}\phi_{0nx}\right)\psi_{0x} \\
= \quad & -i\,(-i)\,(-i)\,(-1)e^{-x}\cos y\left[2\left(\frac{dJ_0(2\omega_n\sqrt{x})}{dx}\right)^2\right. \\
& \left. - 6\frac{d^2J_0(2\omega_n\sqrt{x})}{dx^2}\frac{dJ_0(2\omega_n\sqrt{x})}{dx}\right]\frac{A_n}{\omega_n}\frac{A^*_n}{\omega_n}B \\
= \quad & -i\frac{A_n}{\omega_n}\frac{A^*_n}{\omega_n}Be^{-x}\cos y\left[2\left(\frac{dJ_0(2\omega_n\sqrt{x})}{dx}\right)^2 - 3\frac{d}{dx}\left(\frac{dJ_0(2\omega_n\sqrt{x})}{dx}\right)^2\right]
\end{aligned} \tag{3.53}
$$

with $n = 1, 2$. For brevity, we introduce

$$
\hat{f}_{C3} = \frac{e^{-x}}{\omega_1^2}\left[2\left(\frac{dJ_0(2\omega_1\sqrt{x})}{dx}\right)^2 - 3\frac{d}{dx}\left(\frac{dJ_0(2\omega_1\sqrt{x})}{dx}\right)^2\right]
$$

$$
\hat{f}_{C4} = \frac{e^{-x}}{\omega_2^2}\left[2\left(\frac{dJ_0(2\omega_2\sqrt{x})}{dx}\right)^2 - 3\frac{d}{dx}\left(\frac{dJ_0(2\omega_2\sqrt{x})}{dx}\right)^2\right]
$$

[C-5]. Similarly,

$$
\begin{aligned}
& (\psi^*_0, \phi_{01}, \phi_{02}) \\
= \quad & 2\psi^*_{0xx}\phi_{01x}\phi_{02x} + 3\left(\phi_{01xx}\phi_{02x} + \phi_{02xx}\phi_{01x}\right)\psi^*_{0x} \\
= \quad & B^* i\left(-i\frac{A_1}{\omega_1}\right)\left(-i\frac{A_2}{\omega_2}\right)e^{-x}\cos y\left[2\frac{dJ_0(2\omega_1\sqrt{x})}{dx}\frac{dJ_0(2\omega_2\sqrt{x})}{dx}\right. \\
& \left. - 3\left(\frac{d^2J_0(2\omega_1\sqrt{x})}{dx^2}\frac{dJ_0(2\omega_2\sqrt{x})}{dx} + \frac{d^2J_0(2\omega_2\sqrt{x})}{dx^2}\frac{dJ_0(2\omega_1\sqrt{x})}{dx}\right)\right]
\end{aligned}
$$

$$
\begin{aligned}
&= -i\frac{A_1}{\omega_1}\frac{A_2}{\omega_2}B^* e^{-x}\cos y\left[2\frac{dJ_0(2\omega_1\sqrt{kx})}{dx}\frac{dJ_0(2\omega_2\sqrt{x})}{dx}\right. \\
&\quad \left. -3\frac{d}{dx}\left(\frac{dJ_0(2\omega_1\sqrt{x})}{dx}\frac{dJ_0(2\omega_2\sqrt{x})}{dx}\right)\right] \\
&\equiv \hat{g}_{C5}A_1A_2B^*\cos y
\end{aligned}
\tag{3.54}
$$

[C-6].

$$
\begin{aligned}
&(\psi_{11}, \phi_{01}) \\
&= 2\left[\psi_{11x}\phi_{01x}(-i\omega_1) - i(1-\omega_1)\phi_{01x}\psi_{11x}\right] \\
&\quad -i(1-\omega_1)\psi_{11}\phi_{01xx} - i\omega_1\phi_{01}\left(\psi_{11xx}+\psi_{11yy}\right) \\
&= -i\frac{A_1^*}{\omega_1}B(-i\frac{A_1}{\omega_1})\cos y\left[-i2f_{11x}\frac{dJ_0(2\omega_1\sqrt{x})}{dx}\right. \\
&\quad \left. -i(1-\omega_1)f_{11}\frac{d^2J_0(2\omega_1\sqrt{x})}{dx^2} - i\omega_1 J_0(2\omega_1\sqrt{x})\left(f_{11xx}-f_{11}\right)\right] \\
&= i\frac{A_1}{\omega_1}\frac{A_1^*}{\omega_1}B\cos y\left[2f_{11x}\frac{dJ_0(2\omega_1\sqrt{x})}{dx}\right. \\
&\quad \left. +(1-\omega_1)f_{11}\frac{d^2J_0(2\omega_1\sqrt{x})}{dx^2} + \omega_1 J_0(2\omega_1\sqrt{x})\left(f_{11xx}-f_{11}\right)\right] \\
&\equiv -i\hat{f}_{C6}|A_1|^2B\cos y
\end{aligned}
\tag{3.55}
$$

where f_{11} is defined by Eq. (3.43).

[C-7].

$$
\begin{aligned}
&(\psi_{12}, \phi_{02}) \\
&= 2\left[\psi_{12x}\phi_{02x}(-i\omega_2) - i(1-\omega_2)\phi_{02x}\psi_{12x}\right] \\
&\quad -i(1-\omega_2)\psi_{12}\phi_{02xx} - i\omega_2\phi_{02}\left(\psi_{12xx}+\psi_{12yy}\right) \\
&= -i\frac{A_2^*}{\omega_2}B(-i\frac{A_2}{\omega_2})\cos y\left[-i2f_{12x}\frac{dJ_0(2\omega_2\sqrt{x})}{dx}\right. \\
&\quad \left. -i(1-\omega_2)f_{12}\frac{d^2J_0(2\omega_2\sqrt{x})}{dx^2} - i\omega_2 J_0(2\omega_2\sqrt{x})\left(f_{12xx}-f_{12}\right)\right] \\
&= i\frac{A_2}{\omega_2}\frac{A_2^*}{\omega_2}B\cos y\left[2f_{12x}\frac{dJ_0(2\omega_2\sqrt{x})}{dx}\right. \\
&\quad \left. +(1-\omega_2)f_{121}\frac{d^2J_0(2\omega_2\sqrt{x})}{dx^2} + \omega_2 J_0(2\omega_2\sqrt{x})\left(f_{12xx}-f_{12}\right)\right] \\
&\equiv -i\hat{f}_{C7}|A_2|^2B\cos y
\end{aligned}
\tag{3.56}
$$

where f_{12} is defined by Eq. (3.45).

[C-8].

$$
\begin{aligned}
& (\psi_{13}, \phi_{01}^*) \\
= \; & 2\left[\psi_{13x}\phi_{01x}^*(i\omega_1) - i(1+\omega_1)\phi_{01x}^*\psi_{13x}\right] \\
& -i(1+\omega_1)\psi_{13}\phi_{01xx}^* + i\omega_1\phi_{01}^*\left(\psi_{13xx}+\psi_{13yy}\right) \\
= \; & -i\frac{A_1}{\omega_1}B(i\frac{A_1^*}{\omega_1})\cos y\left[-i2f_{13x}\frac{dJ_0(2\omega_1\sqrt{x})}{dx}\right. \\
& \left. -i(1+\omega_1)f_{13}\frac{d^2J_0(2\omega_1\sqrt{x})}{dx^2} + i\omega_1 J_0(2\omega_1\sqrt{x})\left(f_{13xx}-f_{13}\right)\right] \\
= \; & -i\frac{A_1}{\omega_1}\frac{A_1^*}{\omega_1}B\cos y\left[2f_{13x}\frac{dJ_0(2\omega_1\sqrt{x})}{dx}\right. \\
& \left. +(1+\omega_1)f_{13}\frac{d^2J_0(2\omega_1\sqrt{x})}{dx^2} - \omega_1 J_0(2\omega_1\sqrt{x})\left(f_{13xx}-f_{13}\right)\right] \\
\equiv \; & -i\hat{f}_{C8}|A_1|^2B\cos y
\end{aligned}
\tag{3.57}
$$

where f_{13} is defined by Eq. (3.46).

[C-9].

$$
\begin{aligned}
& (\psi_{14}, \phi_{02}^*) \\
= \; & 2\left[\psi_{14x}\phi_{02x}^*(i\omega_2) - i(1+\omega_2)\phi_{02x}^*\psi_{14x}\right] \\
& -i(1+\omega_2)\psi_{14}\phi_{02xx}^* + i\omega_2\phi_{02}^*\left(\psi_{14xx}+\psi_{14yy}\right) \\
= \; & -i\frac{A_2}{\omega_2}B(i\frac{A_2^*}{\omega_2})\cos y\left[-i2f_{14x}\frac{dJ_0(2\omega_2\sqrt{x})}{dx}\right. \\
& \left. -i(1+\omega_2)f_{14}\frac{d^2J_0(2\omega_2\sqrt{x})}{dx^2} + i\omega_2 J_0(2\omega_2\sqrt{x})\left(f_{14xx}-f_{14}\right)\right] \\
= \; & -i\frac{A_2}{\omega_2}\frac{A_2^*}{\omega_2}B\cos y\left[2f_{14x}\frac{dJ_0(2\omega_2\sqrt{x})}{dx}\right. \\
& \left. +(1+\omega_2)f_{14}\frac{d^2J_0(2\omega_2\sqrt{x})}{dx^2} - \omega_2 J_0(2\omega_2\sqrt{x})\left(f_{14xx}-f_{14}\right)\right] \\
\equiv \; & -i\hat{f}_{C9}|A_2|^2B\cos y
\end{aligned}
\tag{3.58}
$$

where f_{14} is defined by Eq. (3.48).

[C-10].

$$(\psi_{11}^*, \phi_{02})$$

$$
\begin{aligned}
&= 2\left[\psi^*_{11x}\phi_{02x}(-i\omega_2) + i(1-\omega_1)\phi_{02x}\psi^*_{11x}\right] \\
&\quad + i(1-\omega_1)\psi^*_{11}\phi_{02xx} - i\omega_2\phi_{02}\left(\psi^*_{11xx} + \psi^*_{11yy}\right) \\
&= i\frac{A_1}{\omega_1}B^*(-i\frac{A_2}{\omega_2})\cos y\left[-i2f_{11x}\frac{dJ_0(2\omega_2\sqrt{x})}{dx}\right. \\
&\quad \left. + i(1-\omega_1)f_{11}\frac{d^2J_0(2\omega_2\sqrt{x})}{dx^2} - i\omega_2 J_0(2\omega_2\sqrt{x})\left(f_{11xx} - f_{11}\right)\right] \\
&= -i\frac{A_1}{\omega_1}\frac{A_2}{\omega_2}B^*\cos y\left[2f_{11x}\frac{dJ_0(2\omega_2\sqrt{x})}{dx}\right. \\
&\quad \left. -(1-\omega_1)f_{11}\frac{d^2J_0(2\omega_2\sqrt{x})}{dx^2} + \omega_2 J_0(2\omega_2\sqrt{x})\left(f_{11xx} - f_{11}\right)\right] \\
&\equiv \hat{g}_{C10}A_1A_2B^*\cos y
\end{aligned}
\tag{3.59}
$$

where f_{11} is defined by Eq. (3.43).

[C-11].

$$
\begin{aligned}
&(\psi^*_{12}, \phi_{01}) \\
&= 2\left[\psi^*_{12x}\phi_{01x}(-i\omega_1) + i(1-\omega_2)\phi_{01x}\psi^*_{12x}\right] \\
&\quad + i(1-\omega_2)\psi^*_{12}\phi_{01xx} - i\omega_1\phi_{01}\left(\psi^*_{12xx} + \psi^*_{12yy}\right) \\
&= i\frac{A_2}{\omega_2}B^*(-i\frac{A_1}{\omega_1})\cos y\left[-i2f_{12x}\frac{dJ_0(2\omega_1\sqrt{x})}{dx}\right. \\
&\quad \left. + i(1-\omega_2)f_{12}\frac{d^2J_0(2\omega_1\sqrt{x})}{dx^2} - i\omega_1 J_0(2\omega_1\sqrt{x})\left(f_{12xx} - f_{12}\right)\right] \\
&= -i\frac{A_1}{\omega_1}\frac{A_2}{\omega_2}B^*\cos y\left[2f_{12x}\frac{dJ_0(2\omega_1\sqrt{x})}{dx}\right. \\
&\quad \left. -(1-\omega_2)f_{12}\frac{d^2J_0(2\omega_1\sqrt{x})}{dx^2} + \omega_1 J_0(2\omega_1\sqrt{x})\left(f_{12xx} - f_{12}\right)\right] \\
&\equiv \hat{g}_{C11}A_1A_2B^*\cos y
\end{aligned}
\tag{3.60}
$$

where f_{12} is defined by Eq. (3.45).

In summary, we group the terms according to B, B^* and B^2B^*, and get

$$
\mathcal{E}(x) = -i\left(\hat{f}_1(x)|A_1|^2 + \hat{f}_2(x)|A_2|^2\right)B + \hat{g}(x)A_1A_2B^* + \hat{h}(x)B^2B^* \tag{3.61}
$$

where $-i\left(\hat{f}_1(x)|A_1|^2 + \hat{f}_2(x)|A_2|^2\right), \hat{g}, \hat{h}$ are the sum of coefficients of B, B^* and $|B|^2B$ respectively. Specifically

- $i\hat{f}_1(x)$ is collected from [C-3], [C-6] and [C-8], i.e.,

$$\hat{f}_1 = \hat{f}_{C3} + \hat{f}_{C6} + \hat{f}_{C8}. \tag{3.62}$$

- $i\hat{f}_2(x)$ is collected from [C-4], [C-7] and [C-9], i.e.,

$$\hat{f}_2 = \hat{f}_{C4} + \hat{f}_{C7} + \hat{f}_{C9}. \tag{3.63}$$

- $\hat{g}(x)$ is collected from [C-1], [C-5], [C-10] and [C-11], i.e.,

$$\hat{g} = \hat{g}_{C1} + \hat{g}_{C5} + \hat{g}_{C10} + \hat{g}_{C11}. \tag{3.64}$$

- $\hat{h}(x)$ is collected from [C-1] and [C-2], i.e.

$$\hat{h}(x) = \hat{h}_{C1}(x) + \hat{h}_{C2}(x) \tag{3.65}$$

.

3.5.1 Solvability and evolution equation

The homogeneous version of Eq. (3.49) has nontrivial solution $F = e^{-x}$ as described at the first order. By Green's formula,

$$\begin{aligned} \int_0^\infty (H\mathcal{L}F - F\mathcal{L}H)dx &= \int_0^\infty [H(xF_x)_x - F(xH_x)_x]\,dx \\ &= \int_0^\infty [(xHF_x)_x - (xFH_x)_x]\,dx = 0 \end{aligned}$$

Therefore

$$\int_0^\infty F\mathcal{L}H dx = 0 \quad since \quad \mathcal{L}F = 0$$

This gives the solvability condition

$$\int_0^\infty dx e^{-x}\left(-2\frac{\partial B}{\partial \tau}e^{-x} + \mathcal{E}(x)\right) = 0$$

which can be rewritten as

$$\frac{\partial B}{\partial \tau} = f(B)$$

governing the evolution of the edge wave amplitude B for given A_1 and A_2. By collection of the similar terms with respect to B, the evolution equation of the edge wave amplitude can be written as

$$\begin{aligned}\frac{\partial B}{\partial \tau} &= \int_0^\infty dx e^{-x}\mathcal{E}(x) \\ &= -i\left(a_1(\omega_1)|A_1|^2 + a_2(\omega_2)|A_2|^2\right)B + a_3(\omega_1,\omega_2)A_1A_2B^* + \kappa|B|^2B \quad (3.66)\end{aligned}$$

where a_1, a_2, a_3 and κ are constants obtained by numerical integrations

$$[a_1, a_2, a_3, \kappa] = \int_0^\infty e^{-x}[\hat{f}_1(x), \hat{f}_2(x), \hat{g}(x), \hat{h}(x)]dx, \quad (3.67)$$

3.5.2 The coupling coefficients

We now derive the coefficient a_1, a_2 and a_3 from the integral of [C-1] to [C-11] explicitly. [C-1]. From (ϕ_1, ψ_0^*) in (3.51):

$$\begin{aligned}&\int_0^\infty dx e^{-x}\left(-B^*\right)e^{-x}\left(2\frac{d\phi_1}{dx} + \frac{d^2\phi_1}{dx^2}\right) \\ &= -B^*\int_0^\infty dx e^{-2x}\left(2\frac{d\phi_1}{dx} + \frac{d^2\phi_1}{dx^2}\right) \\ &= -B^*\left(-4\phi_1(0) - \left.\frac{d\phi_1(x)}{dx}\right|_{x=0} + 8\int_0^\infty dx e^{-2x}\phi_1(x)\right) \\ &= -B^*\left(-g(0) + 8\int_0^\infty dx e^{-2x}\phi_1(x)\right) \\ &= g(0)B^* - 8B^*\int_0^\infty dx e^{-2x}\phi_1(x) \quad (3.68)\end{aligned}$$

Use has been made of (3.41) and (3.42). We recall that

$$g(0) = 2iB^2 + i\frac{A_1}{\omega_1}\frac{A_2}{\omega_2}\omega_1^2\omega_2^2\left\{4 + \frac{\omega_2^2}{2\omega_1} + \frac{\omega_1^2}{2\omega_2}\right\}$$

from (3.40) and $\phi_1 = 2iB^2\phi_1^e + ie^{i2\varphi}\phi_1^i$ with ϕ_1^e and ϕ_1^i defined in (3.38) and (3.39). Therefore,

$$g(0)B^* = 2iB^2B^* + i\omega_1^2\omega_2^2\left\{4 + \frac{\omega_2^2}{2\omega_1} + \frac{\omega_1^2}{2\omega_2}\right\}\frac{A_1}{\omega_1}\frac{A_2}{\omega_2}B^*$$

and

$$-8B^*\int_0^\infty dx e^{-2x}\phi_1(x)$$

$$
\begin{aligned}
&= -16iB^2B^*\int_0^\infty dxe^{-2x}\phi_1^e - 8ie^{i2\varphi}B^*\int_0^\infty dxe^{-2x}\phi_1^i \\
&= -16iB^2B^*\int_0^\infty dxe^{-2x}\left\{\left[-u_1^e(\infty) - iu_2^e(\infty)\right]J_0(4\sqrt{x})\right. \\
&\quad \left. +u_1^e(x)J_0(4\sqrt{x}) + u_2^e(x)Y_0(4\sqrt{x})\right\} \\
&\quad -8ie^{i2\varphi}B^*\int_0^\infty dxe^{-2x}\left\{\left[-u_1^i(\infty) - iu_2^i(\infty)\right]J_0(4\sqrt{x})\right. \\
&\quad \left. +u_1^i(x)J_0(4\sqrt{x}) + u_2^i(x)Y_0(4\sqrt{x})\right\} \\
&= 16i\int_0^\infty dxe^{-2x}J_0(4\sqrt{x})u_1^e(\infty)B^2B^* + 8ie^{i2\varphi}\int_0^\infty dxe^{-2x}J_0(4\sqrt{x})u_1^i(\infty)B^* \\
&\quad -16i\int_0^\infty dxe^{-2x}J_0(4\sqrt{x})u_1^e(x)B^2B^* - 8ie^{i2\varphi}\int_0^\infty dxe^{-2x}J_0(4\sqrt{x})u_1^i(x)B^* \\
&\quad -16\int_0^\infty dxe^{-2x}J_0(4\sqrt{x})u_2^e(\infty)B^2B^* - 8e^{i2\varphi}\int_0^\infty dxe^{-2x}J_0(4\sqrt{x})u_2^i(\infty)B^* \\
&\quad -16i\int_0^\infty dxe^{-2x}Y_0(4\sqrt{x})u_2^e(x)B^2B^* - 8ie^{i2\varphi}\int_0^\infty dxe^{-2x}Y_0(4\sqrt{x})u_2^i(x)B^*
\end{aligned}
\tag{3.69}
$$

Therefore, the R.H.S. of (3.68)

$$
\begin{aligned}
& g(0)B^* - 8B^*\int_0^\infty dxe^{-2x}\phi_1(x) \\
&= 2iB^2B^* + i\omega_1^2\omega_2^2\left\{4 + \frac{\omega_2^2}{2\omega_1} + \frac{\omega_1^2}{2\omega_2}\right\}\frac{A_1}{\omega_1}\frac{A_2}{\omega_2}B^* \\
&- 16i\pi\kappa_1B^2B^* - 8i\pi\left(4\beta_1 + \omega_1\beta_2 + \omega_2\beta_3\right)\frac{A_1}{\omega_1}\frac{A_2}{\omega_2}B^* \\
&+ 16i\pi\kappa_2B^2B^* + 8i\pi\left(4\beta_4 + \omega_1\beta_5 + \omega_2\beta_6\right)\frac{A_1}{\omega_1}\frac{A_2}{\omega_2}B^* \\
&- 16\pi\kappa_3B^2B^* - 8\pi\left(4\beta_7 + \omega_1\beta_8 + \omega_2\beta_9\right)\frac{A_1}{\omega_1}\frac{A_2}{\omega_2}B^* \\
&- 16i\pi\kappa_4B^2B^* - 8i\pi\left(4\beta_{10} + \omega_1\beta_{11} + \omega_2\beta_{12}\right)\frac{A_1}{\omega_1}\frac{A_2}{\omega_2}B^*
\end{aligned}
$$

with

$$\kappa_1 = \int_0^\infty dxe^{-2x}J_0(4\sqrt{x})\int_0^\infty d\xi e^{-2\xi}Y_0(4\sqrt{\xi})$$

$$\beta_1 = \int_0^\infty dxe^{-2x}J_0(4\sqrt{x})\int_0^\infty d\xi Y_0(4\sqrt{\xi})\frac{dJ_0(2\omega_1\sqrt{\xi})}{d\xi}\frac{dJ_0(2\omega_2\sqrt{\xi})}{d\xi}$$

$$\beta_2 = \int_0^\infty dxe^{-2x}J_0(4\sqrt{x})\int_0^\infty d\xi Y_0(4\sqrt{\xi})J_0(2\omega_1\sqrt{\xi})\frac{d^2J_0(2\omega_2\sqrt{\xi})}{d\xi^2}$$

$$\beta_3 = \int_0^\infty dxe^{-2x}J_0(4\sqrt{x})\int_0^\infty d\xi Y_0(4\sqrt{\xi})J_0(2\omega_2\sqrt{\xi})\frac{d^2J_0(2\omega_1\sqrt{\xi})}{d\xi^2}$$

$$\kappa_2 = \int_0^\infty dx e^{-2x} J_0(4\sqrt{x}) \int_0^x d\xi e^{-2\xi} Y_0(4\sqrt{\xi})$$

$$\beta_4 = \int_0^\infty dx e^{-2x} J_0(4\sqrt{x}) \int_0^x d\xi Y_0(4\sqrt{\xi}) \frac{dJ_0(2\omega_1\sqrt{\xi})}{d\xi} \frac{dJ_0(2\omega_2\sqrt{\xi})}{d\xi}$$

$$\beta_5 = \int_0^\infty dx e^{-2x} J_0(4\sqrt{x}) \int_0^x d\xi Y_0(4\sqrt{\xi}) J_0(2\omega_1\sqrt{\xi}) \frac{d^2 J_0(2\omega_2\sqrt{\xi})}{d\xi^2}$$

$$\beta_6 = \int_0^\infty dx e^{-2x} J_0(4\sqrt{x}) \int_0^x d\xi Y_0(4\sqrt{\xi}) J_0(2\omega_2\sqrt{\xi}) \frac{d^2 J_0(2\omega_1\sqrt{\xi})}{d\xi^2}$$

$$\kappa_3 = \int_0^\infty dx e^{-2x} J_0(4\sqrt{x}) \int_0^\infty d\xi e^{-2\xi} J_0(4\sqrt{\xi})$$

$$\beta_7 = \int_0^\infty dx e^{-2x} J_0(4\sqrt{x}) \int_0^\infty d\xi J_0(4\sqrt{\xi}) \frac{dJ_0(2\omega_1\sqrt{\xi})}{d\xi} \frac{dJ_0(2\omega_2\sqrt{\xi})}{d\xi}$$

$$\beta_8 = \int_0^\infty dx e^{-2x} J_0(4\sqrt{x}) \int_0^\infty d\xi J_0(4\sqrt{\xi}) J_0(2\omega_1\sqrt{\xi}) \frac{d^2 J_0(2\omega_2\sqrt{\xi})}{d\xi^2}$$

$$\beta_9 = \int_0^\infty dx e^{-2x} J_0(4\sqrt{x}) \int_0^\infty d\xi J_0(4\sqrt{\xi}) J_0(2\omega_2\sqrt{\xi}) \frac{d^2 J_0(2\omega_1\sqrt{\xi})}{d\xi^2}$$

$$\kappa_4 = \int_0^\infty dx e^{-2x} Y_0(4\sqrt{x}) \int_0^x d\xi e^{-2\xi} J_0(4\sqrt{\xi})$$

$$\beta_{10} = \int_0^\infty dx e^{-2x} Y_0(4\sqrt{x}) \int_0^x d\xi J_0(4\sqrt{\xi}) \frac{dJ_0(2\omega_1\sqrt{\xi})}{d\xi} \frac{dJ_0(2\omega_2\sqrt{\xi})}{d\xi}$$

$$\beta_{11} = \int_0^\infty dx e^{-2x} Y_0(4\sqrt{x}) \int_0^x d\xi J_0(4\sqrt{\xi}) J_0(2\omega_1\sqrt{\xi}) \frac{d^2 J_0(2\omega_2\sqrt{\xi})}{d\xi^2}$$

$$\beta_{12} = \int_0^\infty dx e^{-2x} Y_0(4\sqrt{x}) \int_0^x d\xi J_0(4\sqrt{\xi}) J_0(2\omega_2\sqrt{\xi}) \frac{d^2 J_0(2\omega_1\sqrt{\xi})}{d\xi^2}$$

[C-2]. From $(\psi_0^*, \psi_0, \psi_0)$ in (3.52):

$$\int_0^\infty dx e^{-x} (-3i) e^{-3x} B^2 B^* = -\frac{3i}{4} B^2 B^*$$

[C-3]. & [C-4]. From $(\psi_0, \phi_{01}, \phi_{01}^*)$ and $(\psi_0, \phi_{02}, \phi_{02}^*)$ in (3.53):

$$\begin{aligned}
&\int_0^\infty dx e^{-x} (-i) e^{-x} \left[2 \left(\frac{dJ_0(2\omega_n\sqrt{x})}{dx} \right)^2 - 3 \frac{d}{dx} \left(\frac{dJ_0(2\omega_n\sqrt{x})}{dx} \right)^2 \right] \frac{A_n}{\omega_n} \frac{A_n^*}{\omega_n} B \\
&= -i \int_0^\infty dx e^{-2x} \left[2 \left(\frac{dJ_0(2\omega_n\sqrt{x})}{dx} \right)^2 - 3 \frac{d}{dx} \left(\frac{dJ_0(2\omega_n\sqrt{x})}{dx} \right)^2 \right] \frac{A_n}{\omega_n} \frac{A_n^*}{\omega_n} B \\
&= -i \left[3 \left(\frac{dJ_0(2\omega_n\sqrt{x})}{dx} \right)^2 \Bigg|_{x=0} - 4 \int_0^\infty dx e^{-2x} \left(\frac{dJ_0(2\omega_n\sqrt{x})}{dx} \right)^2 \right] \frac{A_n}{\omega_n} \frac{A_n^*}{\omega_n} B \\
&= -i \left(3\omega_n^4 - 4\alpha_n \right) \frac{A_n}{\omega_n} \frac{A_n^*}{\omega_n} B
\end{aligned}$$

with

$$\alpha_n = \int_0^\infty dx e^{-2x} \left(\frac{dJ_0\left(2\omega_n \sqrt{x}\right)}{dx} \right)^2$$

with $n = 1, 2$.

[C-5]. From $(\psi_0^*, \phi_{01}, \phi_{02})$ in (3.54):

$$\begin{aligned} & \int_0^\infty dx e^{-x} \left(-i\right) e^{-x} \left[2 \frac{dJ_0(2\omega_1\sqrt{x})}{dx} \frac{dJ_0(2\omega_2\sqrt{x})}{dx} \right. \\ & \left. - 3 \frac{d}{dx} \left(\frac{dJ_0(2\omega_1\sqrt{x})}{dx} \frac{dJ_0(2\omega_2\sqrt{x})}{dx} \right) \right] \frac{A_1}{\omega_1} A_2 B^* \\ = & -i \left[3\omega_1^2 \omega_2^2 - 4\beta_{13} \right] \frac{A_1}{\omega_1} \frac{A_2}{\omega_2} B^* \end{aligned}$$

with

$$\beta_{13} = \int_0^\infty dx e^{-2x} \frac{dJ_0\left(2\omega_1\sqrt{x}\right)}{dx} \frac{dJ_0\left(2\omega_2\sqrt{x}\right)}{dx}$$

[C-6]. From (ψ_{11}, ϕ_{01}) in (3.55):

$$\begin{aligned} & i \int_0^\infty dx e^{-x} \left[2 f_{11x} \frac{dJ_0(2\omega_1\sqrt{x})}{dx} + (1-\omega_1) f_{11} \frac{d^2 J_0(2\omega_1\sqrt{x})}{dx^2} \right. \\ & \left. + \omega_1 J_0(2\omega_1\sqrt{x}) \left(f_{11xx} - f_{11} \right) \right] \frac{A_1}{\omega_1} \frac{A_1^*}{\omega_1} B \\ = & \; i\alpha_3 \frac{A_1}{\omega_1} \frac{A_1^*}{\omega_1} B \end{aligned} \tag{3.70}$$

with

$$\begin{aligned} \alpha_3 \;=\; & \int_0^\infty dx e^{-x} \left[2 f_{11x} \frac{dJ_0(2\omega_1\sqrt{x})}{dx} + (1-\omega_1) f_{11} \frac{d^2 J_0(2\omega_1\sqrt{x})}{dx^2} \right. \\ & \left. + \omega_1 J_0(2\omega_1\sqrt{x}) \left(f_{11xx} - f_{11} \right) \right] \\ = \; & -\omega_1 f_{11x}(0) - \omega_1 (1-\omega_1)^2 f_{11}(0) \\ & + \int_0^\infty dx e^{-x} f_{11} \left[2(1-\omega_1) \frac{dJ_0(2\omega_1\sqrt{x})}{dx} - \frac{d^2 J_0(2\omega_1\sqrt{x})}{dx^2} \right] \end{aligned} \tag{3.71}$$

Use has been made of the generic form of the partial integral

$$\int_0^\infty dx f(x) e^{-x} \frac{dG}{dx} = -f(0)G(0) - \int_0^\infty dx (f' - f) e^{-x} G.$$

[C-7]. From (ψ_{12}, ϕ_{02}) in (3.56):

$$i \int_0^\infty dx e^{-x} \left[2 f_{12x} \frac{dJ_0(2\omega_2\sqrt{x})}{dx} + (1-\omega_2) f_{12} \frac{d^2 J_0(2\omega_2\sqrt{x})}{dx^2} \right.$$

$$
\begin{aligned}
&+\omega_2 J_0(2\omega_2\sqrt{x})\,(f_{12xx} - f_{12})\Big] \frac{A_2}{\omega_2}\frac{A_2^*}{\omega_2} B \\
&= \; i\alpha_4 \frac{A_2}{\omega_2}\frac{A_2^*}{\omega_2} B
\end{aligned}
\tag{3.72}
$$

with

$$
\begin{aligned}
\alpha_4 \;&=\; \int_0^\infty dx e^{-x}\left[2 f_{12x}\frac{dJ_0(2\omega_2\sqrt{x})}{dx} + (1-\omega_2) f_{12}\frac{d^2 J_0(2\omega_2\sqrt{x})}{dx^2}\right. \\
&\quad \left. +\omega_2 J_0(2\omega_2\sqrt{x})\,(f_{12xx} - f_{12})\right] \\
&= \; -\omega_2 f_{12x}(0) - \omega_2(1-\omega_2)^2 f_{12}(0) \\
&\quad + \int_0^\infty dx e^{-x} f_{12}\left[2(1-\omega_2)\frac{dJ_0(2\omega_2\sqrt{x})}{dx} - \frac{d^2 J_0(2\omega_2\sqrt{x})}{dx^2}\right]
\end{aligned}
\tag{3.73}
$$

[C-8]. From (ψ_{13}, ϕ_{01}^*) in (3.57):

$$
\begin{aligned}
&-i\int_0^\infty dx e^{-x}\left[2 f_{13x}\frac{dJ_0(2\omega_1\sqrt{x})}{dx} + (1+\omega_1) f_{13}\frac{d^2 J_0(2\omega_1\sqrt{x})}{dx^2}\right. \\
&\left. -\omega_1 J_0(2\omega_1\sqrt{x})\,(f_{13xx} - f_{13})\right] \frac{A_1}{\omega_1}\frac{A_1^*}{\omega_1} B \\
&= \; -i\alpha_5 \frac{A_1}{\omega_1}\frac{A_1^*}{\omega_1} B
\end{aligned}
\tag{3.74}
$$

with

$$
\begin{aligned}
\alpha_5 \;&=\; \int_0^\infty dx e^{-x}\left[2 f_{13x}\frac{dJ_0(2\omega_1\sqrt{x})}{dx} + (1+\omega_1) f_{13}\frac{d^2 J_0(2\omega_1\sqrt{x})}{dx^2}\right. \\
&\quad \left. -\omega_1 J_0(2\omega_1\sqrt{x})\,(f_{13xx} - f_{13})\right] \\
&= \; \omega_1 f_{13x}(0) + \omega_1(1+\omega_1)^2 f_{13}(0) \\
&\quad + \int_0^\infty dx e^{-x} f_{13}\left[2(1+\omega_1)\frac{dJ_0(2\omega_1\sqrt{x})}{dx} - \frac{d^2 J_0(2\omega_1\sqrt{x})}{dx^2}\right]
\end{aligned}
\tag{3.75}
$$

[C-9]. From (ψ_{14}, ϕ_{02}^*) in (3.58):

$$
\begin{aligned}
&-i\int_0^\infty dx e^{-x}\left[2 f_{14x}\frac{dJ_0(2\omega_2\sqrt{x})}{dx} + (1+\omega_2) f_{14}\frac{d^2 J_0(2\omega_2\sqrt{x})}{dx^2}\right. \\
&\left. -\omega_2 J_0(2\omega_2\sqrt{x})\,(f_{14xx} - f_{14})\right] \frac{A_2}{\omega_2}\frac{A_2^*}{\omega_2} B \\
&= \; -i\alpha_6 \frac{A_2}{\omega_2}\frac{A_2^*}{\omega_2} B
\end{aligned}
\tag{3.76}
$$

with

$$\begin{aligned}\alpha_6 &= \int_0^\infty dx e^{-x} \left[2 f_{14x} \frac{dJ_0(2\omega_2\sqrt{x})}{dx} + (1+\omega_2) f_{14} \frac{d^2 J_0(2\omega_2\sqrt{x})}{dx^2} \right. \\ & \left. -\omega_2 J_0(2\omega_2\sqrt{x}) \left(f_{14xx} - f_{14}\right) \right] \\ &= \omega_2 f_{14x}(0) + \omega_2 (1+\omega_2)^2 f_{14}(0) \\ & + \int_0^\infty dx e^{-x} f_{14} \left[2(1+\omega_2) \frac{dJ_0(2\omega_2\sqrt{x})}{dx} - \frac{d^2 J_0(2\omega_2\sqrt{x})}{dx^2} \right] \end{aligned} \tag{3.77}$$

[C-10]. From (ψ_{11}^*, ϕ_{02}) in (3.59):

$$\begin{aligned} & -i \int_0^\infty dx e^{-x} \left[2 f_{11x} \frac{dJ_0(2\omega_2\sqrt{x})}{dx} - (1-\omega_1) f_{11} \frac{d^2 J_0(2\omega_2\sqrt{x})}{dx^2} \right. \\ & \left. +\omega_2 J_0(2\omega_2\sqrt{x}) \left(f_{11xx} - f_{11}\right) \right] \frac{A_1}{\omega_1} \frac{A_2}{\omega_2} B^* \\ &= -i\beta_{14} \frac{A_1}{\omega_1} \frac{A_2}{\omega_2} B^* \end{aligned} \tag{3.78}$$

with

$$\begin{aligned}\beta_{14} &= \int_0^\infty dx e^{-x} \left[2 f_{11x} \frac{dJ_0(2\omega_2\sqrt{x})}{dx} - (1-\omega_1) f_{11} \frac{d^2 J_0(2\omega_2\sqrt{x})}{dx^2} \right. \\ & \left. +\omega_2 J_0(2\omega_2\sqrt{x}) \left(f_{11xx} - f_{11}\right) \right] \\ &= -\omega_2 f_{11x}(0) - \omega_2 (1-\omega_2)^2 f_{11}(0) \\ & + \int_0^\infty dx e^{-x} f_{11} \left[2(\omega_2 - 1) \frac{dJ_0(2\omega_2\sqrt{x})}{dx} - \frac{d^2 J_0(2\omega_2\sqrt{x})}{dx^2} \right] \end{aligned} \tag{3.79}$$

[C-11]. From (ψ_{12}^*, ϕ_{01}) in (3.60):

$$\begin{aligned} & -i \int_0^\infty dx e^{-x} \left[2 f_{12x} \frac{dJ_0(2\omega_1\sqrt{x})}{dx} - (1-\omega_2) f_{11} \frac{d^2 J_0(2\omega_1\sqrt{x})}{dx^2} \right. \\ & \left. +\omega_1 J_0(2\omega_1\sqrt{x}) \left(f_{12xx} - f_{12}\right) \right] \frac{A_1}{\omega_1} \frac{A_2}{\omega_2} B^* \\ &= -i\beta_{15} \frac{A_1}{\omega_1} \frac{A_2}{\omega_2} B^* \end{aligned} \tag{3.80}$$

with

$$\beta_{15} = \int_0^\infty dx e^{-x} \left[2 f_{12x} \frac{dJ_0(2\omega_1\sqrt{x})}{dx} - (1-\omega_2) f_{11} \frac{d^2 J_0(2\omega_1\sqrt{x})}{dx^2} \right.$$

$$+\omega_1 J_0(2\omega_1\sqrt{x})\left(f_{12xx}-f_{12}\right)\Big]$$

$$\begin{aligned}
&= -\omega_1 f_{12x}(0) - \omega_1(1-\omega_1)^2 f_{12}(0) \\
&\quad + \int_0^\infty dx e^{-x} f_{12}\left[2(\omega_1-1)\frac{dJ_0(2\omega_1\sqrt{x})}{dx} - \frac{d^2J_0(2\omega_1\sqrt{x})}{dx^2}\right]
\end{aligned} \tag{3.81}$$

Collecting the similar terms with respect to B according to (3.67), we get

$$a_1 = \frac{1}{\omega_1^2}\left(3\omega_1^4 - 4\alpha_1 - \alpha_3 + \alpha_5\right) \tag{3.82}$$

$$a_2 = \frac{1}{\omega_2^2}\left(3\omega_2^4 - 4\alpha_2 - \alpha_4 + \alpha_6\right) \tag{3.83}$$

$$\begin{aligned}
a_3 &= \frac{1}{\omega_1\omega_2}\left[i\omega_1^2\omega_2^2\left(4+\frac{\omega_2^2}{2\omega_1}+\frac{\omega_1^2}{2\omega_2}\right) - 8i\pi\left(4\beta_1+\omega_1\beta_2+\omega_2\beta_3\right)\right. \\
&\quad +8i\pi\left(4\beta_4+\omega_1\beta_5+\omega_2\beta_6\right) - 8\pi\left(4\beta_7+\omega_1\beta_8+\omega_2\beta_9\right) \\
&\quad \left. -8i\pi\left(4\beta_{10}+\omega_1\beta_{11}+\omega_2\beta_{12}\right) - i\left(3\omega_1^2\omega_2^2 - 4\beta_{13}+\beta_{14}+\beta_{15}\right)\right]
\end{aligned} \tag{3.84}$$

$$\kappa = 2i - 16i\pi\kappa_1 + 16i\pi\kappa_2 - 16\pi\kappa_3 - 16i\pi\kappa_4 - \frac{3i}{4} \tag{3.85}$$

Substituting a_1, a_2, a_3 and κ into (3.66) we get

$$\begin{aligned}
\frac{\partial B}{\partial \tau} &= -i\left(a_1(\omega_1)|A_1|^2 + a_2(\omega_2)|A_2|^2\right)B + a_3(\omega_1,\omega_2)A_1A_2B^* + \kappa|B|^2B \\
&\equiv -i\tilde{a}B - ibe^{i2\varphi}B^* + \kappa|B|^2B
\end{aligned} \tag{3.86}$$

where $\tilde{a} = a_1(\omega_1)|A_1|^2 + a_2(\omega_2)|A_2|^2$, $b = |a_3(\omega_1,\omega_2)A_1A_2|$ and 2φ is the sum of the two incident waves phases, i.e. $A_1A_2 = |A_1A_2|e^{i2\varphi}$. b is a real number after noticing that a_3 is negative and pure imaginary since $\Re(a_3) \propto 4\beta_7 + \omega_1\beta_8 + \omega_2\beta_9 = 0$ due to $\hat{u}_2(\infty) = 0$ (See Appendix E of last chapter). Change of variable

$$B = \bar{B}e^{i\varphi} \Rightarrow \bar{B} = \frac{B}{e^{i\varphi}} \tag{3.87}$$

will eliminate the phase of the two incident waves 2φ from the governing equation (3.86):

$$\frac{\partial \bar{B}}{\partial \tau} = -i\tilde{a}\bar{B} - ib\bar{B}^* + \kappa\bar{B}^2\bar{B}^* \tag{3.88}$$

Therefore, the phase φ is immaterial to the dynamics. In the following discussion, we will use

$$\frac{\partial B}{\partial \tau} = -i\tilde{a}B - ibB^* + \kappa B^2 B^* \tag{3.89}$$

where we omit the overbar for simplicity.

The normalized integrals are summarized as follows:

- In a_1 and a_2, we have

$$\alpha_n = \int_0^\infty dx e^{-2x} \left(\frac{dJ_0\left(2\omega_n\sqrt{x}\right)}{dx} \right)^2, \quad n = 1, 2$$

$$\alpha_3 = \int_0^\infty dx e^{-x} f_{11} \left[2(1-\omega_1)\frac{dJ_0(2\omega_1\sqrt{x})}{dx} - \frac{d^2 J_0(2\omega_1\sqrt{x})}{dx^2} \right]$$

$$\alpha_4 = \int_0^\infty dx e^{-x} f_{12} \left[2(1-\omega_2)\frac{dJ_0(2\omega_2\sqrt{x})}{dx} - \frac{d^2 J_0(2\omega_2\sqrt{x})}{dx^2} \right]$$

$$\alpha_5 = \int_0^\infty dx e^{-x} f_{13} \left[2(1+\omega_1)\frac{dJ_0(2\omega_1\sqrt{x})}{dx} - \frac{d^2 J_0(2\omega_1\sqrt{x})}{dx^2} \right]$$

$$\alpha_6 = \int_0^\infty dx e^{-x} f_{14} \left[2(1+\omega_2)\frac{dJ_0(2\omega_2\sqrt{x})}{dx} - \frac{d^2 J_0(2\omega_2\sqrt{x})}{dx^2} \right]$$

- In a_3, we have

$$\beta_1 = \int_0^\infty dx e^{-2x} J_0(4\sqrt{x}) \int_0^\infty d\xi Y_0(4\sqrt{\xi}) \frac{dJ_0\left(2\omega_1\sqrt{\xi}\right)}{d\xi} \frac{dJ_0\left(2\omega_2\sqrt{\xi}\right)}{d\xi}$$

$$\beta_2 = \int_0^\infty dx e^{-2x} J_0(4\sqrt{x}) \int_0^\infty d\xi Y_0(4\sqrt{\xi}) J_0\left(2\omega_1\sqrt{\xi}\right) \frac{d^2 J_0\left(2\omega_2\sqrt{\xi}\right)}{d\xi^2}$$

$$\beta_3 = \int_0^\infty dx e^{-2x} J_0(4\sqrt{x}) \int_0^\infty d\xi Y_0(4\sqrt{\xi}) J_0\left(2\omega_2\sqrt{\xi}\right) \frac{d^2 J_0\left(2\omega_1\sqrt{\xi}\right)}{d\xi^2}$$

$$\beta_4 = \int_0^\infty dx e^{-2x} J_0(4\sqrt{x}) \int_0^x d\xi Y_0(4\sqrt{\xi}) \frac{dJ_0\left(2\omega_1\sqrt{\xi}\right)}{d\xi} \frac{dJ_0\left(2\omega_2\sqrt{\xi}\right)}{d\xi}$$

$$\beta_5 = \int_0^\infty dx e^{-2x} J_0(4\sqrt{x}) \int_0^x d\xi Y_0(4\sqrt{\xi}) J_0\left(2\omega_1\sqrt{\xi}\right) \frac{d^2 J_0\left(2\omega_2\sqrt{\xi}\right)}{d\xi^2}$$

$$\beta_6 = \int_0^\infty dx e^{-2x} J_0(4\sqrt{x}) \int_0^x d\xi Y_0(4\sqrt{\xi}) J_0\left(2\omega_2\sqrt{\xi}\right) \frac{d^2 J_0\left(2\omega_1\sqrt{\xi}\right)}{d\xi^2}$$

$$\beta_7 = \int_0^\infty dx e^{-2x} J_0(4\sqrt{x}) \int_0^\infty d\xi J_0(4\sqrt{\xi}) \frac{dJ_0\left(2\omega_1\sqrt{\xi}\right)}{d\xi} \frac{dJ_0\left(2\omega_2\sqrt{\xi}\right)}{d\xi}$$

$$\beta_8 = \int_0^\infty dx e^{-2x} J_0(4\sqrt{x}) \int_0^\infty d\xi J_0(4\sqrt{\xi}) J_0\left(2\omega_1\sqrt{\xi}\right) \frac{d^2 J_0\left(2\omega_2\sqrt{\xi}\right)}{d\xi^2}$$

$$\beta_9 = \int_0^\infty dx e^{-2x} J_0(4\sqrt{x}) \int_0^\infty d\xi J_0(4\sqrt{\xi}) J_0\left(2\omega_2\sqrt{\xi}\right) \frac{d^2 J_0\left(2\omega_1\sqrt{\xi}\right)}{d\xi^2}$$

$$\beta_{10} = \int_0^\infty dx e^{-2x} Y_0(4\sqrt{x}) \int_0^x d\xi J_0(4\sqrt{\xi}) \frac{dJ_0\left(2\omega_1\sqrt{\xi}\right)}{d\xi} \frac{dJ_0\left(2\omega_2\sqrt{\xi}\right)}{d\xi}$$

$$\beta_{11} = \int_0^\infty dx e^{-2x} Y_0(4\sqrt{x}) \int_0^x d\xi J_0(4\sqrt{\xi}) J_0\left(2\omega_1\sqrt{\xi}\right) \frac{d^2 J_0\left(2\omega_2\sqrt{\xi}\right)}{d\xi^2}$$

$$\beta_{12} = \int_0^\infty dx e^{-2x} Y_0(4\sqrt{x}) \int_0^x d\xi J_0(4\sqrt{\xi}) J_0\left(2\omega_2\sqrt{\xi}\right) \frac{d^2 J_0\left(2\omega_1\sqrt{\xi}\right)}{d\xi^2}$$

$$\beta_{13} = \int_0^\infty dx e^{-2x} \frac{dJ_0\left(2\omega_1\sqrt{x}\right)}{dx} \frac{dJ_0\left(2\omega_2\sqrt{x}\right)}{dx}$$

$$\beta_{14} = \int_0^\infty dx e^{-x} f_{11} \left[2(\omega_2 - 1)\frac{dJ_0(2\omega_2\sqrt{x})}{dx} - \frac{d^2 J_0(2\omega_2\sqrt{x})}{dx^2}\right]$$

$$\beta_{15} = \int_0^\infty dx e^{-x} f_{12} \left[2(\omega_1 - 1)\frac{dJ_0(2\omega_1\sqrt{x})}{dx} - \frac{d^2 J_0(2\omega_1\sqrt{x})}{dx^2}\right]$$

All integrals above depend on ω_1 or ω_2.

- In κ we have,

$$\kappa_1 = \int_0^\infty dx e^{-2x} J_0(4\sqrt{x}) \int_0^\infty d\xi e^{-2\xi} Y_0(4\sqrt{\xi}) = 0.007221$$

$$\kappa_2 = \int_0^\infty dx e^{-2x} J_0(4\sqrt{x}) \int_0^x d\xi e^{-2\xi} Y_0(4\sqrt{\xi}) = -0.007085$$

$$\kappa_3 = \int_0^\infty dx e^{-2x} J_0(4\sqrt{x}) \int_0^\infty d\xi e^{-2\xi} J_0(4\sqrt{\xi}) = 0.004579$$

$$\kappa_4 = \int_0^\infty dx e^{-2x} Y_0(4\sqrt{x}) \int_0^x d\xi e^{-2\xi} J_0(4\sqrt{\xi}) = 0.014306$$

Note that the constant

$$\kappa = -0.2302 - 0.1882i \tag{3.90}$$

is identical to the one in the synchronous resonance case. The coefficients a_1, a_2 and the absolute value of a_3 for different ω_1 are plotted in Figure 3-1. Singularities occur at $\omega_1 = 0$ ($\omega_2 = 2$, i.e. twice the frequency of the edge wave, and hence subharmonic resonance is the case. a_2 singularity), $\omega_1 = \sqrt{3} - 1 = 0.732$ (a_1 singularity) , $\omega_1 = 2 - \left(\sqrt{5} - 1\right) = 0.764$ ($\omega_2 = \sqrt{5} - 1$, hence a_2 singularity.) and $\omega_1 = 2 - \left(\sqrt{7} - 1\right) = 0.354$ ($\omega_2 = \sqrt{7} - 1$, hence a_2 singularity.) . The last three cases will be studied later. For example, when $\omega_1 = \sqrt{3} - 1 = 0.732$, this incident wave will interact with the edge wave (mode 0) of eigen frequency 1 to generate harmonic of $\sqrt{3}$, which is the eigen frequency of another edge wave (mode 1). Compared with the synchronous resonance, all these singularities indicate a lower-order resonance.

The special case of $\omega_1 = 1$, $\omega_2 = 1$ corresponds to the synchronous resonance case except here we count the excitation force contribution from the two identical incident waves. Refer to Eq. (3.86) for the detail of the corresponding coefficients. For this special case, $a_1 = a_2 = 0.034$ and $a_3 = -0.152i$. Comparison with α in (2.96) and β in (2.97) from Eq. (2.89) shows that the value of the coefficients in front of the same term is precisely doubled.

3.6 Effects of detuning

Instead of perfect subharmonic resonance, i.e. $\omega_1 + \omega_2 = 2$, we now consider the effects of detuning, i.e.

$$\bar{\omega}_1 + \bar{\omega}_2 = 2(1 + \epsilon^2 \Omega)$$

This frequency mismatch may come from both incident/reflected waves:

$$\Phi_{01} = \phi_{01} e^{-i(\omega_1 + \epsilon^2 \Omega_1)t} + *, \quad \Phi_{02} = \phi_{02} e^{(\omega_2 + \epsilon^2 \Omega_2)t} + * \tag{3.91}$$

This amounts to making replacement

$$A_1 \to A_1 e^{-i\epsilon^2 \Omega_1 t}, \quad A_2 \to A_2 e^{-i\epsilon^2 \Omega_2 t} \tag{3.92}$$

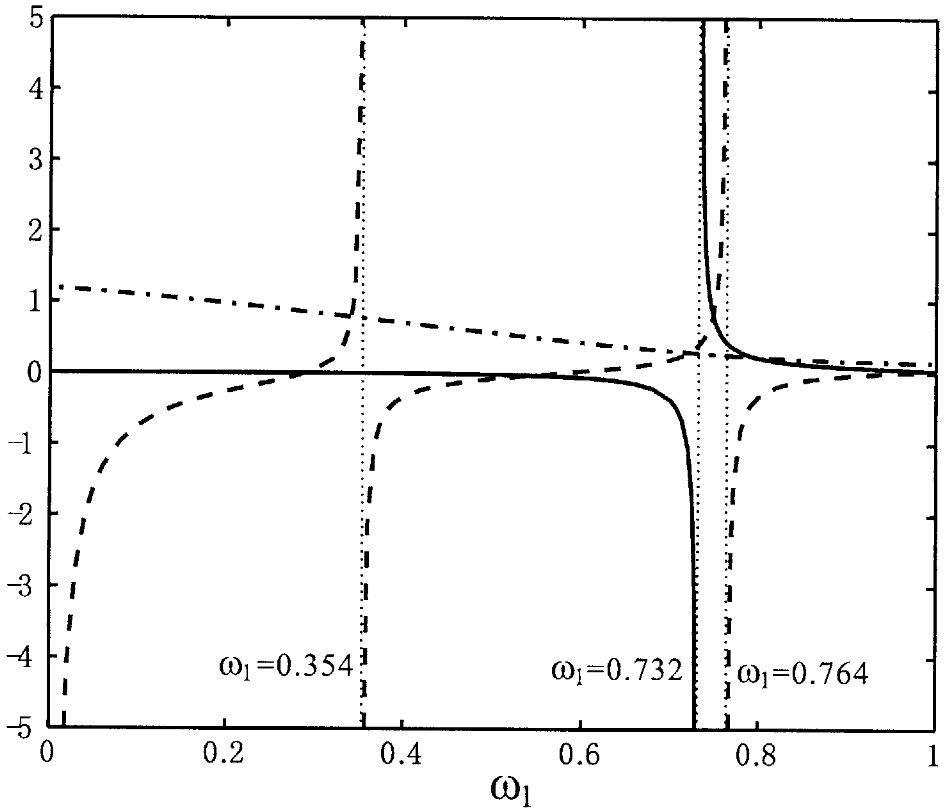

Figure 3-1: Coefficients a_1 (solid lines), a_2 (dash lines) and absolute value of a_3 (dash-dot line) v.s. ω_1. The three vertical dot lines indicate positions of discontinuities at $\omega_1 = 0.354, 0.732$ and 0.764, where resonance occurs.

with

$$\Omega_1 + \Omega_2 = 2\Omega$$

Recall the evolution equation (3.89)

$$\frac{\partial B}{\partial \tau} = -i\tilde{a}B - ibB^* + \kappa|B|^2 B$$

This replacement (3.92) does not change the value of coefficient $\tilde{a}$ since it is related to $|A_1|^2$ and $|A_2|^2$. But A_1A_2 will be changed to

$$A_1A_2e^{-2i\epsilon^2\Omega t} = A_1A_2e^{-2i\Omega\tau}$$

Then the evolution equation (3.89) becomes

$$\frac{\partial B}{\partial \tau} = -i\tilde{a}B - ibe^{-2i\Omega\tau}B^* + \kappa|B|^2 B \tag{3.93}$$

Change of variables $B = \bar{B}e^{-i\Omega\tau}$ gives

$$\frac{\partial B}{\partial \tau} = \left(\frac{\partial \bar{B}}{\partial \tau} - i\Omega\bar{B}\right)e^{-i\Omega\tau}$$

and (3.93) becomes

$$\frac{\partial \bar{B}}{\partial \tau} = -i(\tilde{a} - \Omega)\bar{B} - ib\bar{B}^* + \kappa|\bar{B}|^2\bar{B} \tag{3.94}$$

The detuning merely changes the coefficient of one term as in the synchronous resonance theory. In the following analysis, we omit the overbar for simplicity of the notation, i.e. considering the dynamical system

$$\frac{\partial B}{\partial \tau} = iaB - ibB^* - (\sigma + i\gamma)|B|^2 B \tag{3.95}$$

where $\kappa = -(\sigma + i\gamma)$, with $\sigma = 0.230160$, $\gamma = 0.188212$ from (3.90) and

$$a \equiv \Omega - a_1(\omega_1)|A_1|^2 - a_2(\omega_2)|A_2|^2, \quad b \equiv |a_3(\omega_1, \omega_2)A_1A_2|$$

Due to the normalization, $|A_1| + |A_2| = 2$. Therefore, the maximum of $|A_1||A_2|$ is 1 when $|A_1| = |A_2|$. With zero detuning, we can plot curves of $a_0 = -a_1(\omega_1)|A_1|^2 - a_2(\omega_2)|A_2|^2$ v.s. ω_1 and b v.s. ω_1 for several combination of $(|A_1|, |A_2|)$ in Figure 3-2 and Figure 3-3.

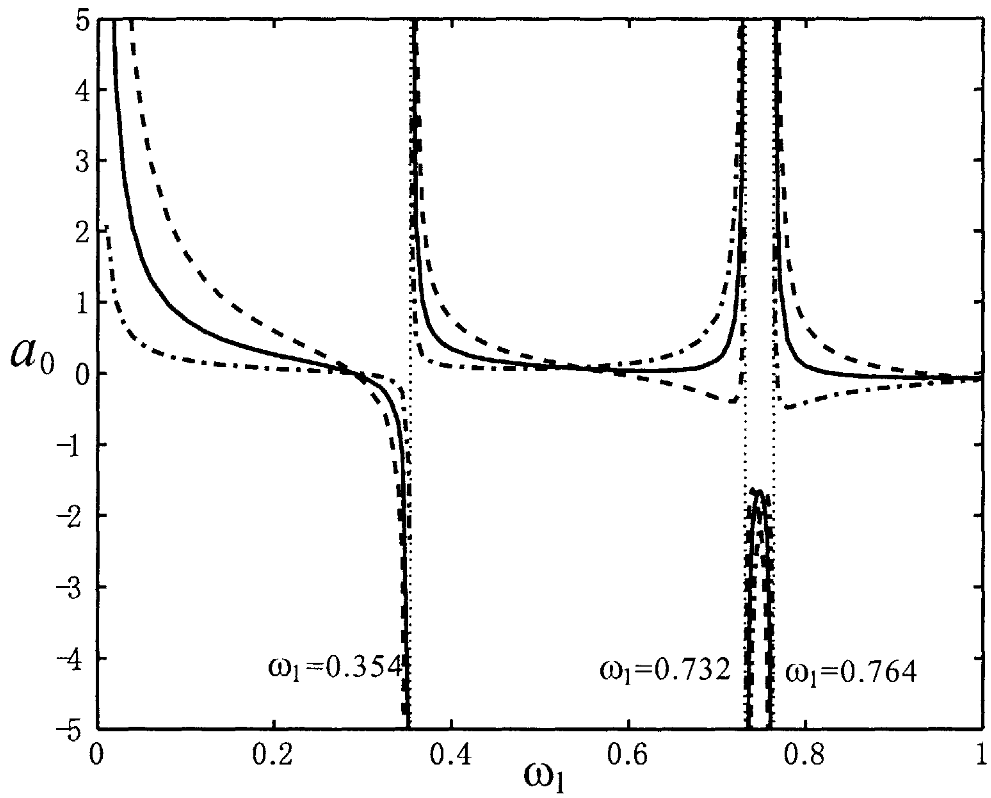

Figure 3-2: Coefficients a_0 v.s. ω_1 for zero detuning $\Omega = 0$ and $(|A_1|, |A_2|) = (\frac{1}{2}, \frac{3}{2})$— dash lines, $(|A_1|, |A_2|) = (1, 1)$— solid lines, $(|A_1|, |A_2|) = (\frac{3}{2}, \frac{1}{2})$— dash-dot lines. Note the singularities at $\omega_1 = 0.354, 0.732$ and 0.764.

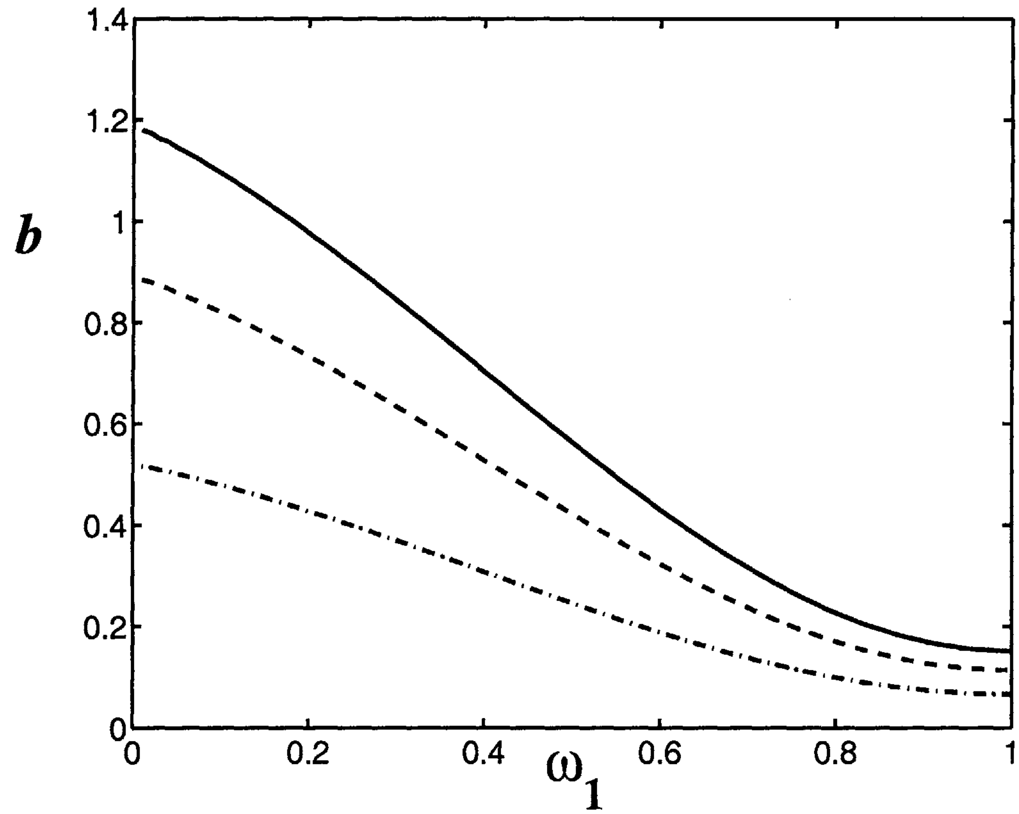

Figure 3-3: Coefficients b v.s. ω_1 for zero detuning $\Omega = 0$ and $(|A_1|, |A_2|) = (\frac{1}{4}, \frac{7}{4})$— dash-dot line, $(|A_1|, |A_2|) = (\frac{1}{2}, \frac{3}{2})$— dash line, $(|A_1|, |A_2|) = (1, 1)$— solid line.

3.7 Initial growth

If the initial edge wave amplitude is much smaller compared to the standing waves, i.e. $|B| << 1$. Therefore, only the linear terms come into play. Equation (3.95) becomes

$$\frac{\partial B}{\partial \tau} = iaB - ibB^* \tag{3.96}$$

$$\frac{\partial^2 B}{\partial \tau^2} = ia\frac{\partial B}{\partial \tau} - ib\frac{\partial B^*}{\partial \tau} = \left(b^2 - a^2\right) B$$

The solution to the above equation is

$$B(\tau) = B(0)e^{\pm\sqrt{b^2-a^2}\ \tau}$$

With zero detuning,

$$r^2 = b^2 - a^2 = |A_1|^2|A_2|^2 \left[|a_3|^2 - \left(a_1\frac{|A_1|}{|A_2|} + a_2\frac{|A_2|}{|A_1|}\right)^2\right].$$

We plot curves of r^2 v.s. ω_1 for several combination of $(|A_1|/|A_2|)$ in Figure 3-4.

From Figure 3-4 we can see that most of parts of the curves are positive, meaning unstable response of dynamical system to the perturbation. The stable response to the perturbation only occurs near the singularities. The growth rate decreases with the increase of ω_1 under the three combinations of $(|A_1|/|A_2|)$. For a certain ω_1, the growth rate is the largest when the two incident waves have almost the same amplitude. The plot suggests a largest growth rate in this case $r = \sqrt{0.9} = 0.95$ at $\omega_1 = 0.18$ around (refer to Figure 3-5). A refined search shows the maximum $r = \sqrt{0.93} = 0.964$ occurs at $|A_1| = 1.15$ when $\omega_1 = 0.14$. Compared with the growth rate of 0.0679 for the synchronous resonance, 0.964 is closed to unity and is a much faster initial growth. Refer to Figure 3-6 for curve of r^2 v.s. $|A_1|$ with different ω_1. In this plot, it is confirmed that the maximum growth rate occurs at $|A_1| = 1.15$.

3.8 Analysis of nonlinear dynamical system

The dynamical system (3.95) has exactly the same form as (2.107) in the synchronous resonance case. Therefore the analysis is the same, except the coefficients a and b

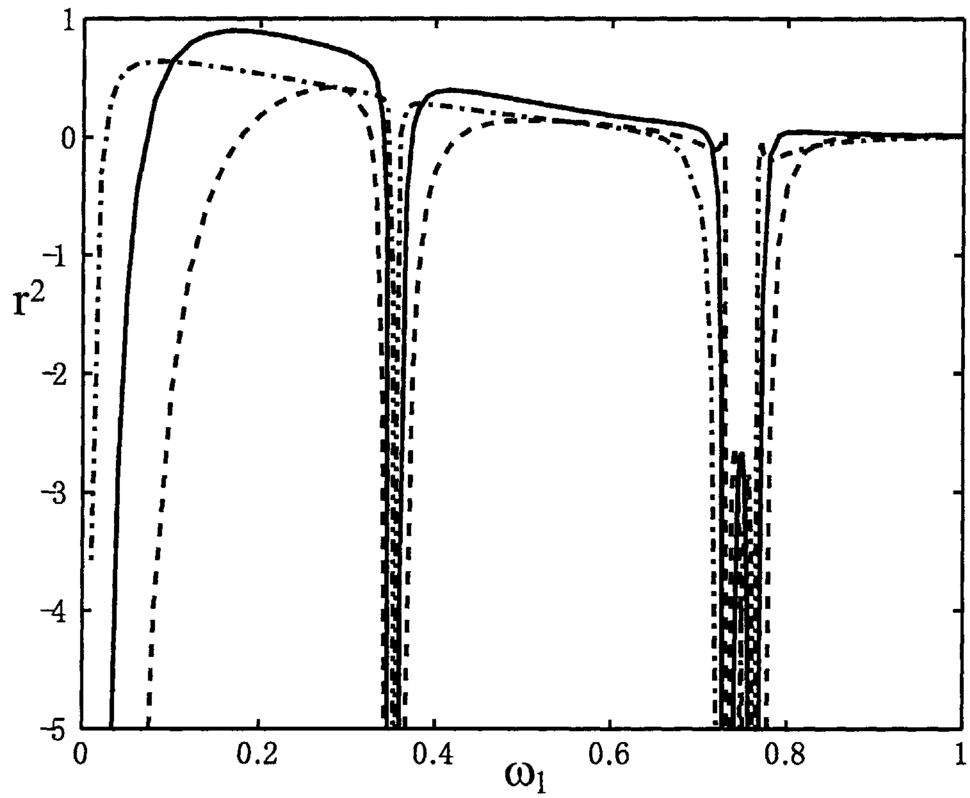

Figure 3-4: Growth rate r^2 v.s. ω_1 for zero detuning $\Omega = 0$ and $(|A_1|, |A_2|) = (\frac{1}{2}, \frac{3}{2})$— dash lines, $(|A_1|, |A_2|) = (1, 1)$— solid lines, $(|A_1|, |A_2|) = (\frac{3}{2}, \frac{1}{2})$—dash-dot lines. Singularities occur at $\omega_1 = 0.354, 0.732$ and 0.764.

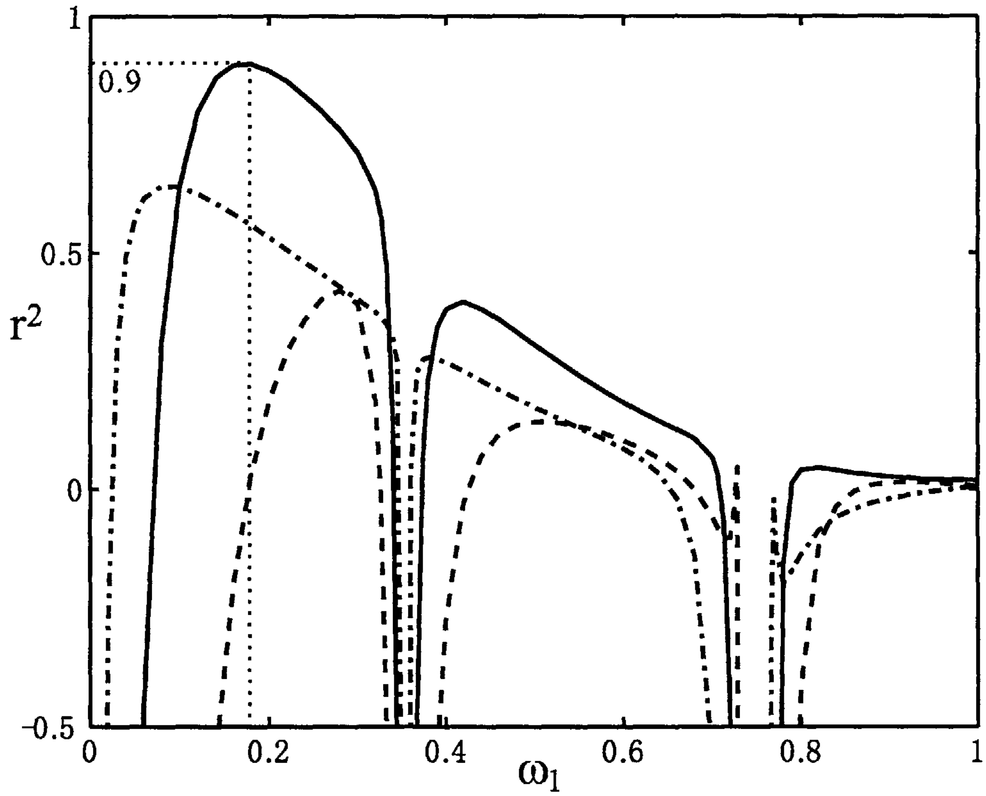

Figure 3-5: A closer look of growth rate r^2 v.s. ω_1 for zero detuning $\Omega = 0$ and $(|A_1|, |A_2|) = (\frac{1}{2}, \frac{3}{2})$— dash lines, $(|A_1|, |A_2|) = (1, 1)$— solid lines, $(|A_1|, |A_2|) = (\frac{3}{2}, \frac{1}{2})$—dash-dot lines. Singularities occur at $\omega_1 = 0.354, 0.732$ and 0.764.

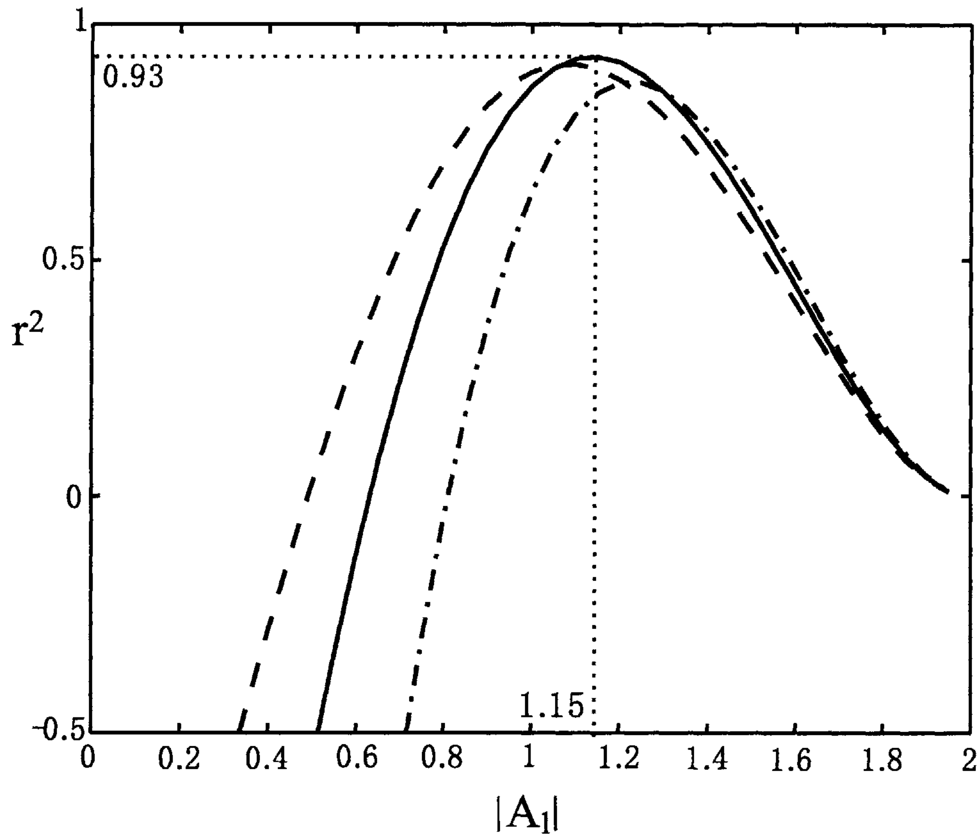

Figure 3-6: Growth rate r^2 v.s. $|A_1|$ for zero detuning $\Omega = 0$ and $\omega_1 = 0.1$— dash-dot line, $\omega_1 = 0.14$— solid line, $\omega_1 = 0.18$— dash line.

have different meanings for the two cases.

$$\frac{\partial B}{\partial \tau} = iaB - ibB^* - (\sigma + i\gamma)|B|^2 B$$

with $\sigma = 0.230160$, $\gamma = 0.188212$ and

$$a \equiv \Omega - a_1(\omega_1)|A_1|^2 - a_2(\omega_2)|A_2|^2, \quad b \equiv |a_3(\omega_1, \omega_2)A_1 A_2| \tag{3.97}$$

At equilibrium we denote $B \equiv \sqrt{I_0}e^{i\theta_0}$, then

$$I_0^{\pm} = \frac{\hat{\gamma}}{\hat{\gamma}^2 + \hat{\sigma}^2}\left[\hat{a} \pm \sqrt{1 + \frac{\hat{\sigma}^2}{\hat{\gamma}^2}(1 - \hat{a}^2)}\right] = \frac{b\gamma}{\gamma^2 + \sigma^2}\left[\hat{a} \pm \sqrt{1 + \frac{\sigma^2}{\gamma^2}(1 - \hat{a}^2)}\right]$$

Therefore, $I_0^{\pm} \propto b$ as

$$\frac{I_0^{\pm}}{b} = \frac{\gamma}{\gamma^2 + \sigma^2}\left[\hat{a} \pm \sqrt{1 + \frac{\sigma^2}{\gamma^2}(1 - \hat{a}^2)}\right]$$

A single curve of equilibrium branch I_0/b v.s. $\hat{a}$ can be drawn and shown in Figure 3-7, where

$$\hat{a} = \frac{a}{b}. \tag{3.98}$$

From the plot we can see that the equilibrium branch curve has exact feature as Figure 2-5 in the synchronous resonance case. Larger b simply means larger mature edge wave amplitude. The four critical points are at $\hat{a} = -1,\ 0.82,\ 1,\ 1.29$, which are four surfaces in the parameterized space $(\omega_1,\ |A_1|,\ \Omega)$. From (3.98) and (3.97) we can get

$$\Omega \equiv \hat{a}|a_3(\omega_1, \omega_2)A_1 A_2| + a_1(\omega_1)|A_1|^2 + a_2(\omega_2)|A_2|^2. \tag{3.99}$$

For each of the four critical $\hat{a}$, we compute Ω for different ω_1 and A_1 and plot them in Figure 3-8 to Figure 3-11.

Alternatively, (3.99) can be rewritten as

$$\hat{a} \equiv \frac{\Omega - a_1(\omega_1)|A_1|^2 - a_2(\omega_2)|A_2|^2}{|a_3(\omega_1, \omega_2)A_1 A_2|}. \tag{3.100}$$

For given ω_1 and A_1, $\hat{a}$ is linearly proportional to Ω. Therefore a straight line can be drawn on the $(\Omega,\ \hat{a})$ plane. The slope of the line is determined by $b \equiv |a_3(\omega_1, \omega_2)A_1 A_2|$ and the $\hat{a}$-intercept is determined by

$$\frac{a_0}{b} \equiv \frac{(-a_1(\omega_1)|A_1|^2 - a_2(\omega_2)|A_2|^2)}{|a_3(\omega_1, \omega_2)A_1 A_2|}.$$

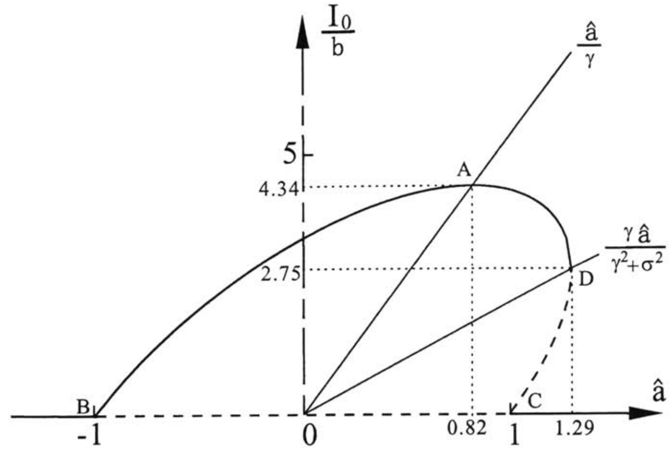

Figure 3-7: Equilibrium branches I_0/b with respect to $\hat{a}$.

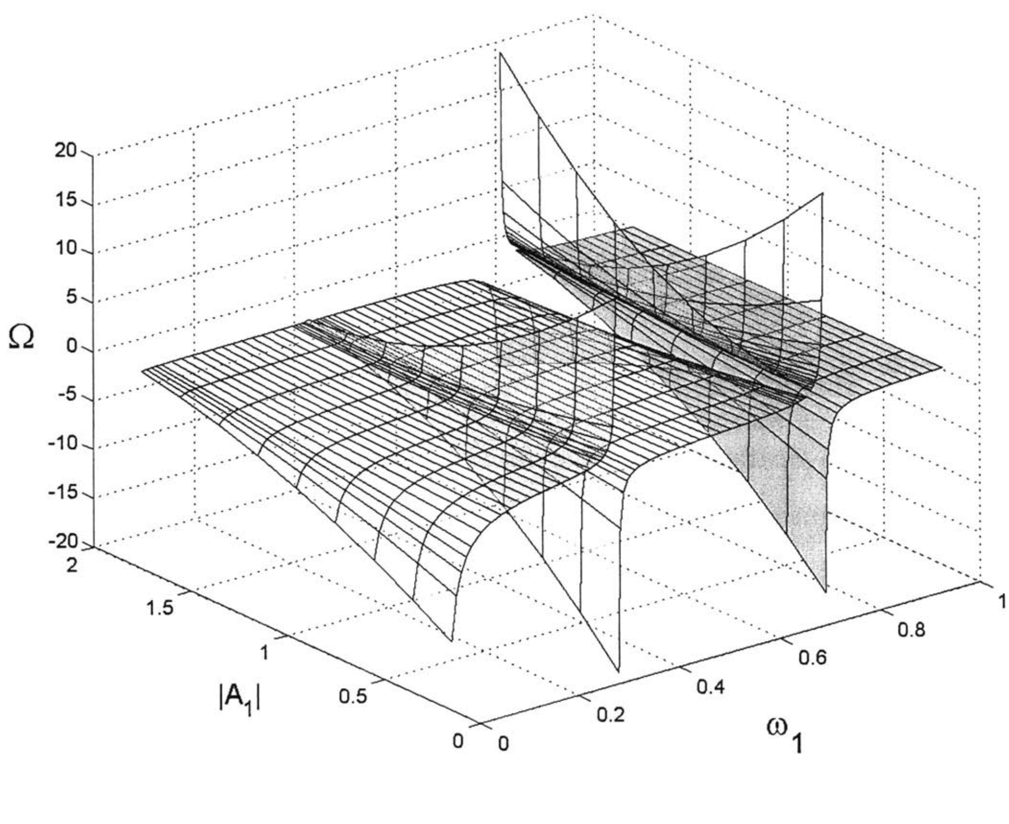

Figure 3-8: Parametrized surface $\hat{a} = -1$.

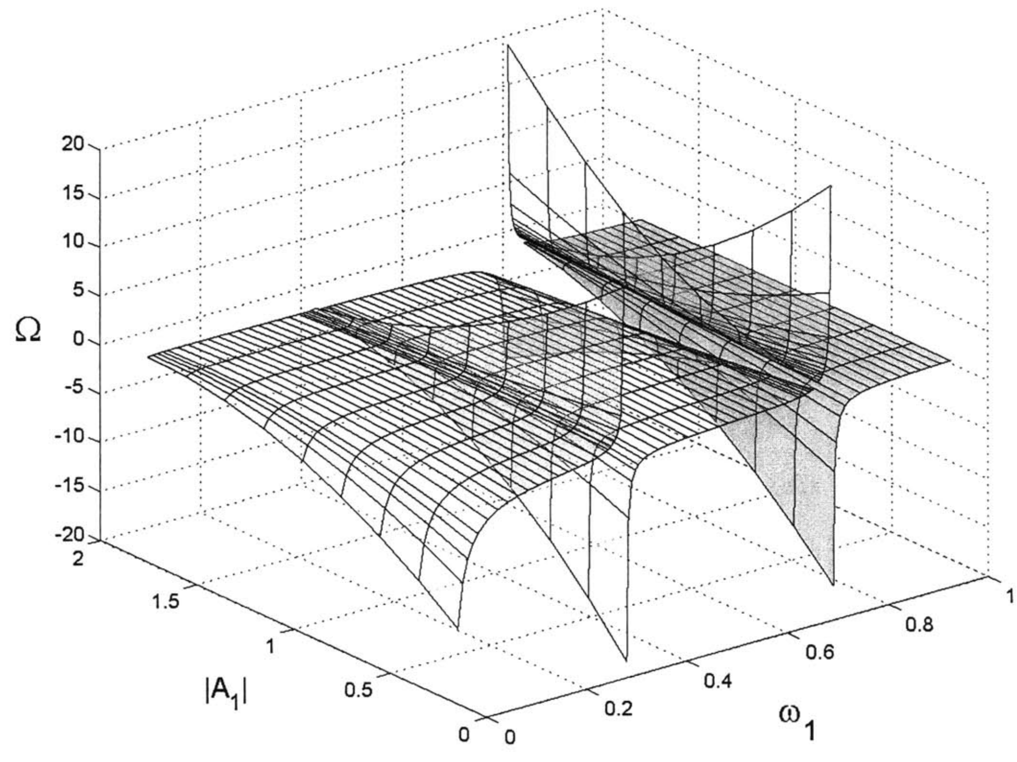

Figure 3-9: Parametrized surface $\hat{a} = 0.82$.

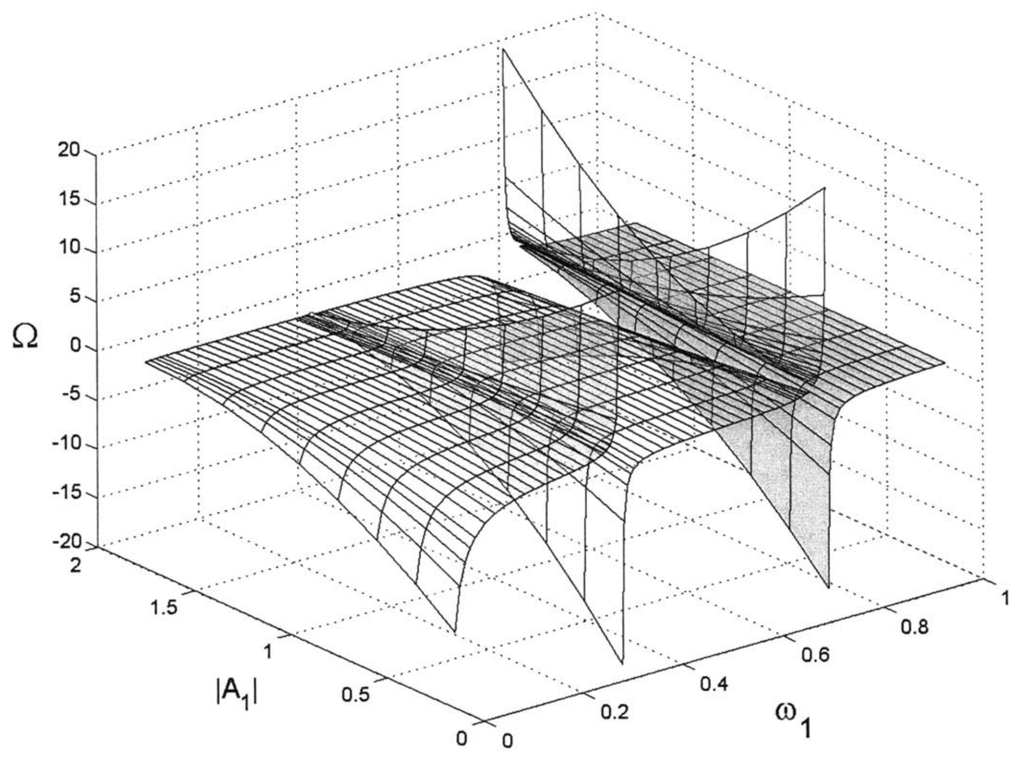

Figure 3-10: Parametrized surface $\hat{a} = 1$.

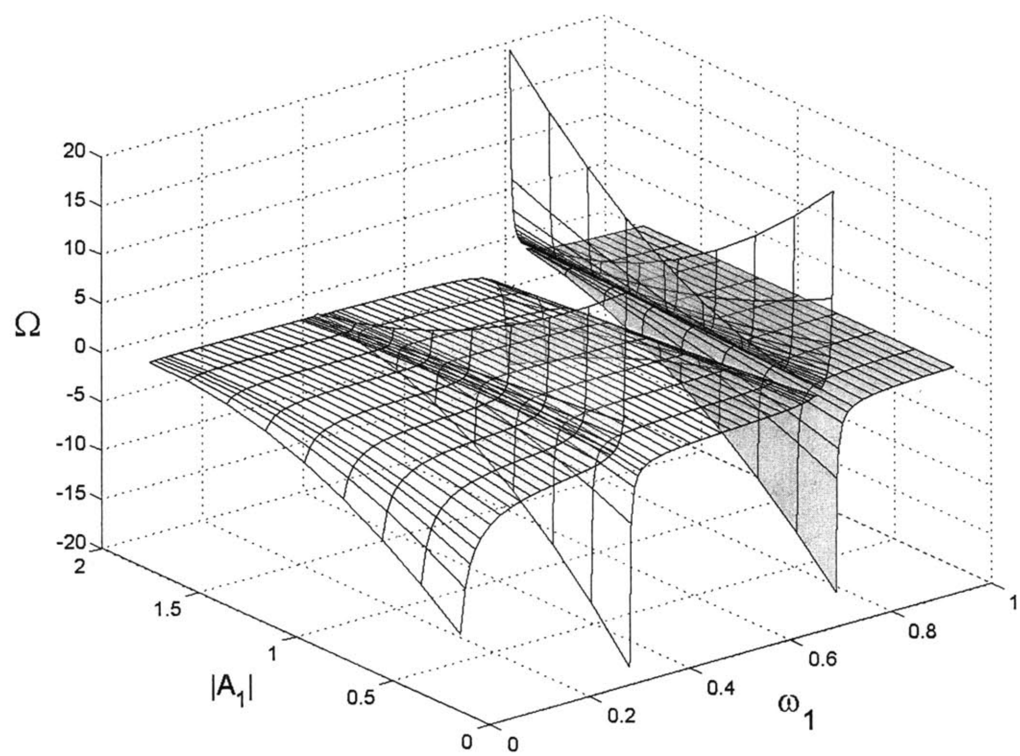

Figure 3-11: Parameterized surface $\hat{a} = 1.29$.

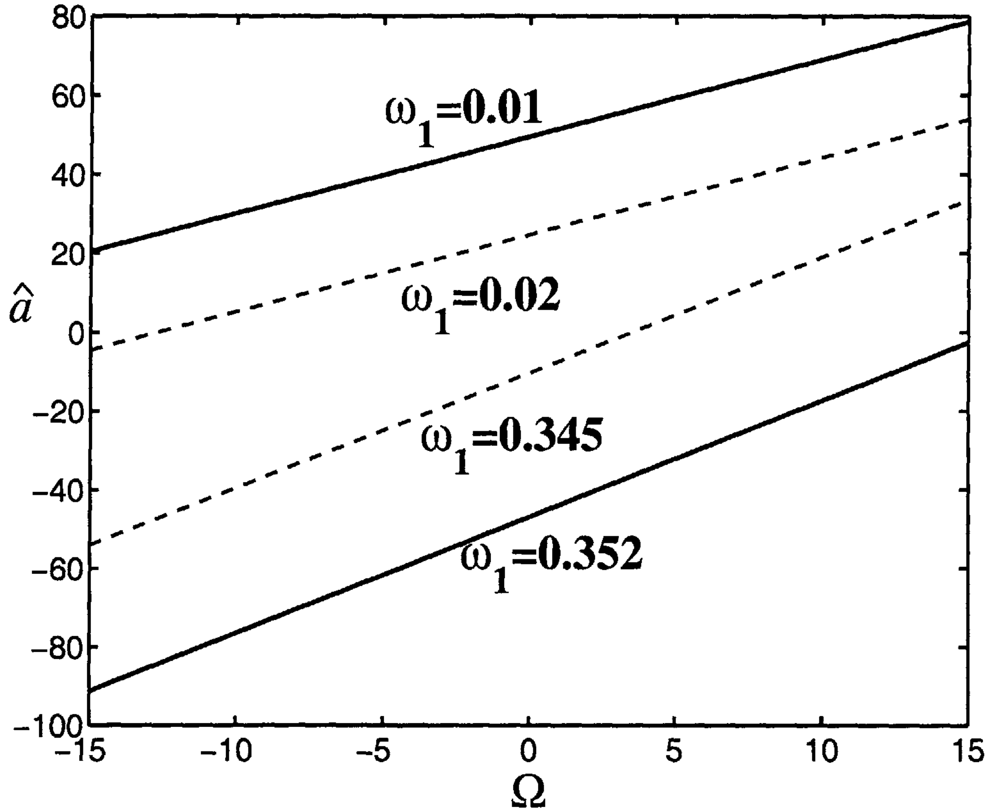

Figure 3-12: $\hat{a}$ v.s. Ω curves for critical value of ω_1 with $A_1 = 0.25, A_2 = 1.75$— First branch of a_0.

Refer to Figure 3-2 and Figure 3-3 for the property of a_0 and b. Basically, b is monotonic with ω_1. But a_0 is only monotonic on the first and the last branches. We also found that different (A_1, A_2) combinations do not affect the features of a_0 too much. Plotted in Figure 3-12 to Figure 3-15 are the $\hat{a}$ v.s. Ω curves for critical value of ω_1 with $A_1 = 0.25, A_2 = 1.75$. We add some intermediate values of ω_1 on the figures, which are plotted in dash lines.

On the other hand, we plot the $\hat{a}$ v.s. ω_1 curve with fixed Ω and A_1 in Figure 3-16, 3-17 and 3-18. Note the singularities at $\omega_1 = 0.354, 0.732$ and 0.764.

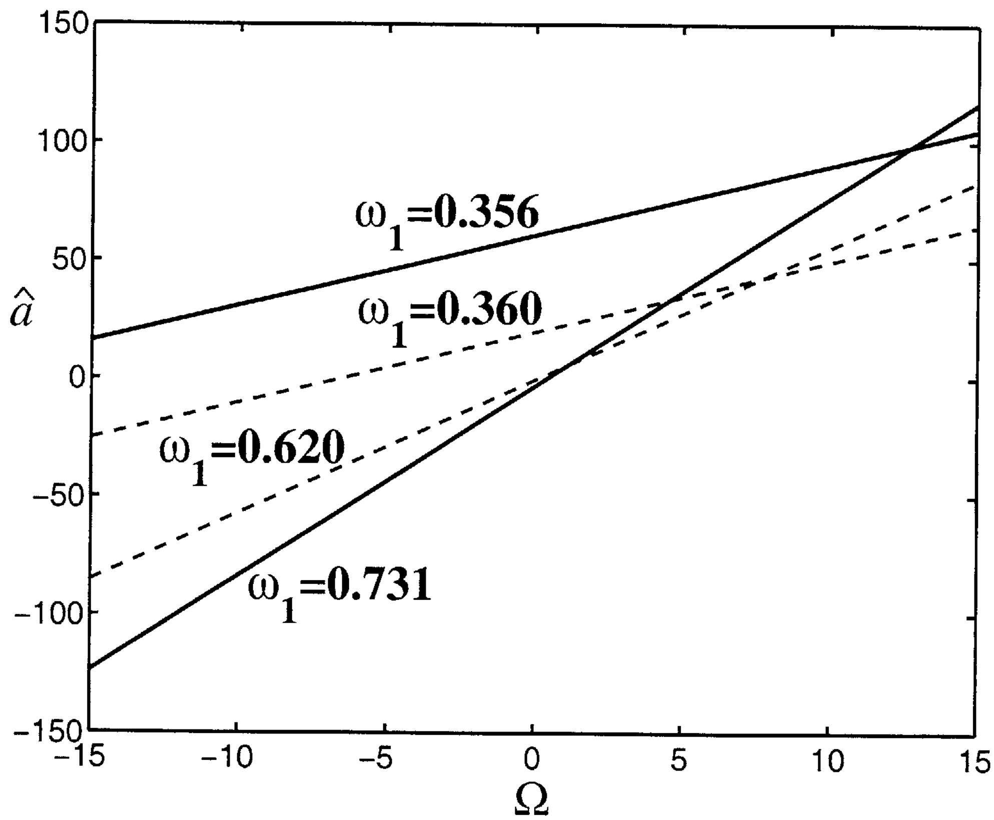

Figure 3-13: $\hat{a}$ v.s. Ω curves for critical value of ω_1 with $A_1 = 0.25, A_2 = 1.75$—Second branch of a_0.

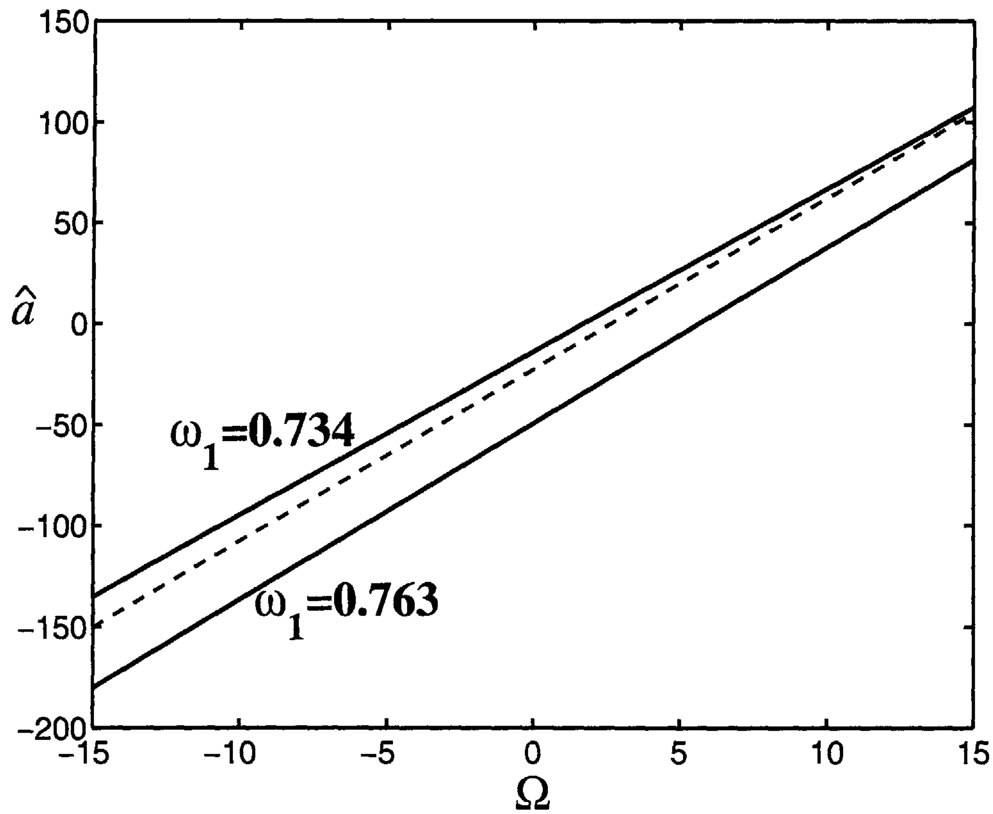

Figure 3-14: $\hat{a}$ v.s. Ω curves for critical value of ω_1 with $A_1 = 0.25, A_2 = 1.75$— Third branch of a_0. The dashed line in the middle is for $\omega_1 = 0.749$.

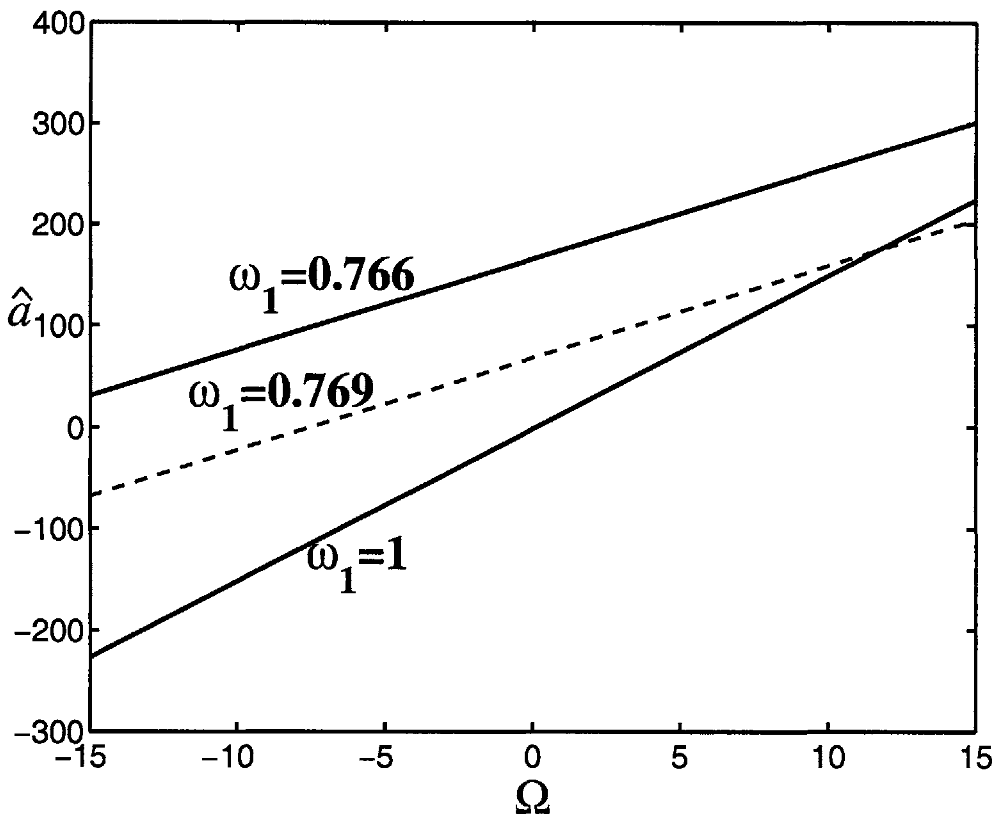

Figure 3-15: $\hat{a}$ v.s. Ω curves for critical value of ω_1 with $A_1 = 0.25, A_2 = 1.75$— Forth branch of a_0

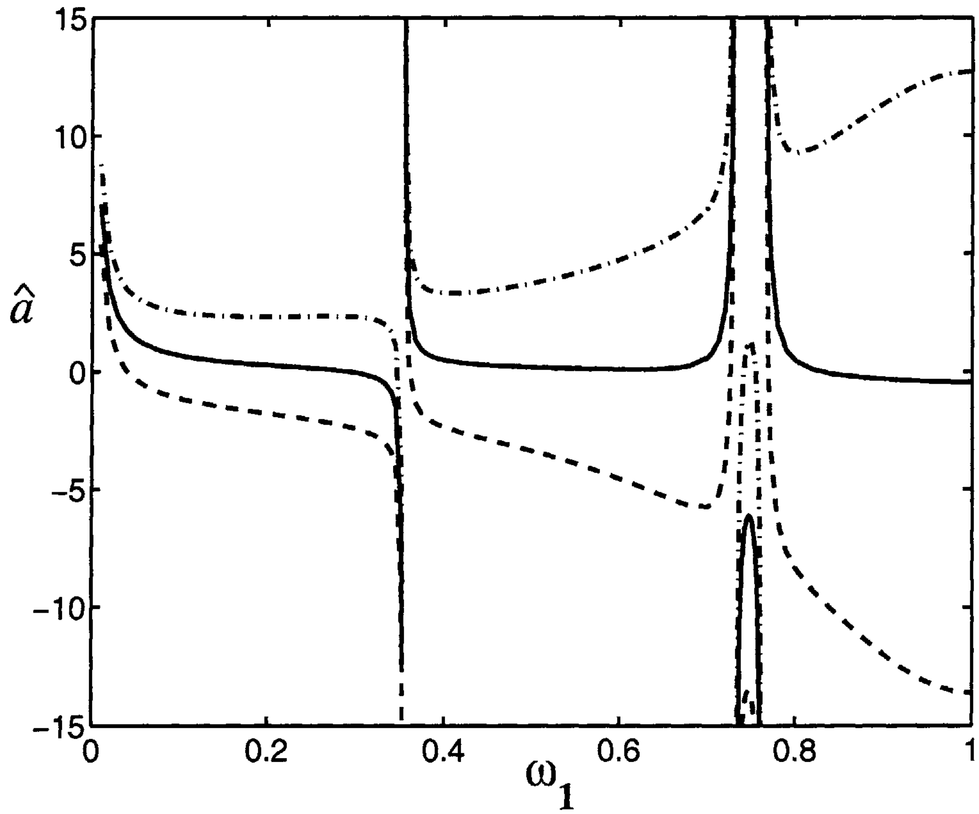

Figure 3-16: $\hat{a}$ v.s. ω_1 curves for $A_1 = 1$ and several Ω's: $\Omega = 0$— solid lines, $\Omega = -2$— dash lines, $\Omega = 2$— dash-dot lines. Note the singularities at $\omega_1 = 0.354, 0.732$ and 0.764.

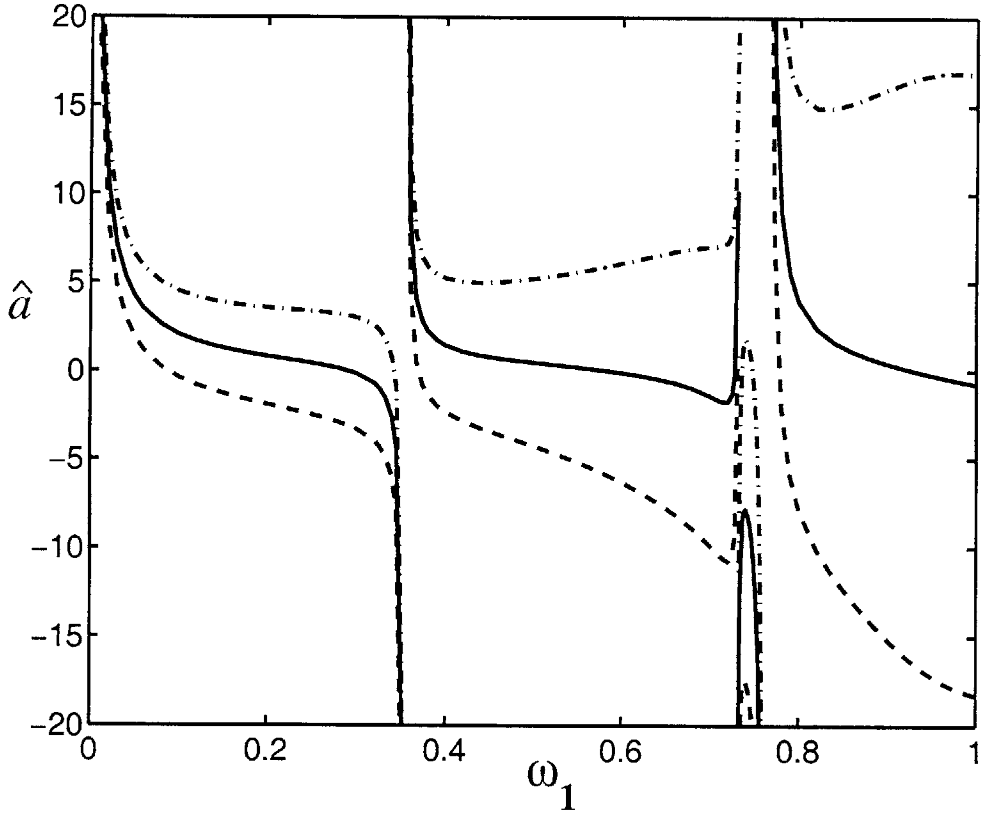

Figure 3-17: $\hat{a}$ v.s. ω_1 curves for $A_1 = 0.5$ and several Ω's: $\Omega = 0$— solid lines, $\Omega = -2$— dash lines, $\Omega = 2$— dash-dot lines. Note the singularities at $\omega_1 = 0.354, 0.732$ and 0.764.

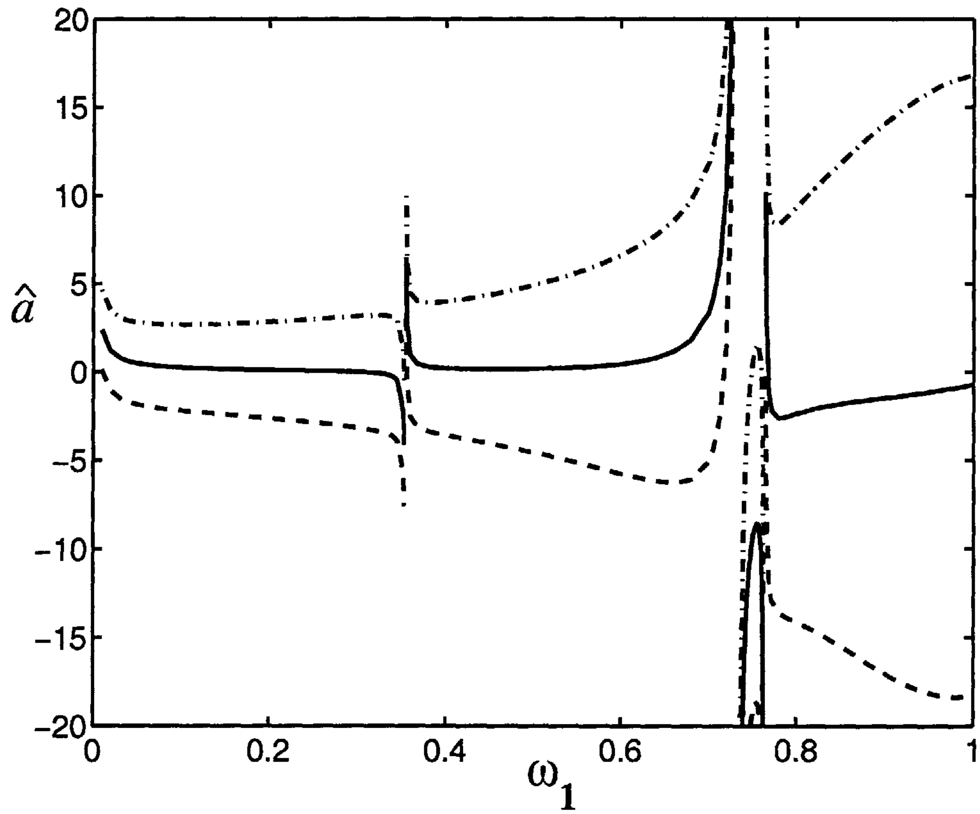

Figure 3-18: $\hat{a}$ v.s. ω_1 curves for $A_1 = 1.5$ and several Ω's: $\Omega = 0$— solid lines, $\Omega = -2$— dash lines, $\Omega = 2$— dash-dot lines. Note the singularities at $\omega_1 = 0.354, 0.732$ and 0.764.

3.9 Conclusion

1. Although we require that $\omega_1 + \omega_2 = 2$, the generation of one edge wave by a pair of incident waves allows a continuous spectrum of frequency within $(0, 1)$;

2. At specific value of ω_1, lower-order resonance occur, which is not appealing for this study, but intriguing a new topic of cross-resonance;

3. The equilibrium of the dynamical system depends on the frequency ω, amplitude A and detuning Ω of the incident waves. Otherwise, it shares the same features of dynamics with the synchronous resonance.

Chapter 4

Resonance of two edge waves by one incident/reflected wave system

In the last chapter, we found that unbounded resonance of two edge waves happens when the eigen frequency of the incident wave and the two edge waves takes some special values. In order to deal with this situation properly, the following multiple scale scheme is proposed: Two edge wave modes are present at leading order, whereas one normally incident/reflected wave exists at one order higher. It is expected that nonlinear interaction of the incident wave and one of the edge wave modes resonates the other edge wave mode. This cross resonance requires that the two edge wave modes share the same longshore dependence $\cos ky$ while the normally incident wave has only x-dependence in the cross-shore direction. Also the incident wave frequency ω must be related to the two edge wave frequencies ω_p and ω_q by

$$\omega = \omega_q \pm \omega_p. \tag{4.1}$$

Later study will show that the choices for different signs on the right hand side of (4.1) make the dynamics of the whole system quite different. Only the plus sign will lead linear instability of the dynamical system, hence is of interest. This resonance triad has been recognized by Guza and Davis [14]. But they only limited their discussion to the initial stage of growth and did not allow the saturation of the edge wave amplitudes. Therefore they did not obtain the complete evolution equations governing the two edge wave amplitudes.

We consider two general edge wave modes p and q of (1.6) sharing the same eigen function in y:

$$\psi'_{0j} = -\frac{igB'_j}{\omega'_j} e^{-kx'} L_j(2kx') \cos ky', \quad j = p, q$$

where we use prime " $'$ " to represent the physical variables in order to distinguish them from the normalized ones to be defined. The two edge waves have the same wave number k, which is related to the channel width W by the eigenvalue condition in y:

$$k = \frac{m\pi}{W}, \quad m = 1, 2, 3...$$

Their eigen frequencies are different according to the eigenvalue condition in x:

$$\omega'_n = \sqrt{(2n+1)kgs}\ , \quad n = 0, 1, 2, ... \tag{4.2}$$

In normalized form the eigen frequencies for these two modes satisfy

$$\omega_j = \omega'_j / \omega'_0 = \sqrt{2j+1}, \quad j = p, q. \tag{4.3}$$

with the scale

$$\omega'_0 = \sqrt{kgs} \tag{4.4}$$

which is the eigen frequency for the lowest 0 mode of edge wave. We assume without loss of generality that $q > p$.

Refer to (2.2) for Airy's nonlinear shallow-water equation and (2.3) and (2.4) for the quadratic and cubic nonlinear terms in physical variables. We introduce the following nondimensionalized variables:

$$x = kx', \quad y = ky', \quad t = \omega'_0 t', \quad \zeta = \frac{\zeta'}{|\bar{A}|}, \quad \Phi = \frac{\omega'_0}{|\bar{A}|g}\Phi'$$

where the scale $|\bar{A}|$ is defined by

$$|\bar{A}| = \left(\frac{s|A'|}{k}\right)^{1/2}. \tag{4.5}$$

where $A' = |A'|e^{i2\varphi}$ is one-half the physical amplitude of the incident/reflected wave at the shoreline. Let us define the small parameter

$$\bar{\epsilon} = \frac{k|\bar{A}|}{s} \ll 1 \tag{4.6}$$

Then

$$A' = \bar{\epsilon}|\bar{A}|e^{i2\varphi} \tag{4.7}$$

and

$$|A'| = \bar{\epsilon}|\bar{A}| = \frac{k}{s}|\bar{A}|^2$$

Physically, $|\bar{A}|$ is the scale of the edge waves when fully resonated.

Upon the substitution into equation (2.2), we obtain

$$-\Phi_{tt} + (x\Phi_x)_x + x\Phi_{yy} = \bar{\epsilon}Q(\Phi) + \bar{\epsilon}^2 C(\Phi) \tag{4.8}$$

where the quadratic and cubic nonlinear terms are

$$Q(\Phi) = 2\left(\Phi_x\Phi_{xt} + \Phi_y\Phi_{yt}\right) + \Phi_t\left(\Phi_{xx} + \Phi_{yy}\right) \tag{4.9}$$

$$C(\Phi) = \frac{1}{2}\left(\Phi_x^2 + \Phi_y^2\right)\left(\Phi_{xx} + \Phi_{yy}\right) + \Phi_x^2\Phi_{xx} + \Phi_y^2\Phi_{yy} + 2\Phi_x\Phi_y\Phi_{xy} \tag{4.10}$$

We also normalized the surface boundary condition to get

$$\zeta + \frac{\partial\Phi}{\partial t} + \frac{\bar{\epsilon}}{2}|\nabla\Phi|^2 = 0. \tag{4.11}$$

As confirmation, a typical linear term is normalized as follows:

$$-\Phi'_{t't'} \rightarrow -\left(\omega'_0\right)^2 \frac{|\bar{A}|g}{\omega'_0}\Phi_{tt}$$

and a typical quadratic nonlinear term as follows:

$$\Phi'_{x'}\Phi'_{x't'} \rightarrow k^2\omega_0\left(\frac{|\bar{A}|g}{\omega'_0}\right)^2\Phi_x\Phi_{xt}$$

The ratio of quadratic nonlinear term to the linear term is the small parameter

$$\bar{\epsilon} = \frac{|\bar{A}|gk^2}{\left(\omega'_0\right)^2} = \frac{sgk}{\left(\omega'_0\right)^2}\frac{k|\bar{A}|}{s} = \frac{k|\bar{A}|}{s}$$

where use has been made of the eigenvalue condition for the lowest 0 mode of edge wave (4.4).

4.1 Harmonics and the nonlinear forcing terms

The proposed perturbation expansion is:

$$\Phi = \Phi_0 + \bar{\epsilon}\Phi_1 + \bar{\epsilon}^2\Phi_2 + \cdots \tag{4.12}$$

At the leading order we assume the co-existence of two edge waves of frequencies ω_p and ω_q:

$$\Phi_0 = \Phi_{0p} + \Phi_{0q} \tag{4.13}$$

where

$$\Phi_{0j} = \psi_{0j}\, e^{-i\omega_j t} + *, \quad \text{with } \psi_{0j} = -i\frac{B_j(\tau)}{\omega_j} e^{-x} L_j(2x)\cos y; \quad j = p,\ q \tag{4.14}$$

are the two edge wave modes with normalized eigen frequencies $\omega_j = \sqrt{2j+1}$. Here L_j is the jth order Laguerre polynomial by

$$L_j(\xi) = \frac{(-1)^j}{j!}\left[\xi^j - \frac{j^2}{1!}\xi^{(j-1)} + \frac{j^2(j-1)^2}{2!}\xi^{(j-2)} - \cdots + (-1)^j j!\right]$$

with $\xi = 2x$ (With this definition, $\frac{dL_j}{dx} = L_j'\frac{d\xi}{dx} = 2L_j'$ since the prime " $'$ " denotes the derivative with respect to argument ξ.). $B_j(\tau)$'s are the slowly varying dimensionless amplitudes of the edge waves at the shoreline in accordance with the linearized free surface boundary condition

$$\frac{\partial \Phi_j}{\partial t} + \zeta_j = 0. \tag{4.15}$$

Besides the incident and reflected waves at the second order O($\bar{\epsilon}$), there are in total ten harmonics generated by the quadratic interaction of the four first-order wave harmonics ($\pm\omega_p$ and $\pm\omega_q$). In order to see which of these harmonics are of our interest, we first gives the details as follows:

[Q-0]. Zeroth harmonic:

$$\begin{aligned}
& (\psi_{0j}, \psi_{0j}^*) \\
= \;& 2\left[\psi_{0jx}\psi_{0jx}^*(i\omega_j) + \psi_{0jx}^*\psi_{0jx}(-i\omega_j) + \psi_{0jy}\psi_{0jy}^*(i\omega_j) + \psi_{0jy}^*\psi_{0jy}(-i\omega_j)\right] \\
& -i\omega_j\psi_{0j}\left(\psi_{0jxx}^* + \psi_{0jyy}^*\right) + i\omega_j\psi_{0j}^*\left(\psi_{0jxx} + \psi_{0jyy}\right) = 0, \quad j = p, q.
\end{aligned} \tag{4.16}$$

[Q-1]. Harmonic $e^{-i(\omega_q-\omega_p)t}$ and its complex conjugate:

$$
\begin{aligned}
& (\psi_{0p}^*, \psi_{0q}) \\
= \;& 2\left[\psi_{0qx}\psi_{0px}^*(i\omega_p) + \psi_{0px}^*\psi_{0qx}(-i\omega_q) + \psi_{0qy}\psi_{0py}^*(i\omega_p) + \psi_{0py}^*\psi_{0qy}(-i\omega_q)\right] \\
& -i\omega_q\psi_{0q}\left(\psi_{0pxx}^* + \psi_{0pyy}^*\right) + i\omega_p\psi_{0p}^*\left(\psi_{0qxx} + \psi_{0qyy}\right) \\
= \;& 2(\omega_p - \omega_q)i\left[\psi_{0px}^*\psi_{0qx} + \psi_{0py}^*\psi_{0qy}\right] \\
& -i\omega_q\psi_{0q}\left(\psi_{0pxx}^* + \psi_{0pyy}^*\right) + i\omega_p\psi_{0p}^*\left(\psi_{0qxx} + \psi_{0qyy}\right) \\
= \;& i\frac{B_p^*}{\omega_p}\left(-i\frac{B_q}{\omega_q}\right) ie^{-2x}\left\{2(\omega_p - \omega_q)\left[(2L_p' - L_p)(2L_q' - L_q)\cos^2 y + L_pL_q\sin^2 y\right]\right. \\
& \left. + \left[-\omega_qL_q\left(4L_p'' - 4L_p'\right) + \omega_pL_p\left(4L_q'' - 4L_q'\right)\right]\cos^2 y\right\} \\
= \;& i\frac{B_p^*B_q}{\omega_p\omega_q}e^{-2x}\left\{2(\omega_p - \omega_q)\left[(4L_p'L_q' - 2L_q'L_p - 2L_p'L_q)\cos^2 y + L_pL_q\right]\right. \\
& \left. + \left[\omega_pL_p\left(4L_q'' - 4L_q'\right) - \omega_qL_q\left(4L_p'' - 4L_p'\right)\right]\cos^2 y\right\} \\
= \;& i\frac{B_p^*B_q}{\omega_p\omega_q}e^{-2x}\left[f_1(x)\cos 2y + g_1(x)\right] \qquad (4.17)
\end{aligned}
$$

with

$$f_1(x) = (\omega_p - \omega_q)(4L_p'L_q' - 2L_q'L_p - 2L_p'L_q) + \frac{1}{2}\left[\omega_pL_p\left(4L_q'' - 4L_q'\right) - \omega_qL_q\left(4L_p'' - 4L_p'\right)\right]$$

$$g_1(x) = f_1(x) + 2(\omega_p - \omega_q)L_pL_q$$

[Q-2]. Harmonic $e^{-i(\omega_p+\omega_q)t}$ and its complex conjugate:

$$
\begin{aligned}
& (\psi_{0p}, \psi_{0q}) \\
= \;& 2\left[\psi_{0qx}\psi_{0px}(-i\omega_p) + \psi_{0px}\psi_{0qx}(-i\omega_q) + \psi_{0qy}\psi_{0py}(-i\omega_p) + \psi_{0py}\psi_{0qy}(-i\omega_q)\right] \\
& -i\omega_q\psi_{0q}\left(\psi_{0pxx} + \psi_{0pyy}\right) - i\omega_p\psi_{0p}\left(\psi_{0qxx} + \psi_{0qyy}\right) \\
= \;& -2(\omega_p + \omega_q)i\left[\psi_{0px}\psi_{0qx} + \psi_{0py}\psi_{0qy}\right] \\
& -i\omega_q\psi_{0q}\left(\psi_{0pxx} + \psi_{0pyy}\right) - i\omega_p\psi_{0p}\left(\psi_{0qxx} + \psi_{0qyy}\right) \\
= \;& -i\frac{B_p}{\omega_p}\left(-i\frac{B_q}{\omega_q}\right)(-i)e^{-2x}\left\{2(\omega_p + \omega_q)\left[(2L_p' - L_p)(2L_q' - L_q)\cos^2 y + L_pL_q\sin^2 y\right]\right. \\
& \left. + \left[\omega_qL_q\left(4L_p'' - 4L_p'\right) + \omega_pL_p\left(4L_q'' - 4L_q'\right)\right]\cos^2 y\right\} \\
= \;& i\frac{B_pB_q}{\omega_p\omega_q}e^{-2x}\left\{2(\omega_p + \omega_q)\left[(4L_p'L_q' - 2L_q'L_p - 2L_p'L_q)\cos^2 y + L_pL_q\right]\right. \\
& \left. + \left[\omega_pL_p\left(4L_q'' - 4L_q'\right) + \omega_qL_q\left(4L_p'' - 4L_p'\right)\right]\cos^2 y\right\} \\
= \;& i\frac{B_pB_q}{\omega_p\omega_q}e^{-2x}\left[f_2(x)\cos 2y + g_2(x)\right] \qquad (4.18)
\end{aligned}
$$

with

$$f_2(x) = (\omega_p+\omega_q)(4L_p'L_q'-2L_q'L_p-2L_p'L_q)+\frac{1}{2}\left[\omega_p L_p\left(4L_q''-4L_q'\right)+\omega_q L_q\left(4L_p''-4L_p'\right)\right]$$

$$g_2(x) = f_2(x) + 2(\omega_p+\omega_q)L_pL_q$$

Use has been made of trigonometric identity

$$\cos^2 y = \frac{1+\cos 2y}{2}$$

[Q-3]. Harmonic $e^{-i2\omega_p t}$ and its complex conjugate:

$$\begin{aligned}
&(\psi_{0p}, \psi_{0p}) \\
=\;& 2(-i\omega_p)\left(\psi_{0px}^2+\psi_{0py}^2\right) - i\omega_p\psi_{0p}\left(\psi_{0pxx}+\psi_{0pyy}\right) \\
=\;& \left(-i\frac{B_p}{\omega_p}\right)^2(-i\omega_p)e^{-2x}\left\{2\left[(2L_p'-L_p)^2\cos^2 y + L_p^2\sin^2 y\right] + L_p\left(4L_p''-4L_p'\right)\cos^2 y\right\} \\
=\;& i\frac{B_p^2}{\omega_p}e^{-2x}\left[f_3(x)\cos 2y + g_3(x)\right] \qquad (4.19)
\end{aligned}$$

with

$$f_3(x) = 2L_p'^2 - 6L_pL_p' + 2L_pL_p''$$

$$g_3(x) = f_3(x) + 2L_p^2$$

[Q-4]. Harmonic $e^{-i2\omega_q t}$ and its complex conjugate:

$$\begin{aligned}
&(\psi_{0q}, \psi_{0q}) \\
=\;& 2(-i\omega_q)\left(\psi_{0qx}^2+\psi_{0qy}^2\right) - i\omega_q\psi_{0q}\left(\psi_{0qxx}+\psi_{0qyy}\right) \\
=\;& \left(-i\frac{B_q}{\omega_q}\right)^2(-i\omega_q)e^{-2x}\left\{2\left[(2L_q'-L_q)^2\cos^2 y + L_q^2\sin^2 y\right] + L_q\left(4L_q''-4L_q'\right)\cos^2 y\right\} \\
=\;& i\frac{B_q^2}{\omega_q}e^{-2x}\left[f_4(x)\cos 2y + g_4(x)\right] \qquad (4.20)
\end{aligned}$$

with

$$f_4(x) = 2L_q'^2 - 6L_qL_q' + 2L_qL_q''$$

$$g_4(x) = f_4(x) + 2L_q^2$$

In summary, there are 4 effective harmonics with their complex conjugates [Q-1] to [Q-4], each of which consists of two parts, the forcing with y dependence and the one without. They will excite two kinds of waves, one trapped and one radiated. We treat the two kinds of responses differently and therefore have eight wave components at the second order besides the known incident and reflected wave. We distinguish the two kinds of responses by different notations – ψ for the trapped wave and ϕ for the radiated wave:

i) $(\psi_{0p}^*, \psi_{0q}) \longrightarrow [\psi_{11}(x,y) + \phi_{11}(x)]\, e^{-i(\omega_q-\omega_p)t}$;

ii) $(\psi_{0p}, \psi_{0q}) \longrightarrow [\psi_{12}(x,y) + \phi_{12}(x)]\, e^{-i(\omega_p+\omega_q)t}$;

iii) $(\psi_{0p}, \psi_{0p}) \longrightarrow [\psi_{13}(x,y) + \phi_{13}(x)]\, e^{-i2\omega_p t}$;

iv) $(\psi_{0q}, \psi_{0q}) \longrightarrow [\psi_{14}(x,y) + \phi_{14}(x)]\, e^{-i2\omega_q t}$.

where ψ_{11}, ψ_{12}, ψ_{13} and ψ_{14} are proportional to $\cos 2y$.

4.2 Multiple-scale expansion

Let the incident and reflected wave have the normalized frequency $\omega = \omega_q + \omega_p = \sqrt{2q+1} + \sqrt{2p+1}$. Case of $\omega = \omega_q - \omega_p = \sqrt{2q+1} - \sqrt{2p+1}$ can be treated similarly and the details are given in the Appendix G. The multiple-scale expansion of the solution is

$$\begin{aligned}\Phi \;=\;& \left[\psi_{0p}(x,y,\tau)e^{-i\omega_p t} + *\right] + \left[\psi_{0q}(x,y,\tau)e^{-i\omega_q t} + *\right] \\ &+\bar{\epsilon}\left[\phi_{11}(x,\tau) + \psi_{11}(x,y,\tau)\right] e^{-i(\omega_q-\omega_p)t} + * \\ &+\bar{\epsilon}\left[\phi_{12}(x,\tau) + \psi_{12}(x,y,\tau)\right] e^{-i(\omega_p+\omega_q)t} + * \\ &+\bar{\epsilon}\left[\phi_{13}(x,\tau) + \psi_{13}(x,y,\tau)\right] e^{-i2\omega_p t} + * \\ &+\bar{\epsilon}\left[\phi_{14}(x,\tau) + \psi_{14}(x,y,\tau)\right] e^{-i2\omega_q t} + * \\ &+\bar{\epsilon}^2\left[\psi_{2p}(x,y,\tau)e^{-i\omega_p t} + *\right] + \bar{\epsilon}^2\left[\psi_{2q}(x,y,\tau)e^{-i\omega_q t} + *\right]\ldots \end{aligned} \qquad (4.21)$$

where the known incident and reflected wave will be incorporated in ϕ_{12} as part of the homogeneous solution. We have two time scales in the system, fast time t and slow time $\tau = \bar{\epsilon}^2 t$. Change of variable will give

$$\frac{\partial}{\partial t} \longrightarrow \frac{\partial}{\partial t} + \bar{\epsilon}^2\frac{\partial}{\partial \tau}, \quad \frac{\partial^2}{\partial t^2} \longrightarrow \frac{\partial^2}{\partial t^2} + 2\bar{\epsilon}^2\frac{\partial}{\partial t}\frac{\partial}{\partial \tau} + \bar{\epsilon}^4\frac{\partial^2}{\partial \tau^2}$$

Substituting 4.21 into Eq. (4.8) and separating different orders, we get

$$
\begin{aligned}
& \left\{\left[\omega_p^2\psi_{0p} + (x\psi_{0px})_x + x\psi_{0pyy}\right] e^{-i\omega_p t} + *\right\} \\
& + \left\{\left[\omega_q^2\psi_{0q} + (x\psi_{0qx})_x + x\psi_{0qyy}\right] e^{-i\omega_q t} + *\right\} \\
& + \bar{\epsilon}\left\{\left[(\omega_q - \omega_p)^2\phi_{11} + (x\phi_{11x})_x\right] e^{-i(\omega_q-\omega_p)t} + *\right\} \\
& + \bar{\epsilon}\left\{\left[(\omega_q - \omega_p)^2\psi_{11} + (x\psi_{11x})_x + x\psi_{11yy}\right] e^{-i(\omega_q-\omega_p)t} + *\right\} \\
& + \bar{\epsilon}\left\{\left[(\omega_p + \omega_q)^2\phi_{12} + (x\phi_{12x})_x\right] e^{-i(\omega_p+\omega_q)t} + *\right\} \\
& + \bar{\epsilon}\left\{\left[(\omega_p + \omega_q)^2\psi_{12} + (x\psi_{12x})_x + x\psi_{12yy}\right] e^{-i(\omega_p+\omega_q)t} + *\right\} \\
& + \bar{\epsilon}\left\{\left[4\omega_p^2\phi_{13} + (x\phi_{13x})_x\right] e^{-i2\omega_p t} + *\right\} \\
& + \bar{\epsilon}\left\{\left[4\omega_p^2\psi_{13} + (x\psi_{13x})_x + x\psi_{13yy}\right] e^{-i2\omega_p t} + *\right\} \\
& + \bar{\epsilon}\left\{\left[4\omega_q^2\phi_{14} + (x\phi_{14x})_x\right] e^{-i2\omega_q t} + *\right\} \\
& + \bar{\epsilon}\left\{\left[4\omega_q^2\psi_{14} + (x\psi_{14x})_x + x\psi_{14yy}\right] e^{-i2\omega_q t} + *\right\} \\
& + \bar{\epsilon}^2\left\{\left[\omega_p^2\psi_{2p} + (x\psi_{2px})_x + x\psi_{2pyy}\right] e^{-i\omega_p t} + *\right\} \\
& + \bar{\epsilon}^2\left\{\left[\omega_q^2\psi_{2q} + (x\psi_{2qx})_x + x\psi_{2qyy}\right] e^{-i\omega_q t} + *\right\} \\
= \; & \bar{\epsilon}\left\{(\psi_{0p}^*, \psi_{0q}) e^{-i(\omega_q-\omega_p)t} + *\right\} + \bar{\epsilon}\left\{(\psi_{0p}, \psi_{0q}) e^{-i(\omega_p+\omega_q)t} + *\right\} \\
& + \bar{\epsilon}\left\{(\psi_{0p}, \psi_{0p}) e^{-i2\omega_p t} + *\right\} + \bar{\epsilon}\left\{(\psi_{0q}, \psi_{0q}) e^{-i2\omega_q t} + *\right\} \\
& + \bar{\epsilon}^2\left\{\left[(\phi_{11}^*, \psi_{0q}) + (\psi_{11}^*, \psi_{0q}) + (\phi_{12}, \psi_{0q}^*) + (\psi_{12}, \psi_{0q}^*)\right] e^{-i\omega_p t} + *\right\} \\
& + \bar{\epsilon}^2\left\{\left[(\phi_{13}, \psi_{0p}^*) + (\psi_{13}, \psi_{0p}^*)\right] e^{-i\omega_p t} + *\right\} \\
& + \bar{\epsilon}^2\left\{\left[(\psi_{0p}, \psi_{0p}, \psi_{0p}^*) + (\psi_{0p}, \psi_{0q}, \psi_{0q}^*)\right] e^{-i\omega_p t} + *\right\} \\
& + \bar{\epsilon}^2\left\{\left[(\phi_{11}, \psi_{0p}) + (\psi_{11}, \psi_{0p}) + (\phi_{12}, \psi_{0p}^*) + (\psi_{12}, \psi_{0p}^*)\right] e^{-i\omega_q t} + *\right\} \\
& + \bar{\epsilon}^2\left\{\left[(\phi_{14}, \psi_{0q}^*) + (\psi_{14}, \psi_{0q}^*)\right] e^{-i\omega_q t} + *\right\} \\
& + \bar{\epsilon}^2\left\{\left[(\psi_{0q}, \psi_{0p}, \psi_{0p}^*) + (\psi_{0q}, \psi_{0q}, \psi_{0q}^*)\right] e^{-i\omega_q t} + *\right\} \\
& + \bar{\epsilon}^2\left\{-2i\omega_p \frac{\partial\psi_{0p}}{\partial\tau} e^{-i\omega_p t} + *\right\} + \bar{\epsilon}^2\left\{-2i\omega_q \frac{\partial\psi_{0q}}{\partial\tau} e^{-i\omega_q t} + *\right\} + \ldots \qquad (4.22)
\end{aligned}
$$

4.3 The leading-order solution

At O(1), we separate different harmonics to get

$$\omega_j^2\psi_{0j} + (x\psi_{0jx})_x + x\psi_{0jyy} = 0, \quad j = p,\ q.$$

With the boundary conditions of no flux at shore and exponential decay at infinity, the first order equations allow the edge wave eigen solutions (Modes with the same y dependence, but different x dependence are of our concern.)

$$\psi_{0j} = -i\frac{B_j(\tau)}{\omega_j}e^{-x}L_j(2x)\cos y, \quad j = p,\ q. \tag{4.23}$$

$B_j(\tau)$'s are the slowly varying dimensionless amplitudes of the edge waves at the shoreline (The physical amplitudes of the edge waves are $B_j' = |\bar{A}|B_j$. The evolution equations governing the complex amplitudes $B_j(\tau)$ are to be obtained at higher order.

For later use note that the functions $F_j = e^{-x}L_j(2x)$, which describe the x dependence of the edge wave modes, are eigen functions of the homogeneous boundary value problems

$$\omega_j^2 F_j + \left[(xF_{jx})_x - xF_j\right] = 0,$$

$$xF_{jx} = 0 \ \ at \ \ x = 0; \quad F_j \to 0, \quad x \sim \infty.$$

4.4 The second-order solution

At $O(\bar{\epsilon})$, there are eight locally generated wave components as mentioned at the end of section 4.1. These harmonics fall into two categories: 1-D outgoing radiated waves (denoted by ϕ_{11} to ϕ_{14}) and 2-D trapped waves (denoted by ψ_{11} to ψ_{14}). The known incident and reflected wave is contained in ϕ_{12} as its homogeneous part. We now pursue the inhomogeneous solutions.

4.4.1 ϕ_{11} to ϕ_{14} — Radiated harmonics

Collecting the second-order terms from (4.22) according to their harmonics, we get four equations governing the four radiated wave components

$$(\omega_q - \omega_p)^2\phi_{11} + (x\phi_{11x})_x = i\frac{B_p^* B_q}{\omega_p\omega_q}e^{-2x}g_1(x)$$

$$(\omega_q + \omega_p)^2\phi_{12} + (x\phi_{12x})_x = i\frac{B_p B_q}{\omega_p\omega_q}e^{-2x}g_2(x)$$

$$4\omega_p^2\phi_{13} + (x\phi_{13x})_x = i\frac{B_p^2}{\omega_p}e^{-2x}g_3(x)$$
$$4\omega_q^2\phi_{14} + (x\phi_{14x})_x = i\frac{B_q^2}{\omega_q}e^{-2x}g_4(x)$$

where we chose the part independent of y from forcing [Q-1] to [Q-4]. Refer to (4.17) $\sim$ (4.20) for the detail of those forcings.

The generic equation governing these four waves can be summarized as

$$\bar{\omega}^2\phi + (x\phi_x)_x = g(x) \tag{4.24}$$

where $\bar{\omega}$ is the generic frequency of the harmonic and $g(x)$ is the corresponding forcing out of the quadratic interaction.

We first rewrite the inhomogeneous Eq. (4.24) in the form

$$\phi_{xx} + \frac{1}{x}\phi_x + \frac{\bar{\omega}^2}{x}\phi = \frac{g(x)}{x} \tag{4.25}$$

Then the particular solution of the inhomogeneous equation will be

$$\phi = C_1 J_0(2\bar{\omega}\sqrt{x}) + C_2 Y_0(2\bar{\omega}\sqrt{x}) + u_1(x)J_0(2\bar{\omega}\sqrt{x}) + u_2(x)Y_0(2\bar{\omega}\sqrt{x}) \tag{4.26}$$

where

$$u_1(x) = -\int_0^x \frac{Y_0(2\bar{\omega}\sqrt{\xi})g(\xi)}{\xi W(J_0,Y_0)(\xi)}d\xi = -\pi\int_0^x Y_0(2\bar{\omega}\sqrt{\xi})g(\xi)d\xi$$
$$u_2(x) = \int_0^x \frac{J_0(2\bar{\omega}\sqrt{\xi})g(\xi)}{\xi W(J_0,Y_0)(\xi)}d\xi = \pi\int_0^x J_0(2\bar{\omega}\sqrt{\xi})g(\xi)d\xi$$

with Wronskian

$$W(J_0,Y_0)(x) = J_0\frac{dY_0}{dx} - Y_0\frac{dJ_0}{dx} = (J_0Y_0' - Y_0J_0')\frac{d(2\bar{\omega}\sqrt{x})}{dx} = \frac{2}{\pi 2\bar{\omega}\sqrt{x}}\frac{2\bar{\omega}}{2\sqrt{x}} = \frac{1}{\pi x}$$

and C_1, C_2 are the constants to be determined by boundary conditions. Use has been made of

$$J_0' = -J_1,\ Y_0' = -Y_1, \quad J_1(z)Y_0(z) - J_0(z)Y_1(z) = \frac{2}{\pi z}$$

The prime " $'$ " denotes the derivative with respect to argument $z = 2\bar{\omega}\sqrt{x}$.

First, for boundedness at the shoreline we require $C_2 = 0$. For confirmation, let us examine the no flux condition at shoreline, i.e.

$$x\phi_x \to 0 \quad as \quad x \to 0 \tag{4.27}$$

As $x \to 0$, we can approximate Bessel functions of the zeroth order by the following ascending series

$$J_0(z) = 1 - \frac{\frac{1}{4}z^2}{(1!)^2} + \frac{(\frac{1}{4}z^2)^2}{(2!)^2} - O(z^6), \quad Y_0(z) = \frac{2}{\pi}\left\{\ln\frac{z}{2} + \gamma\right\} J_0(z) + O(z^2)$$

and their first derivatives by

$$\frac{dJ_0(2\bar{\omega}\sqrt{x})}{dx} = -\bar{\omega}^2 + \frac{1}{2}\bar{\omega}^4 x - O(x^2), \quad \frac{dY_0(2\bar{\omega}\sqrt{x})}{dx} = \frac{1}{\pi x} - O\left(\ln(\bar{\omega}\sqrt{x})\right) \quad (4.28)$$

Upon substitution into (4.27), the first term in solution (4.26) becomes

$$C_1 x\left(J_0(2\bar{\omega}\sqrt{x})\right)_x = C_1\left(-\bar{\omega}^2 x + O(x^2)\right)$$

and the second term becomes

$$C_2 x\left(Y_0(2\bar{\omega}\sqrt{x})\right)_x = C_2\left(\frac{1}{\pi} - O\left(x\ln(\sqrt{x})\right)\right)$$

For the third and fourth terms, $Y_0(2\bar{\omega}\sqrt{x})g(x) \sim g(0)\ln(\bar{\omega}\sqrt{x})$ as $x \to 0$ so that

$$u_1(x) \sim \pi\int_0^x \ln(\bar{\omega}\sqrt{\xi})d\xi \sim \int_0^{\sqrt{x}} \xi\ln(\xi)d\xi \sim x\ln\sqrt{x} + O(x)$$

and $J_0(2\bar{\omega}\sqrt{x})g(x) \to g(0)$ as $x \to 0$ so that

$$u_2(x) = \pi\int_0^x \left[g(0) + O(\xi)\right]d\xi = \pi\left[xg(0) + O(x^2)\right]$$

The third and fourth term become

$$\begin{aligned} & x\left[\left(u_1(x)J_0(2\bar{\omega}\sqrt{x})\right)_x + \left(u_2(x)Y_0(2\bar{\omega}\sqrt{x})\right)_x\right] \\ = \; & x\left(u_1(x)\frac{dJ_0(2\bar{\omega}\sqrt{x})}{dx} + u_2(x)\frac{dY_0(2\bar{\omega}\sqrt{x})}{dx}\right) \\ \sim \; & x\left(-\bar{\omega}^2 x\ln(\sqrt{x}) + g(0)\right) \sim g(0)x \end{aligned}$$

where use has been made of

$$u_{1x}J_0(2\bar{\omega}\sqrt{x}) + u_{2x}Y_0(2\bar{\omega}\sqrt{x}) = -\pi Y_0 g(x)J_0 + \pi J_0 g(x)Y_0 = 0$$

Collecting all four terms, we get at $x = 0$

$$x\phi_x \sim \frac{C_2}{\pi} + g(0)x - C_1\bar{\omega}^2 x + o(x) \quad as \quad x \to 0 \quad (4.29)$$

Therefore, C_2 must be 0 in order for ϕ to satisfy the no-flux condition at the shoreline.

Secondly, a boundary condition at infinity is required for a semi-infinite domain problem. In order to find out what is this boundary, we need study the asymptotic behavior for both the forcing $g(x)$ and the particular solution ϕ at large x.

$$J_0(z) \sim \sqrt{\frac{2}{\pi z}} \cos\left(z - \frac{\pi}{4}\right); \quad Y_0(z) \sim \sqrt{\frac{2}{\pi z}} \sin\left(z - \frac{\pi}{4}\right)$$

$$\frac{dJ_0(2\bar{\omega}\sqrt{x})}{dx} \sim x^{-3/4} \sin\left(2\bar{\omega}\sqrt{x} - \frac{\pi}{4}\right); \quad \frac{d^2 J_0(2\bar{\omega}\sqrt{x})}{dx^2} \sim x^{-5/4} \cos\left(2\bar{\omega}\sqrt{x} - \frac{\pi}{4}\right)$$

Since

$$g(x) \sim e^{-2x}$$

it follows that

$$Y_0(2\bar{\omega}\sqrt{\xi})g(\xi) \sim J_0(2\bar{\omega}\sqrt{\xi})g(\xi) \sim x^{-1/4}e^{-2x}$$

i.e. the integrand of $u_1(x)$ and $u_2(x)$ diminish exponentially at infinity, which guarantees that the integral $u_1(x)$ and $u_2(x)$ converge to a constant as $x \to \infty$. Finally, the solution $\phi \sim x^{-1/4}$ like $J_0(2\bar{\omega}\sqrt{x})$ and $Y_0(2\bar{\omega}\sqrt{x})$ at $x = \infty$.

By comparison we can see that at large x, the forcing $g(x)$ diminishes faster than solution $\phi(x)$ (exponential versus $x^{-1/4}$), i.e. relative to the solution $\phi(x)$, forcing $g(x)$ can be treated as local disturbance. Therefore, the radiation condition applies so that the inhomogeneous solution $\phi(x)$ should appear as an outgoing wave at infinity. It is easy to see that

$$\phi \sim -iu_2(\infty)H_0^{(1)}(2\bar{\omega}\sqrt{x}) \sim -iu_2(\infty)\sqrt{\frac{2}{2\bar{\omega}\pi\sqrt{x}}}e^{i\left(2\bar{\omega}\sqrt{x}-\frac{\pi}{4}\right)} \quad as \quad x \to \infty$$

representing the propagating wave if we let

$$C_1 = -u_1(\infty) - iu_2(\infty).$$

Therefore, the particular solution corresponding to the local forcing $g(x)$ is

$$G(x) = \left[-u_1(\infty) - iu_2(\infty)\right] J_0(2\bar{\omega}\sqrt{x}) + u_1(x)J_0(2\bar{\omega}\sqrt{x}) + u_2(x)Y_0(2\bar{\omega}\sqrt{x}) \quad (4.30)$$

For later uses, we work out some constants as follows. From (4.29) we get

$$\begin{aligned} \left.\frac{dG(x)}{dx}\right|_{x=0} &= C_1(-\bar{\omega}^2) + g(0) \\ &= \bar{\omega}^2\left(u_1(\infty) + iu_2(\infty)\right) + g(0) \end{aligned} \tag{4.31}$$

where $g(0)$ is the excitation force at $x = 0$. And

$$G(0) = C_1 = -u_1(\infty) - iu_2(\infty) \tag{4.32}$$

From (4.31) and (4.32) we can see that

$$\left.\frac{dG(x)}{dx}\right|_{x=0} \equiv -\bar{\omega}^2 G(0) + g(0). \tag{4.33}$$

Solutions to the four outgoing waves are summarized as follows:

$$\begin{aligned} \phi_{11} &= i\frac{B_p^* B_q}{\omega_p\omega_q}G_1(x), \quad \text{with } g(x) = e^{-2x}g_1(x) \text{ and } \bar{\omega} = \omega_q - \omega_p; \\ \phi_{12} &= -i\frac{e^{i2\varphi}}{\omega}J_0(2\omega\sqrt{x}) + i\frac{B_p B_q}{\omega_p\omega_q}G_2(x), \quad \text{with } g(x) = e^{-2x}g_2(x) \text{ and } \bar{\omega} = \omega_q + \omega_p; \\ \phi_{13} &= i\frac{B_p^2}{\omega_p}G_3(x), \quad \text{with } g(x) = e^{-2x}g_3(x) \text{ and } \bar{\omega} = 2\omega_p; \\ \phi_{14} &= i\frac{B_q^2}{\omega_q}G_4(x), \quad \text{with } g(x) = e^{-2x}g_4(x) \text{ and } \bar{\omega} = 2\omega_q. \end{aligned} \tag{4.34}$$

where G_1, G_2, G_3 and G_4 are given by (4.30). We have incorporated the incident wave in the solution $\phi_{12}(x)$, where $A' = \bar{\epsilon}|\bar{A}|e^{i2\varphi}$ is the known incident and reflected wave amplitude at the shoreline and $\omega = \omega_q + \omega_p$ is its frequency.

4.4.2 ψ_{11} to ψ_{14} — Trapped harmonics

Collecting the second-order terms from (4.22) according to their harmonics, we get four equations governing the four trapped wave components

$$(\omega_q - \omega_p)^2\psi_{11} + (x\psi_{11x})_x + x\psi_{11yy} = i\frac{B_p^* B_q}{\omega_p\omega_q}e^{-2x}f_1(x)\cos 2y$$

$$(\omega_q + \omega_p)^2\psi_{12} + (x\psi_{12x})_x + x\psi_{11yy} = i\frac{B_p B_q}{\omega_p\omega_q}e^{-2x}f_2(x)\cos 2y$$

$$4\omega_p^2\psi_{13} + (x\psi_{13x})_x + x\psi_{11yy} = i\frac{B_p^2}{\omega_p}e^{-2x}f_3(x)\cos 2y$$

$$4\omega_q^2\psi_{14} + (x\psi_{14x})_x + x\psi_{11yy} = i\frac{B_q^2}{\omega_q}e^{-2x}f_4(x)\cos 2y$$

where we chose the part with y-dependence from forcing [Q-1] to [Q-4]. Refer to (4.17) $\sim$ (4.20) for the detail of those forcings.

The generic equation governing these four waves can be summarized as

$$\bar{\omega}^2\psi + (x\psi_x)_x + x\psi_{yy} = g(x)\cos 2y$$

where $\bar{\omega}$ is the generic frequency of the harmonic and $g(x)\cos 2y$ is the corresponding forcing out of the quadratic interaction. Since each of the four forcing [Q-1] to [Q-4] has a y dependence of $\cos 2y$, we adopt a solution

$$\psi = f(x)\cos 2y$$

with $f(x)$ satisfying

$$xf_{xx} + f_x + \left[\bar{\omega}^2 - 4x\right]f = g(x) \tag{4.35}$$

Change of variables

$$\xi = 4x, \quad f = e^{-\frac{\xi}{2}}f(\xi)$$

leads to the Laguerre differential equation, which belongs to the class of confluent hypergeometric equation.

$$\xi f'' + (1-\xi)f' + \left(\frac{\bar{\omega}^2}{4} - \frac{1}{2}\right)f = \frac{1}{4}g\left(\frac{\xi}{4}\right)e^{\frac{\xi}{2}}$$

Notice that, for the homogeneous equation,

$$\frac{\bar{\omega}^2}{4} - \frac{1}{2} \neq n, \quad n = 0, 1, 2...$$

where $\bar{\omega}$ is one of the four values

$$\bar{\omega} = \sqrt{2q+1} \pm \sqrt{2p+1}$$

or

$$\bar{\omega} = 2\sqrt{2j+1}, \quad j = p, q$$

Therefore, there is no question of solvability. For $\bar{\omega} = 2\sqrt{2j+1}$,

$$\frac{\bar{\omega}^2}{4} - \frac{1}{2} = 2j + 1 - \frac{1}{2} = 2j + \frac{1}{2}.$$

Therefore, it is obvious that inequality

$$\frac{\bar{\omega}^2}{4} - \frac{1}{2} \neq n$$

holds since both n and j are integers;

For $\bar{\omega} = \sqrt{2q+1} \pm \sqrt{2p+1}$, the eigen value condition is satisfied if

$$\frac{\bar{\omega}^2}{4} - \frac{1}{2} = \frac{2(p+q+1) \pm 2\sqrt{(2q+1)(2p+1)}}{4} - \frac{1}{2} = n$$

or

$$(p+q) \pm \sqrt{(2q+1)(2p+1)} = 2n,$$

or

$$(2q+1)(2p+1) = [(p+q) - 2n]^2$$

which does not hold for the several cases we will study (see Table 4.1).

	(p,q)					
	(0, 1)	(0, 2)	(0, 3)	(1, 2)	(1, 3)	(2, 3)
ω	$\sqrt{3} \pm 1$	$\sqrt{5} \pm 1$	$\sqrt{7} \pm 1$	$\sqrt{5} \pm \sqrt{3}$	$\sqrt{7} \pm \sqrt{3}$	$\sqrt{7} \pm \sqrt{5}$
$\frac{\omega^2}{4} - \frac{1}{2}$	$\frac{1 \pm \sqrt{3}}{2}$	$\frac{2 \pm \sqrt{5}}{2}$	$\frac{3 \pm \sqrt{7}}{2}$	$\frac{3 \pm \sqrt{15}}{2}$	$\frac{4 \pm \sqrt{21}}{2}$	$\frac{5 \pm \sqrt{35}}{2}$

Table 4.1: Check for the eigen value condition for several combinations of (p, q).

The no-flux boundary condition applies at the shoreline, i.e. $xf_x \to 0$ as $x \to 0$. Since the forcing $g(x)$ exponentially decays as x increases, only the homogeneous solution survives at a large distance. As $x \to \infty$, the equation becomes the modified Bessel equation

$$xf_{xx} + f_x - \nu^2 xf = 0, \quad \nu = 2$$

which has the general solution in terms of zeroth-order modified Bessel function of the first and second kind

$$f = C_1 I_0(\nu x) + C_2 K_0(\nu x)$$

Since I_0 grows exponentially in x, whereas K_0 exponentially decays at $x \sim \infty$.

$$I_0(z) \to \frac{1}{\sqrt{2\pi z}} e^z, \quad K_0(z) \to \sqrt{\frac{\pi}{2z}} e^{-z}, \quad as \quad z \to \infty.$$

I_0 must be excluded from our solution and the solution of our problem behaves like K_0, which diminishes like e^{-2x} at ∞. ψ is therefore trapped..

Now we impose a boundary condition at a large distance for our problem as follows:

$$f \to 0 \quad \text{at} \quad x = L$$

with L is large enough so that both forcing $g(x)$ and the homogeneous solution $K_0(x)$ vanish there. Eq. (4.35) can be rewritten as

$$-\frac{d}{dx}(xf_x) + \left[4x - \bar{\omega}^2\right] f_{11} = -g(x)$$

with the corresponding boundary conditions

$$xf_x = 0 \quad \text{as} \quad x \to 0$$

$$xf_x = 0 \quad \text{as} \quad x \to L$$

In Appendix H the numerical formula of the finite element method is given and is used to compute the solutions to the four trapped harmonics f_{11}, f_{12}, f_{13} and f_{14}, which are summarized as follows:

$$\begin{aligned}
\psi_{11} &= i\frac{B_p^* B_q}{\omega_p \omega_q} f_{11}(x)\cos 2y, \quad g(x) = e^{-2x} f_1(x), \quad \bar{\omega} = \omega_q - \omega_p; \\
\psi_{12} &= i\frac{B_p B_q}{\omega_p \omega_q} f_{12}(x)\cos 2y, \quad g(x) = e^{-2x} f_2(x), \quad \bar{\omega} = \omega_q + \omega_p; \\
\psi_{13} &= i\frac{B_p^2}{\omega_p} f_{13}(x)\cos 2y, \quad g(x) = e^{-2x} f_3(x), \quad \bar{\omega} = 2\omega_p; \\
\psi_{14} &= i\frac{B_q^2}{\omega_q} f_{14}(x)\cos 2y, \quad g(x) = e^{-2x} f_4(x), \quad \bar{\omega} = 2\omega_q.
\end{aligned} \tag{4.36}$$

Now f_{11} to f_{14} can be solved by Finite Element Method as described in Appendix H.

4.5 The third-order problem

4.5.1 Governing equations and forcing

At $O(\bar{\epsilon}^2)$, we collect terms of same harmonic and get the governing equations for two edge waves

$$\omega_p^2\psi_{2p} + (x\psi_{2px})_x + x\psi_{2pyy} = -2i\omega_p\frac{\partial\psi_{0p}}{\partial\tau} + \mathcal{E}_p(x)\cos y$$

$$\omega_q^2\psi_{2q} + (x\psi_{2qx})_x + x\psi_{2qyy} = -2i\omega_q\frac{\partial\psi_{0q}}{\partial\tau} + \mathcal{E}_q(x)\cos y$$

where we introduced $\mathcal{E}_p(x)$ to denote the resonance forces with y-dependence of $\cos y$ from the contribution of all the following terms

$$\begin{aligned}&(\phi_{11}^*, \psi_{0q}) + (\psi_{11}^*, \psi_{0q}) + (\phi_{12}, \psi_{0q}^*) + (\psi_{12}, \psi_{0q}^*)\\ &+(\phi_{13}, \psi_{0p}^*) + (\psi_{13}, \psi_{0p}^*) + (\psi_{0p}, \psi_{0p}, \psi_{0p}^*) + (\psi_{0p}, \psi_{0q}, \psi_{0q}^*)\end{aligned} \tag{4.37}$$

and $\mathcal{E}_q(x)$ from

$$\begin{aligned}&(\phi_{11}, \psi_{0p}) + (\psi_{11}, \psi_{0p}) + (\phi_{12}, \psi_{0p}^*) + (\psi_{12}, \psi_{0p}^*)\\ &+(\phi_{14}, \psi_{0q}^*) + (\psi_{14}, \psi_{0q}^*) + (\psi_{0q}, \psi_{0p}, \psi_{0p}^*) + (\psi_{0q}, \psi_{0q}, \psi_{0q}^*)\end{aligned} \tag{4.38}$$

Let $\psi_{2j} = H_j(x)\cos y$ and recall the first-order solution from (4.23), then the governing equation becomes

$$\mathcal{L}_j H_j = -2\frac{\partial B_j}{\partial\tau}F_j(x) + \mathcal{E}_j(x), \quad j = p, q \tag{4.39}$$

where the linear operators are defined by

$$\mathcal{L}_j H_j = \omega_j^2 H_j + \left[(xH_{jx})_x - xH_j\right]$$

Details of forcing $\mathcal{E}_p(x)$ and $\mathcal{E}_q(x)$ are given below:

In $\mathcal{E}_p$, we have

[$\mathcal{E}_p$-1].

$$\begin{aligned}&(\phi_{11}^*, \psi_{0q})\\
= \;& 2\left\{\phi_{11x}^*\psi_{0qx}\left[i(\omega_q - \omega_p) - i\omega_q)\right]\right\} - i\omega_q\psi_{0q}\phi_{11xx}^* + i(\omega_q - \omega_p)\phi_{11}^*(\psi_{0qxx} + \psi_{0qyy})\\
= \;& -i2\omega_p\phi_{11x}^*\psi_{0qx} - i\omega_q\psi_{0q}\phi_{11xx}^* + i(\omega_q - \omega_p)\phi_{11}^*(\psi_{0qxx} + \psi_{0qyy})\\
= \;& -ie^{-x}\cos y\left(-i\frac{B_pB_q^*}{\omega_p\omega_q}\right)\left(-i\frac{B_q}{\omega_q}\right)\left\{2\omega_p\frac{dG_1}{dx}(2L_q' - L_q)\right.\\
&\left.+\omega_q\frac{d^2G_1}{dx^2}L_q - (\omega_q - \omega_p)G_1(4L_q'' - 4L_q')\right\}\\
= \;& i\frac{B_pB_qB_q^*}{\omega_p\omega_q^2}e^{-x}\left\{2\omega_p\frac{dG_1}{dx}(2L_q' - L_q) + \omega_q\frac{d^2G_1}{dx^2}L_q - (\omega_q - \omega_p)G_1(4L_q'' - 4L_q')\right\}\cos y\\
= \;& \hat{h}_{p1}(x)B_pB_qB_q^*\end{aligned} \tag{4.40}$$

$[\mathcal{E}_p\text{-}2]$.

$$
\begin{aligned}
& (\phi_{12}, \psi^*_{0q}) \\
= \;& 2\left\{\phi_{12x}\psi^*_{0qx}\left[-i(\omega_p+\omega_q)+i\omega_q)\right]\right\} + i\omega_q\psi^*_{0q}\phi_{12xx} - i(\omega_p+\omega_q)\phi_{12}(\psi^*_{0qxx}+\psi^*_{0qyy}) \\
= \;& -i2\omega_p\phi_{12x}\psi^*_{0qx} + i\omega_q\psi^*_{0q}\phi_{12xx} - i(\omega_p+\omega_q)\phi_{12}(\psi^*_{0qxx}+\psi^*_{0qyy}) \\
= \;& -ie^{-x}\cos y\left(i\frac{B_pB_q}{\omega_p\omega_q}\right)\left(i\frac{B^*_q}{\omega_q}\right)\left\{2\omega_p\frac{dG_2}{dx}(2L'_q-L_q)\right. \\
& \left.-\omega_q\frac{d^2G_2}{dx^2}L_q + (\omega_p+\omega_q)G_2(4L''_q-4L'_q)\right\} \\
& -ie^{-x}\cos y\left(-i\frac{e^{i2\varphi}}{\omega}\right)\left(i\frac{B^*_q}{\omega_q}\right)\left\{2\omega_p\frac{dJ_0}{dx}(2L'_q-L_q)\right. \\
& \left.-\omega_q\frac{d^2J_0}{dx^2}L_q + (\omega_p+\omega_q)J_0(4L''_q-4L'_q)\right\} \\
= \;& i\frac{B_pB_qB^*_q}{\omega_p\omega_q^2}e^{-x}\left\{2\omega_p\frac{dG_2}{dx}(2L'_q-L_q) - \omega_q\frac{d^2G_2}{dx^2}L_q + (\omega_p+\omega_q)G_2(4L''_q-4L'_q)\right\}\cos y \\
& -i\frac{e^{i2\varphi}B^*_q}{\omega\omega_q}e^{-x}\left\{2\omega_p\frac{dJ_0}{dx}(2L'_q-L_q) - \omega_q\frac{d^2J_0}{dx^2}L_q + (\omega_p+\omega_q)J_0(4L''_q-4L'_q)\right\}\cos y \\
= \;& \hat{h}_{p2}(x)B_pB_qB^*_q + ie^{i2\varphi}\hat{f}_p(x)B^*_q
\end{aligned}
\tag{4.41}
$$

$[\mathcal{E}_p\text{-}3]$.

$$
\begin{aligned}
& (\phi_{13}, \psi^*_{0p}) \\
= \;& 2\left\{\phi_{13x}\psi^*_{0px}\left[-i2\omega_p+i\omega_p\right]\right\} + i\omega_p\psi^*_{0p}\phi_{13xx} - i2\omega_p\phi_{13}(\psi^*_{0pxx}+\psi^*_{0pyy}) \\
= \;& -i2\omega_p\phi_{13x}\psi^*_{0px} + i\omega_p\psi^*_{0p}\phi_{13xx} - i2\omega_p\phi_{13}(\psi^*_{0pxx}+\psi^*_{0pyy}) \\
= \;& -ie^{-x}\cos y\left(i\frac{B_p^2}{\omega_p}\right)\left(i\frac{B^*_p}{\omega_p}\right)\left\{2\omega_p\frac{dG_3}{dx}(2L'_p-L_p)\right. \\
& \left.-\omega_p\frac{d^2G_3}{dx^2}L_p + 2\omega_pG_3(4L''_p-4L'_p)\right\} \\
= \;& i\frac{B_pB_pB^*_p}{\omega_p}e^{-x}\left\{2\frac{dG_3}{dx}(2L'_p-L_p) - \frac{d^2G_3}{dx^2}L_p + 2G_3(4L''_p-4L'_p)\right\}\cos y \\
= \;& \hat{g}_{p1}(x)B_p^2B^*_p
\end{aligned}
\tag{4.42}
$$

$[\mathcal{E}_p\text{-}4]$.

$$
\begin{aligned}
& (\psi^*_{11}, \psi_{0q}) \\
= \;& 2\left\{\psi^*_{11x}\psi_{0qx}\left[-i\omega_q+i(\omega_q-\omega_p)\right] + \psi^*_{11y}\psi_{0qy}\left[-i\omega_q+i(\omega_q-\omega_p)\right]\right\}
\end{aligned}
$$

$$
\begin{aligned}
& -i\omega_q\psi_{0q}\left(\psi^*_{11xx}+\psi^*_{11yy}\right)+i(\omega_q-\omega_p)\psi^*_{11}\left(\psi_{0qxx}+\psi_{0qyy}\right) \\
= & -i2\omega_p\left[\psi^*_{11x}\psi_{0qx}+\psi^*_{11y}\psi_{0qy}\right]-i\omega_q\psi_{0q}\left(\psi^*_{11xx}+\psi^*_{11yy}\right) \\
& +i(\omega_q-\omega_p)\psi^*_{11}\left(\psi_{0qxx}+\psi_{0qyy}\right) \\
= & -ie^{-x}\left(-i\frac{B_pB^*_q}{\omega_p\omega_q}\right)\left(-i\frac{B_q}{\omega_q}\right)\Big[2\omega_p f_{11x}(2L'_q-L_q)\cos 2y\cos y \\
& +2\omega_p f_{11}(-2)L_q(-1)\sin 2y\sin y+\omega_q L_q(f_{11xx}-4f_{11})\cos 2y\cos y \\
& -(\omega_q-\omega_p)f_{11}(4L''_q-4L'_q)\cos 2y\cos y\Big] \\
= & i\frac{B_pB_qB^*_q}{\omega_p\omega_q^2}e^{-x}\Big[\omega_p f_{11x}(2L'_q-L_q)+2\omega_p f_{11}L_q \\
& +\frac{\omega_q}{2}L_q(f_{11xx}-4f_{11})-\frac{\omega_q-\omega_p}{2}f_{11}(4L''_q-4L'_q)\Big]\cos y \\
= & i\frac{B_pB_qB^*_q}{\omega_p\omega_q^2}e^{-x}\Big[\frac{\omega_q}{2}L_q f_{11xx}+\omega_p(2L'_q-L_q)f_{11x} \\
& -\frac{\omega_q-\omega_p}{2}(4L''_q-4L'_q+4L_q)f_{11}\Big]\cos y \\
= & \hat{h}_{p3}(x)B_pB_qB^*_q \qquad (4.43)
\end{aligned}
$$

where terms not proportional to $\cos y$ are discarded. Use has been made of the trigonometric identities

$$
\cos s\cos t=\frac{\cos(s+t)+\cos(s-t)}{2},\qquad \sin s\sin t=\frac{\cos(s-t)-\cos(s+t)}{2}
$$

$[\mathcal{E}_p$-5].

$$
\begin{aligned}
& (\psi_{12},\psi^*_{0q}) \\
= & 2\left\{\psi_{12x}\psi^*_{0qx}\left[i\omega_q-i(\omega_p+\omega_q)\right]+\psi_{12y}\psi^*_{0qy}\left[i\omega_q-i(\omega_p+\omega_q)\right]\right\} \\
& +i\omega_q\psi^*_{0q}\left(\psi_{12xx}+\psi_{12yy}\right)-i(\omega_p+\omega_q)\psi_{12}\left(\psi^*_{0qxx}+\psi^*_{0qyy}\right) \\
= & -i2\omega_p\left[\psi_{12x}\psi^*_{0qx}+\psi_{12y}\psi^*_{0qy}\right]+i\omega_q\psi^*_{0q}\left(\psi_{12xx}+\psi_{12yy}\right) \\
& -i(\omega_p+\omega_q)\psi_{12}\left(\psi^*_{0qxx}+\psi^*_{0qyy}\right) \\
= & -ie^{-x}\left(i\frac{B_pB_q}{\omega_p\omega_q}\right)\left(i\frac{B^*_q}{\omega_q}\right)\Big[2\omega_p f_{12x}(2L'_q-L_q)\cos 2y\cos y \\
& +2\omega_p f_{12}(-2)L_q(-1)\sin 2y\sin y-\omega_q L_q(f_{12xx}-4f_{12})\cos 2y\cos y \\
& +(\omega_p+\omega_q)f_{12}(4L''_q-4L'_q)\cos 2y\cos y\Big] \\
= & i\frac{B_pB_qB^*_q}{\omega_p\omega_q^2}e^{-x}\Big[\omega_p f_{12x}(2L'_q-L_q)+2\omega_p f_{12}L_q
\end{aligned}
$$

$$
\begin{aligned}
& -\frac{\omega_q}{2}L_q(f_{12xx}-4f_{12})+\frac{\omega_p+\omega_q}{2}f_{12}(4L_q''-4L_q')\Big]\cos y \\
= \;& i\frac{B_pB_qB_q^*}{\omega_p\omega_q^2}e^{-x}\Big[\omega_p(2L_q'-L_q)f_{12x}-\frac{\omega_q}{2}L_qf_{12xx} \\
& +\frac{\omega_p+\omega_q}{2}(4L_q''-4L_q'+4L_q)f_{12}\Big]\cos y \\
= \;& \hat{h}_{p4}(x)B_pB_qB_q^*
\end{aligned} \tag{4.44}
$$

$[\mathcal{E}_p\text{-}6]$.

$$
\begin{aligned}
& (\psi_{13},\psi_{0p}^*) \\
= \;& 2\Big\{\psi_{13x}\psi_{0px}^*\left[i\omega_p-i2\omega_p\right]+\psi_{13y}\psi_{0py}^*\left[i\omega_p-i2\omega_p\right]\Big\} \\
& +i\omega_p\psi_{0p}^*\left(\psi_{13xx}+\psi_{13yy}\right)-i2\omega_p\psi_{13}\left(\psi_{0pxx}^*+\psi_{0pyy}^*\right) \\
= \;& -i2\omega_p\left[\psi_{13x}\psi_{0px}^*+\psi_{13y}\psi_{0py}^*\right]+i\omega_p\psi_{0p}^*\left(\psi_{13xx}+\psi_{13yy}\right) \\
& -i2\omega_p\psi_{13}\left(\psi_{0pxx}^*+\psi_{0pyy}^*\right) \\
= \;& -ie^{-x}\left(i\frac{B_p^2}{\omega_p}\right)\left(i\frac{B_p^*}{\omega_p}\right)\Big[2\omega_pf_{13x}(2L_p'-L_p)\cos 2y\cos y \\
& +2\omega_pf_{13}(-2)L_p(-1)\sin 2y\sin y-\omega_pL_p(f_{13xx}-4f_{13})\cos 2y\cos y \\
& +2\omega_pf_{13}(4L_p''-4L_p')\cos 2y\cos y\Big] \\
= \;& i\frac{B_pB_pB_p^*}{\omega_p}e^{-x}\Big[f_{13x}(2L_p'-L_p)+2f_{13}L_p \\
& -\frac{1}{2}L_p(f_{13xx}-4f_{13})+f_{13}(4L_p''-4L_p')\Big]\cos y \\
= \;& i\frac{B_pB_pB_p^*}{\omega_p}e^{-x}\Big[f_{13x}(2L_p'-L_p)-\frac{1}{2}L_pf_{13xx}+f_{13}(4L_p''-4L_p'+4L_p)\Big]\cos y \\
= \;& \hat{g}_{p2}(x)B_p^2B_p^*
\end{aligned} \tag{4.45}
$$

where only terms proportional to $\cos y$ are kept.

$[\mathcal{E}_p\text{-}7]$.

$$
\begin{aligned}
& (\psi_{0p},\psi_{0p},\psi_{0p}^*) \\
= \;& \frac{3}{2}\left(\psi_{0pxx}2\psi_{0px}\psi_{0px}^*+\psi_{0pxx}^*\psi_{0px}\psi_{0px}+\psi_{0pyy}2\psi_{0py}\psi_{0py}^*+\psi_{0pyy}^*\psi_{0py}\psi_{0py}\right) \\
& +\frac{1}{2}\left(\psi_{0pyy}2\psi_{0px}\psi_{0px}^*+\psi_{0pyy}^*\psi_{0px}\psi_{0px}+\psi_{0pxx}2\psi_{0py}\psi_{0py}^*+\psi_{0pxx}^*\psi_{0py}\psi_{0py}\right) \\
& +2\left(\psi_{0px}\psi_{0py}\psi_{0pxy}^*+\psi_{0px}\psi_{0py}^*\psi_{0pxy}+\psi_{0px}^*\psi_{0py}\psi_{0pxy}\right) \\
= \;& \left(-i\frac{B_p}{\omega_p}\right)^2 i\frac{B_p^*}{\omega_p}e^{-3x}\left\{\frac{9}{2}(4L_p''-4L_p'+L_p)(2L_p'-L_p)^2\cos^3 y-\frac{9}{2}L_p^3\cos y\sin^2 y\right.
\end{aligned}
$$

$$
\begin{aligned}
& - \frac{3}{2}(2L_p' - L_p)^2 L_p \cos^3 y + \frac{3}{2}(4L_p'' - 4L_p' + L_p) L_p^2 \cos y \sin^2 y \\
& + 2\left[3(2L_p' - L_p)^2 L_p \cos y \sin^2 y\right]\Big\} \\
= & -i\frac{B_p^2 B_p^*}{\omega_p^3} e^{-3x} \left\{ \left[\frac{9}{2}(4L_p'' - 4L_p' + L_p)(2L_p' - L_p)^2 - \frac{3}{2}(2L_p' - L_p)^2 L_p\right] \cos^3 y \right. \\
& \left. + \left[6(2L_p' - L_p)^2 L_p + \frac{3}{2}(4L_p'' - 4L_p' + L_p) L_p^2 - \frac{9}{2} L_p^3\right] \cos y \sin^2 y \right\} \\
= & -i\frac{B_p^2 B_p^*}{\omega_p^3} e^{-3x} \left\{ \left[\frac{27}{8}(4L_p'' - 4L_p' + L_p)(2L_p' - L_p)^2 - \frac{9}{8}(2L_p' - L_p)^2 L_p\right] \right. \\
& \left. + \left[\frac{3}{2}(2L_p' - L_p)^2 L_p + \frac{3}{8}(4L_p'' - 4L_p' + L_p) L_p^2 - \frac{9}{8} L_p^3\right] \right\} \cos y \\
= & \ \hat{g}_{p3}(x) B_p^2 B_p^* \qquad (4.46)
\end{aligned}
$$

where terms not proportional to $\cos y$ are discarded. Use has been made of

$$
\cos^3 y = \frac{3}{4}\cos y + \frac{1}{4}\cos 3y, \quad \cos y \sin^2 y = \frac{1}{4}\cos y - \frac{1}{4}\cos 3y
$$

[$\mathcal{E}_p$-8].

$$
\begin{aligned}
& (\psi_{0p}, \psi_{0q}, \psi_{0q}^*) \\
= & \ \frac{3}{2}\left(\psi_{0pxx} 2\psi_{0qx}\psi_{0qx}^* + \psi_{0qxx} 2\psi_{0px}\psi_{0qx}^* + \psi_{0qxx}^* 2\psi_{0px}\psi_{0qx}\right) \\
& + \frac{3}{2}\left(\psi_{0pyy} 2\psi_{0qy}\psi_{0qy}^* + \psi_{0qyy} 2\psi_{0py}\psi_{0qy}^* + \psi_{0qyy}^* 2\psi_{0py}\psi_{0qy}\right) \\
& + \frac{1}{2}\left(\psi_{0pyy} 2\psi_{0qx}\psi_{0qx}^* + \psi_{0qyy} 2\psi_{0px}\psi_{0qx}^* + \psi_{0qyy}^* 2\psi_{0px}\psi_{0qx}\right) \\
& + \frac{1}{2}\left(\psi_{0pxx} 2\psi_{0qy}\psi_{0qy}^* + \psi_{0qxx} 2\psi_{0py}\psi_{0qy}^* + \psi_{0qxx}^* 2\psi_{0py}\psi_{0qy}\right) \\
& + 2\left(\psi_{0px}\psi_{0qy}\psi_{0qxy}^* + \psi_{0px}\psi_{0qy}^*\psi_{0qxy} + \psi_{0qx}\psi_{0py}\psi_{0qxy}^*\right) \\
& + 2\left(\psi_{0qx}\psi_{0qy}^*\psi_{0pxy} + \psi_{0qx}^*\psi_{0py}\psi_{0qxy} + \psi_{0qx}^*\psi_{0qy}\psi_{0pxy}\right) \\
= & \left(-i\frac{B_p}{\omega_p}\right)\left(-i\frac{B_q}{\omega_q}\right) i\frac{B_q^*}{\omega_q} e^{-3x} \left\{3(4L_p'' - 4L_p' + L_p)(2L_q' - L_q)^2 \cos^3 y \right. \\
& + 6(4L_q'' - 4L_q' + L_q)(2L_q' - L_q)(2L_p' - L_p)\cos^3 y - 9L_p L_q^2 \cos y \sin^2 y \\
& - (2L_q' - L_q)^2 L_p \cos^3 y - 2L_q(2L_p' - L_p)(2L_q' - L_q)\cos^3 y \\
& + (4L_p'' - 4L_p' + L_p) L_q^2 \cos y \sin^2 y + 2(4L_q'' - 4L_q' + L_q) L_p L_q \cos y \sin^2 y \\
& \left. + 2\left[4(2L_p' - L_p)(2L_q' - L_q) L_q + 2(2L_q' - L_q)^2 L_p\right] \cos y \sin^2 y \right\} \\
= & -i\frac{B_p B_q B_q^*}{\omega_p \omega_q^2} e^{-3x} \left\{ \left[3(4L_p'' - 4L_p' + L_p)(2L_q' - L_q)^2 - (2L_q' - L_q)^2 L_p \right. \right.
\end{aligned}
$$

$$
\begin{aligned}
& + 6(4L_q'' - 4L_q' + L_q)(2L_q' - L_q)(2L_p' - L_p) - 2L_q(2L_p' - L_p)(2L_q' - L_q)\Big] \cos^3 y \\
& + \Big[8(2L_p' - L_p)(2L_q' - L_q)L_q + 4(2L_q' - L_q)^2 L_p \\
& - 9L_p L_q^2 + (4L_p'' - 4L_p' + L_p)L_q^2 + 2(4L_q'' - 4L_q' + L_q)L_p L_q\Big] \cos y \sin^2 y\Big\} \\
= & -i\frac{B_p B_q B_q^*}{\omega_p \omega_q^2} e^{-3x} \Big\{\frac{3}{4}\Big[3(4L_p'' - 4L_p' + L_p)(2L_q' - L_q)^2 - (2L_q' - L_q)^2 L_p \\
& + 6(4L_q'' - 4L_q' + L_q)(2L_q' - L_q)(2L_p' - L_p) - 2L_q(2L_p' - L_p)(2L_q' - L_q)\Big] \\
& + \frac{1}{4}\Big[8(2L_p' - L_p)(2L_q' - L_q)L_q + 4(2L_q' - L_q)^2 L_p \\
& - 9L_p L_q^2 + (4L_p'' - 4L_p' + L_p)L_q^2 + 2(4L_q'' - 4L_q' + L_q)L_p L_q\Big]\Big\} \cos y \\
= & \hat{h}_{p5}(x) B_p B_q B_q^* \qquad (4.47)
\end{aligned}
$$

There is no need to consider terms not proportional to $\cos y$.

In $\mathcal{E}_q$, we have the following terms

$[\mathcal{E}_q\text{-}1]$.

$$
\begin{aligned}
& (\phi_{11}, \psi_{0p}) \\
= & 2\{\phi_{11x}\psi_{0px}[-i(\omega_q - \omega_p) - i\omega_p)]\} - i\omega_p \psi_{0p}\phi_{11xx} - i(\omega_q - \omega_p)\phi_{11}(\psi_{0pxx} + \psi_{0pyy}) \\
= & -i2\omega_q \phi_{11x}\psi_{0px} - i\omega_p \psi_{0p}\phi_{11xx} - i(\omega_q - \omega_p)\phi_{11}(\psi_{0pxx} + \psi_{0pyy}) \\
= & -ie^{-x}\cos y \left(i\frac{B_p^* B_q}{\omega_p \omega_q}\right)\left(-i\frac{B_p}{\omega_p}\right)\Big\{2\omega_q \frac{dG_1}{dx}(2L_p' - L_p) \\
& + \omega_p \frac{d^2 G_1}{dx^2} L_p + (\omega_q - \omega_p) G_1 (4L_p'' - 4L_p')\Big\} \\
= & -i\frac{B_q B_p B_p^*}{\omega_q \omega_p^2} e^{-x}\Big\{2\omega_q \frac{dG_1}{dx}(2L_p' - L_p) + \omega_p \frac{d^2 G_1}{dx^2} L_p \\
& + (\omega_q - \omega_p) G_1 (4L_p'' - 4L_p')\Big\} \cos y \\
= & \hat{h}_{q1}(x) B_q B_p B_p^* \qquad (4.48)
\end{aligned}
$$

$[\mathcal{E}_q\text{-}2]$.

$$
\begin{aligned}
& (\phi_{12}, \psi_{0p}^*) \\
= & 2\Big\{\phi_{12x}\psi_{0px}^*[-i(\omega_p + \omega_q) + i\omega_p)]\Big\} + i\omega_p \psi_{0p}^*\phi_{12xx} - i(\omega_p + \omega_q)\phi_{12}(\psi_{0pxx}^* + \psi_{0pyy}^*) \\
= & -i2\omega_q \phi_{12x}\psi_{0px}^* + i\omega_p \psi_{0p}^*\phi_{12xx} - i(\omega_p + \omega_q)\phi_{12}(\psi_{0pxx}^* + \psi_{0pyy}^*) \\
= & -ie^{-x}\cos y \left(i\frac{B_p B_q}{\omega_p \omega_q}\right)\left(i\frac{B_p^*}{\omega_p}\right)\Big\{2\omega_q \frac{dG_2}{dx}(2L_p' - L_p)
\end{aligned}
$$

$$
\begin{aligned}
& -\omega_p \frac{d^2 G_2}{dx^2} L_p + (\omega_p + \omega_q) G_2 (4L_p'' - 4L_p') \Big\} \\
& -ie^{-x} \cos y \left(-i\frac{e^{i2\varphi}}{\omega}\right) \left(i\frac{B_p^*}{\omega_p}\right) \Big\{ 2\omega_q \frac{dJ_0}{dx}(2L_p' - L_p) \\
& -\omega_p \frac{d^2 J_0}{dx^2} L_p + (\omega_p + \omega_q) J_0 (4L_p'' - 4L_p') \Big\} \\
= \; & i\frac{B_q B_p B_p^*}{\omega_q \omega_p^2} e^{-x} \left\{ 2\omega_q \frac{dG_2}{dx}(2L_p' - L_p) - \omega_p \frac{d^2 G_2}{dx^2} L_p + (\omega_p + \omega_q) G_2 (4L_p'' - 4L_p') \right\} \cos y \\
& -i\frac{e^{i2\varphi} B_p^*}{\omega \omega_p} e^{-x} \left\{ 2\omega_q \frac{dJ_0}{dx}(2L_p' - L_p) - \omega_p \frac{d^2 J_0}{dx^2} L_p + (\omega_p + \omega_q) J_0 (4L_p'' - 4L_p') \right\} \cos y \\
= \; & \hat{h}_{q2}(x) B_q B_p B_p^* + ie^{i2\varphi} \hat{f}_q(x) B_p^* \qquad (4.49)
\end{aligned}
$$

$[\mathcal{E}_q\text{-}3]$.

$$
\begin{aligned}
& (\phi_{14}, \psi_{0q}^*) \\
= \; & 2\left\{ \phi_{14x}\psi_{0qx}^* \left[-i2\omega_q + i\omega_q\right] \right\} + i\omega_q \psi_{0q}^* \phi_{14xx} - i2\omega_q \phi_{14}(\psi_{0qxx}^* + \psi_{0qyy}^*) \\
= \; & -i2\omega_q \phi_{14x}\psi_{0qx}^* + i\omega_q \psi_{0q}^* \phi_{14xx} - i2\omega_q \phi_{14}(\psi_{0qxx}^* + \psi_{0qyy}^*) \\
= \; & -ie^{-x}\cos y \left(i\frac{B_q^2}{\omega_q}\right)\left(i\frac{B_q^*}{\omega_q}\right) \Big\{ 2\omega_q \frac{dG_4}{dx}(2L_q' - L_q) \\
& -\omega_q \frac{d^2 G_4}{dx^2} L_q + 2\omega_q G_4 (4L_q'' - 4L_q') \Big\} \\
= \; & i\frac{B_q B_q B_q^*}{\omega_q} e^{-x} \left\{ 2\frac{dG_4}{dx}(2L_q' - L_q) - \frac{d^2 G_4}{dx^2} L_q + 2G_4(4L_q'' - 4L_q') \right\} \cos y \\
= \; & \hat{g}_{q1}(x) B_q^2 B_q^* \qquad (4.50)
\end{aligned}
$$

$[\mathcal{E}_q\text{-}4]$.

$$
\begin{aligned}
& (\psi_{11}, \psi_{0p}) \\
= \; & 2\left\{ \psi_{11x}\psi_{0px}\left[-i\omega_p - i(\omega_q - \omega_p)\right] + \psi_{11y}\psi_{0py}\left[-i\omega_p - i(\omega_q - \omega_p)\right] \right\} \\
& -i\omega_p \psi_{0p}\left(\psi_{11xx} + \psi_{11yy}\right) - i(\omega_q - \omega_p)\psi_{11}\left(\psi_{0pxx} + \psi_{0pyy}\right) \\
= \; & -i2\omega_q\left[\psi_{11x}\psi_{0px} + \psi_{11y}\psi_{0py}\right] - i\omega_p\psi_{0p}\left(\psi_{11xx} + \psi_{11yy}\right) \\
& -i(\omega_q - \omega_p)\psi_{11}\left(\psi_{0qxx} + \psi_{0qyy}\right) \\
= \; & -ie^{-x}\left(i\frac{B_p^* B_q}{\omega_p \omega_q}\right)\left(-i\frac{B_p}{\omega_p}\right)\Big[2\omega_q f_{11x}(2L_p' - L_p)\cos 2y \cos y \\
& +2\omega_q f_{11}(-2)L_p(-1)\sin 2y \sin y + \omega_p L_p (f_{11xx} - 4f_{11})\cos 2y \cos y \\
& +(\omega_q - \omega_p) f_{11}(4L_p'' - 4L_p')\cos 2y \cos y \Big]
\end{aligned}
$$

$$
\begin{aligned}
&= -i\frac{B_qB_pB_p^*}{\omega_q\omega_p^2}e^{-x}\Big[\omega_q f_{11x}(2L_p'-L_p)+2\omega_q f_{11}L_p \\
&\quad +\frac{\omega_p}{2}L_p(f_{11xx}-4f_{11})+\frac{\omega_q-\omega_p}{2}f_{11}(4L_p''-4L_p')\Big]\cos y \\
&= -i\frac{B_qB_pB_p^*}{\omega_q\omega_p^2}e^{-x}\Big[\frac{\omega_p}{2}L_pf_{11xx}+\omega_q(2L_p'-L_p)f_{11x} \\
&\quad +\frac{\omega_q-\omega_p}{2}f_{11}(4L_p''-4L_p'+4L_p)\Big]\cos y \\
&= \hat{h}_{q3}(x)B_qB_pB_p^* \qquad (4.51)
\end{aligned}
$$

where terms not proportional to $\cos y$ have been discarded.

[$\mathcal{E}_q$-5].

$$
\begin{aligned}
&(\psi_{12},\psi_{0p}^*) \\
&= 2\Big\{\psi_{12x}\psi_{0px}^*\left[i\omega_p-i(\omega_p+\omega_q)\right]+\psi_{12y}\psi_{0py}^*\left[i\omega_p-i(\omega_p+\omega_q)\right]\Big\} \\
&\quad +i\omega_p\psi_{0p}^*\left(\psi_{12xx}+\psi_{12yy}\right)-i(\omega_p+\omega_q)\psi_{12}\left(\psi_{0pxx}^*+\psi_{0pyy}^*\right) \\
&= -i2\omega_q\left[\psi_{12x}\psi_{0px}^*+\psi_{12y}\psi_{0py}^*\right]+i\omega_p\psi_{0p}^*\left(\psi_{12xx}+\psi_{12yy}\right) \\
&\quad -i(\omega_p+\omega_q)\psi_{12}\left(\psi_{0pxx}^*+\psi_{0pyy}^*\right) \\
&= -ie^{-x}\left(i\frac{B_pB_q}{\omega_p\omega_q}\right)\left(i\frac{B_p^*}{\omega_p}\right)\Big[2\omega_q f_{12x}(2L_p'-L_p)\cos 2y\cos y \\
&\quad +2\omega_q f_{12}(-2)L_p(-1)\sin 2y\sin y-\omega_pL_p(f_{12xx}-4f_{12})\cos 2y\cos y \\
&\quad +(\omega_p+\omega_q)f_{12}(4L_p''-4L_p')\cos 2y\cos y\Big] \\
&= i\frac{B_qB_pB_p^*}{\omega_q\omega_p^2}e^{-x}\Big[\omega_q f_{12x}(2L_p'-L_p)+2\omega_q f_{12}L_p \\
&\quad -\frac{\omega_p}{2}L_p(f_{12xx}-4f_{12})+\frac{\omega_p+\omega_q}{2}f_{12}(4L_p''-4L_p')\Big]\cos y \\
&= i\frac{B_qB_pB_p^*}{\omega_q\omega_p^2}e^{-x}\Big[\omega_q(2L_p'-L_p)f_{12x}-\frac{\omega_p}{2}L_pf_{12xx} \\
&\quad +\frac{\omega_p+\omega_q}{2}f_{12}(4L_p''-4L_p'+4L_p)\Big]\cos y \\
&= \hat{h}_{q4}(x)B_qB_pB_p^* \qquad (4.52)
\end{aligned}
$$

[$\mathcal{E}_q$-6].

$$
\begin{aligned}
&(\psi_{14},\psi_{0q}^*) \\
&= 2\Big\{\psi_{14x}\psi_{0qx}^*\left[i\omega_q-i2\omega_q\right]+\psi_{14y}\psi_{0qy}^*\left[i\omega_q-i2\omega_q\right]\Big\} \\
&\quad +i\omega_q\psi_{0q}^*\left(\psi_{14xx}+\psi_{14yy}\right)-i2\omega_q\psi_{14}\left(\psi_{0qxx}^*+\psi_{0qyy}^*\right)
\end{aligned}
$$

$$
\begin{aligned}
&= -i2\omega_q\left[\psi_{14x}\psi^*_{0qx}+\psi_{14y}\psi^*_{0qy}\right]+i\omega_q\psi^*_{0q}\left(\psi_{14xx}+\psi_{14yy}\right)\\
&\quad -i2\omega_q\psi_{14}\left(\psi^*_{0qxx}+\psi^*_{0qyy}\right)\\
&= -ie^{-x}\left(i\frac{B_q^2}{\omega_q}\right)\left(i\frac{B_q^*}{\omega_q}\right)\Big[2\omega_q f_{14x}(2L'_q-L_q)\cos 2y\cos y\\
&\quad +2\omega_q f_{14}(-2)L_q(-1)\sin 2y\sin y-\omega_q L_q(f_{14xx}-4f_{14})\cos 2y\cos y\\
&\quad +2\omega_q f_{14}(4L''_q-4L'_q)\cos 2y\cos y\Big]\\
&= i\frac{B_qB_qB_q^*}{\omega_q}e^{-x}\Big[f_{14x}(2L'_q-L_q)+2f_{14}L_q\\
&\quad -\frac{1}{2}L_q(f_{14xx}-4f_{14})+f_{14}(4L''_q-4L'_q)\Big]\cos y\\
&= i\frac{B_qB_qB_q^*}{\omega_q}e^{-x}\left[(2L'_q-L_q)f_{14x}-\frac{1}{2}L_qf_{14xx}+(4L''_q-4L'_q+4L_q)f_{14}\right]\cos y\\
&= \hat{g}_{q2}(x)B_q^2B_q^* \qquad (4.53)
\end{aligned}
$$

where only terms proportional to $\cos y$ are kept.

$[\mathcal{E}_q\text{-}7]$.

$$
\begin{aligned}
&\quad (\psi_{0q},\psi_{0q},\psi^*_{0q})\\
&= \frac{3}{2}\left(\psi_{0qxx}2\psi_{0qx}\psi^*_{0qx}+\psi^*_{0qxx}\psi_{0qx}\psi_{0qx}+\psi_{0qyy}2\psi_{0qy}\psi^*_{0qy}+\psi^*_{0qyy}\psi_{0qy}\psi_{0qy}\right)\\
&\quad +\frac{1}{2}\left(\psi_{0qyy}2\psi_{0qx}\psi^*_{0qx}+\psi^*_{0qyy}\psi_{0qx}\psi_{0qx}+\psi_{0qxx}2\psi_{0qy}\psi^*_{0qy}+\psi^*_{0qxx}\psi_{0qy}\psi_{0qy}\right)\\
&\quad +2\left(\psi_{0qx}\psi_{0qy}\psi^*_{0qxy}+\psi_{0qx}\psi^*_{0qy}\psi_{0qxy}+\psi^*_{0qx}\psi_{0qy}\psi_{0qxy}\right)\\
&= \left(-i\frac{B_q}{\omega_q}\right)^2 i\frac{B_q^*}{\omega_q}e^{-3x}\Big\{\frac{9}{2}(4L''_q-4L'_q+L_q)(2L'_q-L_q)^2\cos^3 y-\frac{9}{2}L_q^3\cos y\sin^2 y\\
&\quad -\frac{3}{2}(2L'_q-L_q)^2L_q\cos^3 y+\frac{3}{2}(4L''_q-4L'_q+L_q)L_q^2\cos y\sin^2 y\\
&\quad +2\left[3(2L'_q-L_q)^2L_q\cos y\sin^2 y\right]\Big\}\\
&= -i\frac{B_q^2B_q^*}{\omega_q^3}e^{-3x}\Big\{\left[\frac{9}{2}(4L''_q-4L'_q+L_q)(2L'_q-L_q)^2-\frac{3}{2}(2L'_q-L_q)^2L_q\right]\cos^3 y\\
&\quad +\left[6(2L'_q-L_q)^2L_q+\frac{3}{2}(4L''_q-4L'_q+L_q)L_q^2-\frac{9}{2}L_q^3\right]\cos y\sin^2 y\Big\}\\
&= -i\frac{B_q^2B_q^*}{\omega_q^3}e^{-3x}\Big\{\left[\frac{27}{8}(4L''_q-4L'_q+L_q)(2L'_q-L_q)^2-\frac{9}{8}(2L'_q-L_q)^2L_q\right]\\
&\quad +\left[\frac{3}{2}(2L'_q-L_q)^2L_q+\frac{3}{8}(4L''_q-4L'_q+L_q)L_q^2-\frac{9}{8}L_q^3\right]\Big\}\cos y\\
&= \hat{g}_{q3}(x)B_q^2B_q^* \qquad (4.54)
\end{aligned}
$$

$[\mathcal{E}_q\text{-}8]$.

$$
\begin{aligned}
& (\psi_{0q}, \psi_{0p}, \psi_{0p}^*) \\
= \;& \frac{3}{2}\left(\psi_{0qxx}2\psi_{0px}\psi_{0px}^* + \psi_{0pxx}2\psi_{0qx}\psi_{0px}^* + \psi_{0pxx}^*2\psi_{0qx}\psi_{0px}\right) \\
& +\frac{3}{2}\left(\psi_{0qyy}2\psi_{0py}\psi_{0py}^* + \psi_{0pyy}2\psi_{0qy}\psi_{0py}^* + \psi_{0pyy}^*2\psi_{0qy}\psi_{0py}\right) \\
& +\frac{1}{2}\left(\psi_{0qyy}2\psi_{0px}\psi_{0px}^* + \psi_{0pyy}2\psi_{0qx}\psi_{0px}^* + \psi_{0pyy}^*2\psi_{0qx}\psi_{0px}\right) \\
& +\frac{1}{2}\left(\psi_{0qxx}2\psi_{0py}\psi_{0py}^* + \psi_{0pxx}2\psi_{0qy}\psi_{0py}^* + \psi_{0pxx}^*2\psi_{0qy}\psi_{0py}\right) \\
& +2\left(\psi_{0qx}\psi_{0py}\psi_{0pxy}^* + \psi_{0qx}\psi_{0py}^*\psi_{0pxy} + \psi_{0px}\psi_{0qy}\psi_{0pxy}^*\right) \\
& +2\left(\psi_{0px}\psi_{0py}^*\psi_{0qxy} + \psi_{0px}^*\psi_{0qy}\psi_{0pxy} + \psi_{0px}^*\psi_{0py}\psi_{0qxy}\right) \\
= \;& \left(-i\frac{B_q}{\omega_q}\right)\left(-i\frac{B_p}{\omega_p}\right) i\frac{B_p^*}{\omega_p} e^{-3x}\Big\{3(4L_q'' - 4L_q' + L_q)(2L_p' - L_p)^2\cos^3 y \\
& + 6(4L_p'' - 4L_p' + L_p)(2L_p' - L_p)(2L_q' - L_q)\cos^3 y - 9L_qL_p^2\cos y\sin^2 y \\
& - (2L_p' - L_p)^2 L_q \cos^3 y - 2L_p(2L_q' - L_q)(2L_p' - L_p)\cos^3 y \\
& + (4L_q'' - 4L_q' + L_q)L_p^2\cos y\sin^2 y + 2(4L_p'' - 4L_p' + L_p)L_qL_p\cos y\sin^2 y \\
& + 2\left[4(2L_q' - L_q)(2L_p' - L_p)L_p + 2(2L_p' - L_p)^2 L_q\right]\cos y\sin^2 y\Big\} \\
= \;& -i\frac{B_qB_pB_p^*}{\omega_q\omega_p^2}e^{-3x}\Big\{\Big[3(4L_q'' - 4L_q' + L_q)(2L_p' - L_p)^2 - (2L_p' - L_p)^2 L_q \\
& + 6(4L_p'' - 4L_p' + L_p)(2L_p' - L_p)(2L_q' - L_q) - 2L_p(2L_q' - L_q)(2L_p' - L_p)\Big]\cos^3 y \\
& + \Big[8(2L_q' - L_q)(2L_p' - L_p)L_p + 4(2L_p' - L_p)^2 L_q \\
& - 9L_qL_p^2 + (4L_q'' - 4L_q' + L_q)L_p^2 + 2(4L_p'' - 4L_p' + L_p)L_qL_p\Big]\cos y\sin^2 y\Big\} \\
= \;& -i\frac{B_qB_pB_p^*}{\omega_q\omega_p^2}e^{-3x}\Big\{\frac{3}{4}\Big[3(4L_q'' - 4L_q' + L_q)(2L_p' - L_p)^2 - (2L_p' - L_p)^2 L_q \\
& + 6(4L_p'' - 4L_p' + L_p)(2L_p' - L_p)(2L_q' - L_q) - 2L_p(2L_q' - L_q)(2L_p' - L_p)\Big] \\
& + \frac{1}{4}\Big[8(2L_q' - L_q)(2L_p' - L_p)L_p + 4(2L_p' - L_p)^2 L_q \\
& - 9L_qL_p^2 + (4L_q'' - 4L_q' + L_q)L_p^2 + 2(4L_p'' - 4L_p' + L_p)L_qL_p\Big]\Big\}\cos y \\
= \;& \hat{h}_{q5}(x)B_qB_pB_p^* \qquad (4.55)
\end{aligned}
$$

Again, terms not proportional to $\cos y$ have been discarded.

Homogeneous equation 4.39 has nontrivial solutions $F_j = e^{-x}L_j(2x), \quad j = p, q$ as described at the first order. H_j must satisfy a solvability condition which is found by

Green's formula

$$\int_0^\infty (H_j \mathcal{L}_j F_j - F_j \mathcal{L}_j H_j) dx = \int_0^\infty \left[H_j (x F_{jx})_x - F_j (x H_{jx})_x \right] dx$$
$$= \int_0^\infty \left[(x H_j F_{jx})_x - (x F_j H_{jx})_x \right] dx = 0$$

The last equality follows after integration and applying the boundary conditions both at the shoreline and at infinity. Since $\mathcal{L}_j F_j = 0$, we must have

$$\int_0^\infty F_j \mathcal{L}_j H_j dx = 0$$

which gives the solvability condition

$$\int_0^\infty dx F_j(x) \left(-2 \frac{\partial B_j}{\partial \tau} F_j(x) + \mathcal{E}_j(x) \right) = 0$$

In summary, we group the terms in $\mathcal{E}_p(x)$ according to B_q^*, $B_p^2 B_p^*$ and $B_p B_q B_q^*$, and get

$$\mathcal{E}_p(x) \quad = \quad i e^{i2\varphi} \hat{f}_p(x) B_q^* + \hat{g}_p(x) B_p^2 B_p^* + \hat{h}_p(x) B_p B_q B_q^* \tag{4.56}$$

where $ie^{i2\varphi}\hat{f}_p, \hat{g}_p, \hat{h}_p$ are the sum of coefficients of B_q^*, $B_p^2 B_p^*$ and $B_p B_q B_q^*$ respectively. Specifically

- $i\hat{f}_p(x)$ is found in (4.41);
- $\hat{g}_p(x)$ is collected from (4.42), (4.45) and (4.46), i.e.,

$$\hat{g}_p(x) = \hat{g}_{p1} + \hat{g}_{p2} + \hat{g}_{p3} \tag{4.57}$$

- $\hat{h}_p(x)$ is collected from (4.40), (4.41), (4.43), (4.44) and (4.47), i.e.

$$\hat{h}_p(x) = \hat{h}_{p1}(x) + \hat{h}_{p2}(x) + \hat{h}_{p3}(x) + \hat{h}_{p4}(x) + \hat{h}_{p5}(x) \tag{4.58}$$

.

Obviously, $\hat{f}_p$ is real while $\hat{g}_p$ and $\hat{h}_p$ are complex.

Similarly, we group the terms in $\mathcal{E}_q(x)$ according to B_p^*, $B_q^2 B_q^*$ and $B_q B_p B_p^*$, and get

$$\mathcal{E}_q(x) \quad = \quad i e^{i2\varphi} \hat{f}_q(x) B_p^* + \hat{g}_q(x) B_q^2 B_q^* + \hat{h}_q(x) B_q B_p B_p^* \tag{4.59}$$

where $ie^{i2\varphi}\hat{f}_q, \hat{g}_q, \hat{h}_q$ are the sum of coefficients of B_p^*, $B_q^2 B_q^*$ and $B_q B_p B_p^*$ respectively. Specifically

- $i\hat{f}_q(x)$ is found in (4.49);
- $\hat{g}_q(x)$ is collected from (4.50), (4.53) and (4.54), i.e.,

$$\hat{g}_q = \hat{g}_{q1} + \hat{g}_{q2} + \hat{g}_{q3} \tag{4.60}$$

- $\hat{h}_q(x)$ is collected from (4.48), (4.49), (4.51), (4.52) and (4.55), i.e.

$$\hat{h}_q(x) = \hat{h}_{q1}(x) + \hat{h}_{q2}(x) + \hat{h}_{q3}(x) + \hat{h}_{q4}(x) + \hat{h}_{q5}(x) \tag{4.61}$$

-

Again, $\hat{f}_q$ is real while $\hat{g}_q$ and $\hat{h}_q$ are complex.

Therefore, two complex nonlinear ODE's

$$\frac{\partial B_p}{\partial \tau} = ic_1 e^{i2\varphi} B_q^* + c_2 B_p B_p B_p^* + c_3 B_p B_q B_q^*; \tag{4.62}$$

$$\frac{\partial B_q}{\partial \tau} = id_1 e^{i2\varphi} B_p^* + d_2 B_q B_q B_q^* + d_3 B_q B_p B_p^*. \tag{4.63}$$

governs the two edge wave amplitudes B_p and B_q. We have collected terms from the integral of $\mathcal{E}_p(x)$ and $\mathcal{E}_q(x)$ according to their B_p and B_q dependence and defined the coefficients as follows

$$[c_1, c_2, c_3] = \int_0^\infty F_p(x)[\hat{f}_p(x), \hat{g}_p(x), \hat{h}_p(x)]dx, \tag{4.64}$$

$$[d_1, d_2, d_3] = \int_0^\infty F_q(x)[\hat{f}_q(x), \hat{g}_q(x), \hat{h}_q(x)]dx. \tag{4.65}$$

More specifically, we introduce

$$c_2 = c_{21} + c_{22} + c_{23}, \quad c_3 = c_{31} + c_{32} + c_{33} + c_{34} + c_{35}$$

with

$$c_{2j} = \int_0^\infty F_p(x)\hat{g}_{pj}(x)dx, \quad j = 1, 2, 3 \tag{4.66}$$

$$c_{3j} = \int_0^\infty F_p(x)\hat{h}_{pj}(x)dx, \quad j = 1, 2, 3, 4, 5 \tag{4.67}$$

and

$$d_2 = d_{21} + d_{22} + d_{23}, \quad d_3 = d_{31} + d_{32} + d_{33} + d_{34} + d_{35}$$

with

$$d_{2j} = \int_0^\infty F_q(x)\hat{g}_{qj}(x)dx, \quad j = 1, 2, 3 \tag{4.68}$$

$$d_{3j} = \int_0^\infty F_q(x)\hat{h}_{qj}(x)dx, \quad j = 1, 2, 3, 4, 5 \tag{4.69}$$

These coefficients c's and d's are constants obtained by numerical integration, to be given later. Use also has been made of the property of Laguerre polynomial

$$\int_0^\infty F_j^2(x)dx = \int_0^\infty e^{-2x}L_j^2(2x)dx = \frac{1}{2}\int_0^\infty e^{-\xi}L_j^2(\xi)d\xi = \frac{1}{2}$$

As in the case of synchronous resonance, we replace B_j by $B_j e^{i\varphi}$ to eliminate the phase of incident wave,i.e. $e^{i2\varphi}$, from the evolution equation. Without loss of generality we drop $e^{i2\varphi}$ from Eq. (4.62) and Eq. (4.63) to obtain the evolution equation:

$$\frac{\partial B_p}{\partial \tau} = ic_1 B_q^* + c_2 B_p B_p B_p^* + c_3 B_p B_q B_q^*; \tag{4.70}$$

$$\frac{\partial B_q}{\partial \tau} = id_1 B_p^* + d_2 B_q B_q B_q^* + d_3 B_q B_p B_p^*. \tag{4.71}$$

These two nonlinear equations are coupled.

4.6 Initial evolution

The edge wave amplitudes are much smaller than the incident/reflected wave, i.e. $B_p, B_q << 1$. Therefore, the linear terms on the right-hand side of Eq. (4.70) and Eq. (4.71) dominate. The following discussion shows how governing equations behave with different choices of the modes combinations (p, q).

Ignoring nonlinear terms, Eq. (4.70) and (4.71) becomes

$$\frac{\partial B_p}{\partial \tau} = ic_1 B_q^* \quad \text{and} \quad \frac{\partial B_q}{\partial \tau} = id_1 B_p^*. \tag{4.72}$$

which can be manipulated to yield

$$\frac{\partial^2 B_p}{\partial \tau^2} = ic_1\left(-id_1^* B_p\right) = c_1 d_1^* B_p \tag{4.73}$$

The solution to the above equation is

$$B_p = B_p(0)e^{\pm\sqrt{c_1 d_1^*}\ \tau} \tag{4.74}$$

Similarly,

$$\frac{\partial^2 B_q}{\partial \tau^2} = id_1\left(-ic_1^* B_q\right) = c_1^* d_1 B_q \tag{4.75}$$

The solution is

$$B_q = B_q(0)e^{\pm\sqrt{c_1^* d_1}\ \tau} \tag{4.76}$$

We now give a_1 and b_1 for several pairs of (p, q), which can be excited by one incident/reflected wave:

- Case (1). $p = 0,\ q = 1$;

$$\omega_p = 1, \quad \omega_q = \sqrt{3}, \quad \omega = \omega_p + \omega_q = \sqrt{3} + 1, \quad L_p(2x) = 1; \quad L_q(2x) = (1 - 2x)$$

Therefore from $[\mathcal{E}_p\text{-}2]$ we get

$$\begin{aligned} & ic_1 \\ = & \int_0^\infty dx F_p(x)\left\{-i\frac{1}{\omega\omega_q}e^{-x}\left[2\omega_p\frac{dJ_0}{dx}(2L_q' - L_q) - \omega_q\frac{d^2J_0}{dx^2}L_q\right.\right. \\ & \left.\left.+(\omega_p + \omega_q)J_0(4L_q'' - 4L_q')\right]\right\} \\ = & -i\int_0^\infty dx\frac{e^{-2x}}{\omega\sqrt{3}}\left\{(4x - 6)\frac{dJ_0(2\omega\sqrt{x})}{dx} - \sqrt{3}(1 - 2x)\frac{d^2J_0(2\omega\sqrt{x})}{dx^2}\right. \\ & \left.+4cJ_0(2\omega\sqrt{x})\right\} \\ = & \ 0.1410i \end{aligned}$$

And from $[\mathcal{E}_q\text{-}2]$

$$id_1$$

$$
\begin{aligned}
&= \int_0^\infty dx F_q(x) \left\{ -i\frac{1}{\omega\omega_p} e^{-x} \left[2\omega_q \frac{dJ_0}{dx}(2L_p' - L_p) - \omega_p \frac{d^2 J_0}{dx^2} L_p \right.\right. \\
&\quad \left.\left. +(\omega_p + \omega_q) J_0 (4L_p'' - 4L_p') \right] \right\} \\
&= i\int_0^\infty dx \frac{e^{-2x}}{\omega}(1-2x)\left\{ 2\sqrt{3}\frac{dJ_0(2\omega\sqrt{x})}{dx} + \frac{d^2 J_0(2\omega\sqrt{x})}{dx^2} \right\} \\
&= 0.2441i
\end{aligned}
$$

- Case (2). $p = 0,\ q = 2;$

$\omega_p = 1,\ \ \omega_q = \sqrt{5},\ \ \omega = \omega_p + \omega_q = \sqrt{5} + 1,\ \ L_p(2x) = 1;\ \ L_q(2x) = 1 - 4x + 2x^2$

Therefore from [$\mathcal{E}_p$-2] we get

$$
\begin{aligned}
&ic_1 \\
&= \int_0^\infty dx F_p(x) \left\{ -i\frac{1}{\omega\omega_q} e^{-x} \left[2\omega_p \frac{dJ_0}{dx}(2L_q' - L_q) - \omega_q \frac{d^2 J_0}{dx^2} L_q \right.\right. \\
&\quad \left.\left. +(\omega_p + \omega_q) J_0 (4L_q'' - 4L_q') \right] \right\} \\
&= -i\int_0^\infty dx \frac{e^{-2x}}{\omega\sqrt{5}} \left\{ (16x - 10 - 4x^2)\frac{dJ_0(2\omega\sqrt{x})}{dx} \right. \\
&\quad \left. -\sqrt{5}(1 - 4x + 2x^2)\frac{d^2 J_0(2\omega\sqrt{x})}{dx^2} + 4c(3 - 2x) J_0(2\omega\sqrt{x}) \right\} \\
&= 0.1056i
\end{aligned}
$$

And from [$\mathcal{E}_q$-2]

$$
\begin{aligned}
&id_1 \\
&= \int_0^\infty dx F_q(x) \left\{ -i\frac{1}{\omega\omega_p} e^{-x} \left[2\omega_q \frac{dJ_0}{dx}(2L_p' - L_p) - \omega_p \frac{d^2 J_0}{dx^2} L_p \right.\right. \\
&\quad \left.\left. +(\omega_p + \omega_q) J_0 (4L_p'' - 4L_p') \right] \right\} \\
&= i\int_0^\infty dx \frac{e^{-2x}}{\omega}(1 - 4x + 2x^2)\left\{ 2\sqrt{5}\frac{dJ_0(2\omega\sqrt{x})}{dx} + \frac{d^2 J_0(2\omega\sqrt{x})}{dx^2} \right\} \\
&= 0.2360i
\end{aligned}
$$

- Case (3). $p = 1,\ q = 2;$

$\omega_p = \sqrt{3},\ \omega_q = \sqrt{5},\ \omega = \omega_p + \omega_q = \sqrt{5} + \sqrt{3},\ L_p(2x) = 1 - 2x;\ L_q(2x) = 1 - 4x + 2x^2$

Therefore from [$\mathcal{E}_p$-2] we get

$$\begin{aligned}
& ic_1 \\
= & \int_0^\infty dx F_p(x) \left\{ -i \frac{1}{\omega\omega_q} e^{-x} \left[2\omega_p \frac{dJ_0}{dx}(2L_q' - L_q) - \omega_q \frac{d^2 J_0}{dx^2} L_q \right.\right. \\
& \left.\left. +(\omega_p + \omega_q) J_0 (4L_q'' - 4L_q') \right] \right\} \\
= & -i \int_0^\infty dx \frac{e^{-2x}}{\omega\sqrt{5}} (1-2x) \left\{ \sqrt{3}(16x - 10 - 4x^2) \frac{dJ_0(2\omega\sqrt{x})}{dx} \right. \\
& \left. -\sqrt{5}(1 - 4x + 2x^2) \frac{d^2 J_0(2\omega\sqrt{x})}{dx^2} + 4c(3-2x) J_0(2\omega\sqrt{x}) \right\} \\
= & \ 0.0970i
\end{aligned}$$

And from [$\mathcal{E}_q$-2]

$$\begin{aligned}
& id_1 \\
= & \int_0^\infty dx F_q(x) \left\{ -i \frac{1}{\omega\omega_p} e^{-x} \left[2\omega_q \frac{dJ_0}{dx}(2L_p' - L_p) - \omega_p \frac{d^2 J_0}{dx^2} L_p \right.\right. \\
& \left.\left. +(\omega_p + \omega_q) J_0 (4L_p'' - 4L_p') \right] \right\} \\
= & \ i \int_0^\infty dx \frac{e^{-2x}}{\omega\sqrt{3}} (1 - 4x + 2x^2) \left\{ \sqrt{5}(6 - 4x) \frac{dJ_0(2\omega\sqrt{x})}{dx} \right. \\
& \left. +\sqrt{3}(1 - 2x) \frac{d^2 J_0(2\omega\sqrt{x})}{dx^2} + 4c J_0(2\omega\sqrt{x}) \right\} \\
= & \ 0.1524i
\end{aligned}$$

- Case (4). $p = 0, \ q = 3;$

$\omega_p = 1, \ \omega_q = \sqrt{7}, \ \omega = \omega_p + \omega_q = \sqrt{7}+1, \ L_p(2x) = 1; \ L_q(2x) = 1 - 6x + 6x^2 - \frac{4}{3}x^3$

Therefore from [$\mathcal{E}_p$-2] we get

$$\begin{aligned}
& ic_1 \\
= & \int_0^\infty dx F_p(x) \left\{ -i \frac{1}{\omega\omega_q} e^{-x} \left[2\omega_p \frac{dJ_0}{dx}(2L_q' - L_q) - \omega_q \frac{d^2 J_0}{dx^2} L_q \right.\right. \\
& \left.\left. +(\omega_p + \omega_q) J_0 (4L_q'' - 4L_q') \right] \right\} \\
= & -i \int_0^\infty dx \frac{e^{-2x}}{\omega\sqrt{7}} \left\{ (36x - 14 - 20x^2 + \frac{8}{3}x^3) \frac{dJ_0(2\omega\sqrt{x})}{dx} \right. \\
& \left. -\sqrt{7}(1 - 6x + 6x^2 - \frac{4}{3}x^3) \frac{d^2 J_0(2\omega\sqrt{x})}{dx^2} + 8c(3 - 4x + x^2) J_0(2\omega\sqrt{x}) \right\} \\
= & \ 0.0876i
\end{aligned}$$

And from $[\mathcal{E}_q\text{-}2]$

$$
\begin{aligned}
& id_1 \\
= & \int_0^\infty dx F_q(x) \left\{ -i\frac{1}{\omega\omega_p} e^{-x} \left[2\omega_q \frac{dJ_0}{dx}(2L_p' - L_p) - \omega_p \frac{d^2 J_0}{dx^2} L_p \right.\right. \\
& \left.\left. +(\omega_p + \omega_q) J_0 (4L_p'' - 4L_p') \right] \right\} \\
= & \; i \int_0^\infty dx \frac{e^{-2x}}{\omega}(1 - 6x + 6x^2 - \frac{4}{3}x^3) \left\{ 2\sqrt{7} \frac{dJ_0(2\omega\sqrt{x})}{dx} + \frac{d^2 J_0(2\omega\sqrt{x})}{dx^2} \right\} \\
= & \; 0.2318i
\end{aligned}
$$

- Case (5). $p = 1, \; q = 3;$

$$
\omega_p = \sqrt{3}, \; \omega_q = \sqrt{7}, \; \omega = \omega_p + \omega_q = \sqrt{7} + \sqrt{3},
$$

$$
L_p(2x) = 1 - 2x; \quad L_q(2x) = 1 - 6x + 6x^2 - \frac{4}{3}x^3
$$

Therefore from $[\mathcal{E}_p\text{-}2]$ we get

$$
\begin{aligned}
& ic_1 \\
= & \int_0^\infty dx F_p(x) \left\{ -i\frac{1}{\omega\omega_q} e^{-x} \left[2\omega_p \frac{dJ_0}{dx}(2L_q' - L_q) - \omega_q \frac{d^2 J_0}{dx^2} L_q \right.\right. \\
& \left.\left. +(\omega_p + \omega_q) J_0 (4L_q'' - 4L_q') \right] \right\} \\
= & -i \int_0^\infty dx \frac{e^{-2x}}{\omega\sqrt{7}}(1 - 2x) \left\{ \sqrt{3}(36x - 14 - 20x^2 + \frac{8}{3}x^3) \frac{dJ_0(2\omega\sqrt{x})}{dx} \right. \\
& \left. -\sqrt{7}(1 - 6x + 6x^2 - \frac{4}{3}x^3) \frac{d^2 J_0(2\omega\sqrt{x})}{dx^2} + 8c(3 - 4x + x^2) J_0(2\omega\sqrt{x}) \right\} \\
= & \; 0.0807i
\end{aligned}
$$

And from $[\mathcal{E}_q\text{-}2]$

$$
\begin{aligned}
& id_1 \\
= & \int_0^\infty dx F_q(x) \left\{ -i\frac{1}{\omega\omega_p} e^{-x} \left[2\omega_q \frac{dJ_0}{dx}(2L_p' - L_p) - \omega_p \frac{d^2 J_0}{dx^2} L_p \right.\right. \\
& \left.\left. +(\omega_p + \omega_q) J_0 (4L_p'' - 4L_p') \right] \right\} \\
= & \; i \int_0^\infty dx \frac{e^{-2x}}{\omega\sqrt{3}}(1 - 6x + 6x^2 - \frac{4}{3}x^3) \left\{ \sqrt{7}(6 - 4x) \frac{dJ_0(2\omega\sqrt{x})}{dx} \right. \\
& \left. +\sqrt{3}(1 - 2x) \frac{d^2 J_0(2\omega\sqrt{x})}{dx^2} + 4c J_0(2\omega\sqrt{x}) \right\} \\
= & \; 0.1466i
\end{aligned}
$$

- Case (6). $p = 2,\ q = 3;$

$$\omega_p = \sqrt{5},\ \omega_q = \sqrt{7},\ \omega = \omega_p + \omega_q = \sqrt{7} + \sqrt{5},$$

$$L_p(2x) = 1 - 4x + 2x^2; \quad L_q(2x) = 1 - 6x + 6x^2 - \frac{4}{3}x^3$$

Therefore from $[\mathcal{E}_p\text{-}2]$ we get

$$\begin{aligned} & ic_1 \\ = & \int_0^\infty dx F_p(x) \left\{ -i\frac{1}{\omega\omega_q} e^{-x} \left[2\omega_p \frac{dJ_0}{dx}(2L_q' - L_q) - \omega_q \frac{d^2 J_0}{dx^2} L_q \right.\right. \\ & \left.\left. +(\omega_p + \omega_q) J_0 (4L_q'' - 4L_q') \right] \right\} \\ = & -i\int_0^\infty dx \frac{e^{-2x}}{\omega\sqrt{7}}(1 - 4x + 2x^2) \left\{ \sqrt{5}(36x - 14 - 20x^2 + \frac{8}{3}x^3) \frac{dJ_0(2\omega\sqrt{x})}{dx} \right. \\ & \left. -\sqrt{7}(1 - 6x + 6x^2 - \frac{4}{3}x^3)\frac{d^2 J_0(2\omega\sqrt{x})}{dx^2} + 8c(3 - 4x + x^2) J_0(2\omega\sqrt{x}) \right\} \\ = & \ 0.0787i \end{aligned}$$

And from $[\mathcal{E}_q\text{-}2]$

$$\begin{aligned} & id_1 \\ = & \int_0^\infty dx F_q(x) \left\{ -i\frac{1}{\omega\omega_p} e^{-x} \left[2\omega_q \frac{dJ_0}{dx}(2L_p' - L_p) - \omega_p \frac{d^2 J_0}{dx^2} L_p \right.\right. \\ & \left.\left. +(\omega_p + \omega_q) J_0 (4L_p'' - 4L_p') \right] \right\} \\ = & \ i\int_0^\infty dx \frac{e^{-2x}}{\omega\sqrt{5}}(1 - 6x + 6x^2 - \frac{4}{3}x^3) \left\{ \sqrt{7}(10 - 16x + 4x^2) \frac{dJ_0(2\omega\sqrt{x})}{dx} \right. \\ & \left. +\sqrt{5}(1 - 4x + 2x^2)\frac{d^2 J_0(2\omega\sqrt{x})}{dx^2} + 4c(2x - 3) J_0(2\omega\sqrt{x}) \right\} \\ = & \ 0.0931i \end{aligned}$$

The results for all six cases are summarized in Table 4.2:

From Table 4.2 we see that, c_1 and d_1 are all positive real numbers, which makes $c_1^* d_1 = c_1 d_1^* = c_1 d_1$ real and positive. Amplitudes of the two edge wave modes grow or decay exponentially in the rate proportional to $\sqrt{c_1 d_1}$. Therefore, there is linear instability of the edge wave to the incident/reflected wave system so that the nonlinear terms come into play at large t. In Table 4.3 we list the growth rate factor $\sqrt{c_1 d_1}$ for different combination of p and q.

Table 4.2: Coefficients pairs (c_1, d_1) for different edge wave modes combinations.

		q		
		1	2	3
	0	(0.1410, 0.2441)	(0.1056,0.2360)	(0.0876,0.2318)
p	1		(0.0970,0.1524)	(0.0807,0.1466)
	2			(0.0787,0.0931)

Table 4.3: The growth rate factor $\sqrt{c_1 d_1}$ for different edge wave modes combinations.

		q		
		1	2	3
	0	0.1855	0.1579	0.1425
p	1		0.1216	0.1088
	2			0.0856

4.7 Nonlinear evolution equations

In order to see the nonlinear effects of the dynamical system, we work out all the coefficients in the evolution equations. Three specific cases of p, q combination will be discussed. In these cases, we try to make various combinations from different x-modes of the edge wave until some sort of pattern is revealed.

4.7.1 Nonlinear term coefficients for case (1): $p = 0,\ q = 1$

Now we have

$$\omega_p = 1, \quad \omega_q = \sqrt{3}, \quad \omega = \omega_p + \omega_q = \sqrt{3} + 1, \quad L_p(2x) = 1; \quad L_q(2x) = (1 - 2x)$$

We already knew from Table 4.2 that $c_1 = 0.1410$ and $d_1 = 0.2441$ from previous discussion.

$$\begin{aligned}
& f_1(x) \\
= \; & (\omega_p - \omega_q)(4L_p'L_q' - 2L_q'L_p - 2L_p'L_q) + \frac{1}{2}\left[\omega_p L_p \left(4L_q'' - 4L_q'\right) - \omega_q L_q \left(4L_p'' - 4L_p'\right)\right] \\
= \; & 4 - 2\sqrt{3},
\end{aligned}$$

$$g_1(x) = f_1(x) + 2(\omega_p - \omega_q)L_pL_q = 6 - 4\sqrt{3} - 4(1-\sqrt{3})x;$$

$$\begin{aligned}
& f_2(x) \\
= \; & (\omega_p + \omega_q)(4L_p'L_q' - 2L_q'L_p - 2L_p'L_q) + \frac{1}{2}\left[\omega_p L_p \left(4L_q'' - 4L_q'\right) + \omega_q L_q \left(4L_p'' - 4L_p'\right)\right] \\
= \; & 4 + 2\sqrt{3},
\end{aligned}$$

$$g_2(x) = f_2(x) + 2(\omega_p + \omega_q)L_pL_q = 6 + 4\sqrt{3} - 4(1+\sqrt{3})x;$$

$$f_3(x) = 2L_p'^2 - 6L_pL_p' + 2L_pL_p'' = 0,$$

$$g_3(x) = f_3(x) + 2L_p^2 = 2;$$

$$f_4(x) = 2L_q'^2 - 6L_qL_q' + 2L_qL_q'' = 10 - 12x,$$

$$g_4(x) = f_4(x) + 2L_q^2 = 8x^2 - 20x + 12.$$

Referring to (4.36), the numerical solutions to f_{11}, f_{12} and f_{14} are plotted in Figure 4-1. Note that $f_3(x) = 0$ identically, hence $f_{13} = 0$ in this case. Our numerical results by finite element method (Appendix H) show that all of them are close to zero after $x > 4$ (See Figure 4-1.).

Other c's from $\mathcal{E}_p$:

[$\mathcal{E}_p$-1]. From (4.40),

$$\begin{aligned}
& c_{31} \\
= \; & \int_0^\infty dx F_p(x) \left\{ i\frac{1}{\omega_p\omega_q^2} e^{-x} \left[2\omega_p \frac{dG_1}{dx}(2L_q' - L_q) + \omega_q \frac{d^2G_1}{dx^2} L_q \right.\right. \\
& \left.\left. -(\omega_q - \omega_p) G_1 (4L_q'' - 4L_q') \right] \right\}
\end{aligned}$$

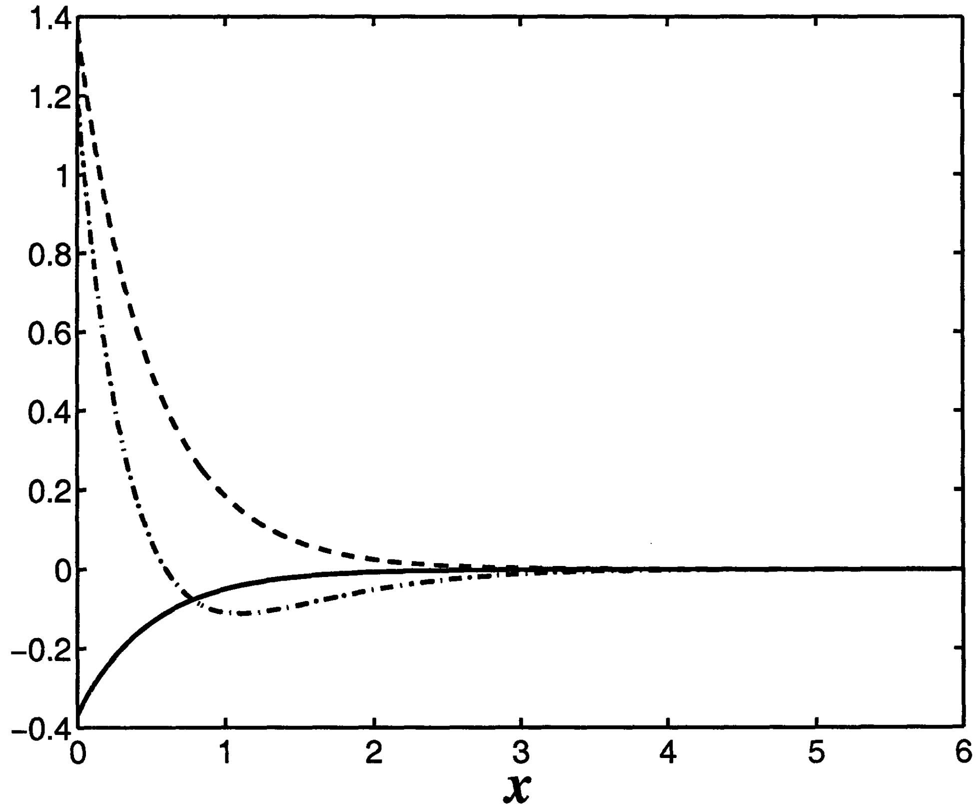

Figure 4-1: Numerical solutions to f_{11}— solid line, f_{12}— dash line, and f_{14}— dash-dot line for Case (1): $p = 0,\ q = 1$.

$$
\begin{aligned}
&= \frac{i}{3}\int_0^\infty dx e^{-2x}\left\{(4x-6)\frac{dG_1}{dx} + \sqrt{3}(1-2x)\frac{d^2G_1}{dx^2} - 4(\sqrt{3}-1)G_1\right\} \\
&= \frac{i}{3}\left\{-\sqrt{3}\frac{dG_1}{dx}(0) - (4\sqrt{3}-6)G_1(0) + \int_0^\infty dx e^{-2x}\left[(8\sqrt{3}-12)+8(1-\sqrt{3})x\right]G_1\right\} \\
&= \frac{i}{3}\left\{-\sqrt{3}g_1(0)+\alpha\right\} = -0.0063 + 0.5412i \qquad (4.77)
\end{aligned}
$$

where use has been made of relation (4.33). And the generic form for the partial integral is

$$
\int_0^\infty dx f(x) e^{-2x}\frac{dG}{dx} = -f(0)G(0) - \int_0^\infty dx (f'-2f)e^{-2x}G.
$$

The integral α can be evaluated as

$$
\alpha = \int_0^\infty dx e^{-2x}\left[(8\sqrt{3}-12)+8(1-\sqrt{3})x\right]G_1 = \sum_{j=1}^{4}\alpha_j = 0.0158 + 0.0190i \qquad (4.78)
$$

where

$$
\begin{aligned}
\alpha_1 &= \pi\int_0^\infty dx e^{-2x}\left[(8\sqrt{3}-12)+8(1-\sqrt{3})x\right]J_0(2\bar{\omega}\sqrt{x})\int_0^\infty d\xi e^{-2\xi}g_1(\xi)Y_0(2\bar{\omega}\sqrt{\xi}) \\
\alpha_2 &= -\pi\int_0^\infty dx e^{-2x}\left[(8\sqrt{3}-12)+8(1-\sqrt{3})x\right]J_0(2\bar{\omega}\sqrt{x})\int_0^x d\xi e^{-2\xi}g_1(\xi)Y_0(2\bar{\omega}\sqrt{\xi}) \\
\alpha_3 &= -i\pi\int_0^\infty dx e^{-2x}\left[(8\sqrt{3}-12)+8(1-\sqrt{3})x\right]J_0(2\bar{\omega}\sqrt{x})\int_0^\infty d\xi e^{-2\xi}g_1(\xi)J_0(2\bar{\omega}\sqrt{\xi}) \\
\alpha_4 &= \pi\int_0^\infty dx e^{-2x}\left[(8\sqrt{3}-12)+8(1-\sqrt{3})x\right]Y_0(2\bar{\omega}\sqrt{x})\int_0^x d\xi e^{-2\xi}g_1(\xi)J_0(2\bar{\omega}\sqrt{\xi})
\end{aligned}
$$

with $\bar{\omega} = \sqrt{3}-1$. Refer to (4.30) for the generic form of solution G_1. Constant α's are given in Table 4.4.

Table 4.4: Coefficients of α's by numerical integration.

α_1	α_2	α_3	α_4
-0.0777	0.0856	0.0190i	0.0079

[$\mathcal{E}_p$-2]. From (4.41),

c_{32}

$$
\begin{aligned}
&= \int_0^\infty dx F_p(x) \left\{ i\frac{1}{\omega_p\omega_q^2} e^{-x} \left[2\omega_p \frac{dG_2}{dx}(2L_q' - L_q) - \omega_q \frac{d^2G_2}{dx^2} L_q \right.\right. \\
&\quad \left.\left. + (\omega_p + \omega_q) G_2 (4L_q'' - 4L_q') \right] \right\} \\
&= \frac{i}{3} \int_0^\infty dx e^{-2x} \left\{ (4x-6)\frac{dG_2}{dx} - \sqrt{3}(1-2x)\frac{d^2G_2}{dx^2} + 4(\sqrt{3}+1)G_1 \right\} \\
&= \frac{i}{3} \left\{ \sqrt{3}\frac{dG_2}{dx}(0) + (4\sqrt{3}+6)G_2(0) + \int_0^\infty dx e^{-2x} \left[8(1+\sqrt{3})x - (8\sqrt{3}+12) \right] G_2 \right\} \\
&= \frac{i}{3} \left\{ \sqrt{3} g_2(0) + \beta \right\} = -0.2329 + 3.9662i \qquad (4.79)
\end{aligned}
$$

The integral β can be evaluated as

$$
\beta = \int_0^\infty dx e^{-2x} \left[8(1+\sqrt{3})x - (8\sqrt{3}+12) \right] G_2 = \sum_{j=1}^{4} \beta_j = -10.4938 + 0.6988i \quad (4.80)
$$

where

$$
\beta_1 = \pi \int_0^\infty dx e^{-2x} \left[8(1+\sqrt{3})x - (8\sqrt{3}+12) \right] J_0(2\bar{\omega}\sqrt{x}) \int_0^\infty d\xi e^{-2\xi} g_2(\xi) Y_0(2\bar{\omega}\sqrt{\xi})
$$

$$
\beta_2 = -\pi \int_0^\infty dx e^{-2x} \left[8(1+\sqrt{3})x - (8\sqrt{3}+12) \right] J_0(2\bar{\omega}\sqrt{x}) \int_0^x d\xi e^{-2\xi} g_2(\xi) Y_0(2\bar{\omega}\sqrt{\xi})
$$

$$
\beta_3 = -i\pi \int_0^\infty dx e^{-2x} \left[8(1+\sqrt{3})x - (8\sqrt{3}+12) \right] J_0(2\bar{\omega}\sqrt{x}) \int_0^\infty d\xi e^{-2\xi} g_2(\xi) J_0(2\bar{\omega}\sqrt{\xi})
$$

$$
\beta_4 = \pi \int_0^\infty dx e^{-2x} \left[8(1+\sqrt{3})x - (8\sqrt{3}+12) \right] Y_0(2\bar{\omega}\sqrt{x}) \int_0^x d\xi e^{-2\xi} g_2(\xi) J_0(2\bar{\omega}\sqrt{\xi})
$$

with $\bar{\omega} = \sqrt{3} + 1$. Refer to (4.30) for the generic form of solution G_2. Constant β's are given in Table 4.5.

Table 4.5: Coefficients of β's by numerical integration.

β_1	β_2	β_3	β_4
-1.8068	-3.4395	0.6988i	-5.2475

[$\mathcal{E}_p$-3]. From (4.42),

$$
\begin{aligned}
&c_{21} \\
&= \int_0^\infty dx F_p(x) \left\{ i\frac{1}{\omega_p} e^{-x} \left[2\frac{dG_3}{dx}(2L_p' - L_p) - \frac{d^2G_3}{dx^2} L_p + 2G_3(4L_p'' - 4L_p') \right] \right\} \\
&= i \int_0^\infty dx e^{-2x} \left\{ -2\frac{dG_3}{dx} - \frac{d^2G_3}{dx^2} \right\}
\end{aligned}
$$

$$
\begin{aligned}
&= i\left\{\frac{dG_3}{dx}(0) + 4G_3(0) - 8\int_0^\infty dx e^{-2x} G_3\right\} \\
&= i\left\{g_3(0) - 8\gamma\right\} = -0.2302 + 0.5618i
\end{aligned} \tag{4.81}
$$

The integral γ can be evaluated as

$$
\gamma = \int_0^\infty dx e^{-2x} G_3 = \sum_{j=1}^{4} \gamma_j = 0.1798 - 0.0288i
$$

where

$$
\begin{aligned}
\gamma_1 &= \pi \int_0^\infty dx e^{-2x} J_0(2\bar{\omega}\sqrt{x}) \int_0^\infty d\xi e^{-2\xi} g_3(\xi) Y_0(2\bar{\omega}\sqrt{\xi}) \\
\gamma_2 &= -\pi \int_0^\infty dx e^{-2x} J_0(2\bar{\omega}\sqrt{x}) \int_0^x d\xi e^{-2\xi} g_3(\xi) Y_0(2\bar{\omega}\sqrt{\xi}) \\
\gamma_3 &= -i\pi \int_0^\infty dx e^{-2x} J_0(2\bar{\omega}\sqrt{x}) \int_0^\infty d\xi e^{-2\xi} g_3(\xi) J_0(2\bar{\omega}\sqrt{\xi}) \\
\gamma_4 &= \pi \int_0^\infty dx e^{-2x} Y_0(2\bar{\omega}\sqrt{x}) \int_0^x d\xi e^{-2\xi} g_3(\xi) J_0(2\bar{\omega}\sqrt{\xi})
\end{aligned}
$$

with $\bar{\omega} = 2$. Refer to (4.30) for the generic form of solution G_3. Constant γ's are given in Table 4.6.

Table 4.6: Coefficients of γ's by numerical integration.

γ_1	γ_2	γ_3	γ_4
0.0454	0.0445	-0.0288i	0.0899

[$\mathcal{E}_p$-4]. From (4.43),

$$
\begin{aligned}
& c_{33} \\
&= \int_0^\infty dx F_p(x) \left\{ \frac{ie^{-x}}{\omega_p \omega_q^2} \left[\frac{\omega_q}{2} L_q f_{11xx} + \omega_p (2L_q' - L_q) f_{11x} \right.\right. \\
&\quad \left.\left. - \frac{\omega_q - \omega_p}{2} (4L_q'' - 4L_q' + 4L_q) f_{11} \right] \right\} \\
&= \frac{i}{3} \int_0^\infty dx e^{-2x} \left\{ \frac{\sqrt{3}}{2} (1 - 2x) f_{11xx} + (2x - 3) f_{11x} - 4(\sqrt{3} - 1)(1 - x) f_{11} \right\} \\
&= \frac{i}{3} \left\{ -\frac{\sqrt{3}}{2} f_{11x}(0) - (2\sqrt{3} - 3) f_{11}(0) \right. \\
&\quad \left. + \int_0^\infty dx e^{-2x} \left[(2\sqrt{3} - 4) + 8(\sqrt{3} - 1)x \right] f_{11} \right\} = -0.1830i
\end{aligned} \tag{4.82}
$$

$[\mathcal{E}_p\text{-}5]$. From (4.44),

$$
\begin{aligned}
& c_{34} \\
= & \int_0^\infty dx F_p(x) \left\{ \frac{ie^{-x}}{\omega_p \omega_q^2} \left[\omega_p (2L_q' - L_q) f_{12x} - \frac{\omega_q}{2} L_q f_{12xx} \right.\right. \\
& \left.\left. + \frac{\omega_p + \omega_q}{2} (4L_q'' - 4L_q' + 4L_q) f_{12} \right] \right\} \\
= & \frac{i}{3} \int_0^\infty dx e^{-2x} \left\{ -\frac{\sqrt{3}}{2} (1-2x) f_{12xx} + (2x-3) f_{12x} + 4(\sqrt{3}+1)(1-x) f_{12} \right\} \\
= & \frac{i}{3} \left\{ \frac{\sqrt{3}}{2} f_{12x}(0) + (2\sqrt{3}+3) f_{12}(0) + \int_0^\infty dx e^{-2x} (-2\sqrt{3}-4) f_{12} \right\} = 1.3050i
\end{aligned} \tag{4.83}
$$

$[\mathcal{E}_p\text{-}6]$. From (4.45),

$$
\begin{aligned}
& c_{22} \\
= & \int_0^\infty dx F_p(x) \left\{ i \frac{1}{\omega_p} e^{-x} \left[f_{13x} (2L_p' - L_p) - \frac{1}{2} L_p f_{13xx} + f_{13} (4L_p'' - 4L_p' + 4L_p) \right] \right\} \\
= & i \int_0^\infty dx e^{-2x} \left\{ -f_{13x} - \frac{1}{2} f_{13xx} + 4 f_{13} \right\} \\
= & i \left\{ \frac{1}{2} f_{13x}(0) + 2 f_{13}(0) \right\} = 0
\end{aligned} \tag{4.84}
$$

$[\mathcal{E}_p\text{-}7]$. From (4.46),

$$
\begin{aligned}
& c_{23} \\
= & \int_0^\infty dx F_p(x) \left\{ -i \frac{1}{\omega_p^3} e^{-3x} \left[\frac{27}{8} (4L_p'' - 4L_p' + L_p)(2L_p' - L_p)^2 - \frac{9}{8} (2L_p' - L_p)^2 L_p \right.\right. \\
& \left.\left. + \frac{3}{2} (2L_p' - L_p)^2 L_p + \frac{3}{8} (4L_p'' - 4L_p' + L_p) L_p^2 - \frac{9}{8} L_p^3 \right] \right\} \\
= & -i \int_0^\infty dx e^{-4x} \left\{ \frac{27}{8} - \frac{9}{8} + \frac{3}{2} + \frac{3}{8} - \frac{9}{8} \right\} \\
= & -3i \int_0^\infty dx e^{-4x} \\
= & -\frac{3i}{4}
\end{aligned} \tag{4.85}
$$

$[\mathcal{E}_p\text{-}8]$. From (4.47),

$$
\begin{aligned}
& c_{35} \\
= & \int_0^\infty -i \frac{1}{\omega_p \omega_q^2} e^{-3x} \left\{ \frac{3}{4} \left[3(4L_p'' - 4L_p' + L_p)(2L_q' - L_q)^2 - (2L_q' - L_q)^2 L_p \right.\right.
\end{aligned}
$$

$$
\begin{aligned}
& + 6(4L_q'' - 4L_q' + L_q)(2L_q' - L_q)(2L_p' - L_p) - 2L_q(2L_p' - L_p)(2L_q' - L_q)\Big] \\
& + \frac{1}{4}\Big[8(2L_p' - L_p)(2L_q' - L_q)L_q + 4(2L_q' - L_q)^2 L_p \\
& - 9L_pL_q^2 + (4L_p'' - 4L_p' + L_p)L_q^2 + 2(4L_q'' - 4L_q' + L_q)L_pL_q\Big]\Big\} F_p(x)dx \\
= & -\frac{i}{3}\int_0^\infty dxe^{-4x}\left\{6L_q^2 + 40L_q + 46\right\} \\
= & -\frac{i}{3}\int_0^\infty dxe^{-4x}\left\{24x^2 - 104x + 92\right\} \\
= & -\frac{23i}{4} \qquad (4.86)
\end{aligned}
$$

Therefore,

$$c_2 \equiv c_{21} + c_{22} + c_{23} = -0.2302 - 0.1882i,$$

$$c_3 \equiv c_{31} + c_{32} + c_{33} + c_{34} + c_{35} = -0.2393 - 0.1207i.$$

Other d's from $\mathcal{E}_q$:

[$\mathcal{E}_q$-1]. From (4.48),

$$
\begin{aligned}
& d_{31} \\
= & \int_0^\infty dxF_q(x)\left\{\frac{ie^{-x}}{\omega_q\omega_p^2}\left[2\omega_q\frac{dG_1}{dx}(2L_p' - L_p) + \omega_p\frac{d^2G_1}{dx^2}L_p\right.\right. \\
& \left.\left. +(\omega_q - \omega_p)G_1(4L_p'' - 4L_p')\right]\right\} \\
= & \frac{i}{\sqrt{3}}\int_0^\infty dxe^{-2x}\left\{-2\sqrt{3}(1-2x)\frac{dG_1}{dx} + (1-2x)\frac{d^2G_1}{dx^2}\right\} \\
= & \frac{i}{\sqrt{3}}\left\{-\frac{dG_1}{dx}(0) - (4-2\sqrt{3})G_1(0) + \int_0^\infty dxe^{-2x}\left[(12-8\sqrt{3}) + 8(\sqrt{3}-1)x\right]G_1\right\} \\
= & \frac{i}{\sqrt{3}}\left\{-g_1(0) - \alpha\right\} = 0.0109 + 0.5268i \qquad (4.87)
\end{aligned}
$$

where α is defined in (4.77) and evaluated in (4.78). Refer to (4.30) for the generic form of solution G_1.

[$\mathcal{E}_q$-2]. From (4.49),

$$
\begin{aligned}
& d_{32} \\
= & \int_0^\infty dxF_q(x)\left\{\frac{ie^{-x}}{\omega_q\omega_p^2}\left[2\omega_q\frac{dG_2}{dx}(2L_p' - L_p) - \omega_p\frac{d^2G_2}{dx^2}L_p\right.\right. \\
& \left.\left. +(\omega_p + \omega_q)G_2(4L_p'' - 4L_p')\right]\right\} \\
= & \frac{i}{\sqrt{3}}\int_0^\infty dxe^{-2x}\left\{-2\sqrt{3}(1-2x)\frac{dG_2}{dx} - (1-2x)\frac{d^2G_2}{dx^2}\right\}
\end{aligned}
$$

$$
\begin{aligned}
&= \frac{i}{\sqrt{3}}\left\{\frac{dG_2}{dx}(0) + (4+2\sqrt{3})G_2(0) + \int_0^\infty dx e^{-2x}\left[8(\sqrt{3}+1)x - (12+8\sqrt{3})\right] G_2\right\} \\
&= \frac{i}{\sqrt{3}}\{g_2(0)+\beta\} = -0.4035 + 1.4055i
\end{aligned}
\tag{4.88}
$$

where β is defined in (4.79) and evaluated in (4.80). Refer to (4.30) for the generic form of solution G_2.

[$\mathcal{E}_q$-3]. From (4.50),

$$
\begin{aligned}
&d_{21} \\
&= \int_0^\infty dx F_q(x)\left\{\frac{i}{\omega_q}e^{-x}\left[2\frac{dG_4}{dx}(2L_q' - L_q) - \frac{d^2G_4}{dx^2}L_q + 2G_4(4L_q'' - 4L_q')\right]\right\} \\
&= \frac{i}{\sqrt{3}}\int_0^\infty dx e^{-2x}\left\{(16x - 8x^2 - 6)\frac{dG_4}{dx} - (1-2x)^2\frac{d^2G_4}{dx^2} + 8(1-2x)G_4\right\} \\
&= \frac{i}{\sqrt{3}}\left\{\frac{dG_4}{dx}(0) + 12G_4(0) + \int_0^\infty dx e^{-2x}\left[16x - 48 - 32x^2\right] G_4\right\} \\
&= \frac{i}{\sqrt{3}}\{g_4(0)+\kappa\} = -0.0501 + 1.6654i
\end{aligned}
\tag{4.89}
$$

The integral κ can be evaluated as

$$
\kappa = \int_0^\infty dx e^{-2x}\left[16x - 48 - 32x^2\right] G_4 = \sum_{j=1}^{4}\kappa_j = -9.1154 + 0.0869i
$$

where

$$
\begin{aligned}
\kappa_1 &= \pi\int_0^\infty dx e^{-2x}\left[16x - 48 - 32x^2\right] J_0(2\bar{\omega}\sqrt{x})\int_0^\infty d\xi e^{-2\xi}g_4(\xi)Y_0(2\bar{\omega}\sqrt{\xi}) \\
\kappa_2 &= -\pi\int_0^\infty dx e^{-2x}\left[16x - 48 - 32x^2\right] J_0(2\bar{\omega}\sqrt{x})\int_0^x d\xi e^{-2\xi}g_4(\xi)Y_0(2\bar{\omega}\sqrt{\xi}) \\
\kappa_3 &= -i\pi\int_0^\infty dx e^{-2x}\left[16x - 48 - 32x^2\right] J_0(2\bar{\omega}\sqrt{x})\int_0^\infty d\xi e^{-2\xi}g_4(\xi)J_0(2\bar{\omega}\sqrt{\xi}) \\
\kappa_4 &= \pi\int_0^\infty dx e^{-2x}\left[16x - 48 - 32x^2\right] Y_0(2\bar{\omega}\sqrt{x})\int_0^x d\xi e^{-2\xi}g_4(\xi)J_0(2\bar{\omega}\sqrt{\xi})
\end{aligned}
$$

with $\bar{\omega} = 2\sqrt{3}$. Refer to (4.30) for the generic form of solution G_4. Constant κ's are given in Table 4.7.

[$\mathcal{E}_q$-4]. From (4.51),

$$
\begin{aligned}
&d_{33} \\
&= \int_0^\infty dx F_q(x)\left\{\frac{ie^{-x}}{\omega_q\omega_p^2}\left[\frac{\omega_p}{2}L_p f_{11xx} + \omega_q(2L_p' - L_p)f_{11x}\right.\right.
\end{aligned}
$$

Table 4.7: Coefficients of κ's by numerical integration.

κ_1	κ_2	κ_3	κ_4
-0.3945	-4.1671	0.0869i	-4.5538

$$
\begin{aligned}
& +\frac{\omega_q-\omega_p}{2} f_{11}(4L_p''-4L_p'+4L_p)\Big]\Big\} \\
= & \frac{i}{\sqrt{3}}\int_0^\infty dx e^{-2x}\left\{\frac{1}{2}(1-2x)f_{11xx}-\sqrt{3}(1-2x)f_{11x}+2(\sqrt{3}-1)(1-2x)f_{11}\right\} \\
= & \frac{i}{\sqrt{3}}\left\{-\frac{1}{2}f_{11x}(0)-(2-\sqrt{3})f_{11}(0)+\int_0^\infty dx e^{-2x}(4-2\sqrt{3})f_{11}\right\}=-0.1830i
\end{aligned} \tag{4.90}
$$

$[\mathcal{E}_q\text{-}5]$. From (4.52),

$$
\begin{aligned}
& d_{34} \\
= & \int_0^\infty dx F_q(x)\left\{\frac{ie^{-x}}{\omega_q\omega_p^2}\Big[\omega_q(2L_p'-L_p)f_{12x}-\frac{\omega_p}{2}L_p f_{12xx}\right. \\
& +\frac{\omega_p+\omega_q}{2}f_{12}(4L_p''-4L_p'+4L_p)\Big]\Big\} \\
= & \frac{i}{\sqrt{3}}\int_0^\infty dx e^{-2x}\left\{-\frac{1}{2}(1-2x)f_{12xx}-\sqrt{3}(1-2x)f_{12x}+2(\sqrt{3}+1)(1-2x)f_{12}\right\} \\
= & \frac{i}{\sqrt{3}}\left\{\frac{1}{2}f_{12x}(0)+(2+\sqrt{3})f_{12}(0)-\int_0^\infty dx e^{-2x}(4+2\sqrt{3})f_{12}\right\}=0.6830i
\end{aligned} \tag{4.91}
$$

$[\mathcal{E}_q\text{-}6]$. From (4.53),

$$
\begin{aligned}
& d_{22} \\
= & \int_0^\infty dx F_q(x)\left\{\frac{i}{\omega_q}e^{-x}\Big[(2L_q'-L_q)f_{14x}-\frac{1}{2}L_q f_{14xx}+(4L_q''-4L_q'+4L_q)f_{14}\Big]\right\} \\
= & \frac{i}{\sqrt{3}}\int_0^\infty dx e^{-2x}\left\{(8x-4x^2-3)f_{14x}-\frac{1}{2}(1-2x)^2 f_{14xx}+8(1-3x+2x^2)f_{14}\right\} \\
= & \frac{i}{\sqrt{3}}\left\{\frac{1}{2}f_{14x}(0)+6f_{14}(0)+\int_0^\infty dx e^{-2x}\left[24x-20\right]f_{14}\right\}=1.0392i
\end{aligned} \tag{4.92}
$$

$[\mathcal{E}_q\text{-}7]$. From (4.54),

$$
\begin{aligned}
& d_{23} \\
= & \int_0^\infty -i\frac{1}{\omega_q^3}e^{-3x}\left\{\Big[\frac{27}{8}(4L_q''-4L_q'+L_q)(2L_q'-L_q)^2-\frac{9}{8}(2L_q'-L_q)^2L_q\Big]\right.
\end{aligned}
$$

$$
\begin{aligned}
& + \left[\frac{3}{2}(2L_q' - L_q)^2 L_q + \frac{3}{8}(4L_q'' - 4L_q' + L_q)L_q^2 - \frac{9}{8}L_q^3\right]\Big\} F_q(x)dx \\
= & -\frac{i}{3\sqrt{3}}\int_0^\infty dx e^{-4x}\left(156 - 276x + 156x^2 - 24x^3\right)(1-2x) \\
= & -\frac{i}{3\sqrt{3}}\int_0^\infty dx e^{-4x}\left\{48x^4 - 336x^3 + 708x^2 - 588x + 156\right\} \\
= & -\frac{47i}{8\sqrt{3}}
\end{aligned} \tag{4.93}
$$

$[\mathcal{E}_q\text{-}8]$. From (4.55),

$$
\begin{aligned}
& d_{35} \\
= & \int_0^\infty -i\frac{1}{\omega_q\omega_p^2}e^{-3x}\left\{\frac{3}{4}\left[3(4L_q'' - 4L_q' + L_q)(2L_p' - L_p)^2 - (2L_p' - L_p)^2 L_q\right.\right. \\
& \left. + 6(4L_p'' - 4L_p' + L_p)(2L_p' - L_p)(2L_q' - L_q) - 2L_p(2L_q' - L_q)(2L_p' - L_p)\right] \\
& + \frac{1}{4}\left[8(2L_q' - L_q)(2L_p' - L_p)L_p + 4(2L_p' - L_p)^2 L_q\right. \\
& \left.\left. - 9L_qL_p^2 + (4L_q'' - 4L_q' + L_q)L_p^2 + 2(4L_p'' - 4L_p' + L_p)L_qL_p\right]\right\} F_q(x)dx \\
= & -\frac{i}{\sqrt{3}}\int_0^\infty dx e^{-4x}\{6L_q + 20\}(1-2x) \\
= & -\frac{i}{\sqrt{3}}\int_0^\infty dx e^{-4x}\left\{24x^2 - 64x + 26\right\} \\
= & -\frac{13i}{4\sqrt{3}}
\end{aligned} \tag{4.94}
$$

Therefore,

$$d_2 \equiv d_{21} + d_{22} + d_{23} = -0.0501 - 0.6873i,$$

$$d_3 \equiv d_{31} + d_{32} + d_{33} + d_{34} + d_{35} = -0.3925 + 0.5558i$$

Case (2): $p = 0,\ q = 2$ and case (3): $p = 1,\ q = 2$ can be treated similarly and details are given in Appendix I. For convenience, we summarized the coefficients in Table 4.8.

4.8 Nonlinear dynamics of Stuart-Landau equations

Recalling from (4.70) and (4.71), we have a pair of coupled equations to deal with:

$$\frac{\partial B_p}{\partial \tau} = ic_1 B_q^* + c_2 B_p B_p B_p^* + c_3 B_p B_q B_q^*; \tag{4.95}$$

$$\frac{\partial B_q}{\partial \tau} = id_1 B_p^* + d_2 B_q B_q B_q^* + d_3 B_q B_p B_p^*. \tag{4.96}$$

Coefficients c's and d's are summarized in Table 4.8 for several (p, q) combinations.

Table 4.8: Coefficients of c's and d's for $\omega = \omega_q + \omega_p$.

		c_1	c_2	c_3
	(0,1)	0.1410	-0.2302-0.1882i	-0.2393-0.1207i
(p,q)	(0,2)	0.1056	-0.2302-0.1882i	-0.1969+0.2098i
	(1,2)	0.0970	-0.0903-0.0478i	-0.1352-0.0318i
		d_1	d_2	d_3
	(0,1)	0.2441	-0.0501-0.6873i	-0.3925+0.5558i
(p,q)	(0,2)	0.2360	-0.0626-0.0121i	-0.3796+0.8419i
	(1,2)	0.1524	-0.0626-0.0121i	-0.1720+1.2832i

4.8.1 Effects of detuning

Instead of perfect resonance, i.e. $\omega = \omega_q + \omega_p$, we now consider the effects of detuning, i.e. some sorts of frequency mismatch may come from the incident/reflected wave:

$$\omega \to \omega + \bar{\epsilon}^2 \Omega$$

This amounts to making replacements

$$\bar{A} \to \bar{A} e^{-i\bar{\epsilon}^2 \Omega t}.$$

Therefore the evolution equations (4.70) and (4.71) become

$$\frac{\partial B_p}{\partial \tau} = ic_1 e^{-i\Omega\tau} B_q^* + c_2 |B_p|^2 B_p + c_3 |B_q|^2 B_p \tag{4.97}$$

$$\frac{\partial B_q}{\partial \tau} = id_1 e^{-i\Omega\tau} B_p^* + d_2 |B_q|^2 B_q + d_3 |B_p|^2 B_q \tag{4.98}$$

Let us make the change of variables

$$B_j = \bar{B}_j e^{-i\Omega_j \tau}, \ j = p, q \tag{4.99}$$

where we require that $\Omega_p + \Omega_q = \Omega$. Then

$$\frac{\partial B_j}{\partial \tau} = \left(\frac{\partial \bar{B}_j}{\partial \tau} - i\Omega_j \bar{B}_j \right) e^{-i\Omega_j \tau}$$

Therefore, Equation (4.97) and (4.98) become

$$\frac{\partial \bar{B}_p}{\partial \tau} = i\Omega_p \bar{B}_p + ic_1 \bar{B}_q^* + c_2 |\bar{B}_p|^2 \bar{B}_p + c_3 |\bar{B}_q|^2 \bar{B}_p \tag{4.100}$$

$$\frac{\partial \bar{B}_q}{\partial \tau} = i\Omega_q \bar{B}_q + id_1 \bar{B}_p^* + d_2 |\bar{B}_q|^2 \bar{B}_q + d_3 |\bar{B}_p|^2 \bar{B}_q \tag{4.101}$$

The detuning adds another new term to the evolution equation as in the classical edge wave theory. Note that only one of Ω_p or Ω_q is arbitrary, since

$$\Omega_p + \Omega_q = \Omega. \tag{4.102}$$

where Ω is the detuning from the incident wave. Physical meaning of $\bar{B}_p$ and $\bar{B}_q$ is as follows: By definition, B_p and B_q are the amplitude of the edge waves. For constant Ω_p and Ω_q with $\Omega_p + \Omega_q = \Omega$, a fixed point solution $\bar{B}_p^0$ and $\bar{B}_q^0$ means that they are time-independent. However, it corresponds to limit cycles for B_p and B_q, since

$$B_p(\tau) = \bar{B}_p^0 e^{-i\Omega_p^0 \tau} \ \text{ and } \ B_q(\tau) = \bar{B}_q^0 e^{-i\Omega_q^0 \tau}$$

are circular trajectories in the phase plane as time increases. Later on we shall show that Ω_p and Ω_q must take the particular value Ω_p^0 and Ω_q^0 in order for $\bar{B}_p$ and $\bar{B}_q$ to have a fixed point solution $\bar{B}_p^0$ and $\bar{B}_q^0$.

4.8.2 Initial growth rate from infinitesimal disturbance with effect of detuning

Consider the initial stage of evolution from $B_p \sim B_q \simeq 0$. Nonlinear terms are ignored and Equation (4.100) and (4.101) become

$$\frac{\partial \bar{B}_p}{\partial \tau} = i\Omega_p \bar{B}_p + ic_1 \bar{B}_q^* \quad \text{and} \quad \frac{\partial \bar{B}_q}{\partial \tau} = i\Omega_q \bar{B}_q + id_1 \bar{B}_p^*. \tag{4.103}$$

which can be manipulated to get

$$\begin{aligned}
\frac{\partial^2 \bar{B}_p}{\partial \tau^2} &= i\Omega_p \frac{\partial \bar{B}_p}{\partial \tau} + ic_1 \frac{\partial \bar{B}_q^*}{\partial \tau} \\
&= i\Omega_p \left(i\Omega_p \bar{B}_p + ic_1 \bar{B}_q^* \right) + ic_1 \left(-i\Omega_q \bar{B}_q^* - id_1 \bar{B}_p \right) \\
&= \left[c_1 d_1 - \Omega_p^2 \right] \bar{B}_p + c_1 \left(\Omega_q - \Omega_p \right) \bar{B}_q^* \\
&= \left[c_1 d_1 - \Omega_p \Omega_q \right] \bar{B}_p - i \left(\Omega_q - \Omega_p \right) \frac{\partial \bar{B}_p}{\partial \tau} \qquad (4.104)
\end{aligned}$$

Similarly, we can get

$$\begin{aligned}
\frac{\partial^2 \bar{B}_q}{\partial \tau^2} &= i\Omega_q \frac{\partial \bar{B}_q}{\partial \tau} + id_1 \frac{\partial \bar{B}_p^*}{\partial \tau} \\
&= i\Omega_q \left(i\Omega_q \bar{B}_q + id_1 \bar{B}_p^* \right) + id_1 \left(-i\Omega_p \bar{B}_p^* - ic_1 \bar{B}_q \right) \\
&= \left[c_1 d_1 - \Omega_q^2 \right] \bar{B}_q + d_1 \left(\Omega_p - \Omega_q \right) \bar{B}_p^* \\
&= \left[c_1 d_1 - \Omega_p \Omega_q \right] \bar{B}_q - i \left(\Omega_p - \Omega_q \right) \frac{\partial \bar{B}_q}{\partial \tau} \qquad (4.105)
\end{aligned}$$

We move all the terms to one side of equation and get

$$\frac{\partial^2 \bar{B}_p}{\partial \tau^2} + i \left(\Omega_q - \Omega_p \right) \frac{\partial \bar{B}_p}{\partial \tau} + \left(\Omega_p \Omega_q - c_1 d_1 \right) \bar{B}_p = 0 \qquad (4.106)$$

$$\frac{\partial^2 \bar{B}_q}{\partial \tau^2} + i \left(\Omega_p - \Omega_q \right) \frac{\partial \bar{B}_q}{\partial \tau} + \left(\Omega_p \Omega_q - c_1 d_1 \right) \bar{B}_q = 0 \qquad (4.107)$$

We assume that the eigen solutions to the above equations are

$$\bar{B}_j = b_j e^{i\sigma_j \tau}, \quad j = p, q$$

Upon substitution into (4.106), we get the eigen value condition

$$\sigma_p^2 + (\Omega_q - \Omega_p)\sigma_p + (c_1 d_1 - \Omega_p \Omega_q) = 0$$

which gives the eigen values

$$\sigma_p^{\pm} = \frac{-(\Omega_q - \Omega_p) \pm \sqrt{(\Omega_q - \Omega_p)^2 - 4(c_1 d_1 - \Omega_p \Omega_q)}}{2}$$

If

$$(\Omega_q - \Omega_p)^2 - 4(c_1 d_1 - \Omega_p \Omega_q) > 0$$

or

$$\Omega^2 > 4c_1d_1 \Rightarrow \Omega < -2\sqrt{c_1d_1}, \text{ or } \Omega > 2\sqrt{c_1d_1}, \tag{4.108}$$

then $\sigma_p^{\pm}$ are real. Use has been made of the relation in (4.102). If this is the case, the edge wave perturbation does not grow and hence is neutrally stable. Otherwise, one of the eigen value σ_p^- has a positive real part and hence the small edge wave perturbation is unstable.

Similarly we get the eigen value condition for σ_q from (4.107)

$$\sigma_q^2 + (\Omega_p - \Omega_q)\sigma_q + (c_1d_1 - \Omega_p\Omega_q) = 0$$

which gives the eigen values

$$\sigma_q^{\pm} = \frac{-(\Omega_p - \Omega_q) \pm \sqrt{(\Omega_p - \Omega_q)^2 - 4(c_1d_1 - \Omega_p\Omega_q)}}{2}$$

Therefore the edge wave perturbation is neutrally stable when $\Omega < -2\sqrt{c_1d_1}$ or $\Omega > 2\sqrt{c_1d_1}$. Otherwise it is unstable.

4.8.3 Energy equation

Multiplying $\bar{B}_p^*$ on both sides of Equation (4.100), we get

$$\frac{\partial \bar{B}_p}{\partial \tau}\bar{B}_p^* = i\Omega_p|B_p|^2 + ic_1\bar{B}_p^*\bar{B}_q^* + c_2|\bar{B}_p|^4 + c_3|\bar{B}_p|^2|\bar{B}_q|^2; \tag{4.109}$$

Added to its complex conjugate, the above equation becomes

$$\frac{\partial|\bar{B}_p|^2}{\partial \tau} = -2c_1\text{Im}\{\bar{B}_p^*\bar{B}_q^*\} + 2\text{Re}\{c_2\}|\bar{B}_p|^4 + 2\text{Re}\{c_3\}|\bar{B}_p|^2|\bar{B}_q|^2 \tag{4.110}$$

which describes the evolution of energy of p-mode edge wave. Similar result can be obtained for mode q:

$$\frac{\partial|\bar{B}_q|^2}{\partial \tau} = -2d_1\text{Im}\{\bar{B}_p^*\bar{B}_q^*\} + 2\text{Re}\{d_2\}|\bar{B}_q|^4 + 2\text{Re}\{d_3\}|\bar{B}_p|^2|\bar{B}_q|^2 \tag{4.111}$$

From Equation (4.110) the nonlinear terms always cause radiation damping for p-mode edge wave due to the fact that the real part of c_2 and c_3 are both negative (See Table 4.8.). Detuning does not affect the energy balance since it is not present in the energy equations. Similar results happen to mode q. The edge waves draw energy from the interaction with the incident wave, if $\text{Im}\{\bar{B}_p^*\bar{B}_q^*\} < 0$.

4.9 Analysis of nonlinear dynamical system for $\bar{B}_p$ and $\bar{B}_q$

Replacing $\bar{B}_j$ with its polar form

$$\bar{B}_j = \sqrt{I_j} e^{i\theta_j}, \quad j = p, q \tag{4.112}$$

we get

$$\frac{\partial \bar{B}_j}{\partial \tau} = \left(\frac{1}{2\sqrt{I_j}} \dot{I}_j + i\sqrt{I_j}\dot{\theta}_j \right) e^{i\theta_j} \tag{4.113}$$

where $I_j = |\bar{B}_j|^2$ is the action variable and θ_j is the angle variable. Also we introduce the new forms for the complex parameters

$$c_2 = -c_2^r - ic_2^i; \quad d_2 = -d_2^r - id_2^i; \quad c_3 = -c_3^r - ic_3^i; \quad d_3 = -d_3^r + id_3^i.$$

so that all c_j^r, c_j^i, d_j^r and d_j^i are real and positive.

Dividing both sides of Eq. (4.100) by $\bar{B}_p$, we get

$$\begin{aligned} L.H.S &= \frac{1}{\bar{B}_p}\frac{\partial \bar{B}_p}{\partial \tau} \\ &= \frac{1}{\sqrt{I_p}e^{i\theta_p}} \left(\frac{1}{2\sqrt{I_p}} \dot{I}_p + i\sqrt{I_p}\dot{\theta}_p \right) e^{i\theta_p} \\ &= \frac{1}{2I_p}\dot{I}_p + i\dot{\theta}_p \end{aligned} \tag{4.114}$$

$$\begin{aligned} R.H.S. &= i\Omega_p + ic_1 \frac{\bar{B}_q^*}{\bar{B}_p} + c_2|\bar{B}_p|^2 + c_3|\bar{B}_q|^2 \\ &= i\Omega_p + ic_1\sqrt{\frac{I_q}{I_p}} e^{-i(\theta_p+\theta_q)} + c_2 I_p + c_3 I_q \\ &= \left\{ c_1\sqrt{\frac{I_q}{I_p}} \sin(\theta_p+\theta_q) - c_2^r I_p - c_3^r I_q \right\} \\ &\quad + i\left\{ \Omega_p + c_1\sqrt{\frac{I_q}{I_p}} \cos(\theta_p+\theta_q) - c_2^i I_p - c_3^i I_q \right\} \end{aligned} \tag{4.115}$$

Separating the real and imaginary parts, we get

$$\frac{1}{2I_p}\dot{I}_p = c_1\sqrt{\frac{I_q}{I_p}}\sin(\theta_p+\theta_q) - c_2^r I_p - c_3^r I_q \tag{4.116}$$

$$\dot{\theta}_p = \Omega_p + c_1\sqrt{\frac{I_q}{I_p}}\cos(\theta_p+\theta_q) - c_2^i I_p - c_3^i I_q \tag{4.117}$$

Similarly we get from Equation (4.101)

$$\frac{1}{2I_q}\dot{I}_q = d_1\sqrt{\frac{I_p}{I_q}}\sin(\theta_p+\theta_q) - d_2^r I_q - d_3^r I_p \tag{4.118}$$

$$\dot{\theta}_q = \Omega_q + d_1\sqrt{\frac{I_p}{I_q}}\cos(\theta_p+\theta_q) - d_2^i I_q + d_3^i I_p \tag{4.119}$$

For initial evolution, we ignore the nonlinear terms of the above equations and get

$$\frac{1}{2I_p}\dot{I}_p = c_1\sqrt{\frac{I_q}{I_p}}\sin(\theta_p+\theta_q) \tag{4.120}$$

$$\dot{\theta}_p = \Omega_p + c_1\sqrt{\frac{I_q}{I_p}}\cos(\theta_p+\theta_q) \tag{4.121}$$

$$\frac{1}{2I_q}\dot{I}_q = d_1\sqrt{\frac{I_p}{I_q}}\sin(\theta_p+\theta_q) \tag{4.122}$$

$$\dot{\theta}_q = \Omega_q + d_1\sqrt{\frac{I_p}{I_q}}\cos(\theta_p+\theta_q) \tag{4.123}$$

Introducing

$$R = \frac{I_p}{I_q}, \quad \Theta = \theta_p + \theta_q$$

we get

$$\dot{R} = \frac{d}{d\tau}\left(\frac{I_p}{I_q}\right) = 2\frac{I_p}{I_q}\left(\frac{1}{2I_p}\dot{I}_p - \frac{1}{2I_q}\dot{I}_q\right)$$
$$\dot{\Theta} = \dot{\theta}_p + \dot{\theta}_q.$$

Therefore, from (4.120) and (4.122) we get

$$\dot{R} = 2R\left(\frac{c_1}{\sqrt{R}} - d_1\sqrt{R}\right)\sin\Theta$$

and from (4.121) and (4.123) we get

$$\dot{\Theta} = \Omega + \left(\frac{c_1}{\sqrt{R}} + d_1\sqrt{R}\right)\cos\Theta.$$

The dynamical system can be reduced to 2-dimensional at the initial stage of evolution. One of the equilibrium is

$$\frac{c_1}{\sqrt{R_0}} - d_1\sqrt{R_0} = 0 \Rightarrow R_0 = \frac{I_p^0}{I_q^0} = \frac{c_1}{d_1} = 0.5776, \tag{4.124}$$

which is independent of detuning Ω.

4.9.1 Fixed point of $\bar{B}_p$ and $\bar{B}_q$

After sufficiently long time evolution the dynamic system reaches its equilibrium, i.e. $\frac{\partial}{\partial\tau} = 0$. $(\bar{B}_p, \bar{B}_q) = (0,0)$ is obviously one fixed point to Equation (4.100) and (4.101). Let us assume that there exists another fixed point (I_p^0, I_q^0) other than the origin $(0,0)$. Let the L.H.S. of Equation (4.116) to (4.119) equal to zero, we get

$$c_1\sqrt{\frac{I_q^0}{I_p^0}}\sin(\theta_p^0 + \theta_q^0) = c_2^r I_p^0 + c_3^r I_q^0 \tag{4.125}$$

$$\Omega_p + c_1\sqrt{\frac{I_q^0}{I_p^0}}\cos(\theta_p^0 + \theta_q^0) = c_2^i I_p^0 + c_3^i I_q^0 \tag{4.126}$$

$$d_1\sqrt{\frac{I_p^0}{I_q^0}}\sin(\theta_p^0 + \theta_q^0) = d_2^r I_q^0 + d_3^r I_p^0 \tag{4.127}$$

$$\Omega_q + d_1\sqrt{\frac{I_p^0}{I_q^0}}\cos(\theta_p^0 + \theta_q^0) = d_2^i I_q^0 - d_3^i I_p^0 \tag{4.128}$$

Eliminating $\sin(\theta_p^0 + \theta_q^0)$ from (4.125) and (4.127), we obtain

$$d_1\sqrt{\frac{I_p^0}{I_q^0}}(c_2^r I_p^0 + c_3^r I_q^0) = c_1\sqrt{\frac{I_q^0}{I_p^0}}(d_2^r I_q^0 + d_3^r I_p^0) \tag{4.129}$$

which can be rewritten as

$$c_2^r R_0^2 + \left(c_3^r - \frac{c_1}{d_1}d_3^r\right)R_0 - \frac{c_1}{d_1}d_2^r = 0 \tag{4.130}$$

which is independent of Ω_p and Ω_q, hence of Ω. We have introduced the amplitude ratio

$$R_0 = \frac{I_p^0}{I_q^0}. \tag{4.131}$$

The above quadratic equation can be solved to get

$$R_0 = \frac{\frac{c_1}{d_1} d_3^r - c_3^r \pm \sqrt{\left(c_3^r - \frac{c_1}{d_1} d_3^r\right)^2 + 4\frac{c_1}{d_1} c_2^r d_2^r}}{2c_2^r}$$

For example, in case $p = 0$, $q = 1$,

$$R_0 = -0.3829, \quad \text{or} \quad R_0 = 0.3283.$$

Obviously, only the positive $R_0 = 0.3283$ is the acceptable root. Thus detuning does not affect the ratio of the two edge wave amplitudes. Similarly, in Case (2): $p = 0$, $q = 2$, $R_0 = 0.2950$ is the acceptable root. And in Case (3): $p = 1$, $q = 2$, $R_0 = 0.5369$ is the acceptable root.

For a complete solution of the fixed point, we need another equation with respect to I_p^0 and I_q^0 besides (4.130). We add (4.125) to (4.127) to get

$$\left[c_1\sqrt{\frac{I_q^0}{I_p^0}} + d_1\sqrt{\frac{I_p^0}{I_q^0}}\right] \sin(\theta_p^0 + \theta_q^0) = c_2^r I_p^0 + c_3^r I_q^0 + d_2^r I_q^0 + d_3^r I_p^0 \tag{4.132}$$

and add (4.126) to (4.128) to get

$$\left[c_1\sqrt{\frac{I_q^0}{I_p^0}} + d_1\sqrt{\frac{I_p^0}{I_q^0}}\right] \cos(\theta_p^0 + \theta_q^0) = c_2^i I_p^0 + c_3^i I_q^0 + d_2^i I_q^0 - d_3^i I_p^0 - \Omega \tag{4.133}$$

Eliminating the trigonometric functions $\sin(\theta_p^0 + \theta_q^0)$ and $\cos(\theta_p^0 + \theta_q^0)$ from (4.132) and (4.133), we get

$$\left[c_1\sqrt{\frac{I_q^0}{I_p^0}} + d_1\sqrt{\frac{I_p^0}{I_q^0}}\right]^2 = \left(c_2^i I_p^0 + c_3^i I_q^0 + d_2^i I_q^0 - d_3^i I_p^0 - \Omega\right)^2 + \left(c_2^r I_p^0 + c_3^r I_q^0 + d_2^r I_q^0 + d_3^r I_p^0\right)^2 \tag{4.134}$$

which can be manipulated to get a quadratic equation for I_q^0 in standard form

$$a(I_q^0)^2 + bI_q^0 + c = 0 \tag{4.135}$$

with the coefficients depending on R_0,

$$a = \left[\left(c_2^i - d_3^i\right) R_0 + c_3^i + d_2^i\right]^2 + \left[\left(c_2^r + d_3^r\right) R_0 + c_3^r + d_2^r\right]^2 \tag{4.136}$$

$$b = -2\Omega \left[\left(c_2^i - d_3^i\right) R_0 + c_3^i + d_2^i\right] \tag{4.137}$$

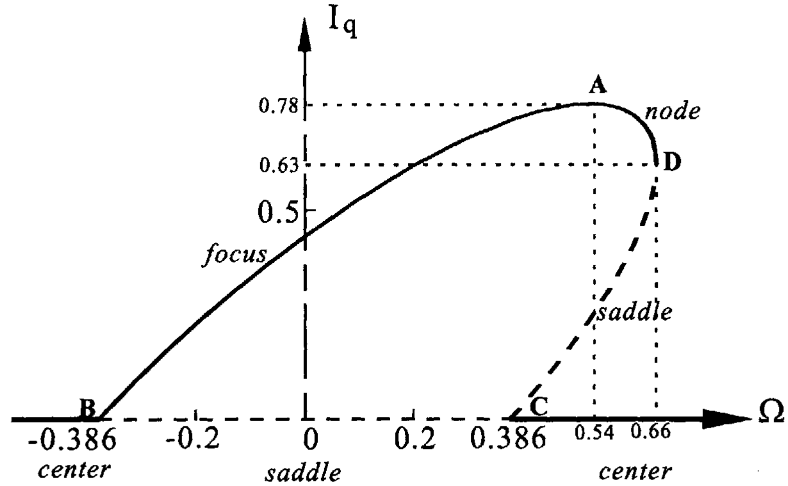

Figure 4-2: Equilibrium branches of I_q^0 v.s. Ω–$p=0$, $q=1$.

$$c = \Omega^2 - \left(c_1/\sqrt{R_0} + d_1\sqrt{R_0}\right)^2 \tag{4.138}$$

Therefore, at dynamic equilibrium

$$I_q^0 = \frac{-b \pm \sqrt{b^2 - 4ac}}{2a} \tag{4.139}$$

Only the positive I_q^0 is of our interest. From (4.139) we see that $I_q^0 = 0$ if and only if $c = 0$, i.e.

$$\Omega^2 = \left(c_1/\sqrt{R_0} + d_1\sqrt{R_0}\right)^2 \Rightarrow \Omega = \pm\left(c_1/\sqrt{R_0} + d_1\sqrt{R_0}\right) \tag{4.140}$$

For Case (1): $p = 0$, $q = 1$, substituting $R_0 = 0.3283$ along with the known coefficients c's and d's from Table 4.8, into (4.136), (4.137) and (4.138), we get

$$a = 0.7163, \quad b = -1.3746\Omega, \quad c = \Omega^2 - 0.1490$$

Therefore, $I_q^0 = 0$ when $\Omega = \pm 0.386$ from (4.140) and the equilibrium branches of finite I_q^0 v.s. Ω are plotted in Figure 4-2. Similar feature is observed for Case (2): $p = 0$, $q = 2$ and Case (3): $p = 1$, $q = 2$, whose equilibrium branches are plotted in Figure 4-3 and Figure 4-4 respectively. The inclination of the curve depends on the sign of the coefficient in b. In case $p = 0$, $q = 2$, $b = 0.7811\Omega$. In case $p = 1$, $q = 2$, $b = 1.2388\Omega$.

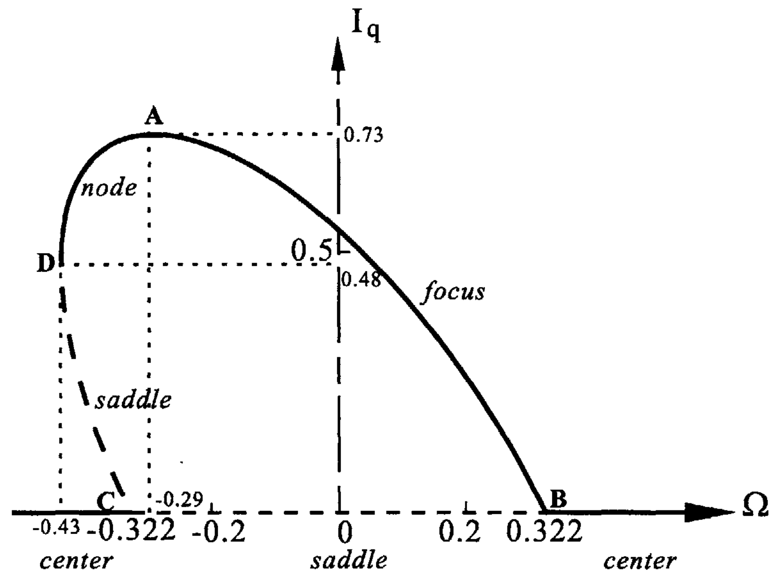

Figure 4-3: Equilibrium branches of I_q^0 v.s. Ω–$p = 0$, $q = 2$.

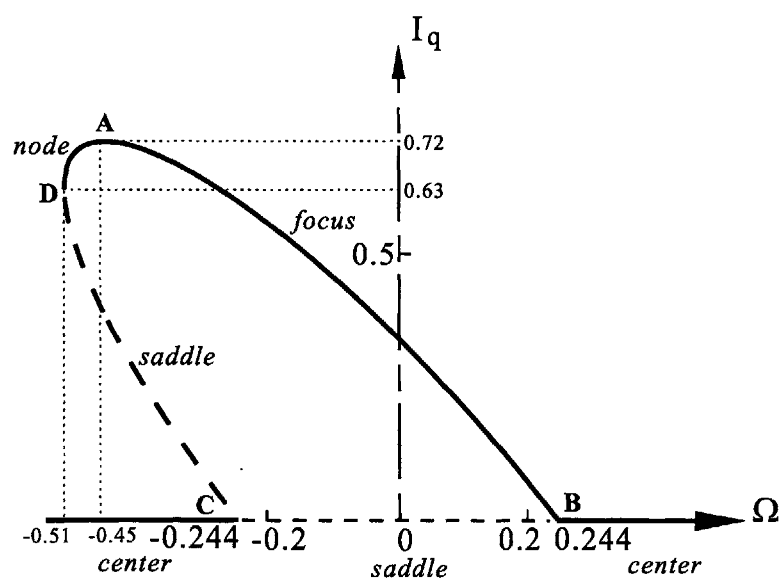

Figure 4-4: Equilibrium branches of I_q^0 v.s. Ω–$p = 1$, $q = 2$.

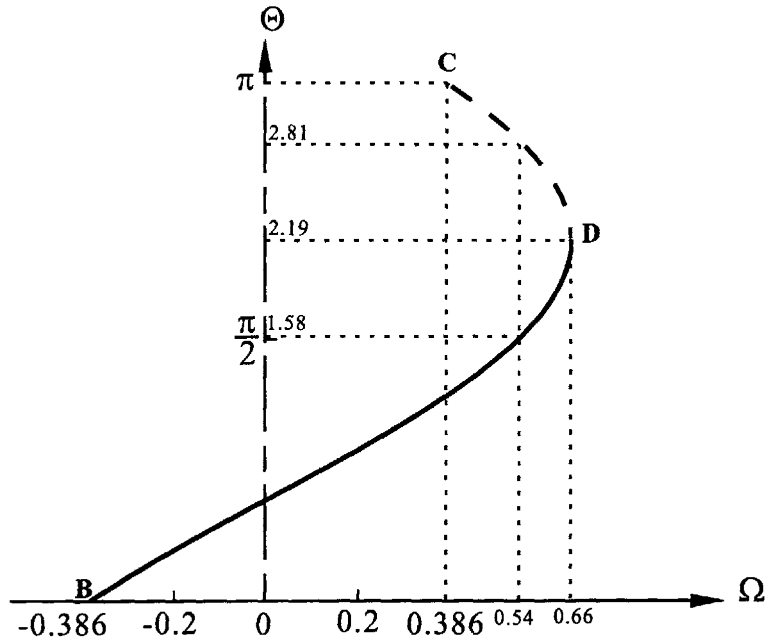

Figure 4-5: Equilibrium branches of Θ^0 v.s. Ω. The solid line represents the stable equilibrium branch and the dot line represents the unstable branch.

Notice that (4.133) can be manipulated to obtain

$$\theta_p^0 + \theta_q^0 = \arccos\left(\frac{c_2^i I_p^0 + c_3^i I_q^0 + d_2^i I_q^0 - d_3^i I_p^0 - \Omega}{c_1\sqrt{\frac{I_q^0}{I_p^0}} + d_1\sqrt{\frac{I_p^0}{I_q^0}}}\right) \tag{4.141}$$

After I_p^0 and I_q^0 are found, we can substitute them into (4.141) to get $\Theta^0 = \theta_p^0 + \theta_q^0$. The curve of Θ^0 v.s. Ω is shown in Figure 4-5.

Upon substitution of (I_p^0, I_q^0, Θ^0) into (4.126) and (4.128), we obtain Ω_p^0 and Ω_q^0 respectively

$$\Omega_p^0 = c_2^i I_p^0 + c_3^i I_q^0 - c_1\sqrt{\frac{I_q^0}{I_p^0}}\cos(\theta_p^0 + \theta_q^0) \tag{4.142}$$

$$\Omega_q^0 = d_2^i I_q^0 - d_3^i I_p^0 + d_1\sqrt{\frac{I_p^0}{I_q^0}}\cos(\theta_p^0 + \theta_q^0) \tag{4.143}$$

The curves of Ω_p^0 and Ω_q^0 v.s. Ω are plotted in Figure 4-6. These two values are the angular speed of the limit cycles. The corresponding edge waves are

$$B_p^0 = \sqrt{I_p^0}e^{i\theta_p^0}e^{-i\left(\omega_p+\bar{\epsilon}^2\Omega_p^0\right)t}; \quad B_q^0 = \sqrt{I_q^0}e^{i\theta_q^0}e^{-i\left(\omega_q+\bar{\epsilon}^2\Omega_q^0\right)t} \tag{4.144}$$

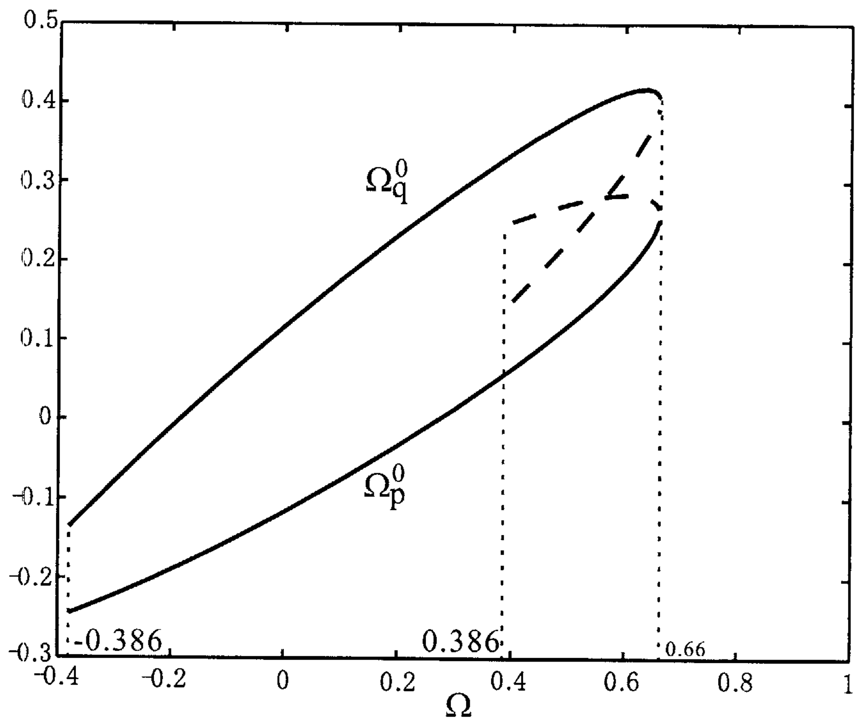

Figure 4-6: Detuning of the two edge wave modes Ω_p^0 and Ω_q^0 v.s. Ω, i.e. the detuning of the incident wave. The solid lines represent the stable equilibrium branch and the dot lines represent the unstable branch.

due to the change of variables in (4.99).

From the above analysis we see that Ω_p and Ω_q must take particular values Ω_p^0 and Ω_q^0 according to (4.142) and (4.143) so that a fixed point for $\bar{B}_p$ and $\bar{B}_q$ can exist. Particularly under perfect resonance, i.e. $\Omega = 0$, we get $\Omega_p^0 = -0.1166$ from (4.142) and $\Omega_q^0 = 0.1166$ from (4.143). From (4.144) we know that

$$\frac{d\theta_j}{d\tau} = -\Omega_j^0, \quad j = p,\ q. \tag{4.145}$$

Therefore, the fixed point of $\bar{B}_p$ and $\bar{B}_q$ corresponds to two limit cycles for B_p and B_q, rotating at the speed of $-\Omega_p^0$ and $-\Omega_q^0$ respectively.

The only thing uncertain is about the equilibrium phase angle θ_p^0 and θ_q^0. We only know the sum of the two, i.e. $\Theta^0 = \theta_p^0 + \theta_q^0$. A direct numerical simulation shows that at equilibrium θ_p^0 and θ_q^0 are not fixed and vary with initial condition. For instance, when detuning $\Omega = 0$, we choose $\Omega_p = \Omega_p^0 = -0.1166$ and $\Omega_q = \Omega_q^0 = 0.1166$ so that a fixed point exists. For this special choice, we allow the dynamical system (4.116) to (4.119) to evolute enough time to reach the steady state. With different initial conditions, we can observe the phase angle θ_p^0 and θ_q^0. Listed in Table 4.9 are several of our records. And the corresponding curves are plotted in Figure 4-7.

Table 4.9: The steady state phase angles θ_p^0 and θ_q^0— $(p = 0, q = 1)$.

$(I_p(0),\ \theta_p(0),\ I_q(0),\ \theta_q(0))$	θ_p^0	θ_q^0	$\Theta^0 = \theta_p^0 + \theta_q^0$	Line in Figure 4-7
(0.01,0.01,0.01,0.01)	-1.6760	2.2990	0.6230	dash-dot
(0.21,0.01,0.21,0.01)	-1.1347	1.7576	0.6229	solid
(0.01,0.21,0.01,0.21)	-1.5274	2.1505	0.6230	dash

4.9.2 Numerical verification for the existence of limit cycles

We define limit cycle by $\dot{I}_p = \dot{I}_q = 0$, and $\dot{\theta}_p + \dot{\theta}_q = 0$ rather than $\dot{\theta}_p = 0$ and $\dot{\theta}_q = 0$ as in the fixed point solution. One of the simplest solution to $\dot{\theta}_p + \dot{\theta}_q = 0$ is $\dot{\theta}_p = -\dot{\theta}_q = \hat{\Omega}$, which means that two phase variables change at constant rate, but in the opposite way. With I_p and I_q being constant, two limit cycles are formed.

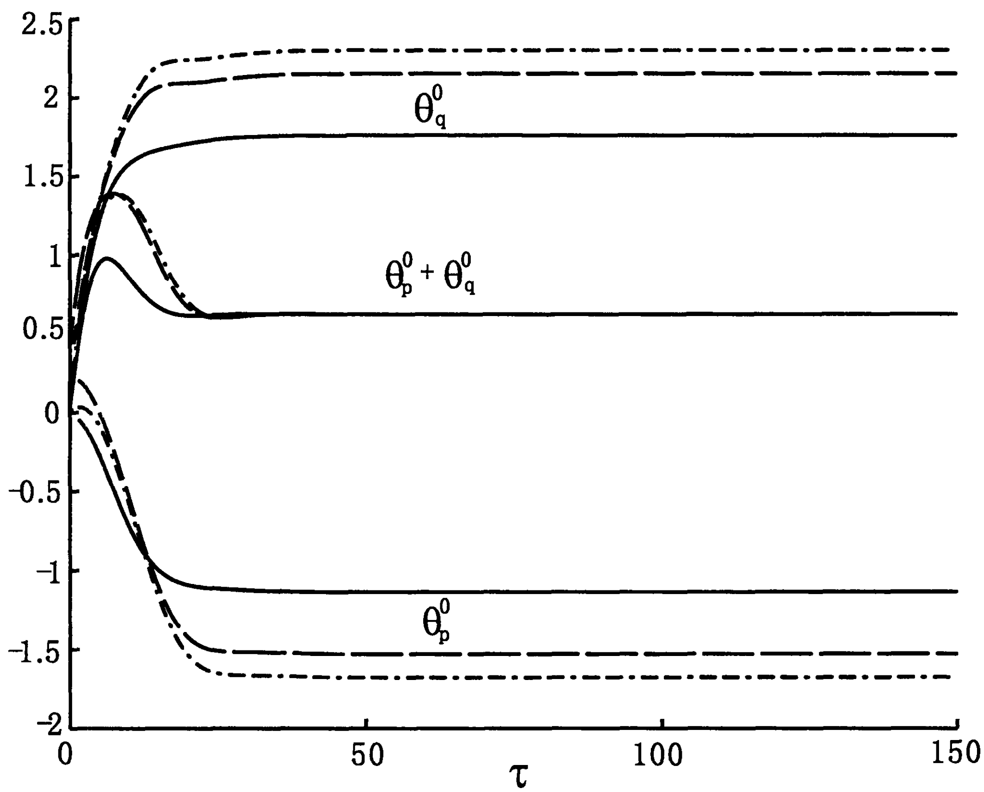

Figure 4-7: Phase angles evolution curves for $\Omega = 0$. $\Omega_p = -0.1166$ and $\Omega_q = 0.1166$.

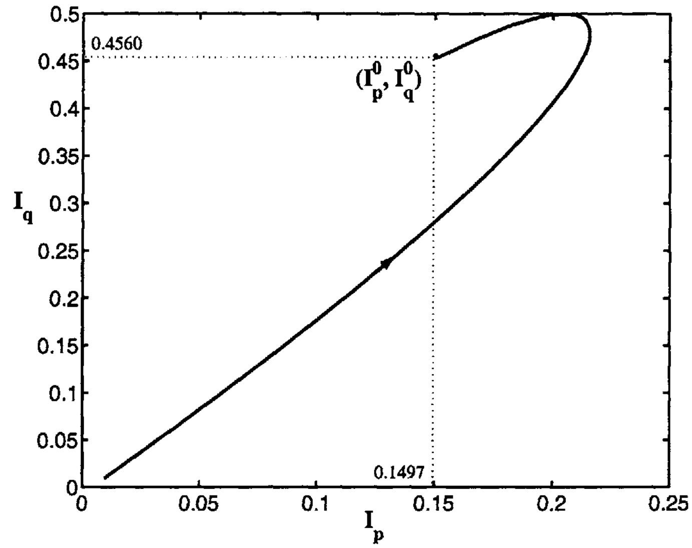

Figure 4-8: Flow map (I_p,I_q) for fixed point (I_p^0,I_q^0)=(0.1497, 0.4560) — ($p = 0, q = 1$).

For the perfect resonance case $\Omega = 0$, we do not introduce Ω_p or Ω_q, i.e. $B_j \equiv \bar{B}_j$, $j = p, q$. A simple numerical simulation of the full nonlinear ODE's (4.116) to (4.119) with $\Omega_p = \Omega_q = 0$ confirms that the dynamical system is attracted to two stable limit cycles, which correspond to the two edge waves amplitudes B_p and B_q. Shown in Figure 4-8 is the flow map projected on the (I_p,I_q) plane with a starting point (I_p, θ_p, I_q, θ_q)=(0.01,0.01,0.01,0.01) with $\Omega = 0$. It converges to equilibrium point (I_p^0,I_q^0)=(0.1497, 0.4560).

From (4.112), we get

$$Re\{B_j\} = \sqrt{I_j}\cos\theta_j, \quad Im\{B_j\} = \sqrt{I_j}\sin\theta_j$$

In the complex plane, we plot in Figure 4-9 the trajectories of ($Re\{B_p\}$, $Im\{B_p\}$) and ($Re\{B_q\}$, $Im\{B_q\}$) respectively. Two limit cycles are revealed, where $B_p^0 = \sqrt{I_p^0} = 0.387$ and $B_q^0 = \sqrt{I_q^0} = 0.675$

From Figure 4-9 we can see that the trajectories rotate in opposite direction as they approach the two limit cycle, meaning that two phase variables vary in opposite way, one increases, another decreases (In this case, θ_p is increasing, while θ_q is decreasing!). When they vary in the same rate so that $\dot{\theta}_p + \dot{\theta}_q = 0$, the steady state is reached and $\theta_p^0 + \theta_q^0 = \Theta^0 = \text{Const}$. (See Figure 4-10.). In this case, we detected a steady state

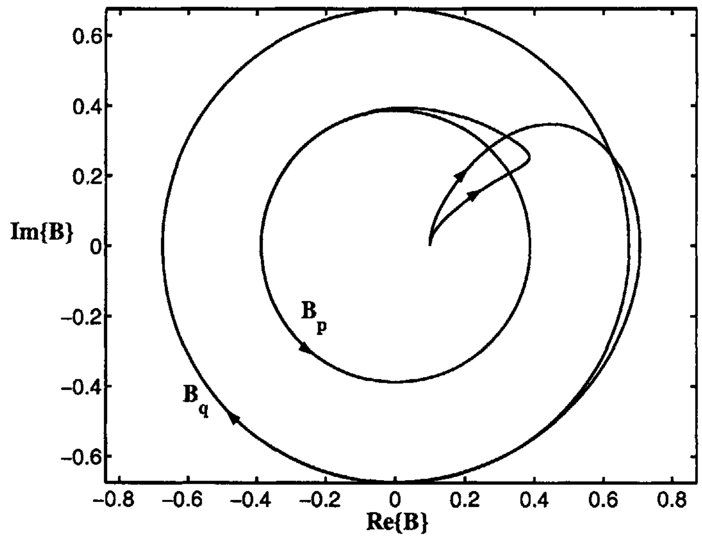

Figure 4-9: Two limit cycles corresponding to two edge wave amplitudes with $\Omega = 0$ ($p = 0, q = 1$). The inner circle is B_p, the outer is B_q.

rotation speed $\dot{\theta}_p = 0.1166$ and $\dot{\theta}_q = -0.1166$, which confirm that $\Omega_p^0 = -0.1166$ and $\Omega_q^0 = 0.1166$ in (4.145) are the condition for the dynamical system $\bar{B}_p$, $\bar{B}_q$ having a non-trivial fixed point. We also found that $\Theta^0 = 0.6230$, which is identical to the one listed in Table 4.9.

Similarly, we carry out the analysis for Case (2): $p = 0, q = 2$ and Case (3): $p = 1, q = 2$. The two limit cycles with $\Omega = 0$ are plotted in Figure 4-11 and 4-12 respectively.

4.9.3 Physical implication of the equilibrium

In order to see the effect of the two edge wave modes competition, we substitute the steady state B_j back into (4.23)

$$\psi_{0j} = -i\frac{|\bar{B}_j^0|}{\omega_j}e^{i(\theta_j^0 - \Omega_j^0\tau)}e^{-x}L_j(2x)\cos y = -i\frac{|\bar{B}_j^0|}{\omega_j}e^{i\theta_j^0}e^{-i\bar{\epsilon}^2\Omega_j^0 t}e^{-x}L_j(2x)\cos y, \quad j = p,\ q. \tag{4.146}$$

where $\dot{\theta}_j = -\Omega_j^0$ is the constant rate of the phase variation of the edge wave at equilibrium. Note that phase of B_j varies with slow time τ with $\tau = \bar{\epsilon}^2 t$. Therefore the two edge waves have slight amount of frequency shift $\bar{\epsilon}^2\Omega_j^0$ like detuning. In order

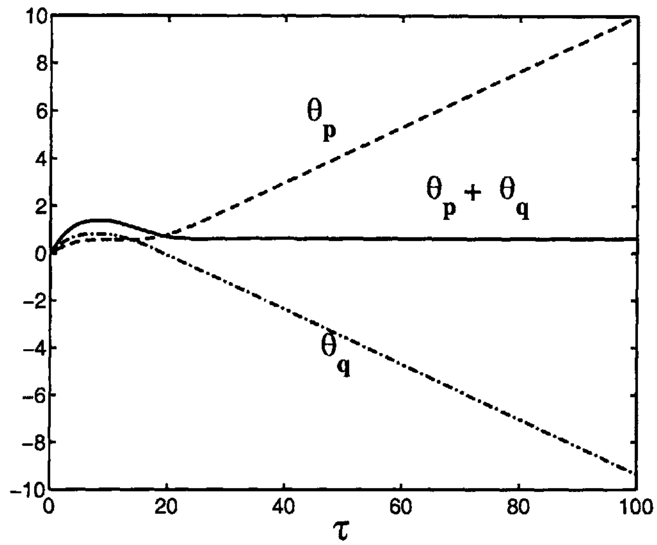

Figure 4-10: Phase angles evolution curves for $\Omega = 0$. $\Omega_p = \Omega_q = 0$.

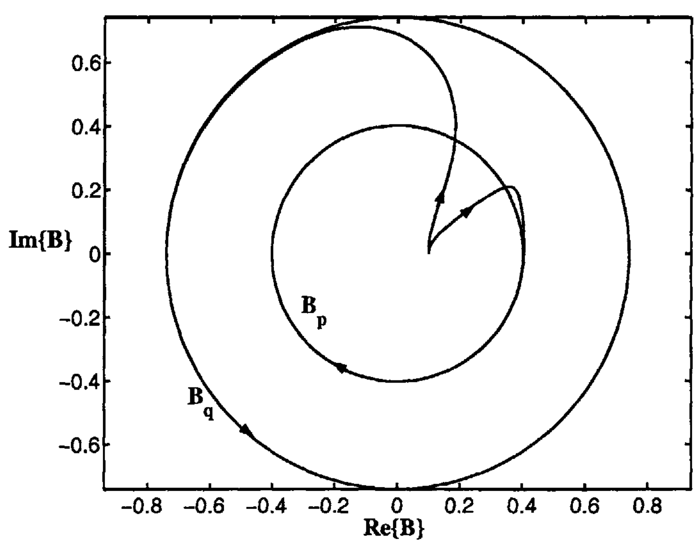

Figure 4-11: Two limit cycles corresponding to two edge wave amplitudes with $\Omega = 0$ ($p = 0, q = 2$). The inner circle is B_p, the outer is B_q.

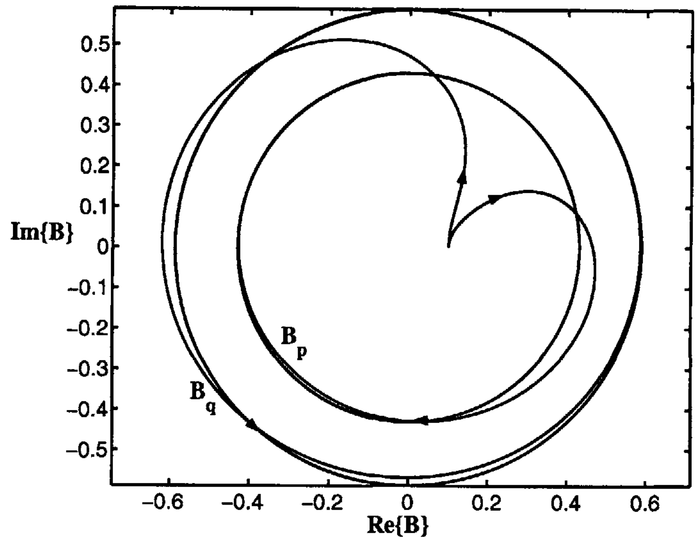

Figure 4-12: Two limit cycles corresponding to two edge wave amplitudes with $\Omega = 0$ $(p = 1, q = 2)$. The inner circle is B_p, the outer is B_q.

to see the visual picture of the free surface elevation as steady state is reached, we add the two edge wave modes together and take the real part to get

$$\begin{aligned} &\zeta_{tot} \\ = \;& \zeta_p + \zeta_q \\ = \;& e^{-x}\cos y\left\{|\bar{B}_p^0|L_p(2x)\cos\left[(\omega_p + \bar{\epsilon}^2\Omega_p^0)t\right] + |\bar{B}_q^0|L_q(2x)\cos\left[(\omega_q + \bar{\epsilon}^2\Omega_q^0)t - \Theta^0\right]\right\} \end{aligned} \tag{4.147}$$

where we have set $\theta_p^0 = 0$ without loss of generality. Hence $\theta_q^0 = \Theta^0$. Use has been made of the free surface boundary condition (4.15).

Recall at the equilibrium for case $p = 0, q = 1$ with zero detuning, the two amplitudes of the edge waves are $|\bar{B}_p^0| = 0.387$ and $|\bar{B}_q^0| = 0.675$. The phases of the two modes are interlocked in the way that $\Omega_p^0 = -0.1166$ while $\Omega_q^0 = 0.1166$, so that $\Theta^0 = \theta_p^0 + \theta_q^0 = 0.623$. Then the instantaneous surface profile is plotted according to (4.147) as shown in Figure 4-13, where $\omega_p = 1$, $\omega_q = \sqrt{3}$, $L_p(2x) = 1$, $L_q(2x) = 1 - 2x$ and we have discarded the detuning Ω_p^0 and Ω_q^0.

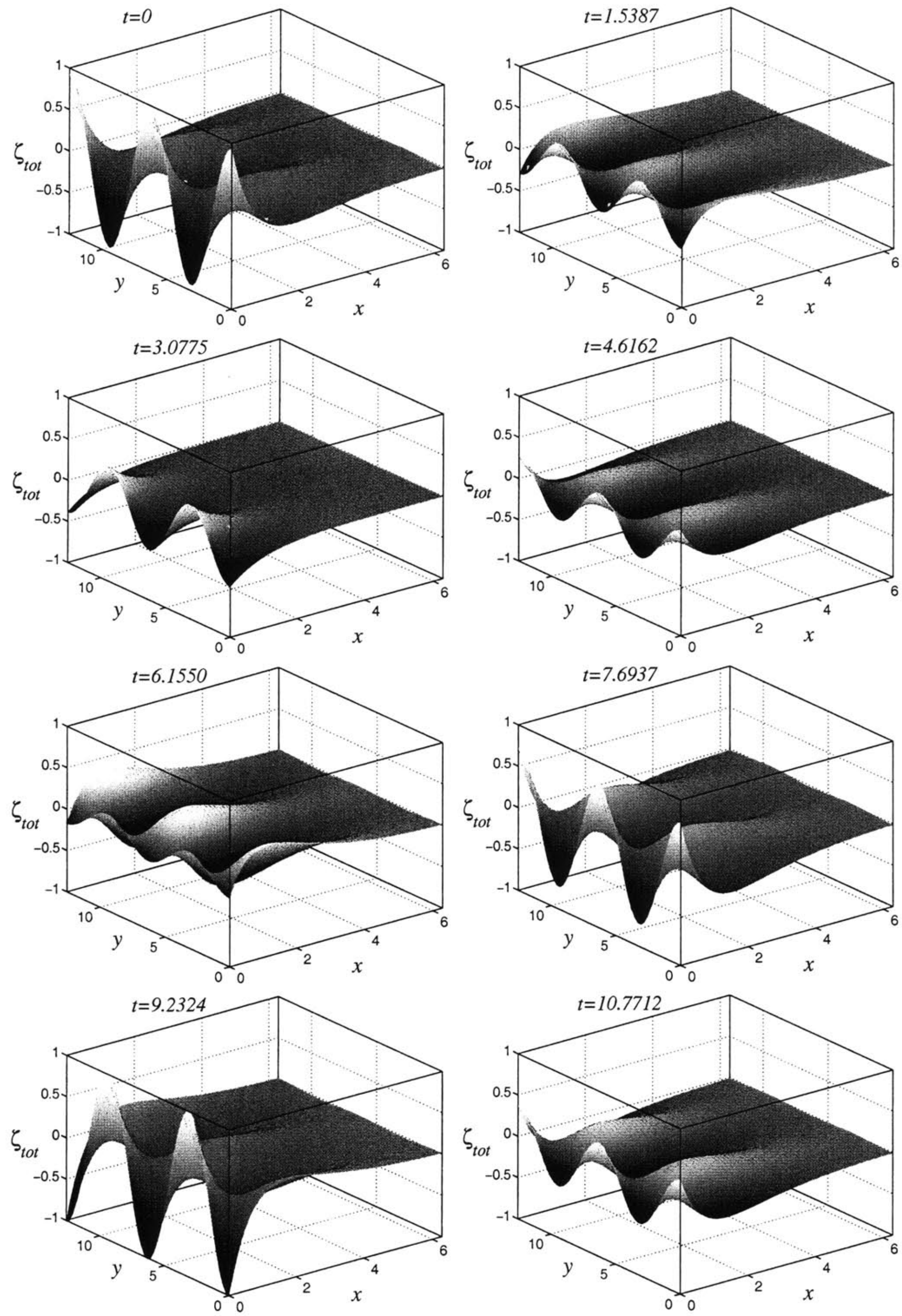

Figure 4-13: The instantaneous surface elevation by addition of two edge wave modes as steady state is reached ($p = 0, q = 1$).

4.9.4 Local stability of limit cycles

The stability of the limit cycles for B_p, B_q is the stability of the fixed point for $\bar{B}_p$, $\bar{B}_q$. In order to analyze the stability of the fixed point, we rearrange the equation (4.116) to (4.119) as follows

$$\dot{I}_p = 2c_1\sqrt{I_p I_q}\sin\Theta - 2c_2^r I_p^2 - 2c_3^r I_p I_q \tag{4.148}$$

$$\dot{I}_q = 2d_1\sqrt{I_p I_q}\sin\Theta - 2d_2^r I_q^2 - 2d_3^r I_p I_q \tag{4.149}$$

$$\dot{\Theta} = \Omega + \left(c_1\sqrt{\frac{I_q}{I_p}} + d_1\sqrt{\frac{I_p}{I_q}}\right)\cos\Theta + \left(d_3^i - c_2^i\right) I_p - \left(c_3^i + d_2^i\right) I_q \tag{4.150}$$

where we have introduced $\Theta = \theta_p + \theta_q$ and added together two equations (4.117) and (4.119). The dynamical system is now reduced to 3-D and its equilibrium (I_p^0, I_q^0, Θ^0) is obtained in the last section.

Linearizing the above equations near the fixed point (I_p^0, I_q^0, Θ^0), we obtain

$$\dot{\mathbf{X}} = \mathbf{A}\left(\mathbf{X} - \mathbf{X}_0\right)$$

with

$$\mathbf{X}^T = \left[I_p, I_q, \Theta\right], \quad \mathbf{X}_0^T = \left[I_p^0, I_q^0, \Theta^0\right]$$

and the coefficient matrix $\mathbf{A}$ equal to

$$\begin{matrix} c_1\sqrt{\frac{I_q^0}{I_p^0}}\sin\Theta^0 - 4c_2^r I_p^0 - 2c_3^r I_q^0 & c_1\sqrt{\frac{I_p^0}{I_q^0}}\sin\Theta^0 - 2c_3^r I_p^0 & 2c_1\sqrt{I_p^0 I_q^0}\cos\Theta^0 \\ d_1\sqrt{\frac{I_q^0}{I_p^0}}\sin\Theta^0 - 2d_3^r I_q^0 & d_1\sqrt{\frac{I_p^0}{I_q^0}}\sin\Theta^0 - 4d_2^r I_q^0 - 2d_3^r I_p^0 & 2d_1\sqrt{I_p^0 I_q^0}\cos\Theta^0 \\ \frac{d_1\sqrt{\frac{I_p^0}{I_q^0}} - c_1\sqrt{\frac{I_q^0}{I_p^0}}}{2I_p^0}\cos\Theta^0 - c_2^i + d_3^i & \frac{c_1\sqrt{\frac{I_q^0}{I_p^0}} - d_1\sqrt{\frac{I_p^0}{I_q^0}}}{2I_q^0}\cos\Theta^0 - c_3^i - d_2^i & -(c_1\sqrt{\frac{I_q^0}{I_p^0}} + d_1\sqrt{\frac{I_p^0}{I_q^0}})\sin\Theta^0 \end{matrix}$$

Therefore, by solving the characteristic equation

$$det(\mathbf{A} - \lambda\mathbf{I}) = 0$$

which is a cubic polynomial, we get the eigen value λ.

In order to see the stability of the fixed point, we need to compute the eigen value of above matrix $\mathbf{A}$ for each fixed point. For case $p = 0$, $q = 1$, our numerical computation shows that all the fixed points on branch AD in Figure 4-2 and Figure

4-5 have three real negative eigen values. Therefore, they are stable nodes. The fixed points on branch AB have one real negative eigen value and one pair of imaginary eigen values, whose real parts are also negative. Therefore, this equilibrium branch is stable focus. On the other hand, the fixed points on branch CD have two real negative eigen values and one real positive eigen value, meaning they are unstable saddle nodes. For example, when $\Omega = 0.54$, the stable equilibrium (I_p^0, I_q^0, Θ^0)=(0.2566, 0.7815, 1.5782) (point S in Figure 4-14 and 4-15) on branch AD has eigen values $\lambda_1 = -0.1739$, $\lambda_2 = -0.4204$ and $\lambda_3 = -0.3740$. While the unstable equilibrium (I_p^0, I_q^0, Θ^0)=(0.0837, 0.2548, 2.8096) (point U in Figure 4-14 and 4-15) on branch CD has eigen values $\lambda_1 = 0.1387$, $\lambda_2 = -0.1075$ and $\lambda_3 = -0.3468$. Theoretically, there exist a stable plane spanned by the two stable eigen vectors of the unstable fixed point U. This surface further expands nonlinearly away from U and demarcates the attraction domains of the two stable fixed points: the nontrivial fixed point S and the trivial fixed point at origin. For $\Omega = 0.54$, this surface is plotted in Figure 4-16. The details are given as follows:

For $\Omega = 0.54$, the unstable equilibrium U is located at

$$\mathbf{X}_0 = \begin{bmatrix} 0.0837 \\ 0.2548 \\ 2.8096 \end{bmatrix}.$$

This fixed point has three eigen values $\lambda_1 = 0.1378$, $\lambda_2 = -0.1075$, $\lambda_3 = -0.3468$. The corresponding eigen vectors are:

$$v_1 = \begin{bmatrix} 0.1300 \\ 0.2686 \\ -0.9544 \end{bmatrix}; \quad v_2 = \begin{bmatrix} 0.7527 \\ 0.5225 \\ -0.4004 \end{bmatrix}; \quad v_3 = \begin{bmatrix} 0.1777 \\ 0.2706 \\ 0.9461 \end{bmatrix}.$$

Therefore, near U a stable plane is spanned by two stable eigen vectors v_2 and v_3. We chose dozens of starting points on this surface by different θ_j according to

$$\mathbf{X}_s = \mathbf{X}_0 + \epsilon(r_2 v_2 + r_3 v_3)$$

where $r_2 = \cos\theta_j$, $r_3 = \sin\theta_j$, and refer to Table 4.10 for the θ_j we used in our numerical simulations. We chose small $\epsilon = 0.0008$ to ensure the starting point on

Table 4.10: Parameter θ_j for the starting point and the corresponding backward evolution time t.

θ_j	0.74	0.79	0.795	0.797	0.798	0.7983	0.7984	0.79847
t	-43	-47.5	-49	-50	-50.8	-51	-51	-51
θ_j	0.7985	0.79852	0.798535	0.79855	0.7986	0.7987	0.8	0.85
t	-51	-51	-50.5	-48.7	-46.2	-44.6	-40.3	-31
θ_j	1.5	2.5	3.5	3.78	3.79	3.80	3.81	3.83
t	-23.3	-22.5	-27.3	-39.8	-42	-44	-45	-44.7
θ_j	3.9	4.1	4.5	5.6	0.5	0.738		
t	-41.9	-38.33	-35.4	-33.6	-38	-43		

the stable plane. Then we run the numerical simulation of the nonlinear dynamical system. When we set the evolution time forward (positive t), trajectories diverge along the unstable eigen direction after the confluence at point U, forming the unstable subspace (the heavy line in Figure 4-16). When we set the evolution time backward (negative t), the trajectories diverge and further expand to form a stable subspace (the surface in Figure 4-16). Refer to Table 4.10 for the truncation time of the backward evolution.

More flow maps for several Ω by numerical simulations are plotted in Figure 4-17 to 4-21.

Table 4.11 and Table 4.12 give the full list of the eigen values on the two equilibrium branches.

The point $I_p = I_q = 0$ corresponds to trivial equilibrium, it is convenient to turn to Cartesian coordinate system. Let $\bar{B}_p = x_1 + iy_1$ and $\bar{B}_q = x_2 + iy_2$, then (4.100) and (4.101) can be converted to four real ODEs

$$\dot{x}_1 = -(\Omega_p - \hat{\Omega})y_1 + c_1 y_2 + (c_2^i y_1 - c_2^r x_1)(x_1^2 + y_1^2) + (c_3^i y_1 - c_3^r x_1)(x_2^2 + y_2^2) \quad (4.151)$$

$$\dot{y}_1 = (\Omega_p - \hat{\Omega})x_1 + c_1 x_2 - (c_2^i x_1 + c_2^r y_1)(x_1^2 + y_1^2) - (c_3^i x_1 + c_3^r y_1)(x_2^2 + y_2^2) \quad (4.152)$$

$$\dot{x}_2 = -(\Omega_q + \hat{\Omega})y_2 + d_1 y_1 + (d_2^i y_2 - d_2^r x_2)(x_2^2 + y_2^2) - (d_3^i y_2 + d_3^r x_3)(x_1^2 + y_1^2) \quad (4.153)$$

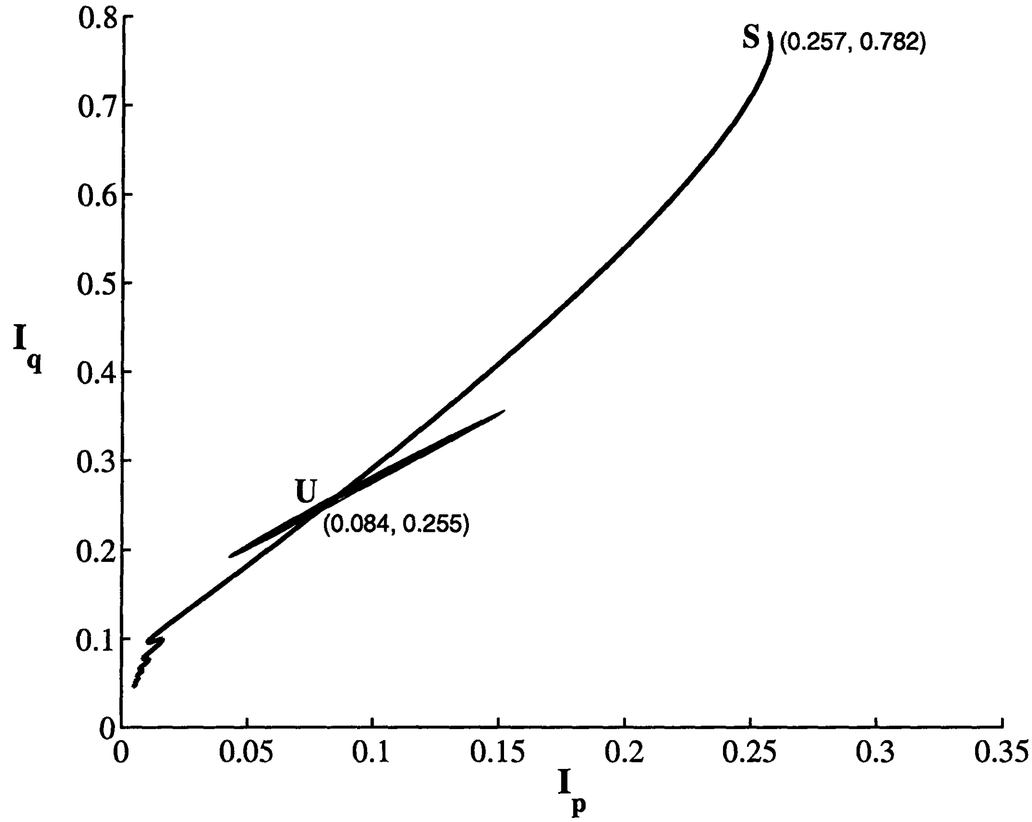

Figure 4-14: Projection of eigen directions of the unstable fixed point U on (I_p, I_q) plane for $\Omega = 0.54$.

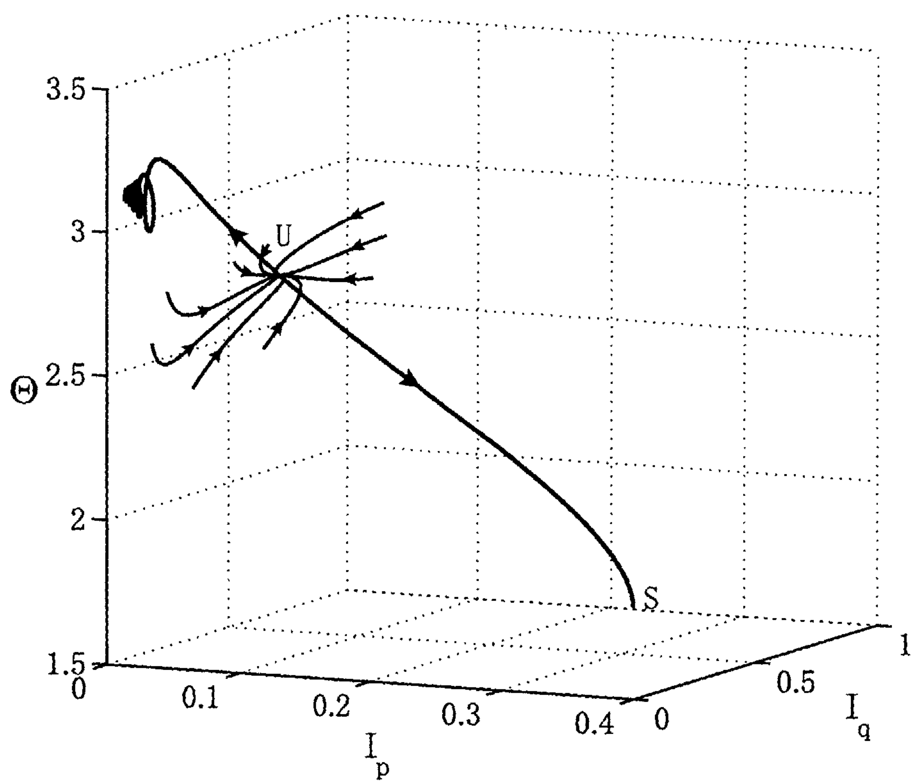

Figure 4-15: The 3D view of the eigen directions of the unstable point U for $\Omega = 0.54$.

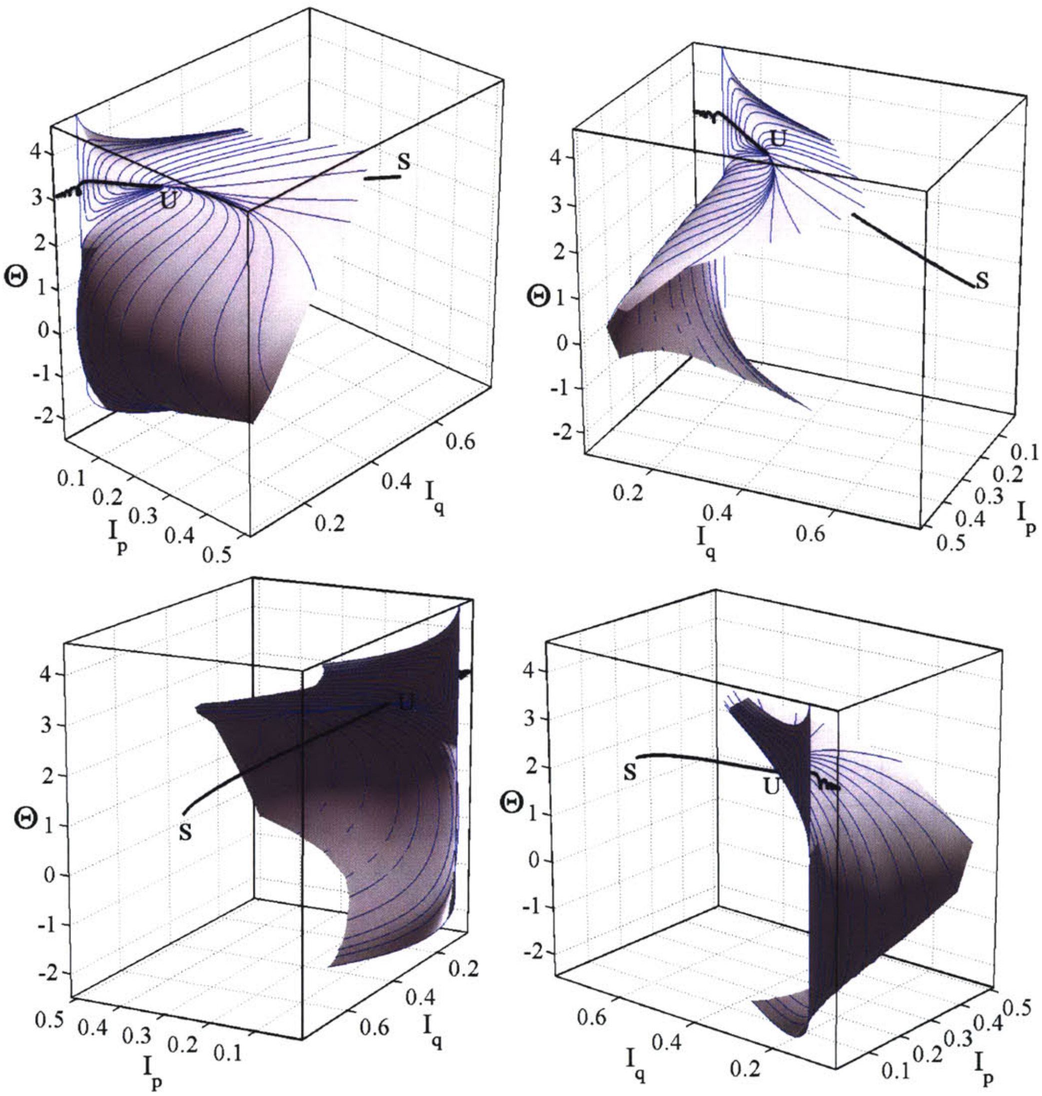

Figure 4-16: The 3D view of the separatix by the unstable fixed point U for $\Omega = 0.54$.

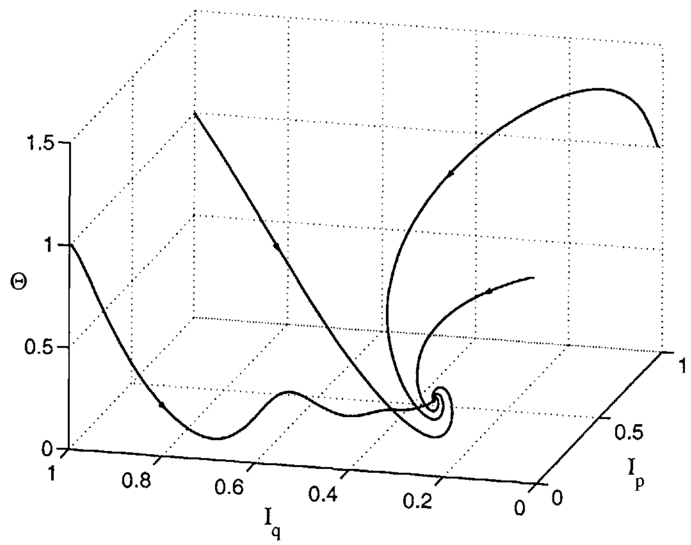

Figure 4-17: Flow map of the nonlinear dynamical system for $\Omega = -0.2$.

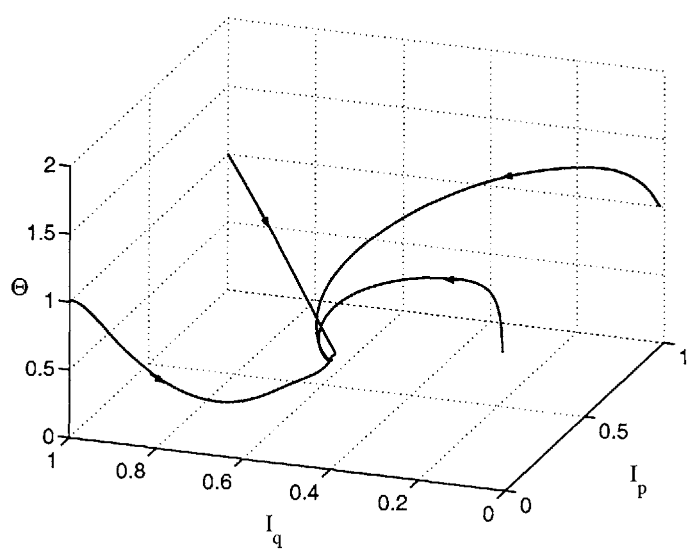

Figure 4-18: Flow map of the nonlinear dynamical system for $\Omega = 0$.

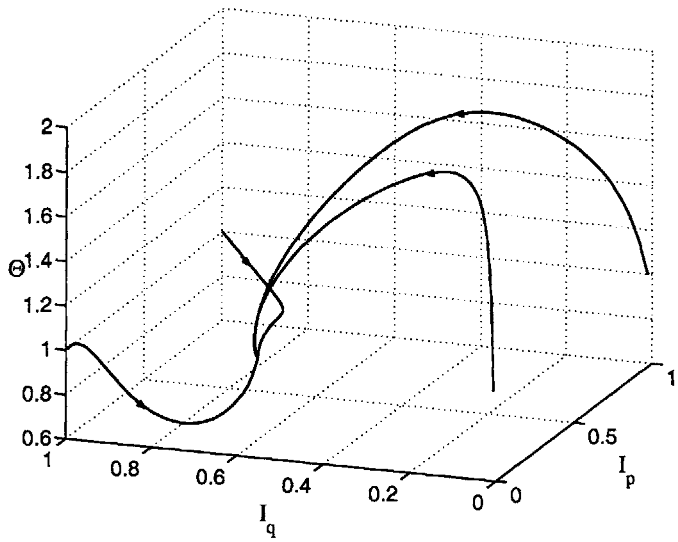

Figure 4-19: Flow map of the nonlinear dynamical system for $\Omega = 0.2$.

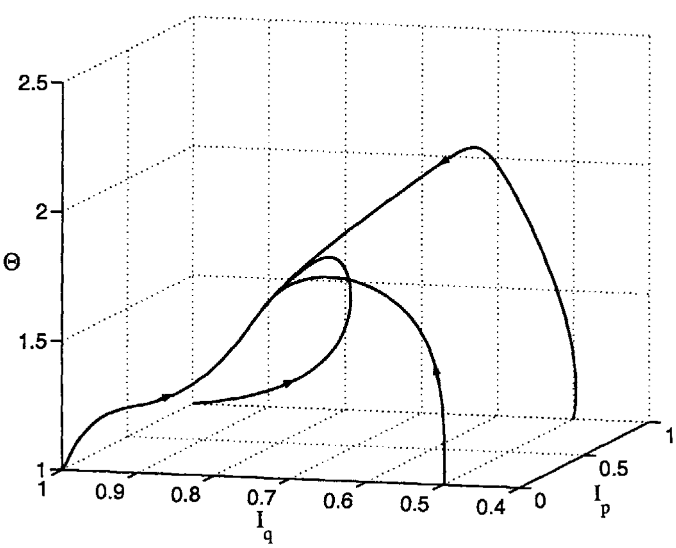

Figure 4-20: Flow map of the nonlinear dynamical system for $\Omega = 0.54$.

Table 4.11: Eigen values for upper nontrivial equilibrium branch BD.

Ω	λ_1	λ_2	λ_3
-0.3800	-0.0004	-0.0052 - 0.1128i	-0.0052 + 0.1128i
-0.3600	-0.0050	-0.0205 - 0.1322i	-0.0205 + 0.1322i
-0.3000	-0.0286	-0.0592 - 0.1746i	-0.0592 + 0.1746i
-0.2400	-0.0545	-0.0933 - 0.2037i	-0.0933 + 0.2037i
-0.1800	-0.0800	-0.1249 - 0.2246i	-0.1249 + 0.2246i
-0.1200	-0.1044	-0.1543 - 0.2395i	-0.1543 + 0.2395i
-0.0600	-0.1275	-0.1819 - 0.2493i	-0.1819 + 0.2493i
0	-0.1493	-0.2079 - 0.2545i	-0.2079 + 0.2545i
0.1000	-0.1823	-0.2475 - 0.2536i	-0.2475 + 0.2536i
0.2000	-0.2105	-0.2829 - 0.2403i	-0.2829 + 0.2403i
0.3000	-0.2317	-0.3143 - 0.2121i	-0.3143 + 0.2121i
0.4000	-0.2385	-0.3435 - 0.1626i	-0.3435 + 0.1626i
0.5000	-0.2043	-0.3800 - 0.0779i	-0.3800 + 0.0779i
0.5200	-0.1900	-0.3887 - 0.0513i	-0.3887 + 0.0513i
0.5300	-0.1821	-0.3930 - 0.0319i	-0.3930 + 0.0319i
0.5360	-0.1772	-0.3955 - 0.0086i	-0.3955 + 0.0086i
0.5400	-0.1739	-0.4204	-0.3740
0.5500	-0.1653	-0.3561	-0.4464
0.5600	-0.1563	-0.3460	-0.4642
0.5800	-0.1373	-0.3326	-0.4914
0.6000	-0.1164	-0.3224	-0.5124
0.6200	-0.0929	-0.3125	-0.5285
0.6400	-0.0643	-0.3002	-0.5390
0.6540	-0.0364	-0.2862	-0.5396
0.6560	-0.0308	-0.2831	-0.5384
0.6580	-0.0243	-0.2792	-0.5365
0.6600	-0.0155	-0.2736	-0.5330

Table 4.12: Eigen values for lower nontrivial equilibrium branch CD.

Ω	λ_1	λ_2	λ_3
0.4000	0.1425	-0.0103	-0.1578
0.4200	0.1466	-0.0242	-0.1852
0.4400	0.1488	-0.0377	-0.2124
0.4600	0.1495	-0.0511	-0.2393
0.4800	0.1488	-0.0646	-0.2660
0.4900	0.1479	-0.0715	-0.2795
0.4920	0.1478	-0.0729	-0.2821
0.4960	0.1473	-0.0757	-0.2875
0.5000	0.1468	-0.0785	-0.2928
0.5200	0.1435	-0.0927	-0.3197
0.5400	0.1387	-0.1075	-0.3468
0.5600	0.1323	-0.1231	-0.3743
0.5800	0.1241	-0.1397	-0.4023
0.6000	0.1133	-0.1577	-0.4312
0.6200	0.0990	-0.1779	-0.4613
0.6400	0.0782	-0.2022	-0.4942
0.6500	0.0625	-0.2179	-0.5128
0.6540	0.0539	-0.2257	-0.5212
0.6560	0.0486	-0.2303	-0.5258
0.6580	0.0421	-0.2358	-0.5310
0.6600	0.0329	-0.2430	-0.5373

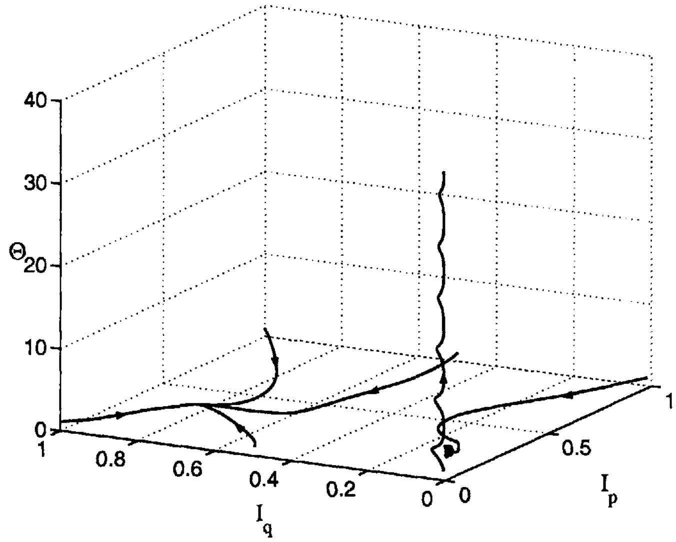

Figure 4-21: Flow map of the nonlinear dynamical system for $\Omega = 0.54$.

$$\dot{y}_2 = (\Omega_q + \hat{\Omega})x_2 + d_1 x_1 - (d_2^i x_2 + d_2^r y_2)(x_2^2 + y_2^2) + (d_3^i x_2 - d_3^r y_2)(x_1^2 + y_1^2) \quad (4.154)$$

The linearized dynamical system around fixed point $(x_1^0, y_1^0, x_2^0, y_2^0) = (0,0,0,0)$ is

$$\begin{pmatrix} \dot{x}_1 \\ \dot{y}_1 \\ \dot{x}_2 \\ \dot{y}_2 \end{pmatrix} = \begin{bmatrix} 0 & -(\Omega_p - \hat{\Omega}) & 0 & c_1 \\ \Omega_p - \hat{\Omega} & 0 & c_1 & 0 \\ 0 & d_1 & 0 & -(\Omega_q + \hat{\Omega}) \\ d_1 & 0 & \Omega_q + \hat{\Omega} & 0 \end{bmatrix} \begin{pmatrix} x_1 \\ y_1 \\ x_2 \\ y_2 \end{pmatrix} \quad (4.155)$$

The characteristic equation $det(\mathbf{A} - \lambda \mathbf{I}) = 0$ leads to

$$\begin{bmatrix} -\lambda & -(\Omega_p - \hat{\Omega}) & 0 & c_1 \\ \Omega_p - \hat{\Omega} & -\lambda & c_1 & 0 \\ 0 & d_1 & -\lambda & -(\Omega_q + \hat{\Omega}) \\ d_1 & 0 & \Omega_q + \hat{\Omega} & -\lambda \end{bmatrix} = 0 \quad (4.156)$$

i.e.

$$\lambda^4 + \left[\left(\Omega_p - \hat{\Omega}\right)^2 + \left(\Omega_q + \hat{\Omega}\right)^2 - 2c_1 d_1\right]\lambda^2 + \left[\left(\Omega_p - \hat{\Omega}\right)\left(\Omega_q + \hat{\Omega}\right) - c_1 d_1\right]^2 = 0$$

which is a quadratic equation for λ^2 and can be rewritten as

$$\lambda^4 + B\lambda^2 + C = 0$$

with abbreviation

$$B = \left[\left(\Omega_p - \hat{\Omega}\right)^2 + \left(\Omega_q + \hat{\Omega}\right)^2 - 2c_1d_1\right]$$

$$C = \left[\left(\Omega_p - \hat{\Omega}\right)\left(\Omega_q + \hat{\Omega}\right) - c_1d_1\right]^2$$

Therefore,

$$\lambda^2 = \frac{-B \pm \sqrt{B^2 - 4C}}{2}$$

- If $B^2 - 4C > 0$, then $\sqrt{B^2 - 4C} < |B|$ since $C > 0$. Therefore,

  i) when $B > 0$, $\sqrt{B^2 - 4C} < B$ and hence $-B \pm \sqrt{B^2 - 4C} < 0$. We have two pair pure imaginary λ's;

  ii) when $B < 0$, $\sqrt{B^2 - 4C} < -B$ and hence $-B \pm \sqrt{B^2 - 4C} > 0$. We have two real and positive λ's and two real and negative λ's;

- If $B^2 - 4C < 0$, then we have one pair complex λ^2's and hence we always have λ with positive real part.

Therefore, we have neutrally stable equilibrium $I_p = I_q = 0$ if and only if $B > 0$ and $B^2 - 4C > 0$.

- For $B^2 - 4C > 0$, we require that

  $$\left[\left(\Omega_p - \hat{\Omega}\right)^2 + \left(\Omega_q + \hat{\Omega}\right)^2 - 2c_1d_1\right]^2 - 4\left[\left(\Omega_p - \hat{\Omega}\right)\left(\Omega_q + \hat{\Omega}\right) - c_1d_1\right]^2 > 0$$

  or

  $$\left\{\left[\left(\Omega_p - \hat{\Omega}\right) + \left(\Omega_q + \hat{\Omega}\right)\right]^2 - 4c_1d_1\right\}\left[\left(\Omega_p - \hat{\Omega}\right) - \left(\Omega_q + \hat{\Omega}\right)\right]^2 > 0$$

  or

  $$\Omega^2 - 4c_1d_1 > 0 \Rightarrow |\Omega| > 2\sqrt{c_1d_1}$$

- For $B > 0$, we require that

  $$\left(\Omega_p - \hat{\Omega}\right)^2 + \left(\Omega_q + \hat{\Omega}\right)^2 - 2c_1d_1 > 0$$

  which leads to

  $$v^2 + (\Omega - v)^2 - 2c_1d_1 > 0 \Rightarrow v^2 - \Omega v + \frac{\Omega^2}{2} - c_1d_1 > 0$$

Since $v = \Omega_p - \hat{\Omega}$ is arbitrary, we require that

$$\Omega^2 - 4\left(\frac{\Omega^2}{2} - c_1 d_1\right) < 0$$

i.e.

$$\Omega^2 > 4c_1 d_1 \Rightarrow |\Omega| > 2\sqrt{c_1 d_1}$$

Therefore, we draw exactly the same conclusions as in Section 4.8.2.

When considering both branches of equilibrium, we found small domains of Ω where both equilibria are stable. In order to see how the dynamical system behaves within that domain, we did some direct numerical simulations. For instance in case $p = 0, q = 1$, we have two small domains at $-0.386 < \Omega < -0.371$ and $0.371 < \Omega < 0.386$.

Shown in Figure 4-22 is the flow map projected on (I_p, I_q) plane for $\Omega = 0.376$. In this simulation, although we chose the starting point (I_p, I_q, Θ)=(0.001, 0.001, 0.01) very close to one of the equilibrium (I_p^0, I_q^0)=(0, 0), the trajectory is attracted by the other equilibrium (I_p^0, I_q^0)=(0.2416, 0.7360) right away. The temporal evolution of I_p and I_q v.s. τ are plotted in Figure 4-23. When we choose a starting point (I_p, I_q, Θ)=(0.00001, 0.00001, 0.1), which is closer to the trivial fixed point than the previous starting point, the trajectory stays close to (I_p^0, I_q^0)=(0, 0) for longer time. But the trajectory is finally attracted by the nontrivial equilibrium as shown in Figure 4-24 and 4-25, where we plot the temporal evolution of I_p and I_q v.s. τ.

For $\Omega = -0.380$ the trajectory shown in Figure 4-26 in the (I_p, I_q) plane stays close to the trivial equilibrium (I_p^0, I_q^0)=(0, 0) with a starting point (I_p, I_q, Θ)=(0.001, 0.001, 0.01). As an alternative, Figure 4-27 and 4-28 show the temporal evolution of I_p and I_q v.s. τ. Since the trivial equilibrium is neutrally stable, the flow map is not attracted to $I_q = 0$, but oscillates at a small distance. In this case the other equilibrium is (I_p^0, I_q^0)=(0.0028, 0.0086). On the other hand, when we choose a starting point (I_p, I_q, Θ)=(0.003, 0.007, 0.1), which is close to the nontrivial fixed point, the trajectory is attracted to (I_p^0, I_q^0)=(0.0028, 0.0086) as shown in Figure 4-29. The numerical simulation also shows a constant slope of 0.58 for the initial development of the two edge wave amplitudes, which confirms the equilibrium state $R_0 = 0.5776$ from (4.124)

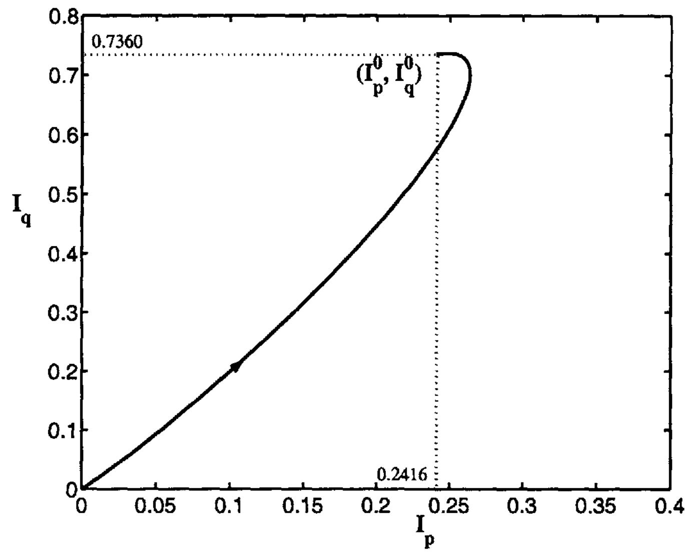

Figure 4-22: Flow map of the nonlinear dynamical system for $\Omega = 0.376$ with a starting point (I_p, I_q, Θ)=(0.001, 0.001, 0.01).

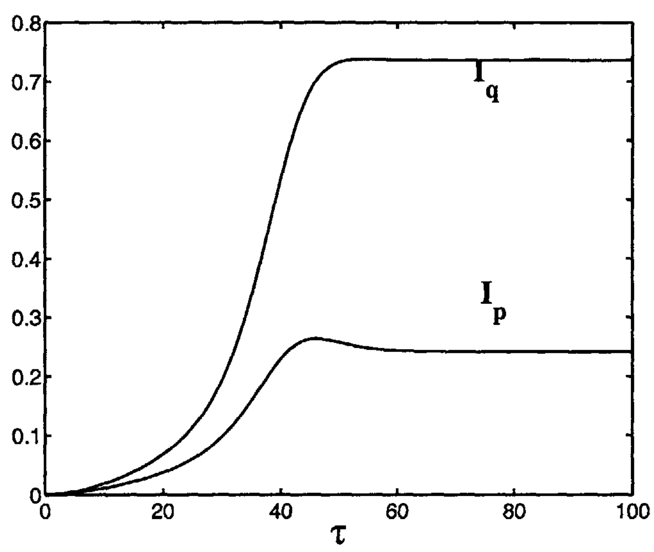

Figure 4-23: Temporal evolution of I_p and I_q v.s. τ for $\Omega = 0.376$ with a starting point (I_p, I_q, Θ)=(0.001, 0.001, 0.01).

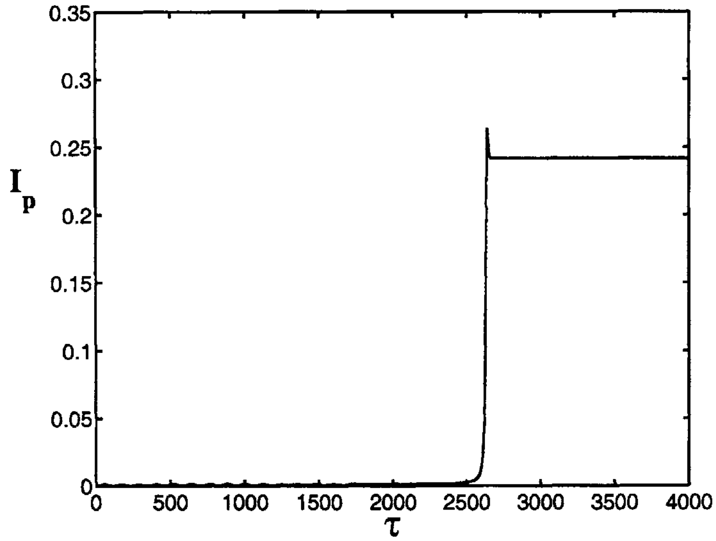

Figure 4-24: Temporal evolution of I_p v.s. τ for $\Omega = 0.376$ with a starting point (I_p, I_q, Θ)=(0.00001, 0.00001, 0.1).

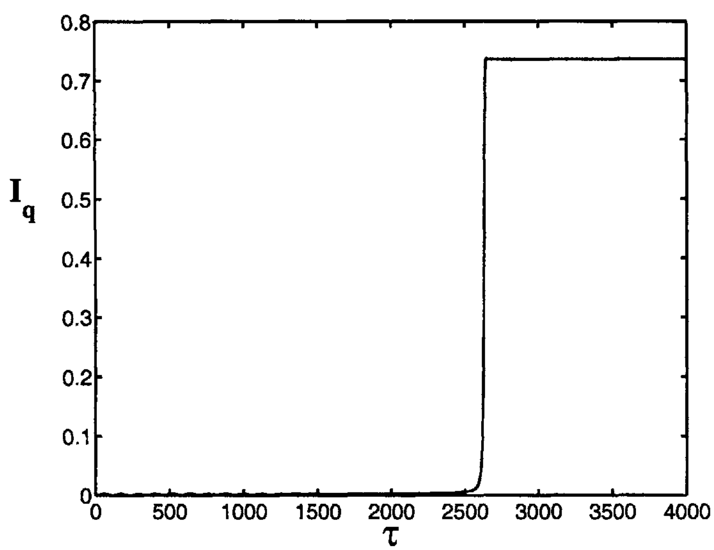

Figure 4-25: Temporal evolution of I_q v.s. τ for $\Omega = -0.380$ with a starting point (I_p, I_q, Θ)=(0.00001, 0.00001, 0.1).

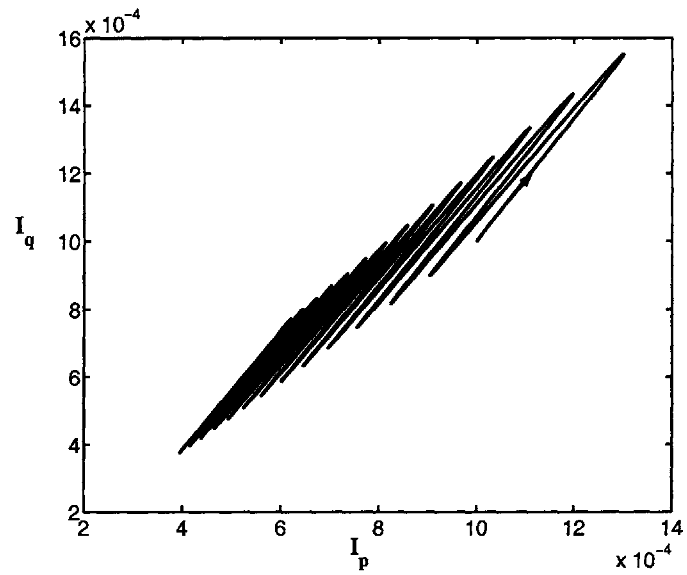

Figure 4-26: Flow map of the nonlinear dynamical system for $\Omega = -0.380$ with a starting point (I_p, I_q, Θ)=(0.001, 0.001, 0.01).

for the initial evolution. Alternatively, we plot the temporal evolution of I_p and I_q v.s. τ in Figure 4-30.

Comparing what happens at $\Omega = 0.376$ and $\Omega = -0.380$, we found that when the nontrivial stable fixed point is far from zero, the attraction is strong. When the nontrivial equilibrium is close to the trivial, the attraction is weak and only shows up when the trajectory is close to it.

Figure 4-31 shows the trajectory in the (I_p, I_q) plane for $\Omega = -0.370$. The flow map is attracted by the only stable equilibrium (I_p^0, I_q^0)=(0.0038, 0.0090) with a starting point (I_p, I_q, Θ)=(0.001, 0.001, 0.01). In this case the trivial equilibrium is unstable.

4.10 Conclusion

1. We dealt with the lower order resonance in this chapter and developed the nonlinear evolution equations governing the two edge wave amplitudes at the third order;

2. We have considered the two edge wave modes sharing same y eigen function,

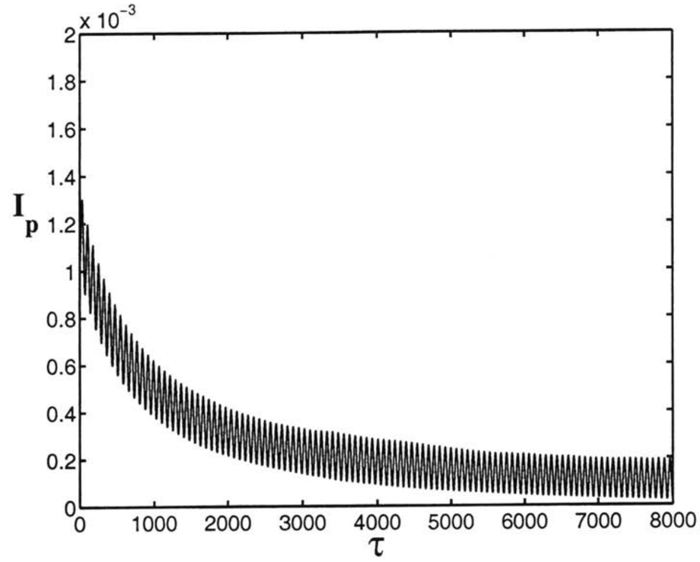

Figure 4-27: Temporal evolution of I_p v.s. τ for $\Omega = -0.380$ with a starting point (I_p, I_q, Θ)=(0.001, 0.001, 0.01).

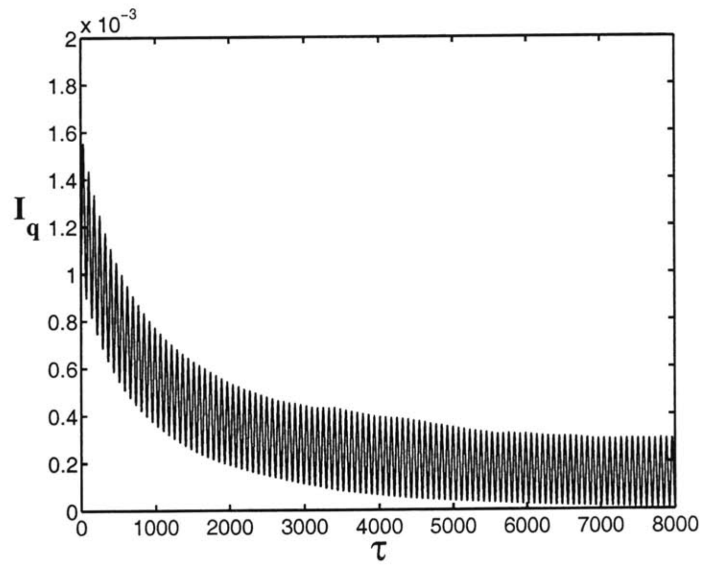

Figure 4-28: Temporal evolution of I_q v.s. τ for $\Omega = -0.380$ with a starting point (I_p, I_q, Θ)=(0.001, 0.001, 0.01).

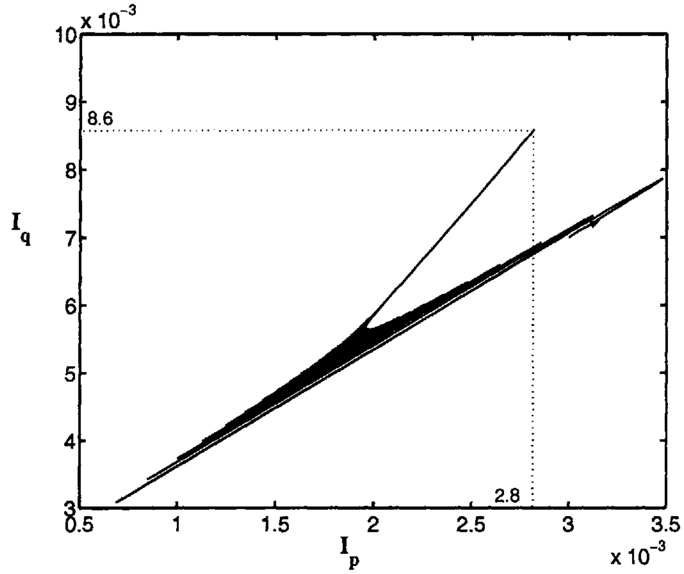

Figure 4-29: Flow map of the nonlinear dynamical system for $\Omega = -0.380$ with a starting point (I_p, I_q, Θ)=(0.003, 0.007, 0.1).

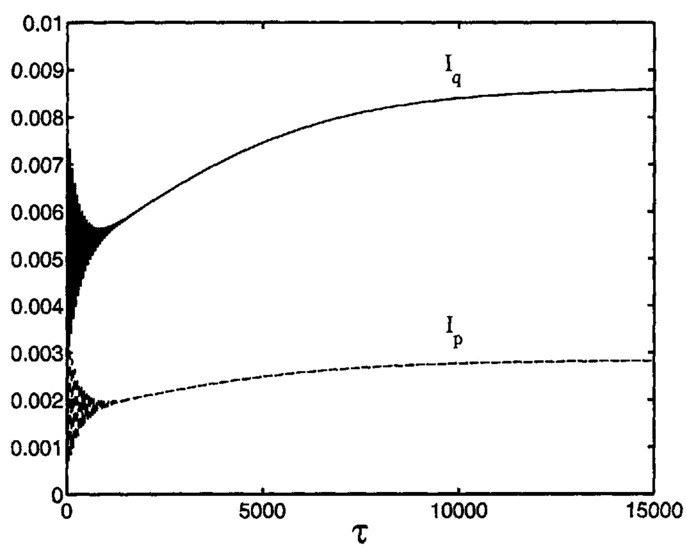

Figure 4-30: Temporal evolution of I_p (dash line) and I_q (solid line) v.s. τ for $\Omega = -0.380$ with a starting point (I_p, I_q, Θ)=(0.003, 0.007, 0.1).

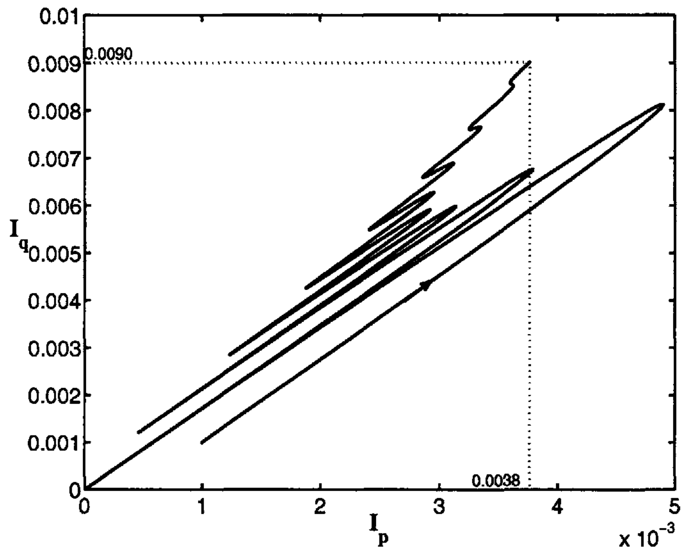

Figure 4-31: Flow map of the nonlinear dynamical system for $\Omega = -0.370$.

which makes the cross resonance possible. The choice of eigen frequency of the incident/reflected wave play a key role in the dynamical system: Unstable under the high frequency incident wave attack, whereas stable under the low frequency attack;

3. Fixed point of the nonlinear system for $\bar{B}_p$ & $\bar{B}_q$ is equivalent to two limit cycles for B_p & B_q. But using a rotation frame as the reference enable us to reduce the four real ODEs to three under the polar coordinate system. The stability of limit cycles is easily analyzed;

4. Detuning of the incident wave does not affect the ratio of the two edge wave amplitudes at equilibrium. But it does change the rotation speed of the limit cycle. Detuning of the incident wave detunes the frequencies of the two edge waves;

5. From the subharmonic resonance analysis we knew that the lower mode of edge wave has a faster initial growth rate. But the two edge waves we considered in this chapter share the same rate of initial growth.

Chapter 5

Other considerations and future works

Other than the nonlinear resonance mechanism discussed in the previous chapters, we have considered two other possibilities for the nonlinear resonance of multiple edge waves. We give the basic idea and some preliminary results in the following two sections. Further work is needed to complete the investigation.

5.1 Competition between two subharmonic edge waves driven by two smaller incident and reflected waves

When we consider two incident/reflected waves, two subharmonic resonance can happen simultaneously. Even though at the initial stage, the two incident waves drive the two edge wave modes separately, nonlinear interaction plays a role soon after either one of them reaches a finite amplitude. Therefore, it is interesting to know what new features these nonlinear terms will provide to the dynamical system. We propose that two edge wave modes are ultimately excited at the first order, by two normally incident waves with eigen frequencies twice those of the two edge waves. The two edge waves are coupled by the third-order nonlinear interaction and therefore it is weak coupling compared with the cross resonance case in Chapter 4, where the coupling is at both the first-order linear terms and third-order nonlinear terms.

The eigen value condition for edge wave is

$$\omega_{nm} = \sqrt{(2n+1)mkgs}\ , \quad n = 0, 1, 2...\ ; \quad m = 1, 2, 3... \tag{5.1}$$

where k is the lowest longshore wave number

$$k = \frac{\pi}{W},$$

with m representing the longshore wave number and n representing the cross-shore mode number, i.e. the corresponding edge wave is

$$\Phi_{nm} = -\frac{igB_{nm}}{\omega_{nm}} e^{-mkx} L_n(2mkx) \cos(mky) e^{-i\omega_{nm}t} + *. \tag{5.2}$$

Please refer to (1.3) and (1.4) for details. Instead of two edge waves having the same y-mode as in classical subharmonic resonance, let's consider two edge waves with different y-mode $0p$ and $0q$ simultaneously, i.e. $(n, m) = (0, p)$ and $(n, m) = (0, q)$

$$\Phi_{0j} = -\frac{igB_j}{\omega_{0j}} e^{-jkx} \cos(jky) e^{-i\omega_{0j}t} + *, \quad j = p, q. \tag{5.3}$$

The eigen value conditions for these two modes are

$$\omega_{0j} = \sqrt{jksg}, \quad j = p, q.$$

After normalization by the lowest mode eigen frequency $\omega_{01} = \sqrt{kgs}$, we get $\omega_{0j}/\omega_{01} = \sqrt{j},\ j = 1, 2, 3....$ In this chapter we consider only the lowest x-mode, i.e. $n = 0$. We assume without loss of generality that $q > p$.

5.1.1 Governing equations

The full version of the nonlinear shallow-water equation is as (2.2) and we use following scales for nondimensionalization:

$$x = kx', \quad y = ky', \quad t = \omega_{01}t', \quad \zeta = \frac{\zeta'}{|\bar{A}|}, \quad \Phi = \frac{\omega_{01}}{|\bar{A}|g}\Phi'$$

where

$$|\bar{A}| = \frac{|\bar{A}_1| + |\bar{A}_2|}{2} \tag{5.4}$$

and $A_1' = \epsilon|\bar{A}_1|e^{i2\varphi_1}$ and $A_2' = \epsilon|\bar{A}_2|e^{i2\varphi_2}$ are one half of the two incident waves amplitudes at shoreline and are taken to be constants. Note that here the definition of $\bar{A}$ is different from the previous cases. Then the same set of dimensionless governing equation as (4.8) is obtained, as well as the small parameter $\bar{\epsilon}$.

$$-\Phi_{tt} + (x\Phi_x)_x + x\Phi_{yy} = \bar{\epsilon}Q(\Phi) + \bar{\epsilon}^2C(\Phi) \tag{5.5}$$

with

$$\bar{\epsilon} = \frac{k|\bar{A}|}{s}$$

and quadratic and cubic nonlinear terms

$$Q(\Phi) = 2\left(\Phi_x\Phi_{xt} + \Phi_y\Phi_{yt}\right) + \Phi_t\left(\Phi_{xx} + \Phi_{yy}\right) \tag{5.6}$$

$$C(\Phi) = \frac{1}{2}\left(\Phi_x^2 + \Phi_y^2\right)\left(\Phi_{xx} + \Phi_{yy}\right) + \Phi_x^2\Phi_{xx} + \Phi_y^2\Phi_{yy} + 2\Phi_x\Phi_y\Phi_{xy} \tag{5.7}$$

The normalized free surface boundary condition becomes

$$\zeta + \frac{\partial\Phi}{\partial t} + \frac{\epsilon}{2}|\nabla\Phi|^2 = 0. \tag{5.8}$$

Using multiple scale expansion similar to the previous chapters, we can derive to get the governing evolution equations

$$\frac{\partial B_p}{\partial\tau} = i\Omega_1 B_p + ia_1|A_1|B_p^* + a_2|B_p|^2B_p - ia_3|B_q|^2B_p \tag{5.9}$$

$$\frac{\partial B_q}{\partial\tau} = i\Omega_2 B_q + ib_1|A_2|B_q^* + b_2|B_q|^2B_q - ib_3|B_p|^2B_q \tag{5.10}$$

where A_1 and A_2 are the normalized incident waves amplitudes and Ω_1 and Ω_2 are their detuning respectively. For example, if $p = 1$, $q = 2$, we get $a_1 = 0.27067$, $a_2 = -0.23016 - 0.18821i$, $a_3 = 0.51753$, $b_1 = 0.76557$, $b_2 = -1.3020 - 1.0647i$, $b_3 = 1.4638i$.

Initially, the two edge waves amplitudes are both small and they grow in different rate independently because they are coupled only by the higher order terms. We distinguish this weak coupling from the strong coupling as the cross resonance case in Chapter 4, where the two edge wave modes share the same initial growth rate.

Replacing B_p and B_q with their polar forms

$$B_p = \sqrt{I_1} e^{i\theta_1}, \quad B_q = \sqrt{I_2} e^{i\theta_2}$$

and further making change of variables

$$J_j = \frac{I_j}{|A_j|}, \quad s_j = \frac{\Omega_j}{|A_j|}, \quad j = 1,\ 2$$

we can rewrite Eqs. (5.9) and (5.9) as

$$\dot{J}_1 = 2|A_1| J_1 \left[a_1 \sin 2\theta_1 - a_2^r J_1\right] \tag{5.11}$$

$$\dot{\theta}_1 = |A_1| \left[a_1 \cos 2\theta_1 + s_1 - a_2^i J_1 - a_3 J_2\right] \tag{5.12}$$

$$\dot{J}_2 = 2|A_2| J_2 \left[b_1 \sin 2\theta_2 - b_2^r J_2\right] \tag{5.13}$$

$$\dot{\theta}_2 = |A_2| \left[b_1 \cos 2\theta_2 + s_2 - b_2^i J_2 - b_3 J_1\right] \tag{5.14}$$

5.1.2 Fixed points

After sufficiently long time evolution, the dynamic system reaches its equilibrium, i.e. $\frac{\partial}{\partial \tau} = 0$. Let the L.H.S. of Equation (5.11) to (5.12) equal to zero, we get

$$J_1 = 0, \quad \text{or} \quad a_1 \sin 2\theta_1 = a_2^r J_1$$

and

$$a_1 \cos 2\theta_1 = a_2^i J_1 + a_3 J_2 - s_1$$

If $J_1 \neq 0$, we can eliminate the θ_1 by recalling the trigonometric identity to get

$$\left(a_2^r J_1\right)^2 + \left(a_2^i J_1 + a_3 J_2 - s_1\right)^2 = a_1^2 \tag{5.15}$$

Similarly, for $J_2 \neq 0$ we can get

$$\left(b_2^r J_2\right)^2 + \left(b_2^i J_2 + b_3 J_1 - s_2\right)^2 = b_1^2 \tag{5.16}$$

Since it is trivial to have both $J_1 = 0$ and $J_2 = 0$, three equilibrium are identified:

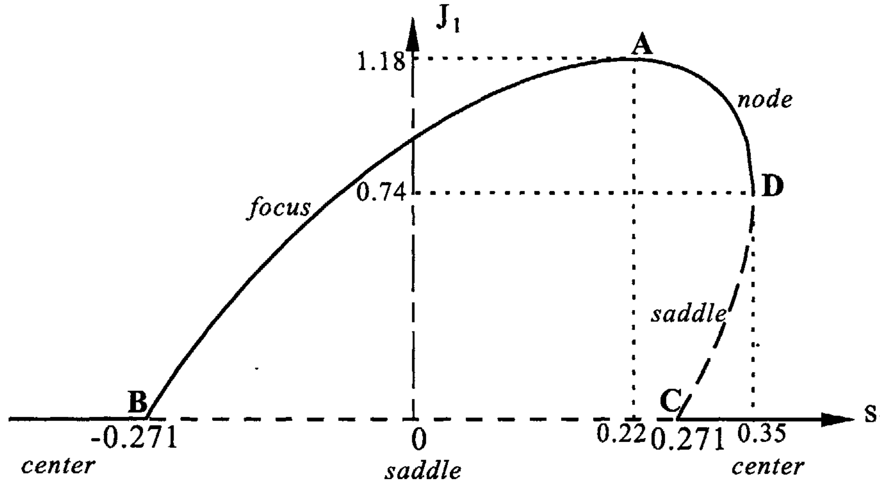

Figure 5-1: Equilibrium branch for $J_2^0 = 0$— Equilibrium of the first kind.

1. Equilibrium of the first kind:

$$J_2 = 0, \quad \text{and} \quad (a_2^r J_1)^2 + \left(a_2^i J_1 - s_1\right)^2 = a_1^2$$

which can be solved to get

$$J_1^0 = \frac{a_2^i s_1 \pm \sqrt{a_1^2 |a_2|^2 - (a_2^r s_1)^2}}{|a_2|^2}$$

The equilibrium branch for $J_2^0 = 0$ is plotted in Figure 5-1.

2. Equilibrium of the second kind:

$$J_1 = 0, \quad \text{and} \quad (b_2^r J_2)^2 + \left(b_2^i J_2 - s_2\right)^2 = b_1^2$$

which can be solved to get

$$J_2^0 = \frac{b_2^i s_2 \pm \sqrt{b_1^2 |b_2|^2 - (b_2^r s_2)^2}}{|b_2|^2}$$

The equilibrium branch for $J_1^0 = 0$ is plotted in Figure 5-2.

3. Equilibrium of the third kind:

Both $J_1 \neq 0$ and $J_2 \neq 0$;

In this case, we need solve two equations (5.15) and (5.16) (two ellipses) to obtain the equilibrium points $(J_1^0, \theta_1^0, J_2^0, \theta_2^0)$. In principle, we can eliminate either one of the

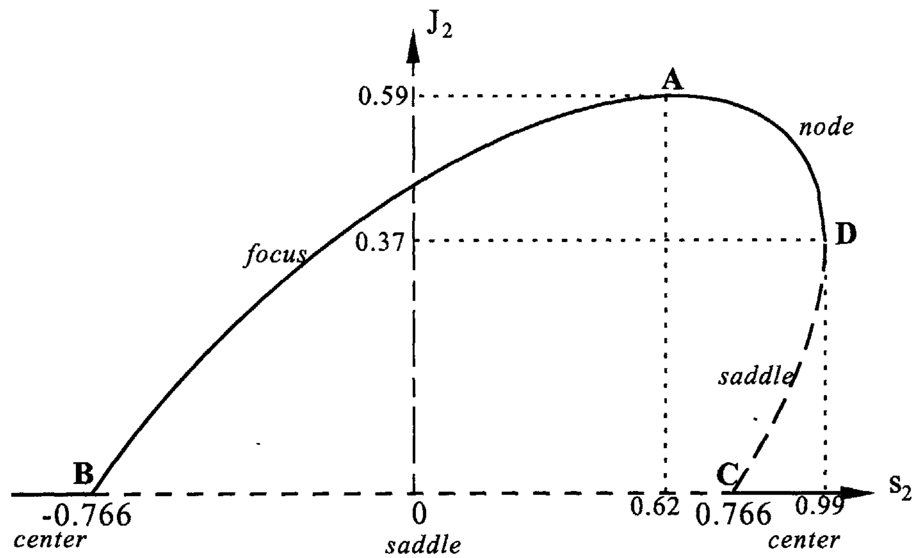

Figure 5-2: Equilibrium branch for $J_1^0 = 0$— Equilibrium of the second kind.

two variables from the two quadratic equations to obtain a quartic equation of only one variable.

In order to discuss the dynamics of the nonlinear system, please refer to Figure 5-3 for the conceptual bifurcation diagram. The straight lines demarcate the equilibrium of first (denoted by **I**) and second kind (denoted by **II**). The equilibrium of the third kind (denoted by **III**) is plotted on top of the first and second kind. The three zero zone are the trivial domains where the dynamical system is at rest.

1. When $s_1 < -0.271$, we have no equilibrium branch drops in the first quadrant of (J_1, J_2) plane. The only fixed point will be (J_1^0, J_2^0)=(0, J_2^0). Therefore, the dynamics of the system is totally governed by the second kind of equilibrium $J_1^0 = 0$ (Refer to Figure 5-2 for the bifurcation diagram.);

2. When $-0.271 < s_1 < 0.271$, we have only one branch of equilibrium in the first quadrant. When $0.271 < s_1 < 0.35$, we have two branches of equilibrium in the first quadrant. As long as s_1 drops in the domain (-0.271, 0.35), we at least have one equilibrium of the first kind. In this case,

i) As $s_2 < -0.766$, the dynamical system is governed by the equilibrium of the first kind;

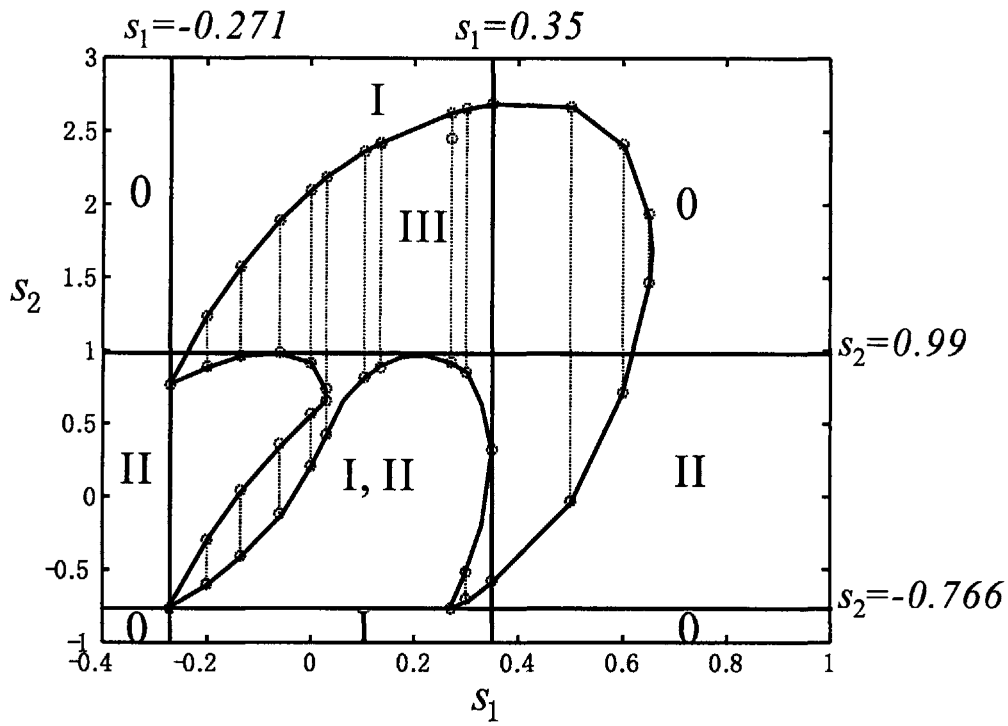

Figure 5-3: The bifurcation diagram.

ii) As $s_2 > 0.99$, the dynamical system is governed by the equilibrium of the first kind and the third kind (if any);

iii) As $-0.766 < s_2 < 0.99$, the dynamical system is governed by the equilibrium of the first kind, the second kind and the third kind (if any);

3. When $s_1 > 0.35$, the two equilibrium branches merge to one in the first quadrant of (J_1, J_2) plane. Because the absence of the first kind equilibrium, the dynamical system is dominated by the equilibrium of second and third kind (if any).

Although the equilibrium branches are obvious by above discussion, the global picture are not clear when co-existence of two fixed points occurs at certain values for parameters s_1 and s_2. How the dynamical system behaves at these parametric values and why it is so. To answer these questions, further study is needed.

5.2 Simultaneous resonance of two subharmonic edge waves of the same eigen frequency by one incident/reflected wave

We study two edge wave modes, sharing the same eigen frequency ω (degeneracy) but different x and y eigen function dependences, excited by one normally incident/reflected wave of twice the frequency. Initially, the two edge wave modes develop separately and one edge wave mode (low) outgrows another (high) mode as in the subharmonic resonance. But as soon as one of the edge wave reaches a finite amplitude, nonlinear effects come into play. The two modes are not independent any more. Since the two edge waves share the same frequency, steady flow could be generated by their interaction at the second order. The eigen frequency of edge wave satisfies

$$\omega_{nm} = \sqrt{(2n+1)mkgs}\ , \quad n = 0, 1, 2...\ ; \quad m = 1, 2, 3... \tag{5.17}$$

where k is the lowest longshore wave number

$$k = \frac{\pi}{W}.$$

We use (m, n) to denote the edge wave mode, where n is the cross-shore modal number and m is the longshore modal number. For simplicity, we limit our study to cases that only one pair of (n, m) can exist, i.e. $(0, q)$ and $(p, 1)$ with $q = 2p + 1$. Hence the normalized eigen frequency

$$\omega_{p1} = \sqrt{(2p+1)}, \quad \omega_{0q} = \sqrt{q}. \tag{5.18}$$

Therefore, $\omega_{p1} = \omega_{0q}$. The corresponding edge waves are

$$\Phi_{p1} = -\frac{igB_p}{\omega_{p1}} e^{-kx} L_p(2kx) \cos ky \ e^{-i\omega_{p1}t} + *. \tag{5.19}$$

and

$$\Phi_{0q} = -\frac{igB_q}{\omega_{0q}} e^{-qkx} \cos(qky) \ e^{-i\omega_{0q}t} + *. \tag{5.20}$$

We have derived the evolution equations for the edge waves amplitudes by multiple-scale expansion

$$\frac{\partial B_p}{\partial \tau} = i\Omega B_p + ic_1 B_p^* + c_2 B_p B_p B_p^* + ic_3 B_p B_q B_q^* + ic_4 B_p B_p B_q^* + ic_5 B_p B_p^* B_q + c_6 B_p^* B_q B_q; \tag{5.21}$$

$$\frac{\partial B_q}{\partial \tau} = i\Omega B_q + id_1 B_q^* + d_2 B_q B_q B_q^* + id_3 B_q B_p B_p^* + id_4 B_p B_p B_p^* + d_5 B_p B_p B_q^*. \tag{5.22}$$

where Ω is the detuning of the incident wave. For case $p = 1,\ q = 3$, the numerically computed coefficients are summarized in Table 5.1 and Table 5.2 below:

Table 5.1: Coefficients c_j's for case $p = 1$, $q = 3$.

c_1	c_2	c_3	c_4	c_5	c_6
0.1288	-0.0903-0.0478i	-2.6018	0.0256	0.0513	-0.3286-0.1657i

Table 5.2: Coefficients d_j's for case $p = 1$, $q = 3$.

d_1	d_2	d_3	d_4	d_5
1.4064	-0.9857-8.2701i	-7.8054	0.0769	-3.5879+4.8391i

Initially, the two edge waves evolve independently due to the weak coupling as in the last section. Mode q possesses a lower x mode and has a much larger growth rate (ten times that of the mode p). Therefore, mode q outgrows mode p during the initial evolution. But soon after it reaches a finite amplitude, the nonlinear terms take effect.

In Cartesian coordinate system, we let

$$B_p = x_1 + iy_1, \quad B_q = x_2 + iy_2,$$

then Eqs. (5.21) and (5.22) become

$$\begin{aligned} \dot{x}_1 &= (c_1 - \Omega)y_1 + (c_2^r x_1 - c_2^i y_1 - c_5 y_2)(x_1^2 + y_1^2) \\ &\quad -c_3 y_1(x_2^2 + y_2^2) + c_4 y_2(x_1^2 - y_1^2) - 2c_4 x_1 y_1 x_2 \\ &\quad +(c_6^i y_1 + c_6^r x_1)(x_2^2 - y_2^2) + 2(c_6^r y_1 - c_6^i x_1)x_2 y_2 \end{aligned} \tag{5.23}$$

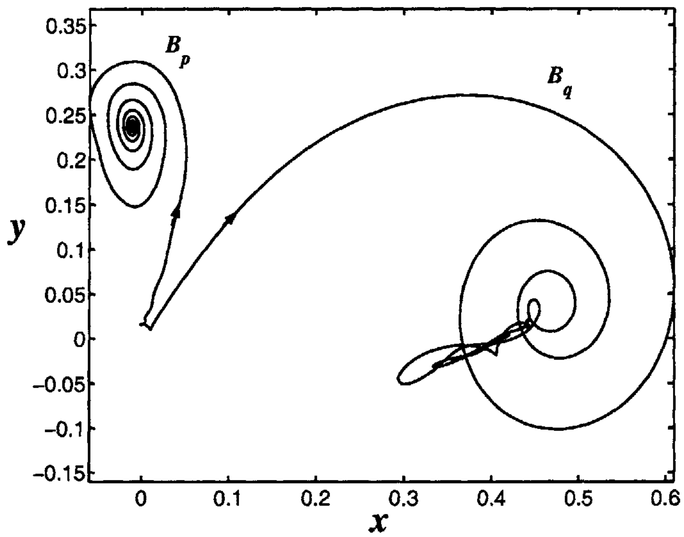

Figure 5-4: Flow map (x_j, y_j), $j = 1, 2$ for $\Omega = 0.5$ — $(p = 1, q = 3)$.

$$\begin{aligned}\dot{y}_1 &= (c_1+\Omega)x_1 + (c_2^i x_1 + c_2^r y_1 + c_5 x_2)(x_1^2+y_1^2) \\ &\quad + c_3 x_1(x_2^2+y_2^2) + c_4 x_2(x_1^2-y_1^2) + 2c_4 x_1 y_1 y_2 \\ &\quad + (c_6^i x_1 - c_6^r y_1)(x_2^2-y_2^2) + 2(c_6^i y_1 + c_6^r x_1)x_2 y_2 \end{aligned} \qquad (5.24)$$

$$\begin{aligned}\dot{x}_2 &= (d_1-\Omega)y_2 + (d_2^r x_2 - d_2^i y_2)(x_2^2+y_2^2) \\ &\quad - (d_3 y_2 + d_4 y_1)(x_1^2+y_1^2) \\ &\quad + (d_5^i y_2 + d_5^r x_2)(x_1^2-y_1^2) + 2(d_5^r y_2 - d_5^i x_2)x_1 y_1 \end{aligned} \qquad (5.25)$$

$$\begin{aligned}\dot{y}_2 &= (d_1+\Omega)x_2 + (d_2^i x_2 + d_2^r y_2)(x_2^2+y_2^2) \\ &\quad + (d_3 x_2 + d_4 x_1)(x_1^2+y_1^2) \\ &\quad + (d_5^i x_2 - d_5^r y_2)(x_1^2-y_1^2) + 2(d_5^i y_2 + d_5^r x_2)x_1 y_1 \end{aligned} \qquad (5.26)$$

Direct numerical simulation shows that the two modes converge to two equilibrium points (see Figure 5-4) (x_1, y_1)= (-0.0114, 0.2367) and (x_2, y_2)= (0.3853, -0.0129) for $\Omega = 0.5$. For mode p it is easy to see the equilibrium, whereas it is difficult for mode q. We plot another Figure 5-5 showing the evolution of x_2 and y_2. The analysis on

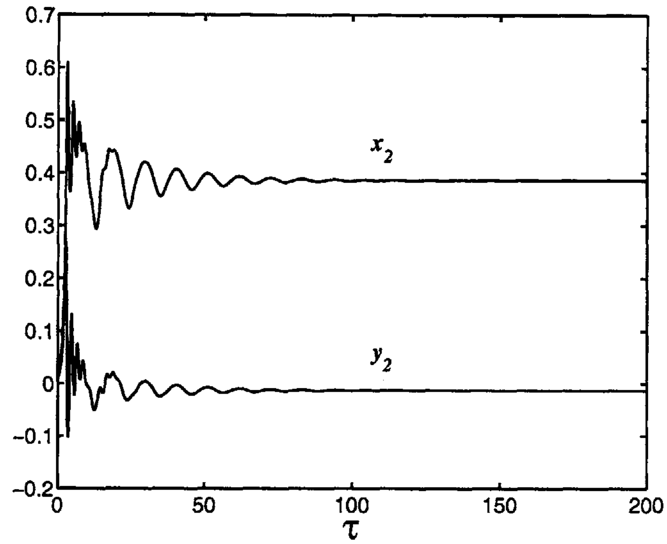

Figure 5-5: Temporal evolution of x_2 and y_2 for $\Omega = 0.5$ — $(p = 1, q = 3)$.

the dynamical system in this case is far from completion. Where is the equilibrium branch for different Ω? How the dynamical system behaves near these equilibrium? Which fixed point to choose when several fixed points coexist? We left these works for the future.

Our study of nonlinear resonance of edge waves originated from Venice gate project, where people found wave energy trapped near the slanted gates in the channel. Due to the similarity of the two problems, it is not difficult to extend the new theory of edge waves to Venice gates. For example, in the past only subharmonic resonance was studied for Venice gates. But nonlinear synchronous resonance could happen too according to the edge wave study. Therefore, the extension of the new developed edge wave theory to Venice gate problem is of industrial interest and demonstrates a direct application.

Appendix A

Analytical solution by Guza and Davis, Rockliff

In their study of subharmonic resonance, Guza and Davis [14], Rockliff [26] have solved the inhomogeneous equation

$$4\bar{\phi}_1 + \left(x\bar{\phi}_{1x}\right)_x = g_i(x) \equiv 2\left(\frac{dJ_0(2\sqrt{x})}{dx}\right)^2 + J_0(2\sqrt{x})\frac{d^2J_0(2\sqrt{x})}{dx^2}. \tag{A.1}$$

to obtain the following simple solution:

$$\bar{\phi}_1(x) = \frac{1}{\sqrt{x}}J_0(2\sqrt{x})J_1(2\sqrt{x}) \tag{A.2}$$

The forcing is just the second part of R.H.S. of (2.36), i.e., $g_i(x)$. Let's first verify that this solution is correct!

By the change of variable $\rho = 2\sqrt{x}$ we can rewrite the solution as

$$\bar{\phi}_1(\rho) = 2\rho^{-1}J_0(\rho)J_1(\rho) \tag{A.3}$$

Let us calculate both sides of (C.1) by evaluating the derivatives

$$\frac{dJ_0(2\sqrt{x})}{dx} = J_0'(\rho)\frac{d\rho}{dx} = -\frac{2}{\rho}J_1(\rho)$$

$$\frac{d^2J_0(2\sqrt{x})}{dx^2} = \left(-\frac{2}{\rho}J_1(\rho)\right)'\frac{d\rho}{dx} = 2\rho^{-1}\left(4\rho^{-2}J_1 - 2\rho^{-1}J_0\right)$$

$$\bar{\phi}_{1x} = \bar{\phi}_{1\rho}\frac{d\rho}{dx} = \frac{1}{\sqrt{x}}\bar{\phi}_{1\rho}$$

$$\left(x\bar{\phi}_{1x}\right)_x = \left(\sqrt{x}\bar{\phi}_{1\rho}\right)_x = \frac{1}{2}\left(\rho\bar{\phi}_{1\rho}\right)_\rho \frac{2}{\rho} = \rho^{-1}\left(\rho\bar{\phi}_{1\rho}\right)_\rho$$

Use has been made of

$$J_1' = J_0 - \rho^{-1}J_1, \quad J_1 = -J_0'$$

With these results, Eq. (A.3) becomes

$$4\bar{\phi}_1 + \rho^{-1}\left(\rho\bar{\phi}_{1\rho}\right)_\rho = 2\left(-\frac{2}{\rho}J_1(\rho)\right)^2 + 4\rho^{-2}J_0(\rho)\left(2\rho^{-1}J_1 - J_0\right). \tag{A.4}$$

Let us see whether two sides are equal.

By substituting (A.3) into L.H.S. of (A.4), we get

$$\bar{\phi}_{1\rho} = -2\rho^{-2}J_0J_1 + 2\rho^{-1}(J_0'J_1 + J_0J_1')$$

$$\left(\rho\bar{\phi}_{1\rho}\right)_\rho = 2(J_0'J_1 + J_0J_1' - \rho^{-1}J_0J_1)_\rho = 4(-2J_0J_1 - \rho^{-1}J_0^2 + 2\rho^{-2}J_0J_1 + 2\rho^{-1}J_1^2)$$

Therefore, L.H.S. of (A.4) becomes

$$L.H.S. = 8\rho^{-1}J_0(\rho)J_1(\rho) + 4\rho^{-1}(-2J_0J_1 - \rho^{-1}J_0^2 + 2\rho^{-2}J_0J_1 + 2\rho^{-1}J_1^2)$$

which is equal to R.H.S. of (A.4). Therefore, $\bar{\phi}_1(x)$ is the inhomogeneous solution of (A.4).

This solution can be used to check the correctness of the solution by variation of parameters. By following the procedure in §2.5, we get the general solution

$$\phi_1^i = C_1^iJ_0(4\sqrt{x}) + C_2^iY_0(4\sqrt{x}) + u_1^i(x)J_0(4\sqrt{x}) + u_2^i(x)Y_0(4\sqrt{x}) \tag{A.5}$$

where

$$u_1^i(x) = -\int_0^x \frac{Y_0(4\sqrt{\xi})g_i(\xi)}{\xi W(J_0, Y_0)(\xi)}d\xi = -\pi\int_0^x Y_0(4\sqrt{\xi})g_i(\xi)d\xi$$
$$u_2^i(x) = \int_0^x \frac{J_0(4\sqrt{\xi})g_i(\xi)}{\xi W(J_0, Y_0)(\xi)}d\xi = \pi\int_0^x J_0(4\sqrt{\xi})g_i(\xi)d\xi$$

with the familiar Wronskian

$$W(J_0, Y_0)(x) = J_0\frac{dY_0}{dx} - Y_0\frac{dJ_0}{dx} = (J_0Y_0' - Y_0J_0')\frac{d(4\sqrt{x})}{dx} = \frac{2}{\pi 4\sqrt{x}}\frac{2}{\sqrt{x}} = \frac{1}{\pi x}$$

From the analysis in last section, $C_2^i = 0$ by the boundary condition at the shore and $C_1^i = -u_1^i(\infty) - iu_2^i(\infty)$ by the radiation condition at infinity. In particular,

Table A.1: Confirmation for the numerical integral of $u_1^i(\infty) = -1, \quad u_2^i(\infty) = 0$.

L	10^4	10^5	2×10^6	10^7	2×10^8
$(u_1^i(\infty) + 1) \quad \times 10^5$	-28.256	-4.9839	-0.48347	-0.15213	0.010019
$u_2^i(\infty) \quad \times 10^5$	28.307	5.2859	0.83997	0.47902	0.33788

$u_1^i(\infty) = -1, \quad u_2^i(\infty) = 0$, as plotted in Figure 2-1 for $u_1^i(x)$ and $u_2^i(x)$. In order to confirm that $u_1^i(\infty) = -1, \quad u_2^i(\infty) = 0$, we list in Table A.1 the numerical integral at high accuracy (10^{-9}) for different truncation of upper limit L.

In summary our solution of (C.1) by variation of parameters is

$$\phi_1^i = J_0(4\sqrt{x}) + u_1^i(x)J_0(4\sqrt{x}) + u_2^i(x)Y_0(4\sqrt{x}) \tag{A.6}$$

which is plotted in Figure A-1 by crosses, and compared with $\bar{\phi}_1(x)$ (solid line). The agreement is perfect. The following paragraph is to confirm that $u_2^i(\infty) = 0$ since $u_2^i(\infty)H_0(4\sqrt{x})$ is the radiation condition in our method of variation of parameter, whereas Guza & Davies' solution gives no radiation!

For large x, we can approximate Bessel function of the nth order by following asymptotic form

$$J_0(z) \sim \sqrt{\frac{2}{\pi z}} \cos\left[z - (2n+1)\frac{\pi}{4}\right], \quad Y_0(z) \sim \sqrt{\frac{2}{\pi z}} \sin\left[z - (2n+1)\frac{\pi}{4}\right].$$

Therefore, Guza & Davies' solution behaves at large z as

$$\begin{aligned} \frac{1}{\sqrt{x}} J_0(2\sqrt{x}) J_1(2\sqrt{x}) &\sim \frac{2}{z}\sqrt{\frac{2}{\pi z}} \cos\left(z - \frac{\pi}{4}\right) \sqrt{\frac{2}{\pi z}} \cos\left(z - \frac{3\pi}{4}\right) \\ &= -\frac{2}{\pi z^2} \cos 2z \end{aligned}$$

where $z = 2\sqrt{x}$. Note that the energy flux rate is

$$P = puh \sim \zeta \frac{\partial \zeta}{\partial x} h \sim \phi \frac{\partial \phi}{\partial x} h$$

Since at large x

$$\phi \sim \frac{\cos 2z}{z^2} \sim \frac{1}{x}$$

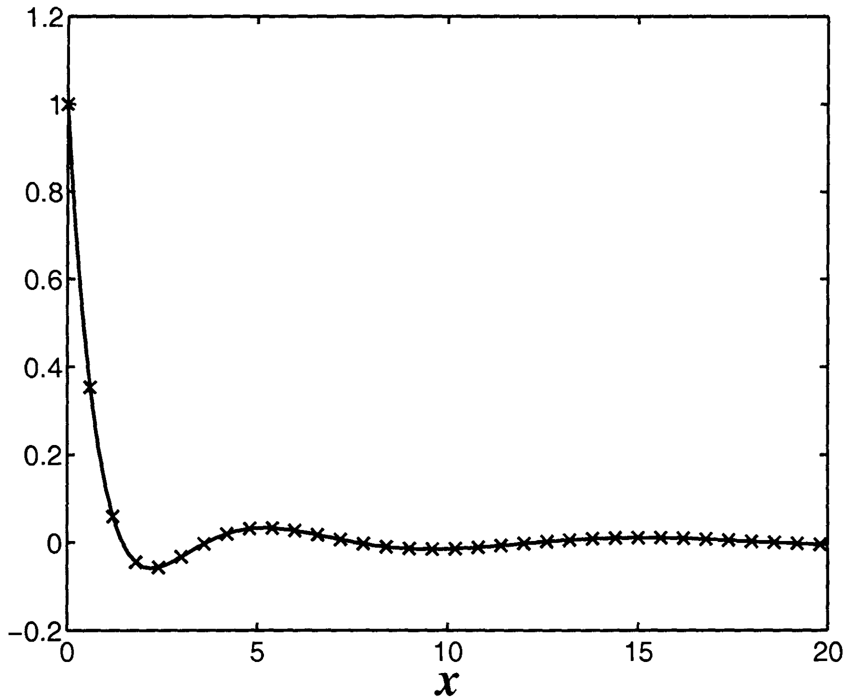

Figure A-1: Comparison of two solutions: Analytical formula — solid line; Solution by variation of parameters — crosses.

$$\frac{\partial\phi}{\partial x} \sim \frac{\sin 2z}{z^2}\frac{dz}{dx} \sim \frac{1}{x}\frac{1}{\sqrt{x}}$$

$$h \sim x$$

we have

$$P \sim \frac{1}{x}\frac{1}{x}\frac{1}{\sqrt{x}}x \sim \frac{1}{x^{3/2}} \to 0$$

Thus, quadratic forcing by the incident/reflected wave does not lead to radiation. Our numerical computation of $u_2^i(\infty)$ shown in Figure 2-1 confirms this result.

Appendix B

Confirmation of $C_2 = 0$ by the no-flux boundary condition at shoreline

Alternatively, let's apply the no-flux boundary condition at the shoreline, i.e.

$$x\phi_{1x} \to 0 \quad as \quad x \to 0$$

As $x \to 0$, Bessel functions of the zeroth order can be approximated by the following ascending series

$$J_0(z) = 1 - \frac{\frac{1}{4}z^2}{(1!)^2} + \frac{(\frac{1}{4}z^2)^2}{(2!)^2} - O(z^6), \quad Y_0(z) = \frac{2}{\pi}\left\{\ln\frac{z}{2} + \gamma\right\} J_0(z) + O(z^2) \quad \text{(B.1)}$$

For later use in (2.93), we first work out the constant $g(0)$ as follows. From (B.1) we see that

$$\frac{dJ_0(2\sqrt{x})}{dx} = -1 + \frac{1}{2}x - O(x^2), \quad \frac{d^2 J_0(2\sqrt{x})}{dx^2} = \frac{1}{2} - O(x)$$

as $x \to 0$. Upon substitution into (2.36), we get

$$g(0) = 2iB^2 + ie^{i2\varphi}\left(2 + \frac{1}{2}\right) = 2iB^2 + \frac{5i}{2}e^{i2\varphi} \quad \text{(B.2)}$$

From (B.1) we also get

$$\frac{dJ_0(4\sqrt{x})}{dx} = -4 + 8x - O(x^2), \quad \frac{dY_0(4\sqrt{x})}{dx} = \frac{1}{\pi x} - O\left(\ln(\sqrt{x})\right) \quad \text{(B.3)}$$

The first term in solution (2.40) becomes

$$C_1 x \left(J_0(4\sqrt{x})\right)_x = C_1\left(-4x + O(x^2)\right)$$

and the second term becomes

$$C_2 x \left(Y_0(4\sqrt{x})\right)_x = C_2\left(\frac{1}{\pi} - O\left(x\ln(\sqrt{x})\right)\right)$$

For the third and fourth terms, $Y_0(4\sqrt{x})g(x) \sim g(0)\ln(2\sqrt{x})$ as $x \to 0$. Making use of (B.2) we get

$$u_1(x) \sim \pi\int_0^x g(0)\ln(2\sqrt{\xi})d\xi \sim \int_0^{\sqrt{x}} g(0)\xi\ln(\xi)d\xi \sim g(0)x\ln\sqrt{x} + O(x)$$

and $J_0(4\sqrt{x})g(x) \to g(0)$ as $x \to 0$ so that

$$u_2(x) = \pi\int_0^x \left[g(0) + O(\xi)\right]d\xi = \pi\left[xg(0) + O(x^2)\right]$$

The third and fourth term becomes

$$\begin{aligned} & x\left[\left(u_1(x)J_0(4\sqrt{x})\right)_x + \left(u_2(x)Y_0(4\sqrt{x})\right)_x\right] \\ = \; & x\left(u_1(x)\frac{dJ_0(4\sqrt{x})}{dx} + u_2(x)\frac{dY_0(4\sqrt{x})}{dx}\right) \\ \sim \; & x\left(-4g(0)x\ln(\sqrt{x}) + g(0)\right) \sim g(0)x \end{aligned}$$

where use has been made of

$$u_{1x}J_0(4\sqrt{x}) + u_{2x}Y_0(4\sqrt{x}) = -\pi Y_0 g(x)J_0 + \pi J_0 g(x)Y_0 = 0$$

Collecting all four terms, we get at $x = 0$

$$x\phi_{1x} \sim \frac{C_2}{\pi} + O\left(x\right) \quad as \quad x \to 0$$

Therefore, $C_2 = 0$ in order that ϕ_1 satisfies the no-flux condition at the shoreline.

Appendix C

Analytical solution similar to Guza and Davis

For later use in the next chapter, we extend the simple solution of Guza & Davies [14] to solve the following equation with a modified forcing term

$$4\hat{\phi}_1 + \left(x\hat{\phi}_{1x}\right)_x = \hat{g}(x). \tag{C.1}$$

where

$$\begin{aligned} \hat{g}(x) &= 4\frac{dJ_0(2\omega_1\sqrt{x})}{dx}\frac{dJ_0(2\omega_2\sqrt{x})}{dx} + \omega_1 J_0(2\omega_1\sqrt{x})\frac{d^2J_0(2\omega_2\sqrt{x})}{dx^2} \\ &\quad + \omega_2 J_0(2\omega_2\sqrt{x})\frac{d^2J_0(2\omega_1\sqrt{x})}{dx^2} \end{aligned} \tag{C.2}$$

with $\omega_1 + \omega_2 = 2$. We try (by guessing) the following solution

$$\hat{\phi}_1(x) = \frac{-\hat{u}_1(\infty)}{2\sqrt{x}}\left[J_0(2\omega_1\sqrt{x})J_1(2\omega_2\sqrt{x}) + J_0(2\omega_2\sqrt{x})J_1(2\omega_1\sqrt{x})\right] \tag{C.3}$$

Refer to (C.5) for the definition of $\hat{u}_1$.

In principle one can check the correctness by direct substitution. We verify instead by comparing with the solution by the method of variation of parameters:

$$\hat{\phi}_1 = \hat{C}_1 J_0(4\sqrt{x}) + \hat{C}_2 Y_0(4\sqrt{x}) + \hat{u}_1(x)J_0(4\sqrt{x}) + \hat{u}_2(x)Y_0(4\sqrt{x}) \tag{C.4}$$

where

$$\hat{u}_1(x) = -\int_0^x \frac{Y_0(4\sqrt{\xi})\hat{g}(\xi)}{\xi W(J_0, Y_0)(\xi)}d\xi = -\pi\int_0^x Y_0(4\sqrt{\xi})\hat{g}(\xi)d\xi \tag{C.5}$$

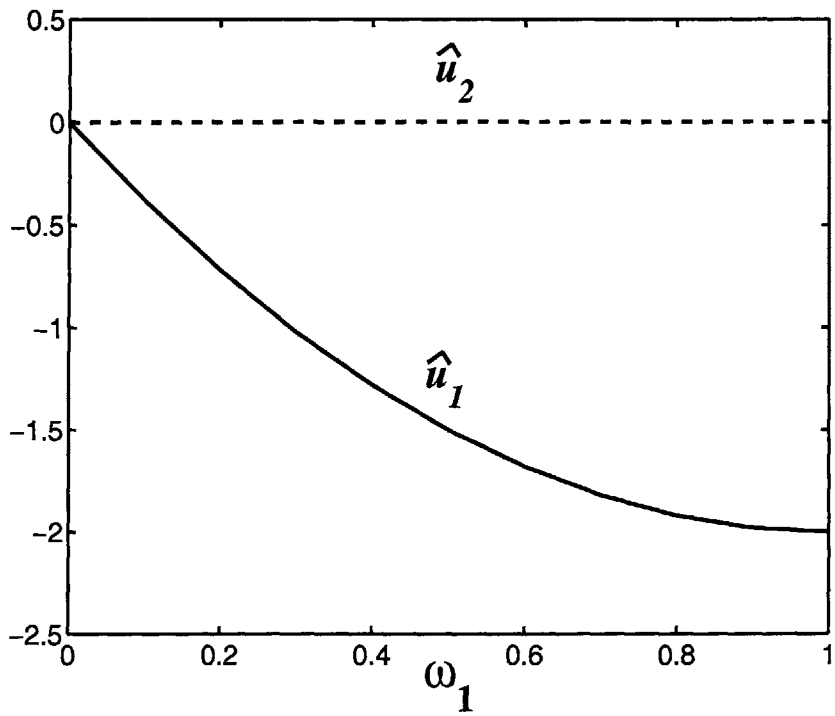

Figure C-1: $\hat{u}_1(\infty)$ and $\hat{u}_2(\infty)$ v.s. ω_1.

$$\hat{u}_2(x) = \int_0^x \frac{J_0(4\sqrt{\xi})\hat{g}(\xi)}{\xi W(J_0, Y_0)(\xi)} d\xi = \pi \int_0^x J_0(4\sqrt{\xi})\hat{g}(\xi) d\xi \tag{C.6}$$

with Wronskian

$$W(J_0, Y_0)(x) = J_0 \frac{dY_0}{dx} - Y_0 \frac{dJ_0}{dx} = (J_0 Y_0' - Y_0 J_0') \frac{d(4\sqrt{x})}{dx} = \frac{2}{\pi 4\sqrt{x}} \frac{2}{\sqrt{x}} = \frac{1}{\pi x}$$

From the analysis in last section, $\hat{C}_2 = 0$ by the boundary condition at shore and $\hat{C}_1 = -\hat{u}_1(\infty) - i\hat{u}_2(\infty)$ by the radiation condition at infinity. For a prescribed ω_1 and $\omega_2 = 2 - \omega_1$, we can evaluate $\hat{u}_1(\infty)$, $\hat{u}_2(\infty)$ numerically. In Figure C-1 the computed $\hat{u}_1(\infty)$ and $\hat{u}_2(\infty)$ are displayed for different ω_1.

Clearly, $\hat{u}_2(\infty)$ is zero irrespective of ω_1. The solution by variation of parameters is

$$\hat{\phi}_1 = -\hat{u}_1(\infty) J_0(4\sqrt{x}) + \hat{u}_1(x) J_0(4\sqrt{x}) + \hat{u}_2(x) Y_0(4\sqrt{x}) \tag{C.7}$$

which is plotted in Figure C-2, C-3, and C-4 for different ω_1. Our guess solution (C.3) is also plotted for comparison.

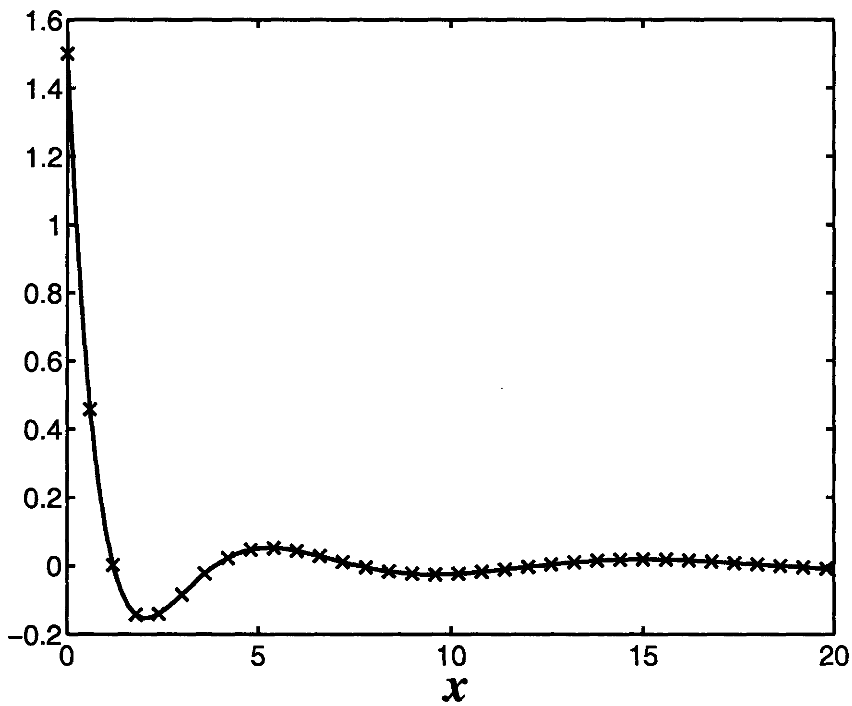

Figure C-2: Comparison of the two solutions for $\omega_1 = 0.5$: Solid line — Eq. (C.3); Crosses — Eq. (C.7).

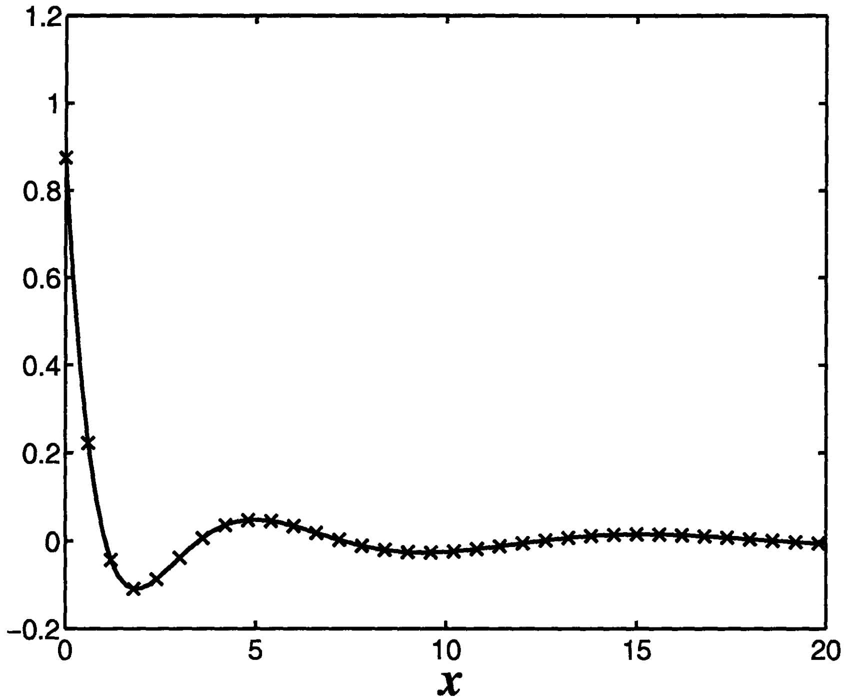

Figure C-3: Comparison of the two solutions for $\omega_1 = 0.25$: Solid line — Eq. (C.3); Crosses — Eq. (C.7).

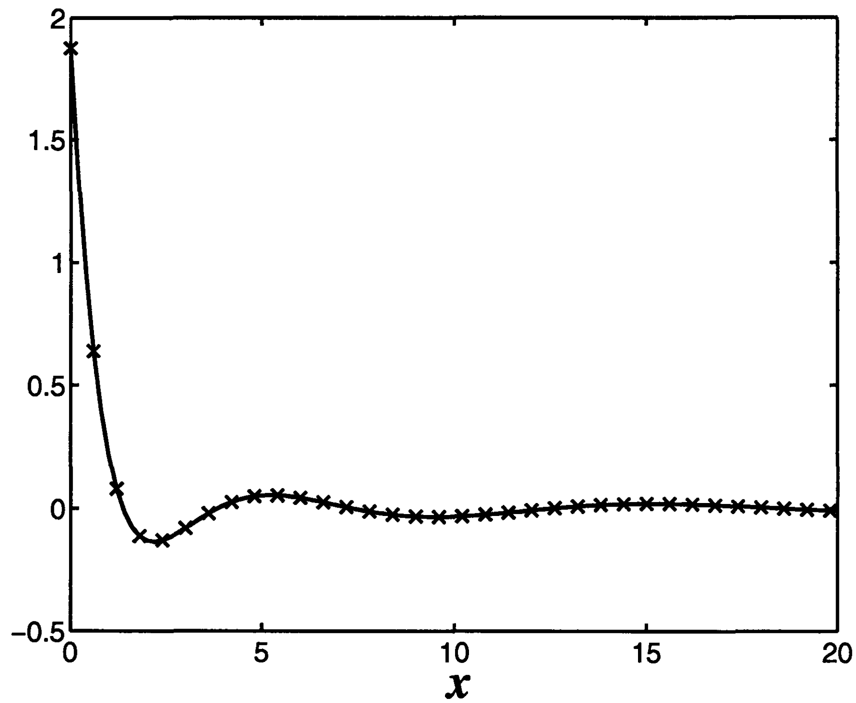

Figure C-4: Comparison of the two solutions for $\omega_1 = 0.75$: Solid line — Eq. (C.3); Crosses — Eq. (C.7).

In our numerical work, the following recursive formulas are used:

$$\frac{dJ_0(2\omega_n\sqrt{x})}{dx} = -\frac{\omega_n}{\sqrt{x}}J_1(2\omega_n\sqrt{x})$$

$$\frac{d^2J_0(2\omega_n\sqrt{x})}{dx^2} = -\frac{\omega_n^2}{x}J_0(2\omega_n\sqrt{x}) + \frac{\omega_n}{x\sqrt{x}}J_1(2\omega_n\sqrt{x})$$

Appendix D

Convergence of integrals

In order to check the convergence of the integrals at the lower (0) and upper limits (∞), we use series expansions around zero and the asymptotic forms at infinity to approximate the integrand.

As $x \to 0$, we can approximate Bessel functions of the zeroth order by following ascending series

$$J_0(z) = 1 - \frac{\frac{1}{4}z^2}{(1!)^2} + \frac{(\frac{1}{4}z^2)^2}{(2!)^2} - O(z^6), \quad Y_0(z) = \frac{2}{\pi}\left\{\ln\frac{z}{2} + \gamma\right\} J_0(z) + O(z^2)$$

and their first derivatives

$$\frac{dJ_0(z)}{dz} \sim -\frac{1}{2}z + O(z^3), \quad \frac{dY_0(z)}{dz} \sim \frac{2}{\pi z} - O\left(\ln\frac{z}{2}\right) \tag{D.1}$$

As $x \to \infty$, we can approximate Bessel functions of the zeroth order by following asymptotic form

$$J_0(z) \sim \sqrt{\frac{2}{\pi z}} \cos\left(z - \frac{\pi}{4}\right), \quad Y_0(z) \sim \sqrt{\frac{2}{\pi z}} \sin\left(z - \frac{\pi}{4}\right)$$

and their first derivatives

$$\frac{dJ_0(z)}{dz} \sim -\sqrt{\frac{2}{\pi z}} + O(z^{-3/2}), \quad \frac{dY_0(z)}{dz} \sim \sqrt{\frac{2}{\pi z}} + O(z^{-3/2}) \tag{D.2}$$

We can make use of these approximations to evaluate the integrals efficiently. Thus in u_1, we divide the integration domain into three segments as follows

$$\left(\int_0^{\epsilon} + \int_{\epsilon}^{L} + \int_L^{\infty}\right) d\xi Y_0(4\sqrt{\xi}) \frac{dJ_0(2\sqrt{\xi})}{d\xi} \frac{dJ_0(2\sqrt{\xi})}{d\xi}$$

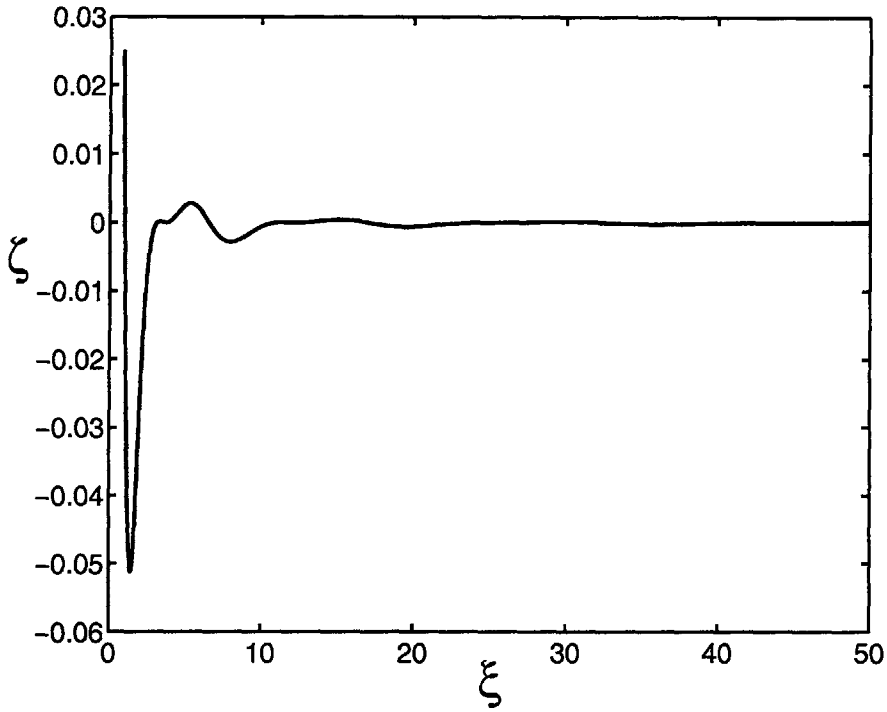

Figure D-1: Behavior of the integrand ζ

where ϵ is small but L is large. Therefore at the two ends, the integration can be approximated by

$$\int_L^\infty d\xi \xi^{-1/4} \xi^{-3/4} \xi^{-3/4} \sim \xi^{-3/4}\Big|_L^\infty \sim -L^{-3/4} \rightarrow 0 \text{ as } L \rightarrow \infty$$

and

$$\int_0^\epsilon d\xi \ln(\sqrt{\xi}) \sim \xi \ln(\sqrt{\xi})\Big|_0^\epsilon \sim \epsilon \ln(\sqrt{\epsilon}) \rightarrow 0 \text{ as } \epsilon \rightarrow 0$$

This assures us that the integral u_1 is finite at both limits 0 and ∞. Also the analysis above tells us the truncation error for our numerical evaluation of the integration. For example, if we use $L = 10000$ as the upper limit to approximate $u_1(\infty)$ in (2.41), the numerical result is only accurate up to the third digit behind the decimal point. To give some quantitative ideas, we plot a typical integrand defined by

$$\zeta = Y_0(4\sqrt{\xi}) \frac{dJ_0(2\sqrt{\xi})}{d\xi} \frac{dJ_0(2\sqrt{\xi})}{d\xi}$$

versus the argument ξ in Figure D-1. It can be seen that it is easy to evaluate the integral by the normal trapezoidal rule.

Appendix E

Numerical solution by finite element method for synchronous resonance

In Section 2.5.2 and 2.5.4 we have found that the boundary-value problems for both the forced trapped wave and the steady potential flow are governed by an equation of the form

$$\frac{d}{dx}(xf_x) - \left[x - w^2\right] f = g(x) \tag{E.1}$$

with the boundary conditions

$$xf_x = 0 \quad \text{as} \quad x \to 0 \tag{E.2}$$

$$f = 0 \quad \text{as} \quad x \to \infty. \tag{E.3}$$

The parameter w is $w = 2$ in (2.56), and $w = 0$ in (2.70).

It is easy to show that the boundary-value problem above is equivalent to the stationarity of the following functional

$$\mathcal{F}(f) = \overbrace{\frac{1}{2}\int_0^\infty \left[p(x)\left(\frac{df}{dx}\right)^2 + q(x)f^2\right] dx}^{I_1} + \underbrace{\int_0^\infty gf\,dx}_{I_2} \tag{E.4}$$

where

$$p(x) = x, \quad q(x) = x - w^2$$

To prove the stationarity we calculate the first variation:

$$\begin{aligned}
\delta\mathcal{F}(f) &= \int_0^\infty \left[p(x)\frac{df}{dx}\frac{d\delta f}{dx} + q(x)f\delta f\right] dx + \int_0^\infty g\delta f dx \\
&= \int_0^\infty \left[\frac{d}{dx}\left(p(x)\frac{df}{dx}\delta f\right) - \frac{d}{dx}\left(p(x)\frac{df}{dx}\right)\delta f + q(x)f\delta f + g\delta f\right] dx \\
&= \left(p(x)\frac{df}{dx}\right)\Big|_0^\infty \delta f + \int_0^\infty \left[-\frac{d}{dx}\left(p(x)\frac{df}{dx}\right) + q(x)f + g\right] dx\delta f
\end{aligned} \tag{E.5}$$

Obviously, $\delta\mathcal{F}(f) = 0$ if f satisfies the conditions (E.1), (E.2) and (E.3). The necessity can also be proven.

We discretize a large but finite region by standard 2-node elements with piece-wise linear potentials :

Within each element $x \in [x_1, x_2]$:

$$f = \sum_{i=1}^{2} f_i N_i(x) \tag{E.6}$$

where f_i is an unknown nodal potential and $N_i(x)$ is a interpolation function

$$N_1 = \frac{x_2 - x}{h}; \quad N_2 = \frac{x - x_1}{h} \tag{E.7}$$

and h is the element length, i.e. $h = x_2 - x_1$.

In matrix form,

$$f = \begin{bmatrix} N_1 & N_2 \end{bmatrix} \begin{bmatrix} f_1 \\ f_2 \end{bmatrix} = \mathbf{N}\left\{\hat{f}\right\} \tag{E.8}$$

therefore,

$$\frac{df}{dx} = \begin{bmatrix} \frac{dN_1}{dx} & \frac{dN_2}{dx} \end{bmatrix} \begin{bmatrix} f_1 \\ f_2 \end{bmatrix} = \begin{bmatrix} -\frac{1}{h} & \frac{1}{h} \end{bmatrix} \begin{bmatrix} f_1 \\ f_2 \end{bmatrix} = \mathbf{B}\left\{\hat{f}\right\} \tag{E.9}$$

Now we can evaluate the two integrals of functional $\mathcal{F}$:

- Integral I_1

$$\frac{1}{2}\int_{el} \left[p(x)\left(\frac{df}{dx}\right)^2 + q(x)f^2\right] dx = \frac{1}{2}\{\hat{f}\}^T [K]^{el} \{\hat{f}\}$$

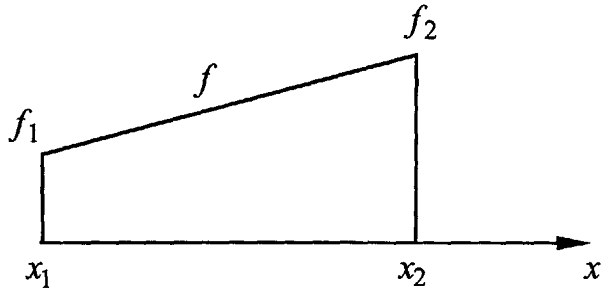

Figure E-1: Local coordinate system for 1-D linear element

where $[K]^{el}$ is the element stiffness matrix

$$[K]^{el}_{ij} = \frac{(-1)^{i+j}}{h^2}\int_{x_1}^{x_2} p dx + \int_{x_1}^{x_2} qN_iN_j dx$$

with

$$\frac{(-1)^{i+j}}{h^2}\int_{x_1}^{x_2} p dx = (-1)^{i+j}\frac{x_1+x_2}{2h}$$

$$\int_{x_1}^{x_2} qN_1N_1 dx = \frac{1}{h^2}\left[\frac{1}{4}x^4 - \frac{2}{3}x_2x^3 + \frac{1}{2}x_2^2x^2\right]_{x_1}^{x_2} - \frac{w^2}{h^2}\left[\frac{1}{3}x^3 - x_2x^2 + x_2^2x\right]_{x_1}^{x_2}$$

$$\int_{x_1}^{x_2} qN_2N_2 dx = \frac{1}{h^2}\left[\frac{1}{4}x^4 - \frac{2}{3}x_1x^3 + \frac{1}{2}x_1^2x^2\right]_{x_1}^{x_2} - \frac{w^2}{h^2}\left[\frac{1}{3}x^3 - x_1x^2 + x_1^2x\right]_{x_1}^{x_2}$$

$$\begin{aligned}&\int_{x_1}^{x_2} qN_1N_2 dx \\ =\ & \frac{1}{h^2}\left[-\frac{x^4}{4} + \frac{x_1+x_2}{3}x^3 - \frac{x_1x_2}{2}x^2\right]_{x_1}^{x_2} - \frac{w^2}{h^2}\left[-\frac{x^3}{3} + \frac{x_1+x_2}{2}x^2 - x_1x_2x\right]_{x_1}^{x_2}\end{aligned}$$

After assemblage and using the global $\hat{f}$, we can get

$$I_1 = \frac{1}{2}\left\{\hat{f}\right\}^T [K]\left\{\hat{f}\right\}$$

- Integral I_2

$$\int_{el} gf dx = \{\hat{f}\}^T [G]^{el}$$

where $[G]^{el}$ is the element load vector

$$[G]^{el}_i = \int_{x_1}^{x_2} gN_i dx, \quad i = 1, 2$$

After assemblage and using the global $\hat{f}$, we can get

$$I_2 = \left\{\hat{f}\right\}^T [G]$$

In summary, the stationary functional becomes

$$\mathcal{F}(\left\{\hat{f}\right\}) \;=\; \frac{1}{2}\left\{\hat{f}\right\}^T [K]\left\{\hat{f}\right\} + \left\{\hat{f}\right\}^T [G] \tag{E.10}$$

By extremizing the functional, the first derivative of $\mathcal{F}$ with respect to unknowns f_i vanishes,

$$[K]\left\{\hat{f}\right\} + [G] = 0 \tag{E.11}$$

which is an algebraic equation system for the nodal coefficients. At the distant boundary $x \gg 1$, $f = 0$ is imposed as the essential boundary condition.

As a simple check, let us consider an analytical solution: $f(x) = -e^{-x}$ which is the exact solution to forcing $g(x) = e^{-x}$, i.e.

$$xf_{xx} + f_x - xf = g(x) = e^{-x}$$

Plotted in Fig. E-2 is the comparison of our numerical solution (solid line) and the exact solution (crosses). The numerical values are listed in Table E.1.

Shown in Figure E-3 are the solutions of $f_{11}(x)$ and $f_{12}(x)$ by FEM computations. We also show in Figure E-3 for comparison the series expansion solutions (refer to Figure 2-3 and Figure 2-4). In addition, they are compared in Table E.2, which shows very good agreement. It may be concluded that the solution for f_{11} by Rockliff and Smith is in error.

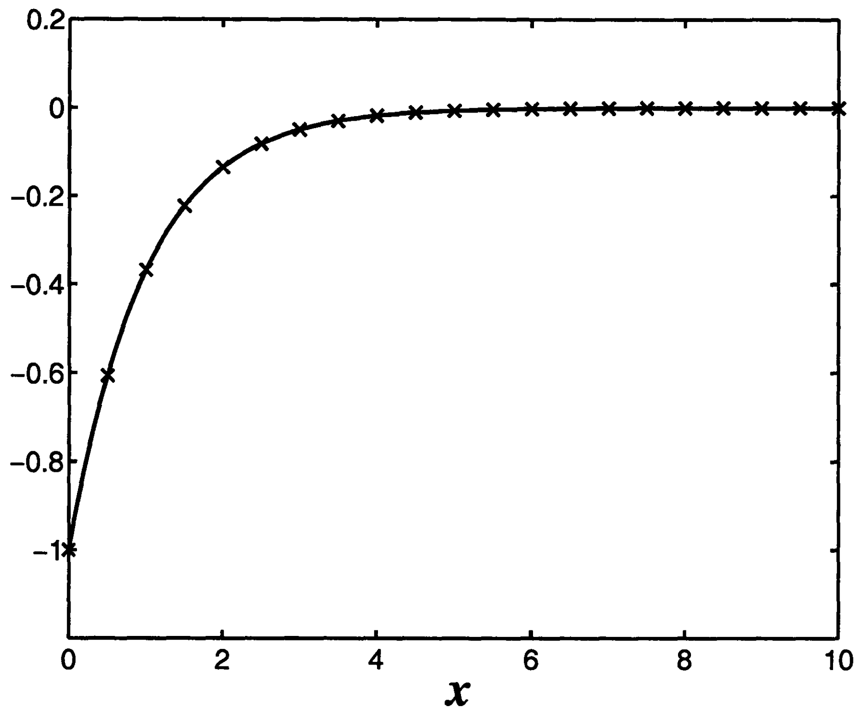

Figure E-2: Numerical solution of $f(x)$ (solid line) and exact solution (dots) for special force $g(x) = e^{-x}$.

Table E.1: Comparison of FEM solution with the exact solution for $g(x) = e^{-x}$. Error is defined by $100 \times \frac{f(EXACT) - f(FEM)}{f(EXACT)}$.

x	$f(x), FEM$	$f(x) = -e^{-x}, EXACT$	Error (%)
0.000000000	-0.999993871	-1.000000000	0.000612926
0.000012167	-0.999981704	-0.999987833	0.000612934
0.000039138	-0.999954733	-0.999960863	0.000612950
0.000098926	-0.999894950	-0.999901079	0.000612987
0.000231457	-0.999762441	-0.999768570	0.000613068
0.000525241	-0.999468767	-0.999474897	0.000613248
0.001176477	-0.998818085	-0.998824215	0.000613648
0.002620082	-0.997377218	-0.997383347	0.000614533
0.005820143	-0.994190632	-0.994196761	0.000616495
0.012913767	-0.987163129	-0.987169258	0.000620850
0.028638311	-0.971761751	-0.971767878	0.000630521
0.063495147	-0.938472554	-0.938478673	0.000652064
0.140762827	-0.868689234	-0.868695319	0.000700465
0.312043267	-0.731943912	-0.731949858	0.000812354
0.691723226	-0.500706984	-0.500712484	0.001098466
1.533365568	-0.215803620	-0.215808127	0.002088555
3.399046955	-0.033402462	-0.033405091	0.007869709
7.534731277	-0.000533893	-0.000534205	0.058322591

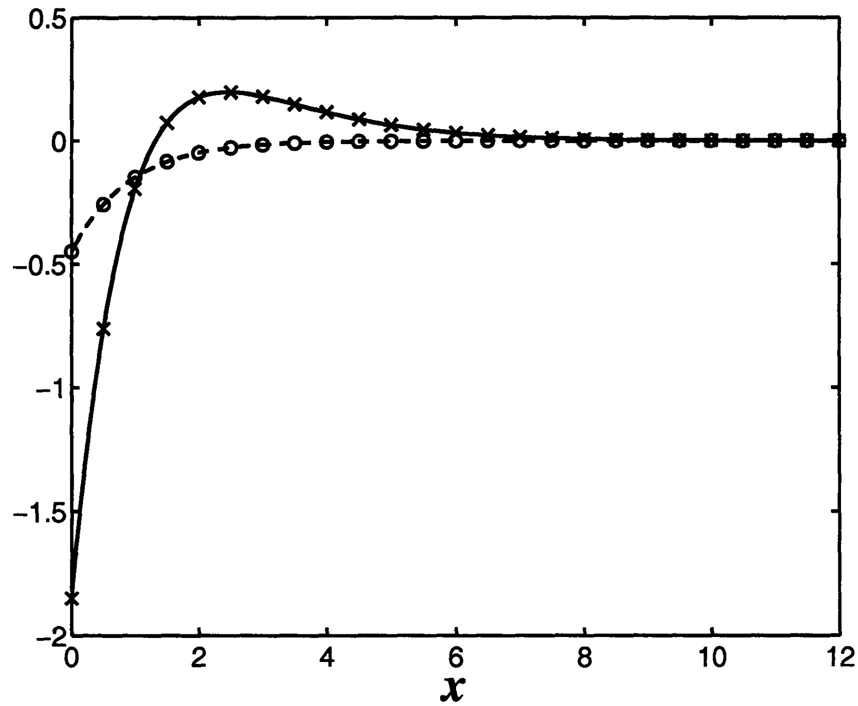

Figure E-3: The numerical solution for f_{11}(solid line) and f_{12}(dashed line). The circles and crosses are their series expansion solutions respectively.

Table E.2: Comparison of FEM solution with the series solution of $f_{11}(x)$ and $f_{12}(x)$.

x	f_{11} (FEM)	f_{11} (SERIES)	f_{12} (FEM)	f_{12} (SERIES)
0.0000000000	-1.8501992842	-1.8501654620	-0.4495540068	-0.4495565083
0.0000121672	-1.8501639900	-1.8501301679	-0.4495479232	-0.4495504248
0.0000391383	-1.8500857546	-1.8500519327	-0.4495344381	-0.4495369398
0.0000989255	-1.8499123379	-1.8498785165	-0.4495045467	-0.4495070487
0.0002314569	-1.8495279656	-1.8494941454	-0.4494382933	-0.4494407959
0.0005252412	-1.8486761341	-1.8486423166	-0.4492914631	-0.4492939671
0.0011764773	-1.8467889099	-1.8467550985	-0.4489661542	-0.4489686611
0.0026200822	-1.8426105950	-1.8425767982	-0.4482458795	-0.4482483929
0.0058201432	-1.8333735959	-1.8333398360	-0.4466533675	-0.4466558950
0.0129137671	-1.8130208417	-1.8129871864	-0.4431434368	-0.4431459948
0.0286383112	-1.7685041395	-1.7684708218	-0.4354612938	-0.4354639143
0.0634951474	-1.6727150220	-1.6726829210	-0.4189052933	-0.4189080304
0.1407628267	-1.4740101149	-1.4739825075	-0.3844224787	-0.3844253822
0.3120432672	-1.0945953876	-1.0945823218	-0.3177983332	-0.3178012981
0.6917232259	-0.4970469865	-0.4970635773	-0.2085137651	-0.2085163053
1.5333655681	0.0837485636	0.0837246300	-0.0821327162	-0.0821346097
3.3990469554	0.1552896131	0.1552837448	-0.0105514550	-0.0105524706
7.5347312771	0.0101678930	0.0101729218	-0.0001199001	-0.0001200686
16.7023656466	0.0000038205	0.0000039386	-0.0000000081	-0.0000000107

Appendix F

Evaluation of the integral in (2.66)

Let us introduce

$$f(\xi) = \xi^n e^{-\xi}$$

for brevity. Therefore, integration by part gives

$$\begin{aligned}
& \int_0^\infty \xi^k \frac{d^n}{d\xi^n} \left(\xi^n e^{-\xi}\right) d\xi \\
= & \int_0^\infty \xi^k \frac{d^n f}{d\xi^n} d\xi \\
= & \int_0^\infty \xi^k d \left(\frac{d^{n-1} f}{d\xi^{n-1}}\right) \\
= & \left[\xi^k \left(\frac{d^{n-1} f}{d\xi^{n-1}}\right)\right]_0^\infty - \int_0^\infty \left(\frac{d^{n-1} f}{d\xi^{n-1}}\right) d\xi^k
\end{aligned}$$

The first term on the R.H.S. is zero since the lowest order term in the brackets would be $n!\xi^{k+1}e^{-\xi}$. The second term can be rewritten as

$$-\int_0^\infty \left(\frac{d^{n-1} f}{d\xi^{n-1}}\right) d\xi^k = -k \int_0^\infty \xi^{k-1} \left(\frac{d^{n-1} f}{d\xi^{n-1}}\right) d\xi = -k \int_0^\infty \xi^{k-1} d \left(\frac{d^{n-2} f}{d\xi^{n-2}}\right)$$

Then we can repeat the first step to obtain

$$\begin{aligned}
\int_0^\infty \xi^k \frac{d^n}{d\xi^n} \left(\xi^n e^{-\xi}\right) d\xi &= \int_0^\infty \xi^k d \left(\frac{d^{n-1} f}{d\xi^{n-1}}\right) \\
&= -k \int_0^\infty \xi^{k-1} d \left(\frac{d^{n-2} f}{d\xi^{n-2}}\right) \\
&= k(k-1) \int_0^\infty \xi^{k-2} d \left(\frac{d^{n-3} f}{d\xi^{n-3}}\right) \\
&= \ldots
\end{aligned} \tag{F.1}$$

If $k < n$, this procedure would stop at

$$\begin{aligned} & (-1)^k k! \int_0^\infty \xi^0 d\left(\frac{d^{n-k-1}f}{d\xi^{n-k-1}}\right) \\ = & (-1)^k k! \left[\frac{d^{n-k-1}f}{d\xi^{n-k-1}}\right]_0^\infty \end{aligned} \quad \text{(F.2)}$$

The lowest order term in the brackets would be $\frac{n!}{(k+1)!}\xi^{k+1}e^{-\xi}$. Therefore the integral is equal to zero.

If $k \geq n$, we can proceed until

$$\begin{aligned} & (-1)^n k(k-1)...(k-n+1) \int_0^\infty \xi^{k-n} f d\xi \\ = & (-1)^n \frac{k!}{(k-n)!} \int_0^\infty \xi^{k-n} \left(\xi^n e^{-\xi}\right) d\xi \\ = & (-1)^n \frac{k!}{(k-n)!} \int_0^\infty \xi^k e^{-\xi} d\xi \\ = & (-1)^n \frac{k!k!}{(k-n)!} \end{aligned} \quad \text{(F.3)}$$

which leads to (2.67).

Appendix G

Low-frequency incident wave — case of $\omega = \omega_q - \omega_p$

Now let us consider the case that incident wave has a frequency equal to the difference of the two edge wave eigen frequencies, i.e. $\omega = \omega_q - \omega_p = \sqrt{2q+1} - \sqrt{2p+1}$.

G.1 Governing equations

We still use the same multiple-scale expansion of the solution as in (4.21) except that the known incident and reflected wave will be incorporated in ϕ_{11} (instead of ϕ_{11} as in the " + " sign case) as part of the homogeneous solution. Therefore at second order, the radiated wave solutions become

i) $\phi_{11} = -i\frac{e^{i2\varphi}}{\omega}J_0(2\omega\sqrt{x}) + i\frac{B_p^* B_q}{\omega_p\omega_q}G_1(x)$, with $g(x) = e^{-2x}g_1(x)$ and $\bar{\omega} = \omega_q - \omega_p$;

ii) $\phi_{12} = i\frac{B_p B_q}{\omega_p\omega_q}G_2(x)$, with $g(x) = e^{-2x}g_2(x)$ and $\bar{\omega} = \omega_q + \omega_p$;

iii) $\phi_{13} = i\frac{B_p^2}{\omega_p}G_3(x)$, with $g(x) = e^{-2x}g_3(x)$ and $\bar{\omega} = 2\omega_p$;

iv) $\phi_{14} = i\frac{B_q^2}{\omega_q}G_4(x)$, with $g(x) = e^{-2x}g_4(x)$ and $\bar{\omega} = 2\omega_q$.

where G_1, G_2, G_3 and G_4 are given by (4.30). We have incorporated the incident wave in the solution $\phi_{11}(x)$, where $A' = \bar{\epsilon}|\bar{A}|e^{i2\varphi}$ is the known incident and reflected wave amplitude at the shoreline and $\omega = \omega_q - \omega_p$ is its frequency.

The solutions to the four trapped harmonics f_{11}, f_{12}, f_{13} and f_{14} are the same:

i) $\psi_{11} = i\frac{B_p^* B_q}{\omega_p\omega_q}f_{11}(x)\cos 2y$, $g(x) = e^{-2x}f_1(x)$, $\bar{\omega} = \omega_q - \omega_p$;

ii) $\psi_{12} = i\frac{B_pB_q}{\omega_p\omega_q} f_{12}(x)\cos 2y, \quad g(x) = e^{-2x} f_2(x), \quad \bar{\omega} = \omega_q + \omega_p;$

iii) $\psi_{13} = i\frac{B_p^2}{\omega_p} f_{13}(x)\cos 2y, \quad g(x) = e^{-2x} f_3(x), \quad \bar{\omega} = 2\omega_p;$

iv) $\psi_{14} = i\frac{B_q^2}{\omega_q} f_{14}(x)\cos 2y, \quad g(x) = e^{-2x} f_4(x), \quad \bar{\omega} = 2\omega_q.$

where f_{11} to f_{14} can be solved by Finite Element Method as described in Appendix H.

At the third order, the forcing terms related to ϕ_{11} and ϕ_{12} change accordingly:

[$\mathcal{E}_p$-1]. Instead of (4.40), we now have

$$\begin{aligned}
&(\phi_{11}^*, \psi_{0q}) \\
= \;& 2\{\phi_{11x}^*\psi_{0qx}[i(\omega_q-\omega_p) - i\omega_q)]\} - i\omega_q\psi_{0q}\phi_{11xx}^* + i(\omega_q-\omega_p)\phi_{11}^*(\psi_{0qxx}+\psi_{0qyy}) \\
= \;& -i2\omega_p\phi_{11x}^*\psi_{0qx} - i\omega_q\psi_{0q}\phi_{11xx}^* + i(\omega_q-\omega_p)\phi_{11}^*(\psi_{0qxx}+\psi_{0qyy}) \\
= \;& -ie^{-x}\cos y\left(-i\frac{B_pB_q^*}{\omega_p\omega_q}\right)\left(-i\frac{B_q}{\omega_q}\right)\left\{2\omega_p\frac{dG_1}{dx}(2L_q'-L_q) + \omega_q\frac{d^2G_1}{dx^2}L_q\right. \\
& \left. -(\omega_q-\omega_p)G_1(4L_q''-4L_q')\right\} \\
& -ie^{-x}\cos y\left(i\frac{e^{-i2\varphi}}{\omega}\right)\left(-i\frac{B_q}{\omega_q}\right)\left\{2\omega_p\frac{dJ_0}{dx}(2L_q'-L_q) + \omega_q\frac{d^2J_0}{dx^2}L_q\right. \\
& \left. -(\omega_q-\omega_p)J_0(4L_q''-4L_q')\right\} \\
= \;& i\frac{B_pB_qB_q^*}{\omega_p\omega_q^2}e^{-x}\left\{2\omega_p\frac{dG_1}{dx}(2L_q'-L_q) + \omega_q\frac{d^2G_1}{dx^2}L_q - (\omega_q-\omega_p)G_1(4L_q''-4L_q')\right\}\cos y \\
& -i\frac{e^{-i2\varphi}B_q}{\omega\omega_q}e^{-x}\left\{2\omega_p\frac{dJ_0}{dx}(2L_q'-L_q) + \omega_q\frac{d^2J_0}{dx^2}L_q - (\omega_q-\omega_p)J_0(4L_q''-4L_q')\right\}\cos y \\
= \;& \hat{h}_{p1}(x)B_pB_qB_q^* + ie^{i2\varphi}\hat{f}_p(x)B_q^* \qquad \text{(G.1)}
\end{aligned}$$

[$\mathcal{E}_p$-2]. Instead of (4.41), we now have

$$\begin{aligned}
&(\phi_{12}, \psi_{0q}^*) \\
= \;& 2\left\{\phi_{12x}\psi_{0qx}^*[-i(\omega_p+\omega_q) + i\omega_q)]\right\} + i\omega_q\psi_{0q}^*\phi_{12xx} - i(\omega_p+\omega_q)\phi_{12}(\psi_{0qxx}^*+\psi_{0qyy}^*) \\
= \;& -i2\omega_p\phi_{12x}\psi_{0qx}^* + i\omega_q\psi_{0q}^*\phi_{12xx} - i(\omega_p+\omega_q)\phi_{12}(\psi_{0qxx}^*+\psi_{0qyy}^*) \\
= \;& -ie^{-x}\cos y\left(i\frac{B_pB_q}{\omega_p\omega_q}\right)\left(i\frac{B_q^*}{\omega_q}\right)\left\{2\omega_p\frac{dG_2}{dx}(2L_q'-L_q) - \omega_q\frac{d^2G_2}{dx^2}L_q\right. \\
& \left. +(\omega_p+\omega_q)G_2(4L_q''-4L_q')\right\} \\
= \;& i\frac{B_pB_qB_q^*}{\omega_p\omega_q^2}e^{-x}\left\{2\omega_p\frac{dG_2}{dx}(2L_q'-L_q) - \omega_q\frac{d^2G_2}{dx^2}L_q + (\omega_p+\omega_q)G_2(4L_q''-4L_q')\right\}\cos y \\
= \;& \hat{h}_{p2}(x)B_pB_qB_q^* \qquad \text{(G.2)}
\end{aligned}$$

$[\mathcal{E}_p\text{-}3]$, $[\mathcal{E}_p\text{-}4]$, $[\mathcal{E}_p\text{-}5]$, $[\mathcal{E}_p\text{-}6]$, $[\mathcal{E}_p\text{-}7]$ and $[\mathcal{E}_p\text{-}8]$ do not change. Similarly,

$[\mathcal{E}_q\text{-}1]$. Instead of (4.48), we now have

$$
\begin{aligned}
& (\phi_{11}, \psi_{0p}) \\
= \; & 2\left\{\phi_{11x}\psi_{0px}\left[-i(\omega_q-\omega_p)-i\omega_p)\right]\right\} - i\omega_p\psi_{0p}\phi_{11xx} - i(\omega_q-\omega_p)\phi_{11}(\psi_{0pxx}+\psi_{0pyy}) \\
= \; & -i2\omega_q\phi_{11x}\psi_{0px} - i\omega_p\psi_{0p}\phi_{11xx} - i(\omega_q-\omega_p)\phi_{11}(\psi_{0pxx}+\psi_{0pyy}) \\
= \; & -ie^{-x}\cos y\left(i\frac{B_p^* B_q}{\omega_p\omega_q}\right)\left(-i\frac{B_p}{\omega_p}\right)\left\{2\omega_q\frac{dG_1}{dx}(2L_p'-L_p)+\omega_p\frac{d^2G_1}{dx^2}L_p\right. \\
& \left. +(\omega_q-\omega_p)G_1(4L_p''-4L_p')\right\} \\
& -ie^{-x}\cos y\left(-i\frac{e^{i2\varphi}}{\omega}\right)\left(-i\frac{B_p}{\omega_p}\right)\left\{2\omega_q\frac{dJ_0}{dx}(2L_p'-L_p)+\omega_p\frac{d^2J_0}{dx^2}L_p\right. \\
& \left. +(\omega_q-\omega_p)J_0(4L_p''-4L_p')\right\} \\
= \; & -i\frac{B_qB_pB_p^*}{\omega_q\omega_p^2}e^{-x}\left\{2\omega_q\frac{dG_1}{dx}(2L_p'-L_p)\right. \\
& \left. +\omega_p\frac{d^2G_1}{dx^2}L_p+(\omega_q-\omega_p)G_1(4L_p''-4L_p')\right\}\cos y \\
& +i\frac{e^{i2\varphi}B_p}{\omega\omega_p}e^{-x}\left\{2\omega_q\frac{dJ_0}{dx}(2L_p'-L_p)+\omega_p\frac{d^2J_0}{dx^2}L_p+(\omega_q-\omega_p)J_0(4L_p''-4L_p')\right\}\cos y \\
= \; & \hat{h}_{q1}(x)B_qB_pB_p^* + ie^{i2\varphi}\hat{f}_q(x)B_p
\end{aligned}
\tag{G.3}
$$

$[\mathcal{E}_q\text{-}2]$. Instead of (4.49), we now have

$$
\begin{aligned}
& (\phi_{12}, \psi_{0p}^*) \\
= \; & 2\left\{\phi_{12x}\psi_{0px}^*\left[-i(\omega_p+\omega_q)+i\omega_p)\right]\right\} + i\omega_p\psi_{0p}^*\phi_{12xx} - i(\omega_p+\omega_q)\phi_{12}(\psi_{0pxx}^*+\psi_{0pyy}^*) \\
= \; & -i2\omega_q\phi_{12x}\psi_{0px}^* + i\omega_p\psi_{0p}^*\phi_{12xx} - i(\omega_p+\omega_q)\phi_{12}(\psi_{0pxx}^*+\psi_{0pyy}^*) \\
= \; & -ie^{-x}\cos y\left(i\frac{B_pB_q}{\omega_p\omega_q}\right)\left(i\frac{B_p^*}{\omega_p}\right)\left\{2\omega_q\frac{dG_2}{dx}(2L_p'-L_p)-\omega_p\frac{d^2G_2}{dx^2}L_p\right. \\
& \left. +(\omega_p+\omega_q)G_2(4L_p''-4L_p')\right\} \\
= \; & i\frac{B_qB_pB_p^*}{\omega_q\omega_p^2}e^{-x}\left\{2\omega_q\frac{dG_2}{dx}(2L_p'-L_p)-\omega_p\frac{d^2G_2}{dx^2}L_p+(\omega_p+\omega_q)G_2(4L_p''-4L_p')\right\}\cos y \\
= \; & \hat{h}_{q2}(x)B_qB_pB_p^*
\end{aligned}
\tag{G.4}
$$

But $[\mathcal{E}_q\text{-}3]$, $[\mathcal{E}_q\text{-}4]$, $[\mathcal{E}_q\text{-}5]$, $[\mathcal{E}_q\text{-}6]$, $[\mathcal{E}_q\text{-}7]$ and $[\mathcal{E}_q\text{-}8]$ do not change.

Then we recall the solvability condition and obtain the governing equations:

$$\frac{\partial B_p}{\partial \tau} = ia_1e^{-i2\varphi}B_q + a_2B_pB_pB_p^* + a_3B_pB_qB_q^*; \tag{G.5}$$

$$\frac{\partial B_q}{\partial \tau} = ib_1 e^{i2\varphi} B_p + b_2 B_q B_q B_q^* + b_3 B_q B_p B_p^*. \tag{G.6}$$

Referring to (4.62) and (4.63) we found that the differences are in the linear terms since they are related to the incident/reflected wave. Therefore, we have different coefficients a_1 and b_1 for different combinations with B_p and B_q. Change of variable from $\bar{B}_j$ to $\bar{B}_j e^{i\varphi}$ eliminates the phase of incident wave from the evolution equation and we get

$$\frac{\partial B_p}{\partial \tau} = ia_1 B_q + a_2 B_p B_p B_p^* + a_3 B_p B_q B_q^*; \tag{G.7}$$

$$\frac{\partial B_q}{\partial \tau} = ib_1 B_p + b_2 B_q B_q B_q^* + b_3 B_q B_p B_p^*. \tag{G.8}$$

G.2 Initial growth

Due to the difference of the linear terms, we expect a different initial evolution of the two edge waves. Ignoring nonlinear terms, Eq. (G.12) and (G.13) becomes

$$\frac{\partial B_p}{\partial \tau} = ia_1 B_q \quad \text{and} \quad \frac{\partial B_q}{\partial \tau} = ib_1 B_p. \tag{G.9}$$

which can be manipulated to get

$$\frac{\partial^2 B_j}{\partial \tau^2} = ib_1 \left(ia_1 B_j \right) = -a_1 b_1 B_j \tag{G.10}$$

The above equation has an eigen solution

$$B_j = B_j(0) e^{\pm i\sqrt{a_1 b_1}\ \tau}, \quad j = p, q \tag{G.11}$$

We now give a_1 and b_1 for several pairs of (p, q), which can be excited by one incident/reflected wave:

- Case (1). $p = 0,\ q = 1;$

$$\omega_p = 1, \quad \omega_q = \sqrt{3}, \quad \omega = \omega_q - \omega_p = \sqrt{3} - 1, \quad L_p(2x) = 1; \quad L_q(2x) = 1 - 2x$$

Therefore from $[\mathcal{E}_p\text{-}1]$ we get

$$\begin{aligned} & ia_1 \\ = & \int_0^\infty dx F_p(x) \left\{ -i \frac{1}{\omega\omega_q} e^{-x} \left[2\omega_p \frac{dJ_0}{dx}(2L_q' - L_q) + \omega_q \frac{d^2 J_0}{dx^2} L_q \right.\right. \\ & \left.\left. -(\omega_q - \omega_p) J_0 (4L_q'' - 4L_q') \right] \right\} \\ = & -i \int_0^\infty dx \frac{e^{-2x}}{\omega\sqrt{3}} \left\{ (4x-6) \frac{dJ_0(2\omega\sqrt{x})}{dx} + \sqrt{3}(1-2x) \frac{d^2 J_0(2\omega\sqrt{x})}{dx^2} \right. \\ & \left. -4cJ_0(2\omega\sqrt{x}) \right\} = 0.0866i \end{aligned}$$

And from $[\mathcal{E}_q\text{-}1]$

$$\begin{aligned} & ib_1 \\ = & \int_0^\infty dx F_q(x) \left\{ i \frac{1}{\omega\omega_p} e^{-x} \left[2\omega_q \frac{dJ_0}{dx}(2L_p' - L_p) + \omega_p \frac{d^2 J_0}{dx^2} L_p \right.\right. \\ & \left.\left. +(\omega_q - \omega_p) J_0 (4L_p'' - 4L_p') \right] \right\} \\ = & -i \int_0^\infty dx \frac{e^{-2x}}{\omega}(1-2x) \left\{ 2\sqrt{3} \frac{dJ_0(2\omega\sqrt{x})}{dx} - \frac{d^2 J_0(2\omega\sqrt{x})}{dx^2} \right\} \\ = & \ 0.1500i \end{aligned}$$

- Case (2). $p = 0, \ q = 2;$

$\omega_p = 1, \ \omega_q = \sqrt{5}, \ \omega = \omega_q - \omega_p = \sqrt{5} - 1, \ L_p(2x) = 1; \ L_q(2x) = 1 - 4x + 2x^2$

Therefore from $[\mathcal{E}_p\text{-}1]$ we get

$$\begin{aligned} & ia_1 \\ = & \int_0^\infty dx F_p(x) \left\{ -i \frac{1}{\omega\omega_q} e^{-x} \left[2\omega_p \frac{dJ_0}{dx}(2L_q' - L_q) + \omega_q \frac{d^2 J_0}{dx^2} L_q \right.\right. \\ & \left.\left. -(\omega_q - \omega_p) J_0 (4L_q'' - 4L_q') \right] \right\} \\ = & -i \int_0^\infty dx \frac{e^{-2x}}{\omega\sqrt{5}} \left\{ (16x - 10 - 4x^2) \frac{dJ_0(2\omega\sqrt{x})}{dx} \right. \\ & \left. +\sqrt{5}(1 - 4x + 2x^2) \frac{d^2 J_0(2\omega\sqrt{x})}{dx^2} - 4c(3-2x) J_0(2\omega\sqrt{x}) \right\} \\ = & \ 0.0751i \end{aligned}$$

And from $[\mathcal{E}_q\text{-}1]$

$$ib_1$$

$$
\begin{aligned}
&= \int_0^\infty dx F_q(x)\left\{i\frac{1}{\omega\omega_p}e^{-x}\left[2\omega_q\frac{dJ_0}{dx}(2L_p'-L_p)+\omega_p\frac{d^2J_0}{dx^2}L_p\right.\right.\\
&\quad \left.\left.+(\omega_q-\omega_p)J_0(4L_p''-4L_p')\right]\right\}\\
&= -i\int_0^\infty dx\frac{e^{-2x}}{\omega}(1-4x+2x^2)\left\{2\sqrt{5}\frac{dJ_0(2\omega\sqrt{x})}{dx}-\frac{d^2J_0(2\omega\sqrt{x})}{dx^2}\right\}\\
&= 0.1680i
\end{aligned}
$$

- Case (3). $p=1,\ q=2;$

$\omega_p=\sqrt{3}, \omega_q=\sqrt{5}, \omega=\omega_q-\omega_p=\sqrt{5}-\sqrt{3}, L_p(2x)=1-2x; L_q(2x)=1-4x+2x^2$

Therefore from [$\mathcal{E}_p$-1] we get

$$
\begin{aligned}
& ia_1\\
&= \int_0^\infty dx F_p(x)\left\{-i\frac{1}{\omega\omega_q}e^{-x}\left[2\omega_p\frac{dJ_0}{dx}(2L_q'-L_q)+\omega_q\frac{d^2J_0}{dx^2}L_q\right.\right.\\
&\quad \left.\left.-(\omega_q-\omega_p)J_0(4L_q''-4L_q')\right]\right\}\\
&= -i\int_0^\infty dx\frac{e^{-2x}}{\omega\sqrt{5}}(1-2x)\left\{\sqrt{3}(16x-10-4x^2)\frac{dJ_0(2\omega\sqrt{x})}{dx}\right.\\
&\quad \left.+\sqrt{5}(1-4x+2x^2)\frac{d^2J_0(2\omega\sqrt{x})}{dx^2}-4c(3-2x)J_0(2\omega\sqrt{x})\right\}\\
&= 0.0647i
\end{aligned}
$$

And from [$\mathcal{E}_q$-1]

$$
\begin{aligned}
& ib_1\\
&= \int_0^\infty dx F_q(x)\left\{i\frac{1}{\omega\omega_p}e^{-x}\left[2\omega_q\frac{dJ_0}{dx}(2L_p'-L_p)+\omega_p\frac{d^2J_0}{dx^2}L_p\right.\right.\\
&\quad \left.\left.+(\omega_q-\omega_p)J_0(4L_p''-4L_p')\right]\right\}\\
&= -i\int_0^\infty dx\frac{e^{-2x}}{\omega\sqrt{3}}(1-4x+2x^2)\left\{\sqrt{5}(6-4x)\frac{dJ_0(2\omega\sqrt{x})}{dx}\right.\\
&\quad \left.-\sqrt{3}(1-2x)\frac{d^2J_0(2\omega\sqrt{x})}{dx^2}+4cJ_0(2\omega\sqrt{x})\right\}\\
&= 0.0671i
\end{aligned}
$$

- Case (4). $p=0,\ q=3;$

$\omega_p=1,\ \omega_q=\sqrt{7},\ \omega=\omega_q-\omega_p=\sqrt{7}-1,\ L_p(2x)=1;\ L_q(2x)=1-6x+6x^2-\frac{4}{3}x^3$

Therefore from [$\mathcal{E}_p$-1] we get

$$\begin{aligned}
& ia_1 \\
= & \int_0^\infty dx F_p(x) \left\{ -i\frac{1}{\omega\omega_q} e^{-x} \left[2\omega_p \frac{dJ_0}{dx}(2L_q' - L_q) + \omega_q \frac{d^2J_0}{dx^2} L_q \right. \right. \\
& \left. \left. -(\omega_q - \omega_p) J_0 (4L_q'' - 4L_q') \right] \right\} \\
= & -i\int_0^\infty dx \frac{e^{-2x}}{\omega\sqrt{7}} \left\{ (36x - 14 - 20x^2 + \frac{8}{3}x^3) \frac{dJ_0(2\omega\sqrt{x})}{dx} \right. \\
& \left. +\sqrt{7}(1 - 6x + 6x^2 - \frac{4}{3}x^3) \frac{d^2J_0(2\omega\sqrt{x})}{dx^2} - 8c(3 - 4x + x^2) J_0(2\omega\sqrt{x}) \right\} \\
= & \ 0.0665i
\end{aligned}$$

And from [$\mathcal{E}_q$-1]

$$\begin{aligned}
& ib_1 \\
= & \int_0^\infty dx F_q(x) \left\{ i\frac{1}{\omega\omega_p} e^{-x} \left[2\omega_q \frac{dJ_0}{dx}(2L_p' - L_p) + \omega_p \frac{d^2J_0}{dx^2} L_p \right. \right. \\
& \left. \left. +(\omega_q - \omega_p) J_0 (4L_p'' - 4L_p') \right] \right\} \\
= & -i\int_0^\infty dx \frac{e^{-2x}}{\omega} (1 - 6x + 6x^2 - \frac{4}{3}x^3) \left\{ 2\sqrt{7} \frac{dJ_0(2\omega\sqrt{x})}{dx} - \frac{d^2J_0(2\omega\sqrt{x})}{dx^2} \right\} \\
= & \ 0.1759i
\end{aligned}$$

- Case (5). $p = 1,\ q = 3;$

$$\omega_p = \sqrt{3}, \quad \omega_q = \sqrt{7}, \quad \omega = \omega_q - \omega_p = \sqrt{7} - \sqrt{3},$$

$$L_p(2x) = 1 - 2x; \quad L_q(2x) = 1 - 6x + 6x^2 - \frac{4}{3}x^3$$

Therefore from [$\mathcal{E}_p$-1] we get

$$\begin{aligned}
& ia_1 \\
= & \int_0^\infty dx F_p(x) \left\{ -i\frac{1}{\omega\omega_q} e^{-x} \left[2\omega_p \frac{dJ_0}{dx}(2L_q' - L_q) + \omega_q \frac{d^2J_0}{dx^2} L_q \right. \right. \\
& \left. \left. -(\omega_q - \omega_p) J_0 (4L_q'' - 4L_q') \right] \right\} \\
= & -i\int_0^\infty dx \frac{e^{-2x}}{\omega\sqrt{7}} (1 - 2x) \left\{ \sqrt{3}(36x - 14 - 20x^2 + \frac{8}{3}x^3) \frac{dJ_0(2\omega\sqrt{x})}{dx} \right. \\
& \left. +\sqrt{7}(1 - 6x + 6x^2 - \frac{4}{3}x^3) \frac{d^2J_0(2\omega\sqrt{x})}{dx^2} - 8c(3 - 4x + x^2) J_0(2\omega\sqrt{x}) \right\} \\
= & \ 0.0607i
\end{aligned}$$

And from $[\mathcal{E}_q\text{-}1]$

$$\begin{aligned}
& ib_1 \\
= & \int_0^\infty dx F_q(x)\left\{i\frac{1}{\omega\omega_p}e^{-x}\left[2\omega_q\frac{dJ_0}{dx}(2L_p'-L_p)+\omega_p\frac{d^2J_0}{dx^2}L_p\right.\right. \\
& \left.\left.+(\omega_q-\omega_p)J_0(4L_p''-4L_p')\right]\right\} \\
= & -i\int_0^\infty dx\frac{e^{-2x}}{\omega\sqrt{3}}(1-6x+6x^2-\frac{4}{3}x^3)\left\{\sqrt{7}(6-4x)\frac{dJ_0(2\omega\sqrt{x})}{dx}\right. \\
& \left.-\sqrt{3}(1-2x)\frac{d^2J_0(2\omega\sqrt{x})}{dx^2}+4cJ_0(2\omega\sqrt{x})\right\} \\
= & 0.0743i
\end{aligned}$$

- Case (6). $p=2,\ q=3;$

$$\omega_p=\sqrt{5},\quad \omega_q=\sqrt{7},\quad \omega=\omega_q-\omega_p=\sqrt{7}-\sqrt{5},$$

$$L_p(2x)=1-4x+2x^2;\quad L_q(2x)=1-6x+6x^2-\frac{4}{3}x^3$$

Therefore from $[\mathcal{E}_p\text{-}1]$ we get

$$\begin{aligned}
& ia_1 \\
= & \int_0^\infty dx F_p(x)\left\{-i\frac{1}{\omega\omega_q}e^{-x}\left[2\omega_p\frac{dJ_0}{dx}(2L_q'-L_q)+\omega_q\frac{d^2J_0}{dx^2}L_q\right.\right. \\
& \left.\left.-(\omega_q-\omega_p)J_0(4L_q''-4L_q')\right]\right\} \\
= & -i\int_0^\infty dx\frac{e^{-2x}}{\omega\sqrt{7}}(1-4x+2x^2)\left\{\sqrt{5}(36x-14-20x^2+\frac{8}{3}x^3)\frac{dJ_0(2\omega\sqrt{x})}{dx}\right. \\
& \left.+\sqrt{7}(1-6x+6x^2-\frac{4}{3}x^3)\frac{d^2J_0(2\omega\sqrt{x})}{dx^2}-8c(3-4x+x^2)J_0(2\omega\sqrt{x})\right\} \\
= & 0.0543i
\end{aligned}$$

And from $[\mathcal{E}_q\text{-}1]$

$$\begin{aligned}
& ib_1 \\
= & \int_0^\infty dx F_q(x)\left\{i\frac{1}{\omega\omega_p}e^{-x}\left[2\omega_q\frac{dJ_0}{dx}(2L_p'-L_p)+\omega_p\frac{d^2J_0}{dx^2}L_p\right.\right. \\
& \left.\left.+(\omega_q-\omega_p)J_0(4L_p''-4L_p')\right]\right\} \\
= & -i\int_0^\infty dx\frac{e^{-2x}}{\omega\sqrt{5}}(1-6x+6x^2-\frac{4}{3}x^3)\left\{\sqrt{7}(10-16x+4x^2)\frac{dJ_0(2\omega\sqrt{x})}{dx}\right. \\
& \left.-\sqrt{5}(1-4x+2x^2)\frac{d^2J_0(2\omega\sqrt{x})}{dx^2}+4c(2x-3)J_0(2\omega\sqrt{x})\right\} \\
= & 0.0643i
\end{aligned}$$

The results for all six cases are summarized in Table G.1:

Table G.1: Coefficients pairs (a_1, b_1) for different edge wave modes combinations. Low frequency incident wave.

		q		
		1	2	3
	0	(0.0866, 0.1500)	(0.0751,0.1680)	(0.0665,0.1759)
p	1		(0.0647,0.0671)	(0.0607,0.743)
	2			(0.0543,0.643)

From Table G.1 we see that, all a_1 and b_1 are positive real numbers, which makes $a_1 b_1$ positive and real for $\omega = \omega_q - \omega_p$. Solution to amplitudes of the two edge wave modes must be periodic, instead of growing or decaying exponentially. Therefore, there is no linear instability of the edge wave perturbations to the incident/reflected wave system.

The nonlinear terms for case $\omega = \omega_q - \omega_p$ is exactly the same as in case $\omega = \omega_q + \omega_p$. Therefore, we have a pair of coupled equations to deal with:

$$\frac{\partial B_p}{\partial \tau} = i a_1 B_q + a_2 B_p B_p B_p^* + a_3 B_p B_q B_q^*; \tag{G.12}$$

$$\frac{\partial B_q}{\partial \tau} = i b_1 B_p + b_2 B_q B_q B_q^* + b_3 B_q B_p B_p^*. \tag{G.13}$$

Coefficients a's and b's are summarized in Table G.2.

G.3 Effects of Detuning

When we consider the effects of detuning, i.e. some sorts of frequency mismatch coming from the incident/reflected wave:

$$\omega \to \omega + \bar{\epsilon}^2 \bar{\Omega}$$

we can always make replacements

$$\bar{A} \to \bar{A} e^{-i\bar{\epsilon}^2 \bar{\Omega} t}$$

Table G.2: Coefficients of a's and b's for $\omega = \omega_q - \omega_p$.

		a_1	a_2	a_3
	(0,1)	0.0866	-0.2302-0.1882i	-0.2393-0.1207i
(p,q)	(0,2)	0.0751	-0.2302-0.1882i	-0.1969+0.2098i
	(1,2)	0.0647	-0.0903-0.0478i	-0.1352-0.0318i
		b_1	b_2	b_3
	(0,1)	0.1500	-0.0501-0.6873i	-0.3925+0.5558i
(p,q)	(0,2)	0.1680	-0.0626-0.0121i	-0.3796+0.8419i
	(1,2)	0.0671	-0.0626-0.0121i	-0.1720+1.2832i

then all the analysis is still the same as in the perfect resonance case. When we look at the evolution equations, (G.12) and (G.13) become

$$\frac{\partial B_p}{\partial \tau} = ia_1 e^{i\bar{\Omega}\tau} B_q + a_2|B_p|^2 B_p + a_3|B_q|^2 B_p \tag{G.14}$$

$$\frac{\partial B_q}{\partial \tau} = ib_1 e^{-i\bar{\Omega}\tau} B_p + b_2|B_q|^2 B_q + b_3|B_p|^2 B_q \tag{G.15}$$

Change of variables $B_j = \bar{B}_j e^{-i\bar{\Omega}_j\tau}$, $j = p, q$ gives

$$\frac{\partial B_j}{\partial \tau} = \left(\frac{\partial \bar{B}_j}{\partial \tau} - i\bar{\Omega}_j \bar{B}_j\right) e^{-i\bar{\Omega}_j\tau}$$

where we require that $\bar{\Omega}_q - \bar{\Omega}_p = \bar{\Omega}$. Therefore, equations (G.14) and (G.15) become

$$\frac{\partial \bar{B}_p}{\partial \tau} = i\bar{\Omega}_p \bar{B}_p + ia_1 \bar{A}^* \bar{B}_q + a_2|\bar{B}_p|^2 \bar{B}_p + a_3|\bar{B}_q|^2 \bar{B}_p \tag{G.16}$$

$$\frac{\partial \bar{B}_q}{\partial \tau} = i\bar{\Omega}_q \bar{B}_q + ib_1 \bar{A} \bar{B}_p + b_2|\bar{B}_q|^2 \bar{B}_q + b_3|\bar{B}_p|^2 \bar{B}_q \tag{G.17}$$

The detuning adds another new term to the evolution equation as in the classical edge wave theory. As in the synchronous resonance analysis, a change of variable will eliminate the phase of incident wave from the evolution equation. For example, we can replace $\bar{B}_p$ by $\bar{B}_p e^{i\varphi}$ and $\bar{B}_q$ by $\bar{B}_q e^{i2\varphi}$, where φ is the phase angle of the incident wave.

G.4 Analysis of nonlinear dynamical system

Replacing $\bar{B}_j$ with its polar form

$$\bar{B}_j = \sqrt{I_j}e^{i\theta_j}, \quad j = p, q$$

we get

$$\frac{\partial \bar{B}_j}{\partial \tau} = \left(\frac{1}{2\sqrt{I_j}}\dot{I}_j + i\sqrt{I_j}\dot{\theta}_j\right)e^{i\theta_j} \tag{G.18}$$

where $I_j = |\bar{B}_j|^2$ is action variable and θ_j is phase variable. Also we introduce the new forms for the complex parameters

$$a_2 = -a_2^r - ia_2^i; \quad b_2 = -b_2^r - ib_2^i; \quad a_3 = -a_3^r - ia_3^i; \quad b_3 = -b_3^r + ib_3^i.$$

Divided by $\bar{B}_p$ on both sides, Equation (G.16) becomes

$$\begin{aligned}
&\frac{1}{\bar{B}_p}\frac{\partial \bar{B}_p}{\partial \tau} \\
= \; & \frac{1}{\sqrt{I_p}e^{i\theta_p}}\left(\frac{1}{2\sqrt{I_p}}\dot{I}_p + i\sqrt{I_p}\dot{\theta}_p\right)e^{i\theta_p} \\
= \; & \frac{1}{2I_p}\dot{I}_p + i\dot{\theta}_p \\
= \; & i\Omega_p + ia_1\frac{\bar{B}_q}{\bar{B}_p} + a_2|\bar{B}_p|^2 + a_3|\bar{B}_q|^2 \\
= \; & i\Omega_p + ia_1\sqrt{\frac{I_q}{I_p}}e^{-i(\theta_p-\theta_q)} + a_2 I_p + a_3 I_q \\
= \; & \left\{a_1\sqrt{\frac{I_q}{I_p}}\sin(\theta_p - \theta_q) - a_2^r I_p - a_3^r I_q\right\} \\
& + i\left\{\Omega_p + a_1\sqrt{\frac{I_q}{I_p}}\cos(\theta_p - \theta_q) - a_2^i I_p - a_3^i I_q\right\}
\end{aligned} \tag{G.19}$$

Separating the real and imaginary parts, we get

$$\frac{1}{2I_p}\dot{I}_p = a_1\sqrt{\frac{I_q}{I_p}}\sin(\theta_p - \theta_q) - a_2^r I_p - a_3^r I_q \tag{G.20}$$

$$\dot{\theta}_p = \Omega_p + a_1\sqrt{\frac{I_q}{I_p}}\cos(\theta_p - \theta_q) - a_2^i I_p - a_3^i I_q \tag{G.21}$$

Similarly we can get from Equation (G.13)

$$\frac{1}{2I_q}\dot{I}_q = -b_1\sqrt{\frac{I_p}{I_q}}\sin(\theta_p - \theta_q) - b_2^r I_q - b_3^r I_p \tag{G.22}$$

$$\dot{\theta}_q = \Omega_q + b_1\sqrt{\frac{I_p}{I_q}}\cos(\theta_p - \theta_q) - b_2^i I_q + b_3^i I_p \tag{G.23}$$

G.5 Fixed point — the equilibrium state

After sufficiently long time evolution, assumes that the dynamic system reaches its equilibrium, i.e. $\frac{\partial}{\partial \tau} = 0$. $(\bar{B}_p, \bar{B}_q) = (0, 0)$ is obviously a fixed point to Equation (G.16) and (G.17). In order to find equilibrium point other than the origin, let the L.H.S. of Equation (G.20) to (G.23) equal to zero. Then we have

$$a_1\sqrt{\frac{I_q}{I_p}}\sin(\theta_p - \theta_q) = a_2^r I_p + a_3^r I_q \tag{G.24}$$

$$\Omega_p + a_1\sqrt{\frac{I_q}{I_p}}\cos(\theta_p - \theta_q) = a_2^i I_p + a_3^i I_q \tag{G.25}$$

$$-b_1\sqrt{\frac{I_p}{I_q}}\sin(\theta_p - \theta_q) = b_2^r I_q + b_3^r I_p \tag{G.26}$$

$$\Omega_q + b_1\sqrt{\frac{I_p}{I_q}}\cos(\theta_p - \theta_q) = b_2^i I_q - b_3^i I_p \tag{G.27}$$

Then we try to eliminate two phase variables and obtain two equations for I_p and I_q:

We can eliminate the phase parts and obtain two equations for I_p^0 and I_q^0:

Eliminating the $\sin(\theta_p - \theta_q)$ function from (G.24) and (G.26), we obtain

$$a_2^r R_0^2 + \left(a_3^r + \frac{a_1}{b_1}b_3^r\right) R_0 + \frac{a_1}{b_1}b_2^r = 0 \tag{G.28}$$

where we have introduced

$$R_0 = \frac{I_p^0}{I_q^0}.$$

The above equation can be solved to get

$$R_0 = \frac{-\frac{a_1}{b_1}b_3^r - a_3^r \pm \sqrt{\left(a_3^r + \frac{a_1}{b_1}b_3^r\right)^2 - 4\frac{a_1}{b_1}a_2^r b_2^r}}{2a_2^r}$$

For example, in Case (1). $p = 0$, $q = 1$,

$$R_0 = -1.9598, \quad \text{or} \quad R_0 = -0.0641.$$

Obviously, none of them is the root we want. Therefore, we don't expect fixed points other than zero. Similar situation holds for the other two cases. In Case (2). $p = 0$, $q = 2$,

$$R_0 = -1.5121, \quad \text{or} \quad R_0 = -0.0804.$$

And in Case (3). $p = 1$, $q = 2$,

$$R_0 = -3.1196, \quad \text{or} \quad R_0 = -0.2143.$$

This tells us that there is no more fixed points other than $(\bar{B}_p, \bar{B}_q)$=(0, 0).

Can we have limit cycle as equilibrium? If so, we can always make change of variables

$$\bar{B}_p \rightarrow \hat{B}_p e^{i\hat{\Omega}_p \tau}, \quad \bar{B}_q \rightarrow \hat{B}_q e^{i\hat{\Omega}_q \tau}$$

Then Eq. (G.16) and (G.17) become

$$\frac{\partial B_p}{\partial \tau} = i(\Omega_p - \hat{\Omega}_p)B_p + ia_1 B_q + a_2|B_p|^2 B_p + a_3|B_q|^2 B_p \tag{G.29}$$

$$\frac{\partial B_q}{\partial \tau} = i(\Omega_q - \hat{\Omega}_q)B_q + ib_1 B_p + b_2|B_q|^2 B_q + b_3|B_p|^2 B_q \tag{G.30}$$

As a result, this change of variable will affect (G.25) and (G.25) only. Like detuning wouldn't affect the ratio of the two edge wave amplitudes, we don't expect limit cycle as the equilibrium either.

Appendix H

Numerical solution by finite element method for cross resonance

From the analysis of Section 4.4.2, we found that the 4 harmonics of trapped waves share the same form of BVP as follows:

$$-\frac{d}{dx}\left(p(x)f_x\right) + q(x)f = -g(x)$$

with the boundary conditions

$$xf_x = 0 \quad \text{as} \quad x \to 0$$

$$xf_x = 0 \quad \text{as} \quad x \to L$$

and

$$p(x) = x, \quad q(x) = 4x - \bar{\omega}^2$$

The parameter $\bar{\omega}$ takes different values according to the harmonics.

It is easy to show that the boundary-value problem above is equivalent to the stationarity of the following functional

$$\mathcal{F}(f) = \overbrace{\frac{1}{2}\int_0^L \left[p(x)\left(\frac{df}{dx}\right)^2 + q(x)f^2\right] dx}^{I_1} + \underbrace{\int_0^L gf dx}_{I_2} \tag{H.1}$$

Please refer to Appendix E for proof of the equivalence. Notice that we have different definition for $q(x)$ in this problem. We still need develop the finite element formula in order to account for this difference.

We discretize a large but finite region by standard 2-node elements (see Figure E) with piece-wise linear potentials :

Within each element $x \in [x_1, x_2]$:

$$f = \sum_{i=1}^{2} f_i N_i(x) \tag{H.2}$$

where f_i is an unknown nodal potential and $N_i(x)$ is a interpolation function

$$N_1 = \frac{x_2 - x}{h}; \quad N_2 = \frac{x - x_1}{h} \tag{H.3}$$

and h is the element length, i.e. $h = x_2 - x_1$.

In matrix form,

$$f = \begin{bmatrix} N_1 & N_2 \end{bmatrix} \begin{bmatrix} f_1 \\ f_2 \end{bmatrix} = \mathbf{N}\left\{\hat{f}\right\} \tag{H.4}$$

therefore,

$$\frac{df}{dx} = \begin{bmatrix} \frac{dN_1}{dx} & \frac{dN_2}{dx} \end{bmatrix} \begin{bmatrix} f_1 \\ f_2 \end{bmatrix} = \begin{bmatrix} -\frac{1}{h} & \frac{1}{h} \end{bmatrix} \begin{bmatrix} f_1 \\ f_2 \end{bmatrix} = \mathbf{B}\left\{\hat{f}\right\} \tag{H.5}$$

Now we can evaluate the two integrals of functional $\mathcal{F}$:

- I_1

$$\frac{1}{2}\int_{el}\left[p(x)\left(\frac{df}{dx}\right)^2 + q(x)f^2\right]dx = \frac{1}{2}\{\hat{f}\}^T [K]^{el}\{\hat{f}\}$$

where $[K]^{el}$ is the element stiffness matrix

$$[K]^{el}_{ij} = \frac{(-1)^{i+j}}{h^2}\int_{x_1}^{x_2} p dx + \int_{x_1}^{x_2} qN_iN_j dx$$

with

$$\frac{(-1)^{i+j}}{h^2}\int_{x_1}^{x_2} p dx = (-1)^{i+j}\frac{x_1 + x_2}{2h}$$

$$\int_{x_1}^{x_2} qN_1N_1 dx = \frac{4}{h^2}\left[\frac{1}{4}x^4 - \frac{2}{3}x_2x^3 + \frac{1}{2}x_2^2x^2\right]_{x_1}^{x_2} - \frac{\bar{\omega}^2}{h^2}\left[\frac{1}{3}x^3 - x_2x^2 + x_2^2x\right]_{x_1}^{x_2}$$

$$\int_{x_1}^{x_2} qN_2N_2 dx = \frac{4}{h^2}\left[\frac{1}{4}x^4 - \frac{2}{3}x_1x^3 + \frac{1}{2}x_1^2x^2\right]_{x_1}^{x_2} - \frac{\bar{\omega}^2}{h^2}\left[\frac{1}{3}x^3 - x_1x^2 + x_1^2x\right]_{x_1}^{x_2}$$

$$\int_{x_1}^{x_2} qN_1N_2dx$$
$$= \frac{4}{h^2}\left[-\frac{x^4}{4}+\frac{x_1+x_2}{3}x^3-\frac{x_1x_2}{2}x^2\right]_{x_1}^{x_2} - \frac{\bar{\omega}^2}{h^2}\left[-\frac{x^3}{3}+\frac{x_1+x_2}{2}x^2-x_1x_2x\right]_{x_1}^{x_2}$$

After assemblage and using the global $\hat{f}$, we can get

$$I_1 = \frac{1}{2}\left\{\hat{f}\right\}^T [K] \left\{\hat{f}\right\}$$

- I_2

$$\int_{el} gf dx = \{\hat{f}\}^T [G]^{el}$$

where $[G]^{el}$ is the element load vector

$$[G]_i^{el} = \int_{x_1}^{x_2} gN_i dx, \quad i = 1, 2$$

After assemblage and using the global $\hat{f}$, we can get

$$I_2 = \left\{\hat{f}\right\}^T [G]$$

In summary, the stationary functional becomes

$$\mathcal{F}(\left\{\hat{f}\right\}) = \frac{1}{2}\left\{\hat{f}\right\}^T [K] \left\{\hat{f}\right\} + \left\{\hat{f}\right\}^T [G] \tag{H.6}$$

By Rayleigh-Ritz principle, the first derivative of $\mathcal{F}$ with respect to unknowns f_i vanishes. Therefore

$$[K]\left\{\hat{f}\right\} + [G] = 0 \tag{H.7}$$

which can be solved to get the numerical solution of $f = \left\{\hat{f}\right\} = -[K]^{-1}[G]$ within the range of $x \in [0, L]$. Beyond L, $f = 0$ uniformly.

Appendix I

The coefficients c's and d's for other two cases

I.1 Case (2). $p = 0,\ q = 2$

Now we have

$$\omega_p = 1,\ \omega_q = \sqrt{5},\ \omega = \omega_p + \omega_q = \sqrt{5} + 1,\ L_p(2x) = 1;\ L_q(2x) = (1 - 4x + 2x^2)$$

We already knew from Table 4.2 that $c_1 = 0.1056$ and $d_1 = 0.2360$ from previous discussion.

$$\begin{aligned} & f_1(x) \\ = \ & (\omega_p - \omega_q)(4L_p'L_q' - 2L_q'L_p - 2L_p'L_q) + \frac{1}{2}\left[\omega_p L_p \left(4L_q'' - 4L_q'\right) - \omega_q L_q \left(4L_p'' - 4L_p'\right)\right] \\ = \ & (-8 + 4\sqrt{5})x + 10 - 4\sqrt{5}, \end{aligned}$$

$$g_1(x) = f_1(x) + 2(\omega_p - \omega_q)L_p L_q = (4 - 4\sqrt{5})x^2 + (-16 + 12\sqrt{5})x + 12 - 6\sqrt{5};$$

$$\begin{aligned} & f_2(x) \\ = \ & (\omega_p + \omega_q)(4L_p'L_q' - 2L_q'L_p - 2L_p'L_q) + \frac{1}{2}\left[\omega_p L_p \left(4L_q'' - 4L_q'\right) + \omega_q L_q \left(4L_p'' - 4L_p'\right)\right] \\ = \ & (-4\sqrt{5} - 8)x + 4\sqrt{5} + 10, \end{aligned}$$

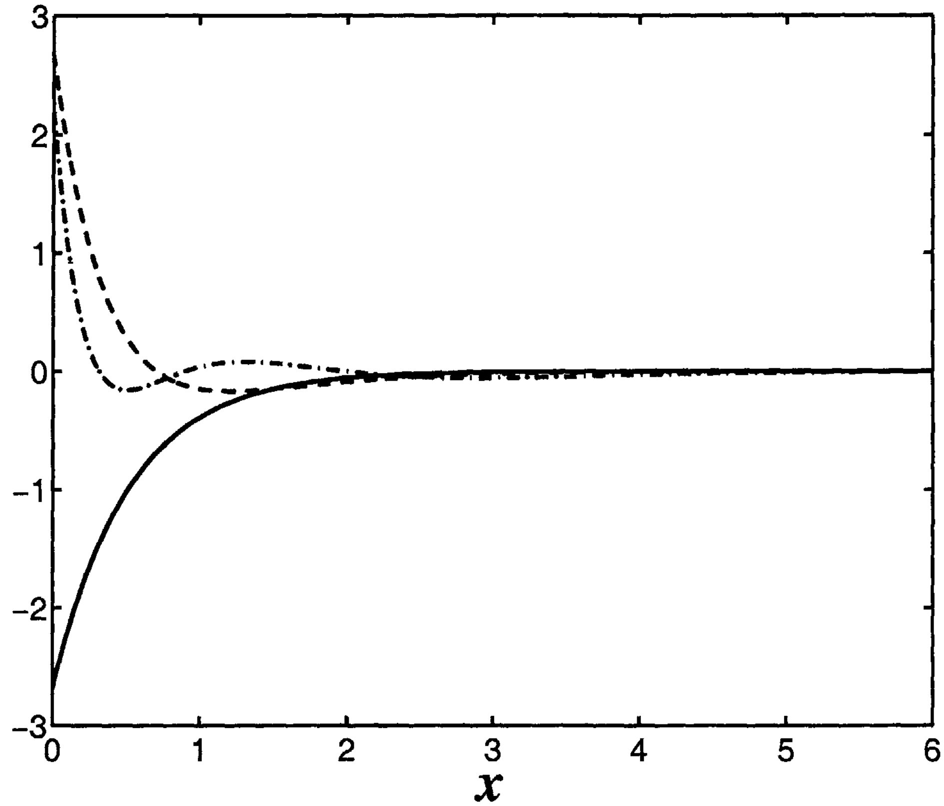

Figure I-1: Numerical solutions to f_{11}— solid line, f_{12}— dash line, and f_{14}— dash-dot line for Case (2). $p = 0,\ q = 2$.

$$g_2(x) = f_2(x) + 2(\omega_p + \omega_q)L_pL_q = (4\sqrt{5}+4)x^2 + (-12\sqrt{5}-16)x + 6\sqrt{5} + 12;$$

$$f_3(x) = 2L_p'^2 - 6L_pL_p' + 2L_pL_p'' = 0,$$

$$g_3(x) = f_3(x) + 2L_p^2 = 2;$$

$$f_4(x) = 2L_q'^2 - 6L_qL_q' + 2L_qL_q'' = -24x^3 + 92x^2 - 100x + 30,$$

$$g_4(x) = f_4(x) + 2L_q^2 = 8x^4 - 56x^3 + 132x^2 - 116x + 32.$$

Numerical solutions to f_{11}, f_{12} and f_{14} are plotted in Figure I-1. Again, $f_{13} = 0$ due to the forcing $f_3(x) = 0$ in this case. Our numerical results show that all of them are close to zero after $x > 6$.

Other c's from $\mathcal{E}_p$:

$[\mathcal{E}_p\text{-}1]$.

$$
\begin{aligned}
& c_{31} \\
= & \int_0^\infty dx F_p(x) \left\{ i \frac{1}{\omega_p \omega_q^2} e^{-x} \left[2\omega_p \frac{dG_1}{dx}(2L_q' - L_q) + \omega_q \frac{d^2 G_1}{dx^2} L_q \right.\right. \\
& \left.\left. -(\omega_q - \omega_p) G_1 (4L_q'' - 4L_q') \right] \right\} \\
= & \frac{i}{5} \int_0^\infty dx e^{-2x} \left\{ (-4x^2 + 16x - 10) \frac{dG_1}{dx} + \sqrt{5}(1 - 4x + 2x^2) \frac{d^2 G_1}{dx^2} \right. \\
& \left. -(\sqrt{5} - 1)(12 - 8x) G_1 \right\} \\
= & \frac{i}{5} \left\{ -\sqrt{5} \frac{dG_1}{dx}(0) - (6\sqrt{5} - 10) G_1(0) \right. \\
& \left. + \int_0^\infty dx e^{-2x} \left[(8\sqrt{5} - 8)x^2 + (32 - 24\sqrt{5})x + 12\sqrt{5} - 24 \right] G_1 \right\} \\
= & \frac{i}{5} \left\{ -\sqrt{5} g_1(0) + \alpha \right\} = -0.0135 + 0.5504i
\end{aligned} \tag{I.1}
$$

where use has been made of relation (4.33). And the generic form for the integral by part is

$$\int_0^\infty dx f(x) e^{-2x} \frac{dG}{dx} = -f(0)G(0) - \int_0^\infty dx (f' - 2f) e^{-2x} G.$$

The integral α can be evaluated as

$$
\begin{aligned}
\alpha &= \int_0^\infty dx e^{-2x} \left[(8\sqrt{5} - 8)x^2 + (32 - 24\sqrt{5})x + 12\sqrt{5} - 24 \right] G_1 \\
&= \sum_{j=1}^{4} \alpha_j = -0.4150 + 0.0677i
\end{aligned} \tag{I.2}
$$

where

$$
\begin{aligned}
\alpha_1 &= \pi \int_0^\infty dx e^{-2x} \left[(8\sqrt{5} - 8)x^2 + (32 - 24\sqrt{5})x + 12\sqrt{5} - 24 \right] J_0(2\bar{\omega}\sqrt{x}) \\
& \int_0^\infty d\xi e^{-2\xi} g_1(\xi) Y_0(2\bar{\omega}\sqrt{\xi}) = -0.3023
\end{aligned}
$$

$$
\begin{aligned}
\alpha_2 &= -\pi \int_0^\infty dx e^{-2x} \left[(8\sqrt{5} - 8)x^2 + (32 - 24\sqrt{5})x + 12\sqrt{5} - 24 \right] J_0(2\bar{\omega}\sqrt{x}) \\
& \int_0^x d\xi e^{-2\xi} g_1(\xi) Y_0(2\bar{\omega}\sqrt{\xi}) = 0.0948
\end{aligned}
$$

$$
\begin{aligned}
\alpha_3 &= -i\pi \int_0^\infty dx e^{-2x} \left[(8\sqrt{5} - 8)x^2 + (32 - 24\sqrt{5})x + 12\sqrt{5} - 24 \right] J_0(2\bar{\omega}\sqrt{x}) \\
& \int_0^\infty d\xi e^{-2\xi} g_1(\xi) J_0(2\bar{\omega}\sqrt{\xi}) = 0.0677i
\end{aligned}
$$

$$\alpha_4 = \pi \int_0^\infty dx e^{-2x} \left[(8\sqrt{5}-8)x^2 + (32-24\sqrt{5})x + 12\sqrt{5} - 24 \right] Y_0(2\bar{\omega}\sqrt{x}) \int_0^x d\xi e^{-2\xi} g_1(\xi) J_0(2\bar{\omega}\sqrt{\xi}) = -0.2075$$

with $\bar{\omega} = \sqrt{5} - 1$. Refer to (4.30) for the generic form of solution G_1.

[$\mathcal{E}_p$-2].

$$\begin{aligned}
& c_{32} \\
= & \int_0^\infty dx F_p(x) \left\{ i \frac{1}{\omega_p \omega_q^2} e^{-x} \left[2\omega_p \frac{dG_2}{dx}(2L_q' - L_q) - \omega_q \frac{d^2 G_2}{dx^2} L_q \right. \right. \\
& \left. \left. + (\omega_p + \omega_q) G_2 (4L_q'' - 4L_q') \right] \right\} \\
= & \frac{i}{5} \int_0^\infty dx e^{-2x} \left\{ (-4x^2 + 16x - 10) \frac{dG_2}{dx} - \sqrt{5}(1 - 4x + 2x^2) \frac{d^2 G_2}{dx^2} \right. \\
& \left. + (\sqrt{5} + 1)(12 - 8x) G_2 \right\} \\
= & \frac{i}{5} \left\{ \sqrt{5} \frac{dG_2}{dx}(0) + (6\sqrt{5} + 10) G_2(0) \right. \\
& \left. + \int_0^\infty dx e^{-2x} \left[(-8\sqrt{5} - 8)x^2 + (32 + 24\sqrt{5})x - 12\sqrt{5} - 24 \right] G_2 \right\} \\
= & \frac{i}{5} \left\{ \sqrt{5} g_2(0) + \beta \right\} = -0.1833 + 7.0219i
\end{aligned} \tag{I.3}$$

The integral β can be evaluated as

$$\begin{aligned}
\beta &= \int_0^\infty dx e^{-2x} \left[(-8\sqrt{5} - 8)x^2 + (32 + 24\sqrt{5})x - 12\sqrt{5} - 24 \right] G_2 \\
&= \sum_{j=1}^{4} \beta_j = -21.7234 + 0.9166i
\end{aligned} \tag{I.4}$$

where

$$\beta_1 = \pi \int_0^\infty dx e^{-2x} \left[(-8\sqrt{5} - 8)x^2 + (32 + 24\sqrt{5})x - 12\sqrt{5} - 24 \right] J_0(2\bar{\omega}\sqrt{x}) \int_0^\infty d\xi e^{-2\xi} g_2(\xi) Y_0(2\bar{\omega}\sqrt{\xi}) = -3.0316$$

$$\beta_2 = -\pi \int_0^\infty dx e^{-2x} \left[(-8\sqrt{5} - 8)x^2 + (32 + 24\sqrt{5})x - 12\sqrt{5} - 24 \right] J_0(2\bar{\omega}\sqrt{x}) \int_0^x d\xi e^{-2\xi} g_2(\xi) Y_0(2\bar{\omega}\sqrt{\xi}) = -7.8277$$

$$\beta_3 = -i\pi \int_0^\infty dx e^{-2x} \left[(-8\sqrt{5} - 8)x^2 + (32 + 24\sqrt{5})x - 12\sqrt{5} - 24 \right] J_0(2\bar{\omega}\sqrt{x}) \int_0^\infty d\xi e^{-2\xi} g_2(\xi) J_0(2\bar{\omega}\sqrt{\xi}) = 0.9166i$$

$$\beta_4 = \pi \int_0^\infty dx e^{-2x} \left[(-8\sqrt{5}-8)x^2 + (32+24\sqrt{5})x - 12\sqrt{5} - 24 \right] Y_0(2\bar{\omega}\sqrt{x})$$
$$\int_0^x d\xi e^{-2\xi} g_2(\xi) J_0(2\bar{\omega}\sqrt{\xi}) = -10.8641$$

with $\bar{\omega} = \sqrt{5}+1$. Refer to (4.30) for the generic form of solution G_2.

$[\mathcal{E}_p$-3].

$$\begin{aligned}
& c_{21} \\
&= \int_0^\infty dx F_p(x) \left\{ i\frac{1}{\omega_p} e^{-x} \left[2\frac{dG_3}{dx}(2L_p' - L_p) - \frac{d^2G_3}{dx^2} L_p + 2G_3(4L_p'' - 4L_p') \right] \right\} \\
&= i \int_0^\infty dx e^{-2x} \left\{ -2\frac{dG_3}{dx} - \frac{d^2G_3}{dx^2} \right\} \\
&= i \left\{ \frac{dG_3}{dx}(0) + 4G_3(0) - 8\int_0^\infty dx e^{-2x} G_3 \right\} \\
&= i \{ g_3(0) - 8\gamma \} = -0.2302 + 0.5618i
\end{aligned}$$

The integral γ can be evaluated as

$$\gamma = \int_0^\infty dx e^{-2x} G_3 = \sum_{j=1}^4 \gamma_j = 0.1798 - 0.0288i$$

where

$$\begin{aligned}
\gamma_1 &= \pi \int_0^\infty dx e^{-2x} J_0(2\bar{\omega}\sqrt{x}) \int_0^\infty d\xi e^{-2\xi} g_3(\xi) Y_0(2\bar{\omega}\sqrt{\xi}) = 0.0454 \\
\gamma_2 &= -\pi \int_0^\infty dx e^{-2x} J_0(2\bar{\omega}\sqrt{x}) \int_0^x d\xi e^{-2\xi} g_3(\xi) Y_0(2\bar{\omega}\sqrt{\xi}) = 0.0445 \\
\gamma_3 &= -i\pi \int_0^\infty dx e^{-2x} J_0(2\bar{\omega}\sqrt{x}) \int_0^\infty d\xi e^{-2\xi} g_3(\xi) J_0(2\bar{\omega}\sqrt{\xi}) = -0.0288i \\
\gamma_4 &= \pi \int_0^\infty dx e^{-2x} Y_0(2\bar{\omega}\sqrt{x}) \int_0^x d\xi e^{-2\xi} g_3(\xi) J_0(2\bar{\omega}\sqrt{\xi}) = 0.0899
\end{aligned}$$

with $\bar{\omega} = 2$. Refer to (4.30) for the generic form of solution G_3.

$[\mathcal{E}_p$-4].

$$\begin{aligned}
& c_{33} \\
&= \int_0^\infty dx F_p(x) \left\{ \frac{ie^{-x}}{\omega_p \omega_q^2} \left[\frac{\omega_q}{2} L_q f_{11xx} + \omega_p(2L_q' - L_q) f_{11x} \right. \right. \\
&\quad \left. \left. - \frac{\omega_q - \omega_p}{2}(4L_q'' - 4L_q' + 4L_q) f_{11} \right] \right\} \\
&= \frac{i}{5} \left\{ -\frac{\sqrt{5}}{2} f_{11x}(0) - (3\sqrt{5} - 5) f_{11}(0) \right. \\
&\quad \left. + \int_0^\infty dx e^{-2x} \left[(-4\sqrt{5}+8)x + 4\sqrt{5} - 10 \right] f_{11} \right\} = -0.0587i
\end{aligned}$$

[$\mathcal{E}_p$-5].

$$
\begin{aligned}
& c_{34} \\
= & \int_0^\infty dx F_p(x) \left\{ \frac{ie^{-x}}{\omega_p \omega_q^2} \left[\omega_p (2L_q' - L_q) f_{12x} - \frac{\omega_q}{2} L_q f_{12xx} \right.\right. \\
& \left.\left. + \frac{\omega_p + \omega_q}{2} (4L_q'' - 4L_q' + 4L_q) f_{12} \right] \right\} \\
= & \frac{i}{5} \left\{ \frac{\sqrt{5}}{2} f_{12x}(0) + (3\sqrt{5} + 5) f_{12}(0) \right. \\
& \left. + \int_0^\infty dx e^{-2x} \left[(4\sqrt{5} + 8)x - 4\sqrt{5} - 10 \right] f_{12} \right\} = 2.7587i
\end{aligned}
$$

[$\mathcal{E}_p$-6].

$$
\begin{aligned}
& c_{22} \\
= & \int_0^\infty dx F_p(x) \left\{ i \frac{1}{\omega_p} e^{-x} \left[f_{13x} (2L_p' - L_p) - \frac{1}{2} L_p f_{13xx} + f_{13} (4L_p'' - 4L_p' + 4L_p) \right] \right\} \\
= & i \int_0^\infty dx e^{-2x} \left\{ -f_{13x} - \frac{1}{2} f_{13xx} + 4 f_{13} \right\} \\
= & i \left\{ \frac{1}{2} f_{13x}(0) + 2 f_{13}(0) \right\} = 0
\end{aligned}
$$

[$\mathcal{E}_p$-7].

$$
\begin{aligned}
& c_{23} \\
= & \int_0^\infty dx F_p(x) \left\{ -i \frac{1}{\omega_p^3} e^{-3x} \left[\frac{27}{8} (4L_p'' - 4L_p' + L_p)(2L_p' - L_p)^2 - \frac{9}{8} (2L_p' - L_p)^2 L_p \right.\right. \\
& \left.\left. + \frac{3}{2} (2L_p' - L_p)^2 L_p + \frac{3}{8} (4L_p'' - 4L_p' + L_p) L_p^2 - \frac{9}{8} L_p^3 \right] \right\} \\
= & -i \int_0^\infty dx e^{-4x} \left\{ \frac{27}{8} - \frac{9}{8} + \frac{3}{2} + \frac{3}{8} - \frac{9}{8} \right\} \\
= & -3i \int_0^\infty dx e^{-4x} \\
= & -\frac{3i}{4}
\end{aligned}
$$

[$\mathcal{E}_p$-8].

$$
\begin{aligned}
& c_{35} \\
= & \int_0^\infty -i \frac{1}{\omega_p \omega_q^2} e^{-3x} \left\{ \frac{3}{4} \left[3(4L_p'' - 4L_p' + L_p)(2L_q' - L_q)^2 - (2L_q' - L_q)^2 L_p \right.\right. \\
& \left. + 6(4L_q'' - 4L_q' + L_q)(2L_q' - L_q)(2L_p' - L_p) - 2L_q (2L_p' - L_p)(2L_q' - L_q) \right]
\end{aligned}
$$

$$
\begin{aligned}
&+\frac{1}{4}\Big[8(2L_p'-L_p)(2L_q'-L_q)L_q+4(2L_q'-L_q)^2L_p \\
&-9L_pL_q^2+(4L_p''-4L_p'+L_p)L_q^2+2(4L_q''-4L_q'+L_q)L_pL_q\Big]\Big\}F_p(x)dx \\
= &-\frac{i}{5}\int_0^\infty dxe^{-4x}\Big\{24x^4-256x^3+824x^2-968x+362\Big\} \\
= &-\frac{161i}{16}
\end{aligned}
$$

Therefore,

$$c_2 \equiv c_{21}+c_{22}+c_{23} = -0.2302-0.1882i;$$

$$c_3 \equiv c_{31}+c_{32}+c_{33}+c_{34}+c_{35} = -0.1969+0.2098i.$$

Other d's from $\mathcal{E}_q$:

[$\mathcal{E}_q$-1].

$$
\begin{aligned}
&d_{31} \\
= &\int_0^\infty dxF_q(x)\left\{\frac{ie^{-x}}{\omega_q\omega_p^2}\left[2\omega_q\frac{dG_1}{dx}(2L_p'-L_p)+\omega_p\frac{d^2G_1}{dx^2}L_p\right.\right. \\
&\left.\left.+(\omega_q-\omega_p)G_1(4L_p''-4L_p')\right]\right\} \\
= &\frac{i}{\sqrt{5}}\left\{-\frac{dG_1}{dx}(0)-(6-2\sqrt{5})G_1(0)\right. \\
&\left.+\int_0^\infty dxe^{-2x}\left[(8-8\sqrt{5})x^2+(24\sqrt{5}-32)x+24-12\sqrt{5}\right]G_1\right\} \\
= &\frac{i}{\sqrt{5}}\{-g_1(0)-\alpha\} = 0.0303+0.8190i
\end{aligned}
$$

α is defined in (I.1) and evaluated in (I.2).

[$\mathcal{E}_q$-2].

$$
\begin{aligned}
&d_{32} \\
= &\int_0^\infty dxF_q(x)\left\{\frac{ie^{-x}}{\omega_q\omega_p^2}\left[2\omega_q\frac{dG_2}{dx}(2L_p'-L_p)-\omega_p\frac{d^2G_2}{dx^2}L_p\right.\right. \\
&\left.\left.+(\omega_p+\omega_q)G_2(4L_p''-4L_p')\right]\right\} \\
= &\frac{i}{\sqrt{5}}\left\{\frac{dG_2}{dx}(0)+(6+2\sqrt{5})G_2(0)\right. \\
&\left.+\int_0^\infty dxe^{-2x}\left[(-8\sqrt{5}-8)x^2+(24\sqrt{5}+32)x-12\sqrt{5}-24\right]G_2\right\} \\
= &\frac{i}{\sqrt{5}}\{g_2(0)+\beta\} = -0.4099+1.6516i
\end{aligned}
$$

β is defined in (I.3) and evaluated in (I.4).

[$\mathcal{E}_q$-3].

$$\begin{aligned}
& d_{21} \\
= & \int_0^\infty dx F_q(x) \left\{ \frac{i}{\omega_q} e^{-x} \left[2\frac{dG_4}{dx}(2L_q' - L_q) - \frac{d^2G_4}{dx^2} L_q + 2G_4(4L_q'' - 4L_q') \right] \right\} \\
= & \frac{i}{\sqrt{5}} \left\{ \frac{dG_4}{dx}(0) + 20G_4(0) \right. \\
& \left. + \int_0^\infty dx e^{-2x} \left[-32x^4 + 224x^3 - 528x^2 + 464x - 128 \right] G_4 \right\} \\
= & \frac{i}{\sqrt{5}} \{ g_4(0) + \kappa \} = -0.0626 + 4.7096i
\end{aligned}$$

The integral κ can be evaluated as

$$\begin{aligned}
\kappa &= \int_0^\infty dx e^{-2x} \left[-32x^4 + 224x^3 - 528x^2 + 464x - 128 \right] G_4 \\
&= \sum_{j=1}^4 \kappa_j = -21.4691 + 0.1400i
\end{aligned}$$

where

$$\begin{aligned}
\kappa_1 = & \pi \int_0^\infty dx e^{-2x} \left[-32x^4 + 224x^3 - 528x^2 + 464x - 128 \right] J_0(2\bar{\omega}\sqrt{x}) \\
& \int_0^\infty d\xi e^{-2\xi} g_4(\xi) Y_0(2\bar{\omega}\sqrt{\xi}) = -1.0838
\end{aligned}$$

$$\begin{aligned}
\kappa_2 = & -\pi \int_0^\infty dx e^{-2x} \left[-32x^4 + 224x^3 - 528x^2 + 464x - 128 \right] J_0(2\bar{\omega}\sqrt{x}) \\
& \int_0^x d\xi e^{-2\xi} g_4(\xi) Y_0(2\bar{\omega}\sqrt{\xi}) = -9.6430
\end{aligned}$$

$$\begin{aligned}
\kappa_3 = & -i\pi \int_0^\infty dx e^{-2x} \left[-32x^4 + 224x^3 - 528x^2 + 464x - 128 \right] J_0(2\bar{\omega}\sqrt{x}) \\
& \int_0^\infty d\xi e^{-2\xi} g_4(\xi) J_0(2\bar{\omega}\sqrt{\xi}) = 0.1400i
\end{aligned}$$

$$\begin{aligned}
\kappa_4 = & \pi \int_0^\infty dx e^{-2x} \left[-32x^4 + 224x^3 - 528x^2 + 464x - 128 \right] Y_0(2\bar{\omega}\sqrt{x}) \\
& \int_0^x d\xi e^{-2\xi} g_4(\xi) J_0(2\bar{\omega}\sqrt{\xi}) = -10.7423
\end{aligned}$$

with $\bar{\omega} = 2\sqrt{5}$. Refer to (4.30) for the generic form of solution G_4.

$[\mathcal{E}_q\text{-}4]$.

$$
\begin{aligned}
& d_{33} \\
= & \int_0^\infty dx F_q(x)\left\{\frac{ie^{-x}}{\omega_q\omega_p^2}\left[\frac{\omega_p}{2}L_p f_{11xx}+\omega_q(2L'_p-L_p)f_{11x}\right.\right. \\
& \left.\left. +\frac{\omega_q-\omega_p}{2}f_{11}(4L''_p-4L'_p+4L_p)\right]\right\} \\
= & \frac{i}{\sqrt{5}}\left\{-\frac{1}{2}f_{11x}(0)-(3-\sqrt{5})f_{11}(0)\right. \\
& \left. +\int_0^\infty dx e^{-2x}\left[(4\sqrt{5}-8)x+10-4\sqrt{5}\right]f_{11}\right\}=-0.6326i
\end{aligned}
$$

$[\mathcal{E}_q\text{-}5]$.

$$
\begin{aligned}
& d_{34} \\
= & \int_0^\infty dx F_q(x)\left\{\frac{ie^{-x}}{\omega_q\omega_p^2}\left[\omega_q(2L'_p-L_p)f_{12x}-\frac{\omega_p}{2}L_p f_{12xx}\right.\right. \\
& \left.\left. +\frac{\omega_p+\omega_q}{2}f_{12}(4L''_p-4L'_p+4L_p)\right]\right\} \\
= & \frac{i}{\sqrt{5}}\left\{\frac{1}{2}f_{12x}(0)+(3+\sqrt{5})f_{12}(0)\right. \\
& \left. +\int_0^\infty dx e^{-2x}\left[(4\sqrt{5}+8)x-4\sqrt{5}-10\right]f_{12}\right\}=0.9326i
\end{aligned}
$$

$[\mathcal{E}_q\text{-}6]$.

$$
\begin{aligned}
& d_{22} \\
= & \int_0^\infty dx F_q(x)\left\{\frac{i}{\omega_q}e^{-x}\left[(2L'_q-L_q)f_{14x}-\frac{1}{2}L_q f_{14xx}+(4L''_q-4L'_q+4L_q)f_{14}\right]\right\} \\
= & \frac{i}{\sqrt{5}}\left\{\frac{1}{2}f_{14x}(0)+10f_{14}(0)\right. \\
& \left. +\int_0^\infty dx e^{-2x}\left[48x^3-184x^2+200x-60\right]f_{14}\right\}=2.2695i
\end{aligned}
$$

$[\mathcal{E}_q\text{-}7]$.

$$
\begin{aligned}
& d_{23} \\
= & \int_0^\infty -i\frac{1}{\omega_q^3}e^{-3x}\left\{\left[\frac{27}{8}(4L''_q-4L'_q+L_q)(2L'_q-L_q)^2-\frac{9}{8}(2L'_q-L_q)^2L_q\right]\right. \\
& \left. +\left[\frac{3}{2}(2L'_q-L_q)^2L_q+\frac{3}{8}(4L''_q-4L'_q+L_q)L_q^2-\frac{9}{8}L_q^3\right]\right\}F_q(x)dx \\
= & -\frac{i}{5\sqrt{5}}\int_0^\infty dx e^{-4x}\left\{48x^8-864x^7+5832x^6-20112x^5\right.
\end{aligned}
$$

$$+39180x^4 - 44184x^3 + 28038x^2 - 9060x + 1110\Big\}$$

$$= -\frac{2001i}{128\sqrt{5}}$$

$[\mathcal{E}_q\text{-}8]$.

$$\begin{aligned} & d_{35} \\ = & \int_0^\infty -i\frac{1}{\omega_q\omega_p^2}e^{-3x}\left\{\frac{3}{4}\left[3(4L_q'' - 4L_q' + L_q)(2L_p' - L_p)^2 - (2L_p' - L_p)^2 L_q\right.\right. \\ & + 6(4L_p'' - 4L_p' + L_p)(2L_p' - L_p)(2L_q' - L_q) - 2L_p(2L_q' - L_q)(2L_p' - L_p)\Big] \\ & + \frac{1}{4}\Big[8(2L_q' - L_q)(2L_p' - L_p)L_p + 4(2L_p' - L_p)^2 L_q \\ & \left.\left. - 9L_qL_p^2 + (4L_q'' - 4L_q' + L_q)L_p^2 + 2(4L_p'' - 4L_p' + L_p)L_qL_p\right]\right\} F_q(x)dx \\ = & -\frac{i}{\sqrt{5}}\int_0^\infty dxe^{-4x}\left\{24x^4 - 176x^3 + 380x^2 - 288x + 56\right\} \\ = & -\frac{69i}{16\sqrt{5}} \end{aligned}$$

Therefore,

$$d_2 \equiv d_{21} + d_{22} + d_{23} = -0.0626 - 0.0121i;$$

$$d_3 \equiv d_{31} + d_{32} + d_{33} + d_{34} + d_{35} = -0.3796 + 0.8419i.$$

I.2 Case (3). $p = 1,\ q = 2$

Now we have

$$\omega_p = \sqrt{3}, \quad \omega_q = \sqrt{5}, \quad \omega = \omega_p + \omega_q = \sqrt{5} + \sqrt{3},$$

$$L_p(2x) = 1 - 2x; \quad L_q(2x) = (1 - 4x + 2x^2)$$

We already knew from Table 4.2 that $c_1 = 0.0970$ and $d_1 = 0.1524$ from previous discussion.

$$\begin{aligned} & f_1(x) \\ = & (\omega_p - \omega_q)(4L_p'L_q' - 2L_q'L_p - 2L_p'L_q) + \frac{1}{2}\left[\omega_pL_p\left(4L_q'' - 4L_q'\right) - \omega_qL_q\left(4L_p'' - 4L_p'\right)\right] \\ = & (20\sqrt{3} - 16\sqrt{5})x^2 + (-44\sqrt{3} + 36\sqrt{5})x + 20\sqrt{3} - 16\sqrt{5}, \end{aligned}$$

$$
\begin{aligned}
& g_1(x) \\
= \; & f_1(x) + 2(\omega_p - \omega_q) L_p L_q \\
= \; & (-8\sqrt{3} + 8\sqrt{5})x^3 + (-36\sqrt{5} + 40\sqrt{3})x^2 + (-56\sqrt{3} + 48\sqrt{5})x + 22\sqrt{3} - 18\sqrt{5};
\end{aligned}
$$

$$
\begin{aligned}
& f_2(x) \\
= \; & (\omega_p + \omega_q)(4L_p' L_q' - 2L_q' L_p - 2L_p' L_q) + \frac{1}{2}\left[\omega_p L_p \left(4L_q'' - 4L_q'\right) + \omega_q L_q \left(4L_p'' - 4L_p'\right)\right] \\
= \; & (20\sqrt{3} + 16\sqrt{5})x^2 + (-44\sqrt{3} - 36\sqrt{5})x + 20\sqrt{3} + 16\sqrt{5},
\end{aligned}
$$

$$
\begin{aligned}
& g_2(x) \\
= \; & f_2(x) + 2(\omega_p + \omega_q) L_p L_q \\
= \; & (-8\sqrt{3} - 8\sqrt{5})x^3 + (36\sqrt{5} + 40\sqrt{3})x^2 + (-56\sqrt{3} - 48\sqrt{5})x + 22\sqrt{3} + 18\sqrt{5};
\end{aligned}
$$

$$
f_3(x) = 2L_p'^2 - 6L_p L_p' + 2L_p L_p'' = 10 - 12x,
$$

$$
g_3(x) = f_3(x) + 2L_p^2 = 8x^2 - 20x + 12;
$$

$$
f_4(x) = 2L_q'^2 - 6L_q L_q' + 2L_q L_q'' = -24x^3 + 92x^2 - 100x + 30,
$$

$$
g_4(x) = f_4(x) + 2L_q^2 = 8x^4 - 56x^3 + 132x^2 - 116x + 32.
$$

Numerical solutions to f_{11}, f_{12}, f_{13} and f_{14} are plotted in Figure I-2. Our numerical results show that all of them become pretty close to zero after $x > 6$.

Other c's from $\mathcal{E}_p$:

[$\mathcal{E}_p$-1].

$$
\begin{aligned}
& c_{31} \\
= \; & \int_0^\infty dx F_p(x) \left\{ i \frac{1}{\omega_p \omega_q^2} e^{-x} \left[2\omega_p \frac{dG_1}{dx}(2L_q' - L_q) + \omega_q \frac{d^2 G_1}{dx^2} L_q \right.\right. \\
& \left.\left. -(\omega_q - \omega_p) G_1 (4L_q'' - 4L_q') \right] \right\} \\
= \; & \frac{i}{5\sqrt{3}} \left\{ -\sqrt{5} \frac{dG_1}{dx}(0) - (8\sqrt{5} - 10\sqrt{3}) G_1(0) + \int_0^\infty dx e^{-2x} \left[(16\sqrt{3} - 16\sqrt{5})x^3 \right.\right. \\
& \left.\left. +(72\sqrt{5} - 80\sqrt{3})x^2 + (-96\sqrt{5} + 112\sqrt{3})x + 36\sqrt{5} - 44\sqrt{3} \right] G_1 \right\} \\
= \; & \frac{i}{5\sqrt{3}} \left\{ -\sqrt{5} g_1(0) + \alpha \right\} = -0.0010 + 0.5793i \qquad \text{(I.5)}
\end{aligned}
$$

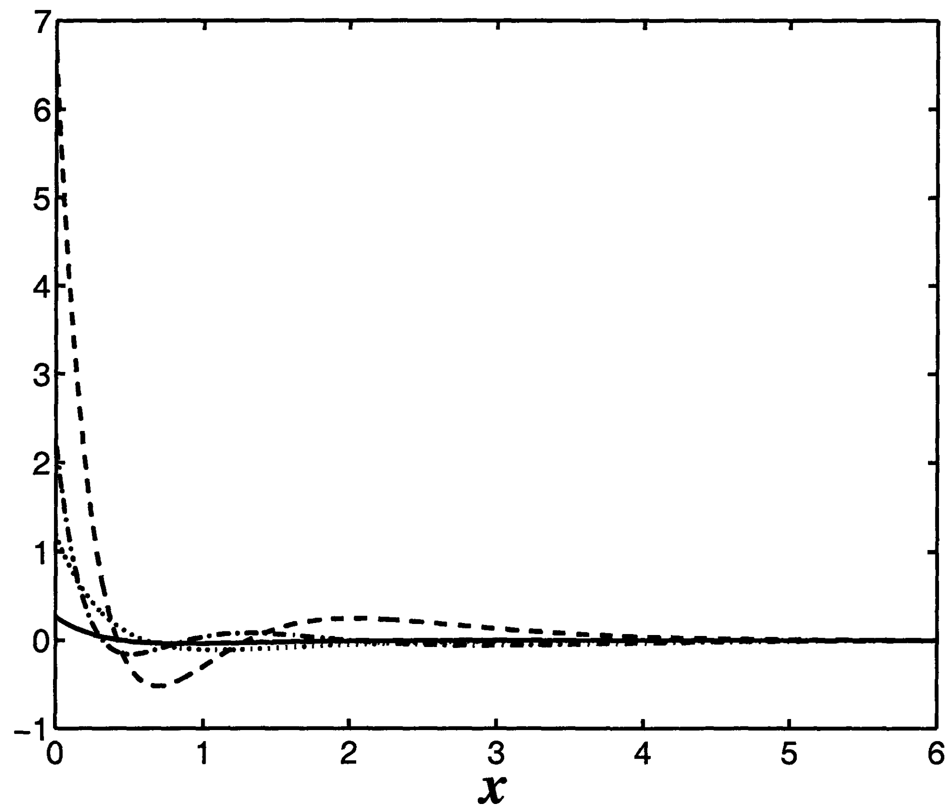

Figure I-2: Numerical solutions to f_{11}— solid line, f_{12}— dash line, f_{13}— dot line, and f_{14}— dash-dot line for Case (3): $p = 1,\ q = 2$.

where use has been made of relation (J.6). And the general form for the integral by part is

$$\int_0^\infty dx f(x)e^{-2x}\frac{dG}{dx} = -f(0)G(0) - \int_0^\infty dx(f' - 2f)e^{-2x}G.$$

The integral α can be evaluated as

$$\begin{aligned}\alpha &= \int_0^\infty dxe^{-2x}\Big[(16\sqrt{3}-16\sqrt{5})x^3 + (72\sqrt{5}-80\sqrt{3})x^2 \\ &\quad +(-96\sqrt{5}+112\sqrt{3})x + 36\sqrt{5} - 44\sqrt{3}\Big]G_1 = \sum_{j=1}^{4}\alpha_j = 0.2223 + 0.0084i\end{aligned} \tag{I.6}$$

where

$$\begin{aligned}\alpha_1 &= \pi\int_0^\infty dxe^{-2x}\Big[(16\sqrt{3}-16\sqrt{5})x^3 + (72\sqrt{5}-80\sqrt{3})x^2 + (-96\sqrt{5}+112\sqrt{3})x \\ &\quad +36\sqrt{5}-44\sqrt{3}\Big]J_0(2\bar{\omega}\sqrt{x})\int_0^\infty d\xi e^{-2\xi}g_1(\xi)Y_0(2\bar{\omega}\sqrt{\xi}) = -0.0749 \\ \alpha_2 &= -\pi\int_0^\infty dxe^{-2x}\Big[(16\sqrt{3}-16\sqrt{5})x^3 + (72\sqrt{5}-80\sqrt{3})x^2 + (-96\sqrt{5}+112\sqrt{3})x \\ &\quad +36\sqrt{5}-44\sqrt{3}\Big]J_0(2\bar{\omega}\sqrt{x})\int_0^x d\xi e^{-2\xi}g_1(\xi)Y_0(2\bar{\omega}\sqrt{\xi}) = 0.1861 \\ \alpha_3 &= -i\pi\int_0^\infty dxe^{-2x}\Big[(16\sqrt{3}-16\sqrt{5})x^3 + (72\sqrt{5}-80\sqrt{3})x^2 + (-96\sqrt{5}+112\sqrt{3})x \\ &\quad +36\sqrt{5}-44\sqrt{3}\Big]J_0(2\bar{\omega}\sqrt{x})\int_0^\infty d\xi e^{-2\xi}g_1(\xi)J_0(2\bar{\omega}\sqrt{\xi}) = 0.0084i \\ \alpha_4 &= \pi\int_0^\infty dxe^{-2x}\Big[(16\sqrt{3}-16\sqrt{5})x^3 + (72\sqrt{5}-80\sqrt{3})x^2 + (-96\sqrt{5}+112\sqrt{3})x \\ &\quad +36\sqrt{5}-44\sqrt{3}\Big]Y_0(2\bar{\omega}\sqrt{x})\int_0^x d\xi e^{-2\xi}g_1(\xi)J_0(2\bar{\omega}\sqrt{\xi}) = 0.1112\end{aligned}$$

with $\bar{\omega} = \sqrt{5} - \sqrt{3}$. Refer to (4.30) for the generic form of solution G_1.

[$\mathcal{E}_p$-2].

$$\begin{aligned}&c_{32} \\ &= \int_0^\infty dxF_p(x)\left\{i\frac{1}{\omega_p\omega_q^2}e^{-x}\left[2\omega_p\frac{dG_2}{dx}(2L_q' - L_q) - \omega_q\frac{d^2G_2}{dx^2}L_q\right.\right. \\ &\quad \left.\left.+(\omega_p+\omega_q)G_2(4L_q'' - 4L_q')\right]\right\} \\ &= \frac{i}{5\sqrt{3}}\left\{\sqrt{5}\frac{dG_2}{dx}(0) + (8\sqrt{5}+10\sqrt{3})G_2(0) + \int_0^\infty dxe^{-2x}\Big[(16\sqrt{3}+16\sqrt{5})x^3\right. \\ &\quad \left.+(-72\sqrt{5}-80\sqrt{3})x^2 + (96\sqrt{5}+112\sqrt{3})x - 36\sqrt{5} - 44\sqrt{3}\Big]G_2\right\} \\ &= \frac{i}{5\sqrt{3}}\left\{\sqrt{5}g_2(0) + \beta\right\} = -0.1342 + 8.5220i\end{aligned} \tag{I.7}$$

The integral β can be evaluated as

$$\begin{aligned}\beta &= \int_0^\infty dxe^{-2x}\left[(-8\sqrt{5}-8)x^2+(32+24\sqrt{5})x-12\sqrt{5}-24\right]G_2 \\ &= \sum_{j=1}^{4}\beta_j = -101.40+1.1625i \qquad \text{(I.8)}\end{aligned}$$

where

$$\begin{aligned}\beta_1 &= \pi\int_0^\infty dxe^{-2x}\left[(16\sqrt{3}+16\sqrt{5})x^3+(-72\sqrt{5}-80\sqrt{3})x^2+(96\sqrt{5}+112\sqrt{3})x\right. \\ &\left.-36\sqrt{5}-44\sqrt{3}\right]J_0(2\bar{\omega}\sqrt{x})\int_0^\infty d\xi e^{-2\xi}g_2(\xi)Y_0(2\bar{\omega}\sqrt{\xi}) = -6.8783\end{aligned}$$

$$\begin{aligned}\beta_2 &= -\pi\int_0^\infty dxe^{-2x}\left[(16\sqrt{3}+16\sqrt{5})x^3+(-72\sqrt{5}-80\sqrt{3})x^2+(96\sqrt{5}+112\sqrt{3})x\right. \\ &\left.-36\sqrt{5}-44\sqrt{3}\right]J_0(2\bar{\omega}\sqrt{x})\int_0^x d\xi e^{-2\xi}g_2(\xi)Y_0(2\bar{\omega}\sqrt{\xi}) = -43.8005\end{aligned}$$

$$\begin{aligned}\beta_3 &= -i\pi\int_0^\infty dxe^{-2x}\left[(16\sqrt{3}+16\sqrt{5})x^3+(-72\sqrt{5}-80\sqrt{3})x^2+(96\sqrt{5}+112\sqrt{3})x\right. \\ &\left.-36\sqrt{5}-44\sqrt{3}\right]J_0(2\bar{\omega}\sqrt{x})\int_0^\infty d\xi e^{-2\xi}g_2(\xi)J_0(2\bar{\omega}\sqrt{\xi}) = 1.1625i\end{aligned}$$

$$\begin{aligned}\beta_4 &= \pi\int_0^\infty dxe^{-2x}\left[(16\sqrt{3}+16\sqrt{5})x^3+(-72\sqrt{5}-80\sqrt{3})x^2+(96\sqrt{5}+112\sqrt{3})x\right. \\ &\left.-36\sqrt{5}-44\sqrt{3}\right]Y_0(2\bar{\omega}\sqrt{x})\int_0^x d\xi e^{-2\xi}g_2(\xi)J_0(2\bar{\omega}\sqrt{\xi}) = -50.7244\end{aligned}$$

with $\bar{\omega} = \sqrt{5}+\sqrt{3}$. Refer to (4.30) for the generic form of solution G_2.

[$\mathcal{E}_p$-3].

$$\begin{aligned}&c_{21} \\ &= \int_0^\infty dxF_p(x)\left\{i\frac{1}{\omega_p}e^{-x}\left[2\frac{dG_3}{dx}(2L_p'-L_p)-\frac{d^2G_3}{dx^2}L_p+2G_3(4L_p''-4L_p')\right]\right\} \\ &= \frac{i}{\sqrt{3}}\left\{\frac{dG_3}{dx}(0)+12G_3(0)-8\int_0^\infty dxe^{-2x}\left(4x^2-10x+6\right)G_3\right\} \\ &= \frac{i}{\sqrt{3}}\left\{g_3(0)-8\gamma\right\} = -0.0903+2.3049i\end{aligned}$$

The integral γ can be evaluated as

$$\gamma = \int_0^\infty dxe^{-2x}\left(4x^2-10x+6\right)G_3 = \sum_{j=1}^{4}\gamma_j = 1.0010-0.0195i$$

where

$$\gamma_1 = \pi \int_0^\infty dx e^{-2x} \left(4x^2 - 10x + 6\right) J_0(2\bar{\omega}\sqrt{x}) \int_0^\infty d\xi e^{-2\xi} g_3(\xi) Y_0(2\bar{\omega}\sqrt{\xi}) = 0.0888$$

$$\gamma_2 = -\pi \int_0^\infty dx e^{-2x} \left(4x^2 - 10x + 6\right) J_0(2\bar{\omega}\sqrt{x}) \int_0^x d\xi e^{-2\xi} g_3(\xi) Y_0(2\bar{\omega}\sqrt{\xi}) = 0.4116$$

$$\gamma_3 = -i\pi \int_0^\infty dx e^{-2x} \left(4x^2 - 10x + 6\right) J_0(2\bar{\omega}\sqrt{x}) \int_0^\infty d\xi e^{-2\xi} g_3(\xi) J_0(2\bar{\omega}\sqrt{\xi}) = -0.0195i$$

$$\gamma_4 = \pi \int_0^\infty dx e^{-2x} \left(4x^2 - 10x + 6\right) Y_0(2\bar{\omega}\sqrt{x}) \int_0^x d\xi e^{-2\xi} g_3(\xi) J_0(2\bar{\omega}\sqrt{\xi}) = 0.5006$$

with $\bar{\omega} = 2\sqrt{3}$. Refer to (4.30) for the generic form of solution G_3.

[$\mathcal{E}_p$-4].

$$\begin{aligned} & c_{33} \\ = & \int_0^\infty dx F_p(x) \left\{ \frac{ie^{-x}}{\omega_p \omega_q^2} \left[\frac{\omega_q}{2} L_q f_{11xx} + \omega_p (2L_q' - L_q) f_{11x} \right.\right. \\ & \left.\left. - \frac{\omega_q - \omega_p}{2} (4L_q'' - 4L_q' + 4L_q) f_{11} \right] \right\} \\ = & \frac{i}{5\sqrt{3}} \left\{ -\frac{\sqrt{5}}{2} f_{11x}(0) - (4\sqrt{5} - 5\sqrt{3}) f_{11}(0) + \int_0^\infty dx e^{-2x} \left[(16\sqrt{5} - 20\sqrt{3}) x^2 \right.\right. \\ & \left.\left. + (-36\sqrt{5} + 44\sqrt{3}) x + 16\sqrt{5} - 20\sqrt{3} \right] f_{11} \right\} = 0.1505i \end{aligned}$$

[$\mathcal{E}_p$-5].

$$\begin{aligned} & c_{34} \\ = & \int_0^\infty dx F_p(x) \left\{ \frac{ie^{-x}}{\omega_p \omega_q^2} \left[\omega_p (2L_q' - L_q) f_{12x} - \frac{\omega_q}{2} L_q f_{12xx} \right.\right. \\ & \left.\left. + \frac{\omega_p + \omega_q}{2} (4L_q'' - 4L_q' + 4L_q) f_{12} \right] \right\} \\ = & \frac{i}{5\sqrt{3}} \left\{ \frac{\sqrt{5}}{2} f_{12x}(0) + (4\sqrt{5} + 5\sqrt{3}) f_{12}(0) + \int_0^\infty dx e^{-2x} \left[(-16\sqrt{5} - 20\sqrt{3}) x^2 \right.\right. \\ & \left.\left. + (36\sqrt{5} + 44\sqrt{3}) x - 16\sqrt{5} - 20\sqrt{3} \right] f_{12} \right\} = 3.9558i \end{aligned}$$

[$\mathcal{E}_p$-6].

$$\begin{aligned} & c_{22} \\ = & \int_0^\infty dx F_p(x) \left\{ i \frac{1}{\omega_p} e^{-x} \left[f_{13x} (2L_p' - L_p) - \frac{1}{2} L_p f_{13xx} + f_{13} (4L_p'' - 4L_p' + 4L_p) \right] \right\} \\ = & \frac{i}{\sqrt{3}} \left\{ \frac{1}{2} f_{13x}(0) + 6 f_{13}(0) + \int_0^\infty dx e^{-2x} \left[24x - 20 \right] f_{12} \right\} = 1.0392i \end{aligned}$$

$[\mathcal{E}_p\text{-}7]$.

$$
\begin{aligned}
& c_{23} \\
= & \int_0^\infty dx F_p(x) \left\{ -i\frac{1}{\omega_p^3} e^{-3x} \left[\frac{27}{8}(4L_p'' - 4L_p' + L_p)(2L_p' - L_p)^2 - \frac{9}{8}(2L_p' - L_p)^2 L_p \right. \right. \\
& \left. \left. + \frac{3}{2}(2L_p' - L_p)^2 L_p + \frac{3}{8}(4L_p'' - 4L_p' + L_p)L_p^2 - \frac{9}{8}L_p^3 \right] \right\} \\
= & -\frac{i}{3\sqrt{3}} \int_0^\infty dx e^{-4x} \left\{ 48x^4 - 336x^3 + 708x^2 - 588x + 156 \right\} \\
= & -\frac{47i}{8\sqrt{3}}
\end{aligned}
$$

$[\mathcal{E}_p\text{-}8]$.

$$
\begin{aligned}
& c_{35} \\
= & \int_0^\infty -i\frac{1}{\omega_p\omega_q^2} e^{-3x} \left\{ \frac{3}{4} \left[3(4L_p'' - 4L_p' + L_p)(2L_q' - L_q)^2 - (2L_q' - L_q)^2 L_p \right. \right. \\
& \left. + 6(4L_q'' - 4L_q' + L_q)(2L_q' - L_q)(2L_p' - L_p) - 2L_q(2L_p' - L_p)(2L_q' - L_q) \right] \\
& + \frac{1}{4} \left[8(2L_p' - L_p)(2L_q' - L_q)L_q + 4(2L_q' - L_q)^2 L_p \right. \\
& \left. \left. - 9L_pL_q^2 + (4L_p'' - 4L_p' + L_p)L_q^2 + 2(4L_q'' - 4L_q' + L_q)L_pL_q \right] \right\} F_p(x)dx \\
= & -\frac{i}{5\sqrt{3}} \int_0^\infty dx e^{-4x} \left\{ 96x^6 - 1280x^5 + 5800x^4 \right. \\
& \left. -12128x^3 + 12616x^2 - 6280x + 1178 \right\} = -\frac{3669i}{160\sqrt{3}}
\end{aligned}
$$

Therefore,

$$c_2 \equiv c_{21} + c_{22} + c_{23} = -0.0903 - 0.0478i;$$

$$c_3 \equiv c_{31} + c_{32} + c_{33} + c_{34} + c_{35} = -0.1352 - 0.0318i.$$

Other d's from $\mathcal{E}_q$:

$[\mathcal{E}_q\text{-}1]$.

$$
\begin{aligned}
& d_{31} \\
= & \int_0^\infty dx F_q(x) \left\{ \frac{ie^{-x}}{\omega_q\omega_p^2} \left[2\omega_q \frac{dG_1}{dx}(2L_p' - L_p) + \omega_p \frac{d^2G_1}{dx^2} L_p \right. \right. \\
& \left. \left. +(\omega_q - \omega_p)G_1(4L_p'' - 4L_p') \right] \right\} \\
= & \frac{i}{3\sqrt{5}} \left\{ -\sqrt{3}g_1(0) - \alpha \right\} = 0.0012 + 0.5205i
\end{aligned}
$$

α is defined in (I.5) and evaluated in (I.6).

$[\mathcal{E}_q\text{-}2]$.

$$\begin{aligned} & d_{32} \\ = & \int_0^\infty dx F_q(x) \left\{ \frac{ie^{-x}}{\omega_q \omega_p^2} \left[2\omega_q \frac{dG_2}{dx}(2L'_p - L_p) - \omega_p \frac{d^2G_2}{dx^2} L_p \right.\right. \\ & \left.\left. +(\omega_p + \omega_q) G_2 (4L''_p - 4L'_p) \right] \right\} \\ = & \frac{i}{3\sqrt{5}} \left\{ \sqrt{3} g_2(0) + \beta \right\} = -0.1733 + 5.1147i \end{aligned}$$

β is defined in (I.7) and evaluated in (I.8).

$[\mathcal{E}_q\text{-}3]$.

$$\begin{aligned} & d_{21} \\ = & \int_0^\infty dx F_q(x) \left\{ \frac{i}{\omega_q} e^{-x} \left[2\frac{dG_4}{dx}(2L'_q - L_q) - \frac{d^2G_4}{dx^2} L_q + 2G_4(4L''_q - 4L'_q) \right] \right\} \\ = & \frac{i}{\sqrt{5}} \left\{ \frac{dG_4}{dx}(0) + 20G_4(0) \right. \\ & \left. + \int_0^\infty dx e^{-2x} \left[-32x^4 + 224x^3 - 528x^2 + 464x - 128 \right] G_4 \right\} \\ = & \frac{i}{\sqrt{5}} \{ g_4(0) + \kappa \} = -0.0626 + 4.7096i \end{aligned}$$

The integral κ can be evaluated as

$$\begin{aligned} \kappa &= \int_0^\infty dx e^{-2x} \left[-32x^4 + 224x^3 - 528x^2 + 464x - 128 \right] G_4 \\ &= \sum_{j=1}^{4} \kappa_j = -21.4691 + 0.1400i \end{aligned}$$

where

$$\begin{aligned} \kappa_1 = & \pi \int_0^\infty dx e^{-2x} \left[-32x^4 + 224x^3 - 528x^2 + 464x - 128 \right] J_0(2\bar{\omega}\sqrt{x}) \\ & \int_0^\infty d\xi e^{-2\xi} g_4(\xi) Y_0(2\bar{\omega}\sqrt{\xi}) = -1.0838 \end{aligned}$$

$$\begin{aligned} \kappa_2 = & -\pi \int_0^\infty dx e^{-2x} \left[-32x^4 + 224x^3 - 528x^2 + 464x - 128 \right] J_0(2\bar{\omega}\sqrt{x}) \\ & \int_0^x d\xi e^{-2\xi} g_4(\xi) Y_0(2\bar{\omega}\sqrt{\xi}) = -9.6430 \end{aligned}$$

$$\kappa_3 = -i\pi \int_0^\infty dx e^{-2x} \left[-32x^4 + 224x^3 - 528x^2 + 464x - 128\right] J_0(2\bar{\omega}\sqrt{x}) \int_0^\infty d\xi e^{-2\xi} g_4(\xi) J_0(2\bar{\omega}\sqrt{\xi}) = 0.1400i$$

$$\kappa_4 = \pi \int_0^\infty dx e^{-2x} \left[-32x^4 + 224x^3 - 528x^2 + 464x - 128\right] Y_0(2\bar{\omega}\sqrt{x}) \int_0^x d\xi e^{-2\xi} g_4(\xi) J_0(2\bar{\omega}\sqrt{\xi}) = -10.7423$$

with $\bar{\omega} = 2\sqrt{5}$. Refer to (4.30) for the generic form of solution G_4.

$[\mathcal{E}_q$-4].

$$\begin{aligned} &d_{33} \\ =& \int_0^\infty dx F_q(x) \left\{ \frac{ie^{-x}}{\omega_q \omega_p^2} \left[\frac{\omega_p}{2} L_p f_{11xx} + \omega_q (2L_p' - L_p) f_{11x} \right.\right. \\ &\left.\left. + \frac{\omega_q - \omega_p}{2} f_{11} (4L_p'' - 4L_p' + 4L_p) \right] \right\} \\ =& \frac{i}{3\sqrt{5}} \left\{ -\frac{\sqrt{3}}{2} f_{11x}(0) - (4\sqrt{3} - 3\sqrt{5}) f_{11}(0) + \int_0^\infty dx e^{-2x} \left[(20\sqrt{3} - 16\sqrt{5}) x^2 \right.\right. \\ &\left.\left. + (-44\sqrt{3} + 36\sqrt{5}) x + 20\sqrt{3} - 16\sqrt{5} \right] f_{11} \right\} = 0.1417i \end{aligned}$$

$[\mathcal{E}_q$-5].

$$\begin{aligned} &d_{34} \\ =& \int_0^\infty dx F_q(x) \left\{ \frac{ie^{-x}}{\omega_q \omega_p^2} \left[\omega_q (2L_p' - L_p) f_{12x} - \frac{\omega_p}{2} L_p f_{12xx} \right.\right. \\ &\left.\left. + \frac{\omega_p + \omega_q}{2} f_{12} (4L_p'' - 4L_p' + 4L_p) \right] \right\} \\ =& \frac{i}{3\sqrt{5}} \left\{ \frac{\sqrt{3}}{2} f_{12x}(0) + (4\sqrt{3} + 3\sqrt{5}) f_{12}(0) + \int_0^\infty dx e^{-2x} \left[(-20\sqrt{3} - 16\sqrt{5}) x^2 \right.\right. \\ &\left.\left. + (44\sqrt{3} + 36\sqrt{5}) x - 20\sqrt{3} - 16\sqrt{5} \right] f_{12} \right\} = 2.4615i \end{aligned}$$

$[\mathcal{E}_q$-6].

$$\begin{aligned} &d_{22} \\ =& \int_0^\infty dx F_q(x) \left\{ \frac{i}{\omega_q} e^{-x} \left[(2L_q' - L_q) f_{14x} - \frac{1}{2} L_q f_{14xx} + (4L_q'' - 4L_q' + 4L_q) f_{14} \right] \right\} \\ =& \frac{i}{\sqrt{5}} \left\{ \frac{1}{2} f_{14x}(0) + 10 f_{14}(0) \right. \\ &\left. + \int_0^\infty dx e^{-2x} \left[48x^3 - 184x^2 + 200x - 60 \right] f_{14} \right\} = 2.2695i \end{aligned}$$

$[\mathcal{E}_q\text{-}7]$.

$$
\begin{aligned}
& d_{23} \\
= \; & \int_0^\infty -i\frac{1}{\omega_q^3}e^{-3x}\left\{\left[\frac{27}{8}(4L_q''-4L_q'+L_q)(2L_q'-L_q)^2-\frac{9}{8}(2L_q'-L_q)^2L_q\right]\right. \\
& \left.+\left[\frac{3}{2}(2L_q'-L_q)^2L_q+\frac{3}{8}(4L_q''-4L_q'+L_q)L_q^2-\frac{9}{8}L_q^3\right]\right\}F_q(x)dx \\
= \; & -\frac{i}{5\sqrt{5}}\int_0^\infty dxe^{-4x}\left\{48x^8-864x^7+5832x^6-20112x^5\right. \\
& \left.+39180x^4-44184x^3+28038x^2-9060x+1110\right\} \\
= \; & -\frac{2001i}{128\sqrt{5}}
\end{aligned}
$$

$[\mathcal{E}_q\text{-}8]$.

$$
\begin{aligned}
& d_{35} \\
= \; & \int_0^\infty -i\frac{1}{\omega_q\omega_p^2}e^{-3x}\left\{\frac{3}{4}\left[3(4L_q''-4L_q'+L_q)(2L_p'-L_p)^2-(2L_p'-L_p)^2L_q\right.\right. \\
& \left.+6(4L_p''-4L_p'+L_p)(2L_p'-L_p)(2L_q'-L_q)-2L_p(2L_q'-L_q)(2L_p'-L_p)\right] \\
& +\frac{1}{4}\left[8(2L_q'-L_q)(2L_p'-L_p)L_p+4(2L_p'-L_p)^2L_q\right. \\
& \left.\left.-9L_qL_p^2+(4L_q''-4L_q'+L_q)L_p^2+2(4L_p''-4L_p'+L_p)L_qL_p\right]\right\}F_q(x)dx \\
= \; & -\frac{i}{3\sqrt{5}}\int_0^\infty dxe^{-4x}\left\{96x^6-1120x^5+4608x^4-8976x^3+8788x^2-4008x+614\right\} \\
= \; & -\frac{1493i}{96\sqrt{5}}
\end{aligned}
$$

Therefore,

$$d_2 \equiv d_{21}+d_{22}+d_{23} = -0.0626-0.0121i;$$

$$d_3 \equiv d_{31}+d_{32}+d_{33}+d_{34}+d_{35} = -0.1720+1.2832i.$$

Appendix J

Subharmonic resonance as a special case

A special case is the two edge waves have same period, which is twice that of the incident wave. It turns out to be the classical subharmonic resonance [22]. For simplicity, we consider the edge wave with the lowest x-mode, which produces the quadratic nonlinear forcing for second order outgoing wave only. Assume the incident and reflected wave has a normalized frequency 2, the multiple-scale expansion of the solution is

$$\begin{aligned}\Phi &= \left[\psi_0(x,y,\tau)e^{-it}+*\right]+\bar{\epsilon}\left[\phi_1(x,\tau)e^{-i2t}+*\right]\\ &+ \bar{\epsilon}^2\left[\psi_2(x,y,\tau)e^{-it}+*\right]\ldots\end{aligned} \tag{J.1}$$

where the known incident and reflected wave will be incorporated in solution ϕ_1 as part of the homogeneous solution. We have two time scales in the system, fast time t and slow time $\tau=\bar{\epsilon}^2 t$. Change of variable will give

$$\frac{\partial}{\partial t}\longrightarrow\frac{\partial}{\partial t}+\bar{\epsilon}^2\frac{\partial}{\partial\tau},\quad \frac{\partial^2}{\partial t^2}\longrightarrow\frac{\partial^2}{\partial t^2}+2\bar{\epsilon}^2\frac{\partial}{\partial t}\frac{\partial}{\partial\tau}+\bar{\epsilon}^4\frac{\partial^2}{\partial\tau^2}$$

Plugging J.1 into Eq. (4.8) and separate different orders, we get

$$\begin{aligned}&\left\{\left[\psi_0+(x\psi_{0x})_x+x\psi_{0yy}\right]e^{-it}+*\right\}\\ +\;&\bar{\epsilon}\left\{\left[2^2\phi_1+(x\phi_{1x})_x\right]e^{-i2t}+*\right\}\end{aligned}$$

$$
\begin{aligned}
&+ \quad \bar{\epsilon}^2 \left\{ \left[\psi_2 + (x\psi_{2x})_x + x\psi_{2yy} \right] e^{-it} + * \right\} \\
&= \quad \bar{\epsilon} \left\{ (\psi_0, \psi_0) e^{-i2t} + * \right\} \\
&+ \quad \bar{\epsilon}^2 \left\{ \left[(\phi_1, \psi_0^*) + (\psi_0, \psi_0, \psi_0^*) \right] e^{-it} + * \right\} \\
&+ \quad \bar{\epsilon}^2 \left\{ -2i \frac{\partial \psi_0}{\partial \tau} e^{-it} + * \right\} \ldots
\end{aligned}
\tag{J.2}
$$

At O(1), we have homogeneous equation

$$\psi_0 + (x\psi_{0x})_x + x\psi_{0yy} = 0$$

With the no flux boundary condition at shoreline and exponential decay at infinity, the first order equation allow the edge wave eigen solution

$$\psi_0 = -iB(\tau)e^{-x}\cos y. \tag{J.3}$$

$B(\tau)$'s are the slowly varying dimensionless amplitudes of the edge wave at shore. As always the evolution equations governing $B(\tau)$ are to be obtained at higher order. We fit in the coefficients for amplitude B so that the normalized boundary condition

$$\frac{\partial \Phi}{\partial t} + \zeta = 0.$$

For later uses note that the factor $F = e^{-x}$, which describe the x dependence of the edge wave modes, satisfies

$$F + \left[(xF_x)_x - xF \right] = 0,$$

$$xF_x = 0 \;\; at \;\; x = 0; \quad F \to 0, \;\; x \sim \infty.$$

At O($\bar{\epsilon}$), we are going to combine the input wave with a local nonlinearly generated wave component to form the whole solution $\phi_1(x)e^{-i2t}$. It can be obtained totally by analytical method.

$$2^2\phi_1 + (x\phi_{1x})_x = (\psi_0, \psi_0)$$

Nonlinear local forcing

$$
\begin{aligned}
(\psi_0, \psi_0) &= -2i\left(\psi_{0x}^2 + \psi_{0y}^2\right) - i\psi_0\left(\psi_{0xx} + \psi_{0yy}\right) \\
&= -i(-iB)^2 e^{-2x}\left\{2\left[\cos^2 y + \sin^2 y\right] + \cos y\left(\cos y - \cos y\right)\right\} \\
&= 2iB^2 e^{-2x}
\end{aligned}
$$

Therefore, the inhomogeneous solution corresponding to the local forcing $g(x) = e^{-2x}$ is

$$\begin{aligned} G(x) &= [-u_1(\infty) - iu_2(\infty)]\, J_0(4\sqrt{x}) + u_1(x)J_0(4\sqrt{x}) + u_2(x)Y_0(4\sqrt{x}) \\ &= -iu_2(\infty)J_0(4\sqrt{x}) + [u_1(x) - u_1(\infty)]\, J_0(4\sqrt{x}) + u_2(x)Y_0(4\sqrt{x}) \end{aligned}$$

$$u_1(x) = -\int_0^x \frac{Y_0(4\sqrt{\xi})g(\xi)}{\xi W(J_0, Y_0)(\xi)} d\xi = -\pi \int_0^x Y_0(4\sqrt{\xi})e^{-2\xi} d\xi$$

$$u_2(x) = \int_0^x \frac{J_0(4\sqrt{\xi})g(\xi)}{\xi W(J_0, Y_0)(\xi)} d\xi = \pi \int_0^x J_0(4\sqrt{\xi})e^{-2\xi} d\xi$$

The whole solution for second order wave $\phi_1(x)e^{-i2t}$ including the input wave is

$$\phi_1(x) = -\frac{i}{2}J_0(4\sqrt{x}) + 2iB^2G(x)$$

For later uses, we now work out some constants as follows. From (4.29) we get

$$\begin{aligned} \left.\frac{dG(x)}{dx}\right|_{x=0} &= -4(-u_1(\infty) - iu_2(\infty)) + g(0) \\ &= 4\,(u_1(\infty) + iu_2(\infty)) + g(0) \end{aligned} \tag{J.4}$$

where $g(0)$ is the exciting force at $x = 0$, which is 1 here. And

$$G(0) = -u_1(\infty) - iu_2(\infty) \tag{J.5}$$

From (J.4) and (J.5) we can see that

$$\left.\frac{dG(x)}{dx}\right|_{x=0} \equiv -4G(0) + g(0). \tag{J.6}$$

At $O(\bar{\epsilon}^2)$, the governing equations become

$$\mathcal{L}H = -2\frac{\partial B}{\partial \tau}F(x) + \mathcal{E}(x) \tag{J.7}$$

where we have introduced

$$\psi_2 = H(x)\cos y$$

and linear operators

$$\mathcal{L}F = F + [(xF_x)_x - xF]\,.$$

And $\mathcal{E}(x)$ denotes all the third-order quadratic and cubic resonance forces for the edge wave ψ_0.

$$\mathcal{E}(x)\cos y \quad = \quad (\phi_1, \psi_0^*) + (\psi_0, \psi_0, \psi_0^*)$$

1.

$$\begin{aligned}
& (\phi_1, \psi_0^*) \\
= \quad & 2\left\{\phi_{1x}\psi_{0x}^*(-2i+i)\right\} + i\psi_0^*\phi_{1xx} \\
= \quad & -2i\phi_{1x}\psi_{0x}^* + i\psi_0^*\phi_{1xx} \\
= \quad & ie^{-x}\cos y\,(iB^*)\left\{2iB^2\left[2\frac{dG}{dx}+\frac{d^2G}{dx^2}\right] - \frac{i}{2}\left[2\frac{dJ_0}{dx}+\frac{d^2J_0}{dx^2}\right]\right\} \\
= \quad & \frac{i}{2}B^*e^{-x}\left(2\frac{dJ_0}{dx}+\frac{d^2J_0}{dx^2}\right)\cos y - 2iB^2B^*e^{-x}\left(2\frac{dG}{dx}+\frac{d^2G}{dx^2}\right)\cos y.
\end{aligned}$$

2.

$$\begin{aligned}
& (\psi_0, \psi_0, \psi_0^*) \\
= \quad & \psi_{0xx}2\psi_{0x}\psi_{0x}^* + \psi_{0xx}^*\psi_{0x}\psi_{0x} + \psi_{0yy}2\psi_{0y}\psi_{0y}^* + \psi_{0yy}^*\psi_{0y}\psi_{0y} \\
& +2\left(\psi_{0x}\psi_{0y}\psi_{0xy}^* + \psi_{0x}\psi_{0y}^*\psi_{0xy} + \psi_{0x}^*\psi_{0y}\psi_{0xy}\right) \\
= \quad & (-iB)^2\,iB^*e^{-3x}\left\{3\cos^3 y - 3\cos y\sin^2 y + 6\cos y\sin^2 y\right\} \\
= \quad & -iB^2B^*e^{-3x}3\left[\cos^2 y + \sin^2 y\right]\cos y \\
= \quad & -3iB^2B^*e^{-3x}\cos y
\end{aligned}$$

Homogeneous equation J.7 has nontrivial solutions $F = e^{-x}$ as described at first order.

$$\begin{aligned}
& \int_0^\infty (H\mathcal{L}F - F\mathcal{L}H)dx = \int_0^\infty \left[H(xF_x)_x - F(xH_x)_x\right]dx \\
= \quad & \int_0^\infty \left[(xHF_x)_x - (xFH_x)_x\right]dx = 0
\end{aligned}$$

by the boundary conditions both at shoreline and at infinity. Therefore

$$\int_0^\infty F\mathcal{L}H dx = 0 \quad \textit{since} \quad \mathcal{L}F = 0$$

Solvability condition gives

$$\int_0^\infty dx F(x)\left(-2\frac{\partial B}{\partial \tau}F(x) + \mathcal{E}(x)\right) = 0$$

which can be rewritten as follows:

$$\frac{\partial B}{\partial \tau} = \frac{i}{2}aB^* - 2ibB^2B^* - 3icB^2B^*. \tag{J.8}$$

This is the equation governing the evolution of the edge wave amplitude B. a, b and c are constants obtained through numerical integrals. Use has been made of

$$\int_0^\infty F^2(x)dx = \int_0^\infty e^{-2x}dx = \frac{1}{2}$$

1.

$$\begin{aligned} a &= \int_0^\infty e^{-x}\left[e^{-x}\left(2\frac{dJ_0}{dx} + \frac{d^2J_0}{dx^2}\right)\right]dx \\ &= \int_0^\infty e^{-2x}\left(2\frac{dJ_0}{dx} + \frac{d^2J_0}{dx^2}\right)dx \\ &= -\frac{dJ_0}{dx}\bigg|_{x=0} - 4J_0(0) + 8\int_0^\infty e^{-2x}J_0dx \\ &= 4 - 4 + 8\int_0^\infty e^{-2x}J_0dx \\ &= 8\int_0^\infty e^{-2x}J_0(4\sqrt{x})dx = \frac{8}{2e^2} = 8 \times 0.06767 = 0.5413 \end{aligned}$$

2.

$$\begin{aligned} b &= \int_0^\infty e^{-x}\left[e^{-x}\left(2\frac{dG}{dx} + \frac{d^2G}{dx^2}\right)\right]dx \\ &= \int_0^\infty e^{-2x}\left(2\frac{dG}{dx} + \frac{d^2G}{dx^2}\right)dx \\ &= -\frac{dG}{dx}\bigg|_{x=0} - 4G(0) + 8\int_0^\infty e^{-2x}G(x)dx \\ &= -1 + 8\int_0^\infty e^{-2x}G(x)dx \\ &= -1 + 8\pi\sum_{j=1}^{3} b_j = -1 + 8\pi \times (0.028612 - 0.0045789i) = -0.28089 - 0.11508i \end{aligned}$$

$$b_1 = -i\int_0^\infty e^{-2x}J_0(4\sqrt{x})dx\int_0^\infty J_0(4\sqrt{\xi})e^{-2\xi}d\xi = \frac{-i}{4e^4} = -0.0045789i$$

$$\begin{aligned} b_2 &= \int_0^\infty e^{-2x}J_0(4\sqrt{x})dx\left(\int_0^\infty Y_0(4\sqrt{\xi})e^{-2\xi}d\xi - \int_0^x Y_0(4\sqrt{\xi})e^{-2\xi}d\xi\right) \\ &= \int_0^\infty e^{-2x}J_0(4\sqrt{x})dx\int_x^\infty Y_0(4\sqrt{\xi})e^{-2\xi}d\xi = 0.014306 \end{aligned}$$

$$b_3 = \int_0^\infty e^{-2x} Y_0(4\sqrt{x})dx \int_0^x J_0(4\sqrt{\xi})e^{-2\xi}d\xi = 0.014306$$

Actually $b_2 = b_3$ by property of double integral:

$$\int_a^b f(x)dx \int_x^b g(y)dy = \int_a^b g(x)dx \int_0^x f(y)dy$$

3.

$$\begin{aligned} c &= \int_0^\infty e^{-x}\left(e^{-3x}\right)dx \\ &= \int_0^\infty e^{-4x}dx \\ &= \frac{1}{4} \end{aligned}$$

Plugging these coefficients back into (J.8) we get

$$\frac{\partial B}{\partial \tau} = i\alpha B^* - (\beta + i\gamma)B^2 B^* \tag{J.9}$$

with

$$\alpha = 0.2707, \quad \beta = 0.2302, \quad \gamma = 0.1882$$

J.1 Initial growth rate

The edge wave amplitudes are much smaller compared to the standing waves, i.e. $B << 1$. Therefore, only the linear terms come into play. Equation (J.9) becomes

$$\frac{\partial B}{\partial \tau} = i\alpha B^*. \tag{J.10}$$

which can be manipulated to get

$$\frac{\partial^2 B}{\partial \tau^2} = i\alpha\left(-i\alpha B\right) = \alpha^2 B \tag{J.11}$$

which has a solution

$$B = B(0)e^{\pm\alpha\tau} \tag{J.12}$$

i.e. the growth rate is 0.2707. Notice that

$$\tau = \bar{\epsilon}^2 t = \bar{\epsilon}\frac{k|\bar{A}|}{s}\omega_0 t' = \frac{\omega_0^3|A'|}{gs^2}t' = \frac{1}{8}\frac{\omega^3|A'|}{gs^2}t'$$

where ω is the incident wave frequency and ω_0 is the edge wave frequency. For the subharmonic resonance in our study, $\omega = 2\omega_0$.

J.2 Equilibrium state — mature edge wave amplitude

When equilibrium state is reached after a certain time of evolution, $\frac{\partial B}{\partial \tau} = 0$, then

$$i\alpha B^* - (\beta + i\gamma)B^2 B^* = 0 \Rightarrow B^2 = \frac{i\alpha}{\beta + i\gamma} \Rightarrow |B| = 0.954$$

where we have discarded the trivial fixed point $B = 0$. Returning back to the physical amplitude,

$$|B'| = 0.954\left(\frac{s|A'|}{k}\right)^{1/2} = 0.954\frac{s}{\omega_0}\left(g|A'|\right)^{1/2} = 0.954\frac{2s}{\omega}\left(g|A'|\right)^{1/2} = 1.908s\left(\frac{g|A'|}{\omega^2}\right)^{1/2}.$$

The maximum excursion at the shoreline

$$X_R = \frac{2|B'|}{s} = 3.816\left(\frac{g|A'|}{\omega^2}\right)^{1/2}.$$

Stability analysis around the fixed point will be similar to the synchronous resonance case.

Bibliography

[1] Abramowitz, M. and I. A. Stegun (1972). Handbook of Mathematical Functions, Dover, New York.

[2] A. M. Batista and I. L. Caldas, S. R. Lopes and R. L. Viana, W. Horton and P. J. Morrison, (2006), Nonlinear three-mode interaction and drift-wave trubulence in a tokamak edge plasma, Physics of Plasmas, 13:042510-1-10.

[3] Bowen, A.J. and Inman, D. L. (1969), Rip currents; part 2: laboratory and field observations. J. Geophys. Res., 74: 5479-5490.

[4] Bowen, A. J., and D. L. Inman, Edge waves and crescentic bars, J. Geophys. Res., 76, 8662C8671, 1971.

[5] Coco, G., T. J. O'Hare, and D. A. Huntley (1999), Beach cusps: A comparison of data and theories for their formation, J. Coastal Res., 15(3), 741C749.

[6] Coco, G., D. A. Huntley, and T. J. O'Hare, Investigation of a self-organisation model for beach cusp formation and development, J. Geophys. Res., 105, 21,991C22,002, 2000.

[7] Eckart, C. (1951), Surface waves on water of variable depth, Wave Rep. 100, pp. 51C12, Scripps Inst. of Oceanogr., La Jolla, Calif.

[8] Elgar, S., J. Oltman-Shay, and P. Howd, (1989), Observations of infragravity-frequency long waves, 1, Coupling to wind waves, EOS Trans. Am. Geophys. Union, 70, pp. 1333.

[9] Fathei Ali and Michael Menzinger, (1999), On the local stability of limit cycles, Chaos, Vol. 9, No. 2, 348-356.

[10] Galvin, C.J. (1964), Resonant edge waves on laboratory beaches. EOS Trans. Am. Geophys. Union, 46, pp. 112 (abstracts).

[11] Greenspan, H. The generation of edge waves by moving pressure distributions. J. Fluid Mech. 1 (1956), 574-592.

[12] Guza, R. T., and Bowen , A. J. Finite amplitude edge waves. J. Mar. Res. 34 (1976), 269C293.

[13] Guza, R. T., and A. J. Bowen (1981), On the amplitude of beach cusps, J. Geophys. Res., 86(C5), 4125C4132.

[14] Guza, R. T., and R. E. Davis (1974), Excitation of edge waves by waves incident on a beach, J. Geophys. Res., 79(9), 1285C1291.

[15] Guza, R. T., and D. Inman (1975), Edge waves and beach cusps, J. Geophys. Res., 80(21), 2997C3012.

[16] R. A. Holman, and A.J. Bowen, Bars, bumps, and holes: Models for the generation of complex beach topography, J. Geophys. Res., 87(C1), 457C468, 1982.

[17] Holland, K. T., and R. A. Holman, Field observations of beach cusps and swash motions, Mar. Geol., 134, 77C93, 1996.

[18] Howd, P.A., J. Oltman-Shay, and R.A. Holman, (1991), Wave variance partitioning in the trough of a barred beach, J. Geophys. Res., 96(C7),12, 781-12,795.

[19] Igor S. Aranson, Lorenz Kramer (2002), The world of the complex Ginzburg-Landau equation, Reviews of Modern Physics, Vol. 74, No. 1, 99C143.

[20] Inman, D. L., and R. T. Guza (1982), The origin of swash cusps on beaches, Mar. Geol., 49, 133C148.

[21] Komar, P., Observations of beach cusps at Mono Lake, California, Geol. Soc. Am. Bull., 84, 3593C3600, 1973.

[22] Chiang C. Mei, Michael Stiassnie & Dick K.-P. Yue, (2005), *Theory and applications of ocean surface waves. Part 2: Nonlinear aspects* World Scientific, pp. 642C655.

[23] Minzoni, A.A. and Whitham, G.B. On the excitation of edge waves on beaches. J. Fluid Mech. 79 (1977), 273-287.

[24] Okihiro, M., R.T. Guza, and R.J. Seymour, (1992), Bound infragravity waves, J. Geophys. Res., 97(C7),11, 453-11,469.

[25] P. L.-F. Liu, H. Yeh, P. Lin, K.-T. Chang, Y.-S. Cho, (1998), Generation and evolution of edge-wave packets, Physics of Fluids, Vol. 10, No. 7, 1635-1657.

[26] Rockliff, Nicole, (1978), Finite amplitude effects in free and forced edge waves, Math. Proc. Camb. Phil. Soc., 83, pp. 463-479.

[27] Rockliff, Nicole, and Ronald Smith, (1985), Topographic effects on nonlinear edge waves, Geophys. Astrophys. Fluid Dynamics, 34, pp. 201-226.

[28] S. R. Lopes and A. C.-L. Chian, (1996), Controlling chaos in nonlinear three-wave coupling, Physical Review E, Vol. 54, No. 1, 170-174.

[29] Stokes, G.G. Report on recent researches in hydrodynamics. Rep. Brit. Assoc. (1846), 1-20.

[30] Ursell, F. Trapping modes in the theory of surface waves. Proc. Cambridge Philos. Soc. 47 (1951), 347-358.

[31] Ursell, F. (1952), Edge waves on a sloping beach, Proc. R. Soc. London, Ser. A, 214, 79C97.

[32] Werner, B. T., and T. M. Fink, Beach cusps as self-organized patterns, Science, 260, 968C971, 1993.

[33] Yolanda Ciriano, Giovanni Coco, K. R. Bryan, and Steve Elgar, (2005), Field observations of swash zone infragravity motions and beach cusp evolution, J. Geophys. Res., Vol. 110, No. C2, C02018.